ISSN 2313–5891 (Online)
ISSN 2304–974X (Print)

Ukrainian Food Journal

Volume 8, Issue 4
2019

Kyiv **Київ**

2019

Ukrainian Food Journal is an international scientific journal that publishes innovative papers of the experts in the fields of food science, engineering and technology, chemistry, economics and management.

Ukrainian Food Journal – міжнародне наукове періодичне видання для публікації результатів досліджень фахівців у галузі харчової науки, техніки та технології, хімії, економіки і управління.

Ukrainian Food Journal is abstracted and indexed by scientometric databases:

Ukrainian Food Journal індексується наукометричними базами:

Index Copernicus (2012)
EBSCO (2013)
Google Scholar (2013)
UlrichsWeb (2013)
CABI full text (2014)
Online Library of University of Southern Denmark (2014)
Directory of Research Journals Indexing (DRJI) (2014)
Directory of Open Access scholarly Resources (ROAD) (2014)
European Reference Index for the Humanities and the Social Sciences (ERIH PLUS) (2014)
Directory of Open Access Journals (DOAJ) (2015)
InfoBase Index (2015)
Chemical Abstracts Service Source Index (CASSI) (2016)
FSTA (Food Science and Technology Abstracts) (2018)
Emerging Sourses Citaton Index (2018)

Ukrainian Food Journal включено у перелік наукових фахових видань України з технічних наук, категорія А (Наказ Міністерства освіти і науки України № 358 від 15.03.2019)

Editorial office address:

National University
of Food Technologies
Volodymyrska str., 68
Ukraine, Kyiv 01601

Адреса редакції:

Національний університет
харчових технологій
вул. Володимирська, 68
Київ 01601

e-mail: **ufj_nuft@meta.ua**

Scientific Council of the National University of Food Technologies recommends the Journal for printing. Protocol № 5, 28.11.2019

Рекомендовано вченою радою Національного університету харчових технологій. Протокол № 5 від 28.11.2019

Ukrainian Food Journal publishes original research articles, short communications, scientific news in the related fields and also literature reviews.

Topics coverage:

Food engineering	Food nanotechnologies
Food chemistry	Food processing
Food microbiology	Economics and management in food industry
Physical property of food	Automation of food processes
Food quality and safety	Food packaging

Periodicity of the journal – 4 isues per year.

Reviewing a Manuscript for Publication. All scientific articles submitted for publication in "Ukrainian Food Journal" are double-blind peer-reviewed by at least two academics appointed by the Editors' Board: one from the Editorial Board and one, not affiliated to the Board and/or the Publisher.

Copyright. Authors submitting articles for publication are expected to provide an electronic statement confirming that their work is not an infringement of any existing copyright and will not indemnify the publisher against any breach of legislation and/or international standards in academic publishing. For the ease of dissemination all papers and other contributions become the legal copyright of the publisher unless agreed otherwise.

Academic ethics policy. The Editorial Board of "Ukrainian Food Journal" strictly follows all internationally acknowledged rules and regulations on academic publishing and academic ethics. For more details on this see: Miguel Roig (2003, 2006) "Avoiding plagiarism, self-plagiarism, and other questionable writing practices. A guide to ethical writing". The Editorial Board suggests all potential contributors of the journal, reviewers and readers to dully follow this guidance in order to avoid misconceptions.

For a **Full guide for All Authors** please visit our website:

http://ufj.ho.ua

International Editorial Board

Contents

Effect of ultrafine grinding on functional properties of soybean by-products

Fang Wang[1,2], Valerii Sukmanov[1], Jie Zeng[2]

1 – Sumy National Agrarian University, Sumy, Ukraine
2 – Henan Institute of Science and Technology, Xinxiang, PR China

Keywords:

Grinding
Soybean
By-product
Functional

Article history:

Received 21.11.2018
Received in revised form 24.04.2019
Accepted 28.11.2019

Corresponding author:

Jie Zeng
E-mail: zengjie623@163.com

DOI:
10.24263/2304-974X-2019-8-4-3

Abstract

Introduction. The ultrafine grinding technology of soybean by-products can effectively increase the content of dietary fiber in the bean dregs, and improve the taste and quality of the product.

Material and methods. Superfine pulverizer KCW-701S; laser particle size distribution meter BT-9300H; scanning electron microscope. The bean dregs were subjected to ultrafine pulverization treatment at 50, 40, 30, and 20 Hz, and untreated as a control group.

Result and discussion. The water solubility and expansion of ultrafine powdered soybean by-products has increased, compare with the control group. As the frequency decreased, the water solubility and expansion of the soybean by-products were significant change. When the frequency was 30 Hz, the water solubility was 20.84%, and the expansion was 11.03 mL/g. As the frequency decrease, the water holding capacity showed a downward trend. When the frequency was 20 Hz, the water holding capacity reached the lowest 6.53g/g, and compared with the control group (10.92g/g), the difference was significant ($p<0.05$). The oil holding capacity was no significant change.

The color of the soybean by-products has a significant change, after ultrafine grinding. The brightness L^* value of the soybean by-products has been greatly improved, and it has changed from the original wheat yellow to the creamy-white. The a^* and b^* values gradually decreased. The microscopic structure of the soybean by-products was made changes to scanning electron microscopes. As the pulverization frequency decreased, the soybean by-products powder became finer and smoother. The particle size of the bean dregs gradually reduced. When the frequency was at 30Hz, the median diameter D50 was 47.95 μm, but when the frequency was less than 30 Hz, the particle size of the bean dregs increased, and the same as a result of scanning electron microscope.

Conclusion. Ultrafine grinding was used to treat soybean by-products, in the physical and chemical properties has obvious changes. The water solubility and expansion was significantly improved, and much higher than the control group. The frequency of ultrathin grinding of 30 Hz is rational, and can be used for ultrafine grinding of soybean by-products and their subsequent use in the production of bakery products.

Introduction

China is a main producer of soybean products and the cultivation and processing industry of beans have a long history. Soybean can be made into various products, such as tofu, yuba, ferment soybean and so on [1] (Miao K., 2010). Built on the vigorous development of China's soybean industry, the domestic soybean food industry can produce tens of thousands of tons of wet bean dregs each year, with a residue up to 70%. The development of soybeans has brought great economic benefits of the food industry, which can produce 15 million tons per year [2–4] (Golbitz P., 1995; Ruan C., 2014; Liu X., 2008). soybean by-products is full of nutrients, containing 50% dietary fiber, 25% protein, 10% fat, 33% isoflavones, slightly higher amino acid content than soy milk, as well as calcium, phosphorus, iron and B vitamins. Therefore, soybean by-products have the nutritional characteristics of high fiber, high protein, low fat, and low reducing sugar, and is rich in mineral elements of high potassium, low sodium, high calcium and high magnesium et al [5–8] (Li B., 2012; Bowles S., 2006; Iskander F. Y., 1987; Wang D. L., 2010). The main ingredients of the soybean by-products were dietary fiber and protein, with high nutritional and health value, and it is a good dietary fiber raw material. However, the direct consumption of dried soybean by-products was rough, and most of the current soybean by-products were used as animal feeds, even the waste was directly thrown away. On the one hand, it caused pollution to the environment, on the other hand, it also caused waste of resources.

Ultrafine grinding use of mechanical force or fluid dynamics to overcome the internal cohesive force of the solid to break it. In the process of ultrafine grinding, the soybean by-products are modified by friction, extrusion, collision and other forces [9] (Xiang Z. N., 2006). Ultrafine grinding was based on the principle of micron technology. Can make the product finer and more surface active. Ultra-finely pulverized products of excellent physical and chemical properties, and improved utilization [10] (Liu S. L., 2007). At present, most countries used ultrafine grinding technology to treat pollen, tea, wheat bran, rice bran, peel, rice, soybean, beet pulp, animal bone, seaweed, edible fungus and other raw materials, which can preserve nutrients and improve taste [11] (Zhang M., 2005). Ultrafine grinding technology can be supported in both micron and submicron scales. This technology is being applied to cereals, such as whole wheat flour modification and related technologies [12] (Rosa N. N., 2013).

Nowadays, the ultrafine grinding technology can effectively increase the content of dietary fiber in the soybean by-products, and improve the taste and quality of the product. Therefore, it is necessary to develop and utilize the soybean by-products. In the research fresh bean dregs were used as raw materials, dried by hot air, and the water content was controlled below 10%. Used the small ultrafine grinding KCW-701S, the water solubility, swelling, water holding capacity and oil holding capacity of the soybean by-products were analyzed, and the color, microstructure, particle size and thermodynamic properties of the bean dregs were measured, and the soybean by-products were used in baked goods. It provided a theoretical reference to the further research and application of soybean by-products in baked goods.

The laboratory mainly adopts the ultrafine powder machine KCW-701S which is specially designed for the ultra-fine grinding and pulverizing processing with variable conditions. The main engine speed and fan speed can be adjusted under the action of the inverter, which can meet the crushing conditions of different requirements. The fineness range is 120-1500 mesh, the crushing cost is low, and the continuity can work. The inverter adjustment range is 50-20Hz. As the frequency decreases, the strength of the material is smaller. The principle is as follows: the material enters through the inlet, and is partially

pressed and ground through the grinding tank. The fineness of the material is caused by the airflow caused by the air-selecting motor, and 90% of the fine powder of the collecting bucket is effectively collected.

Materials and methods

Test materials

Soybean by-products, bought in the local market. Superfine grinding KCW-701S (Beijing Yujie Yucheng Machinery Equipment Co., Ltd.). Laser particle size distribution meter BT-9300H (Dandong Baxter). Scanning electron microscopes: (US FEI company).

Test methods

Process flows of bean dregs ultrafine powder.

(1) Fresh soybean by-products → hot air dried → ordinary crushes → ultrafine grinding → sealed spare

(2) Operation points: The fresh wet soybean by-products were dried, then subjected to ordinary grinding, passed through 40 mesh sieve, and finally the ordinary pulverized bean dregs were subjected to ultrafine grinding, at different frequency, and sealed for use.

(3) Pretreatment: fresh wet soybean by-products are evenly spread to a thickness of about 1 cm at 50 °C, and dried by hot air. Moisture of dried soybean by-products were controlled below 10% [13] (Cheng J. J., 2018). Smashed through a 40 mesh sieves and sealed to prevent moisture absorption from the soybean by-products**.**

(4) Superfine grinding: dry soybean by-products, take 500g into the pulverizer, set different frequency to smash for 8min, collect different frequency of soybean by-products powder, and set aside.

Test designed. The soybean by-products were treated with different frequencies using an ultrafine grinding. Soy slag was ultra-finely pulverized by adjusting the frequency converter. The frequency range was 50–20 Hz. The smaller the frequency, the finer the powder. The soybean by-products were measured for water solubility, expansion, water holding capacity, oil holding capacity, color, scanning electron microscopes, particle size distribution, and differential scanning calorimetry.

Determination of ultrafine grinding of soybean by-products physical and chemical properties

Effect of ultrafine grinding on water solubility content of soybean by-products. Refer to [14] (Li M. J., 2015). A sample of 0.500g of soybean by-products were weighed and placed in 200 mL beakers. 50 mL of distilled water was weighed and placed in a constant temperature water bath at 90 °C for constant stirring. After 30 mins, centrifuge at 3000 r/min for 15 min, pour the resulting supernatant into a Petri dish, and dry to a constant weight at 105 °C to weigh the residue (the total mass of the Petri dish and residue—Petri dish quality).

Water solubility = residue mass ÷ sample quality × 100%

Effect of ultrafine grinding on the expansion content of soybean by-products. The measurement method was referred to [15-17] (P. Rupérez, & Saura-Calixto F., 2001; Chau C. F., & Huang Y. L., 2003; Turnbull C. M., Baxter A. L., & Johnson S. K., 2005) Weigh

1.000 g of the sample of a container with a graduated surface, add 10 mL of distilled water, stir, and let it stand at room temperature for 24 h. Record the volume of the sample at this time.

Calculation method: set the sample mass to N_0, and the expanded volume was N_1

expansion = volume after expansion ÷ sample mass × 100%

expansion = $N_1 \div N_0 \times 100\%$

Effect of ultrafine grinding on the water holding capacity of soybean by-products. Weigh about 0.2 g of soybean by-products into a centrifuge tube, add 10 mL of water, stir evenly, place at room temperature for 1 h, centrifuge at 3000 r/min for 20 min, discard the supernatant, and weight of the centrifuge tube [15, 16] (P. Rupérez, & Saura-Calixto F., 2001; Chau C. F., & Huang Y. L., 2003).

Water holding capacity = (centrifuge tube and residue mass after centrifugation – centrifuge tube mass—dry weight of sample)÷dry weight of sample

Effect of ultrafine grinding on the oil holding capacity of soybean by-products. Take about 0.2 g of soybean by-products sample, place it in a constant weight centrifuge tube, add 5 mL of soybean oil, mix well, and let it stand for 30 min, shaking once every 5 min. After that, centrifuge at 4500 r/min for 25 min to remove the upper loose fat and weigh the total mass of the centrifuge tube and residue [18] (Tu Z. C., 2014).

Oil holding capacity = (centrifuge tube and residue total mass—sample quality – centrifuge tube quality)÷sample quality.

Characteristics of ultra-micro soybean by-products powder

Changes in the color of soybean by-products by ultrafine grinding. Refer to [19] (Huang S. Y., 2015). *L** was the brightness of the sample (100 was white, 0 was black); *a** was the red-greenness of the sample (positive value was red, negative was green); *b** was the yellowness of the sample (positive value was yellow, negative value was blue).

Ultrafine grinding on the particle size analysis of soybean by-products. Refer to [20] (Cheng J. J. 2018). 0.5g of soybean by-products powder was placed in a beaker, 30 ml of water was added, stirring was continued and dispersion was carried out using ultrasonic waves, and the obtained suspension was slowly added to a laser particle size analyzer. The refractive index was 1.5, the control shading ratio was 12%. The median diameter value of the soybean by-products at different frequencies was measured.

Effect of ultrafine grinding on the microstructure of soybean by-products. Refer to [21] (Gao C., 2013) for minor modifications. Weigh a small amount of soybean by-products powder, spread it on the conductive adhesive, put the tray into the ion sputtering apparatus to spray gold for 90s, use the average current of 15mA, the vacuum degree was 7–8Pa, the end of the gold spray, take out the tray, transfer to a scanning electron microscope, scan detection, take a magnification of 500 times, take a picture, and save the picture.

Analysis of differential scanning calorimetry of soybean by-products by ultrafine grinding

Refer to [21] (Gao C., 2013). The thermal stability of the sample was measured and analyzed, used a differential calorimeter. A small amount (2–5mg) of the sample was weighed into a crucible, and then placed in a pressure tested at room temperature under a lid, and transferred to a differential calorimeter for detection. Measuring range was 25–200 °C, and the temperature increase rate was set to 5 °C/min.

Statistical design and data analysis

All data were assayed at least three times and the results were expressed as mean±standard deviation (X±SD). Data and mapping were analyzed used statistical software WPS (Excel), and SPSS analysis software was used to test. The level at which significant differences were reported was setting $p<0.05$.

Results and discussion

Effect of ultrafine grinding on physical and chemical properties of soybean by-products

Effect of ultrafine grinding on water solubility of soybean by-products. As can be seen from Figure 1, the ultrafine grinding was used to soybean by-products, the water solubility significantly higher. As frequency of ultrafine grinding decreased, the soybean by-products powder was fine and the water solubility did not change significantly. However, when the frequency was 30 Hz, the water solubility was 20.84%, which was significantly higher than that of the untreated sample (12.02%), and the difference was significant ($p<0.05$). This may be due to the mechanical force of the bean dregs during the pulverization process, and the protein present in the soybean by-products were denatured, resulting in a decrease in water solubility. Secondly, some of the insoluble fiber in the soybean by-products were converted into soluble fiber, and the water solubility was affected to some extent [22] (Zhu K. X., 2010).

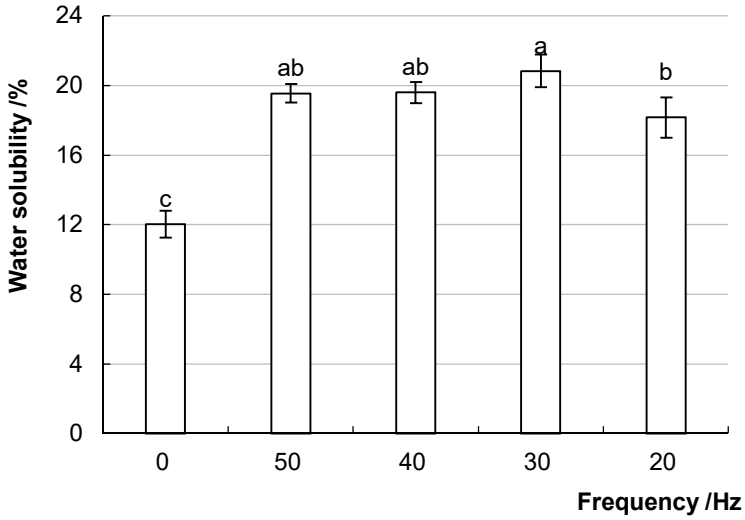

Figure 1. Effect of ultrafine grinding on water solubility of soybean by-products
[a-c] Different parameter superscripts in the figure indicate significant differences (p < 0.05)

Effect of ultrafine grinding on the expansion of soybean by-products. As can be seen from Figure 2, the ultrafine grinding soybean by-products has higher expansion than the untreated bean dregs (9.11%). Because the pulverized soybean by-products residue has a small specific surface area and the sample have high expansion. The frequency of the ultrafine grinding affects the expansion of the soybean by-products, when the frequency was 30 Hz, the expansion property was highest (11.03%). when the frequency was lower than 30 Hz, the expansion property was slightly lower. It indicated that the structure of dietary fiber in soybean by-products were damaged in a certain frequency range after ultrafine grinding, and the macromolecular substance decreased with the decrease of frequency, and the expansion of soybean by-products were affected.

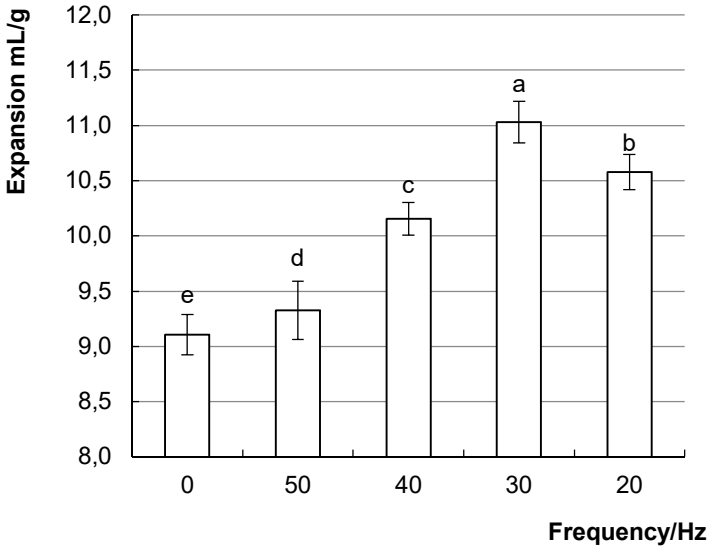

Figure 2. Effect of ultrafine grinding on the expansion of soybean by-products
[a-b] Different parameter superscripts in the figure indicate significant differences ($p < 0.05$)

Effect of ultrafine grinding on water holding capacity of soybean by-products. The water holding capacity of the soybean by-products indicates the water absorption capacity of the soybean by-products. As can be observed in Figure 3, the water holding capacity of the soybean by-products decreased with the decreased of the frequency. When the frequency was right on 20 Hz, the water holding capacity of the soybean by-products were at least 6.53g/g. It showed that the water holding capacity was linked to the specific surface area and porosity of the soybean by-products. After the ultrafine powder, the porous structure of the surface of the soybean by-products were destroyed, the water holding capacity for reduced. On the other hand, it may be that the particle size of the soybean by-products reduced, the retention capacity of the water and the adsorption capacity was all reduced, and the water holding capacity of the soybean by-products after the ultrafine grinding was gradually decreased.

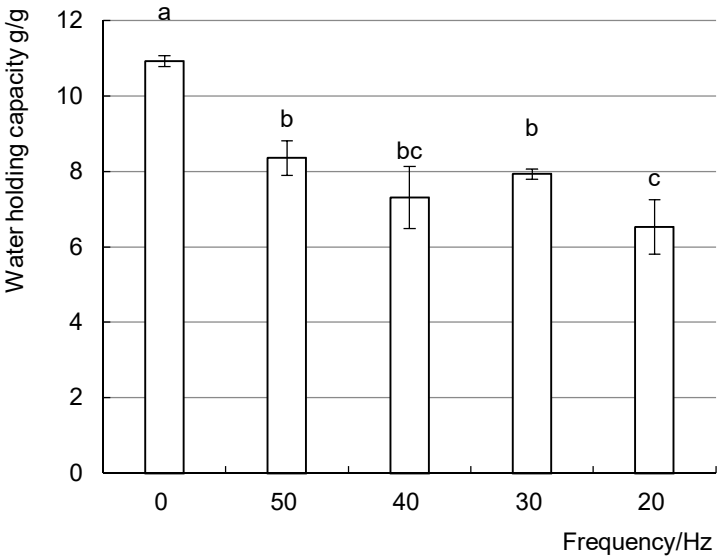

Figure 3. Effect of ultrafine grinding on the water holding capacity of soybean by-products
[a-c] Different parameter superscripts in the figure indicate significant differences (p < 0.05)

Effect of ultrafine grinding on the oil holding capacity of soybean by-products. The size of the oil holding capacity was mainly related to the structure and content of the protein in the material. As can be observed in Figure 4, the oil holding power of the soybean by-products were no significant change.

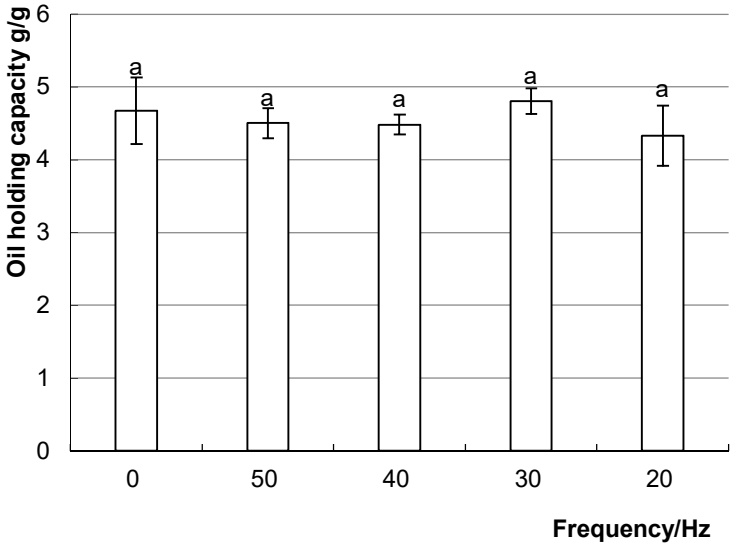

Figure 4. Effect of ultrafine grinding on the oil holding capacity of soybean by-products
[a-d] Different parameter superscripts in the figure indicate significant differences (p < 0.05)

As the frequency of ultrafine grinding decreases, the oil holding capacity gradually decreased. When the frequency reaches 20 Hz, the oil holding capacity was 4.33g/g. Compared with control group (4.68g/g), the overall decline was 7%. Because the soybean by-products undermines the structure of the soybean by-products, under the strong agitation of mechanical force, the greater the damage, the oil holding capacity was smaller. This result was significantly correlated with the water holding capacity of the soybean by-products.

Effect of ultrafine grinding on the characteristics of soybean by-products

Effect of different frequencies on the color of soybean by-products. As can be show in Table 1, the color of bean dregs has changed significantly.

Table 1

Changes in color at different frequencies

Frequency/Hz	*L**	*a**	*b**
0	80.46±0.5^{e}	2.78±0.2^{a}	18.79±0.27^{a}
50	83.08±0.09^{d}	1.85±0.08^{b}	17.56±0.29^{b}
40	86.26±0.86^{c}	1.48±0.09^{c}	15.76±0.71^{c}
30	88.32±0.29^{b}	0.98±0.14^{d}	13.87±0.30^{d}
20	89.75±0.37^{a}	0.64±0.13^{e}	13.24±0.74^{d}

Note: The difference between the lowercase letters of the peers indicates that the difference is significant (P<0.05)

Ultrafine grinding increases the brightness of the soybean by-products, and as the frequency decreases, the *L** value gradually increases. The *a** value and the *b** value slightly decreased, and the difference was significant ($p<0.05$). Therefore, with the stirring of the mechanical force, the ultrafine grinding can increase the color and brightness of the soybean by-products, improve the color of the soybean by-products, and make the flour of the soybean by-products more delicate and shiny [23] (Ren, S. G., 2009).

Effect of different frequencies on the microstructure of ultrafine powder of soybean by-products. It can be seen from Figure 5 that under the same multiples, the Control group dregs have a large, uneven structure and an irregular network structure. When the frequency was at 50-20 Hz, the particles of the soybean by-products became smaller, and the structure of the soybean by-products changes. When the frequency was 50-40 Hz, the particle shape was remarkably small, and the particles gradually become uniform. When the frequency was set to 30 Hz, the particles of the soybean by-products become fine and uniform. When the frequency was 20 Hz, the pulverization force was enormous, and the soybean by-products were fine, but some uneven agglomeration occurs. This was caused by the reduction of the frequency converter, which increases the strength of the pulverization. Under the strong mechanical shearing action, the specific surface area was obviously increased, and some particles were aggregated, so that the porous network structure of the soybean by-products were destroyed. Therefore, it was further verified that as the particle size was further reduced, the retention capacity and adsorption capacity of the water were reduced, resulting in a decrease in the expansion and water holding capacity of the sample after treatment, which was consistent with the measurement results of the properties of the soybean by-products.

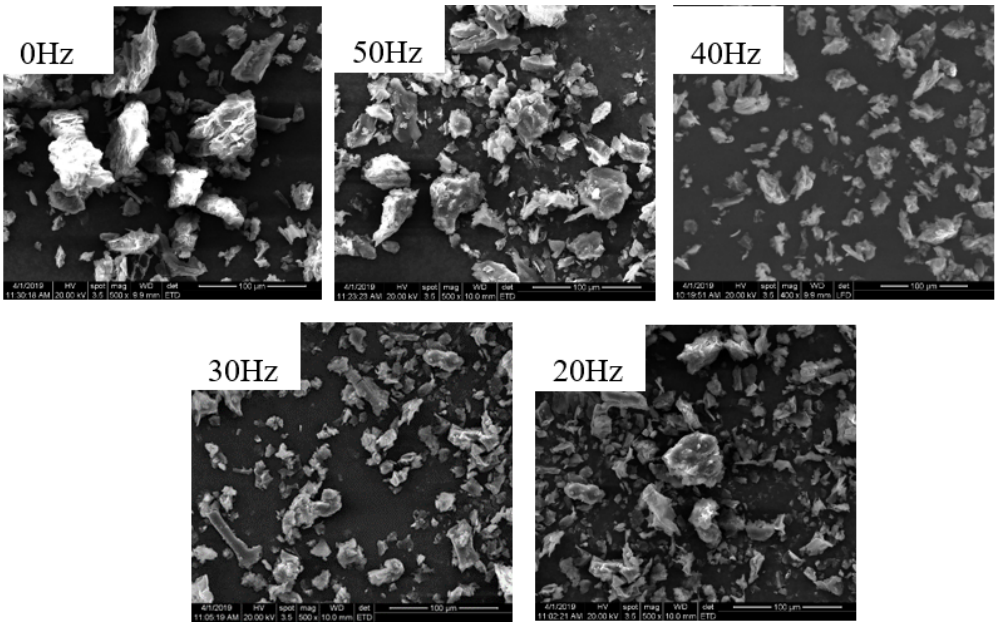

Figure 5. Effect of different frequencies on the microstructure of ultrafine powder of soybean by-products

Effect of different frequencies on the median diameter of ultrafine powder of soybean by-products

It can be seen from Figbre 6 that the different frequencies of ultrafine pulverization have a great influence on the median diameter of the soybean by-products. As the pulverization frequency decreases, the median particle size of the powder decreases significantly, but when the frequency was higher than 30 Hz, the particle size of the soybean by-products tends to increase. Because the material particles were mainly subjected to centrifugal force and medium viscosity resistance in the body, only the centrifugal force was less than the viscous resistance of the medium, the pulverized material particles pass through the classifying wheel impeller, and as the airflow enters the powder collecting system. The smaller the set frequency, the faster the rotation speed, and the higher the tangential speed of the centrifugal force field, the stronger the centrifugal force field formed. At the same time, the more collisions and the stronger the strength of the material in the machine cavity, the smaller the particle size of the obtained powder [24, 25] (Jin-Xingliu C., 2009; Wang L. D., 2016). However, if the pulverization speed was too large, the total surface area of the powder may increase, the surface energy may increase, and the powder may re-aggregate, resulting in a larger particle size [26] (Xie Y. F., 2016). This phenomenon was consistent with the particle size measurement results.

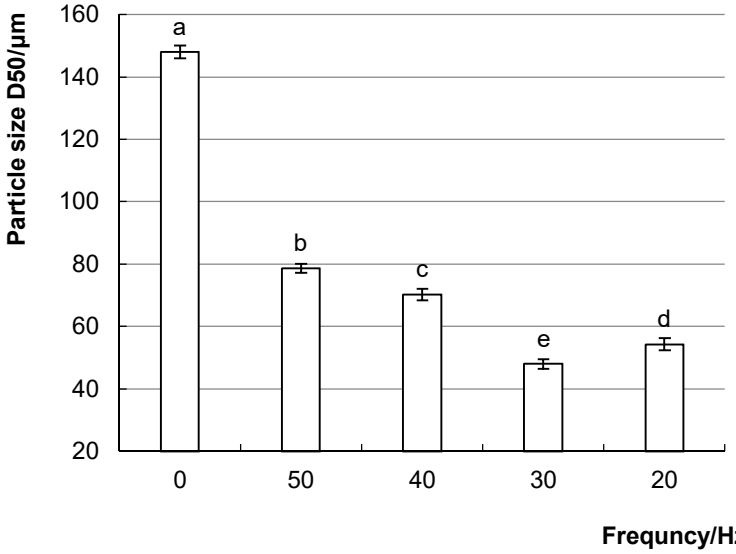

Figure 6. Effect of different frequencies of the median diameter of ultrafine powder of soybean by-products

[a-d] Different parameter superscripts in the figure indicate significant differences ($p < 0.05$)

Effect of different frequencies of the thermal stability of ultrafine powder of soybean by-products. As can be seen from Table 2, compared with the original soybean by-products, As the different frequencies decrease, the onset temperature (To), peak temperature (Tp), and termination temperature (Tc) of the ultrafine grinding soybean by-products changed. The initial temperature of the ultra-finely pulverized soybean residues increased from 32.66 °C to 34.03 °C; The peak temperature gradually increased from 84.88 °C to 87.39 °C; The termination temperature rises from 138.32 °C to 139.99 °C; The enthalpy (ΔH) increased from 150.9 °C to 174.4 °C. Compared with the original soybean by-products, the initial temperature, the peak temperature, the termination temperature, and the enthalpy value all decreased first and then increased. It shows that the soybean by-products have thermal stability and safety, and there was no unidentified substance, which has no adverse effect on the soybean by-products. This conclusion can be a superfine grinding soybean by-products powder, which was of great significance as a dietary fiber for baking food.

Table 2

Effect of different frequencies of the thermal stability of ultrafine powder of soybean by-products

Frequency/Hz	To (□)	Tp (□)	Tc (□)	ΔH (□)
0	34.18	88.45	152.95	188.7
50	32.66	84.88	138.32	150.9
40	33.11	78.41	131.91	158
30	33.42	73.77	129.02	153.6
20	34.03	87.39	139.99	174.4

Conclusion

Ultrafine grinding has a certain influence on the physical and chemical properties of soybean by-products. Compared with the Control group, the water solubility and expansion of soybean by-products by ultrafine grinding had improved. With the decreased of the frequency, the water solubility and expansion of the soybean by-products were significant change, When the frequency was 30 Hz, the water solubility was 20.84%, and the expansion was 11.03 mL/g. As the frequency decreased, the water holding capacity showed a downward trend. When the frequency was 20 Hz, the water holding capacity reached the lowest 6.53g/g, and compared with the control group (10.92g/g), the difference was significant ($p<0.05$). The oil holding capacity was no significant change.

With the decreased of the ultrafine pulverization frequency, the color L^* value of the bean dregs increased, and the a^* and b^* values gradually decreased. After ultrafine grinding, the L^* value brightness was greatly improved, from the wheat yellow color was changed to creamy-white, it indicated that ultrafine grinding can improve the color of the material. Observed by scanning electron microscopy, the microstructure of the ultrafine powder of different frequency has changed significantly. The surface was rough and uneven. With the decrease of the speed, the bean powder becomes fine and the surface of the particles becomes smooth and the powder becomes fine. After the particle size observation, the grain size of the bean dregs after ultrafine pulverization decreased significantly. (The ultra-fine grinding frequency was 30 Hz, the D50 was 47.95μm). However, when the frequency was lower than 30 Hz, the particle size of the soybean by-products has a tendency to rise significantly. Through the analysis of differential scanning calorimetry of the soybean by-products, the soybean by-products have thermal stability and safety, and there was no unidentified substance, which has no adverse effect on the soybean by-products. Therefore, after analysis of multiple indicators, when the frequency of ultrafine pulverization was adjusted to 30 Hz, the soybean by-products particles were uniform and the texture was fine. This conclusion can provide theoretical basis of the production of soybean by-products biscuits.

References

1. Mateos-Aparicio I., Mateos-Peinado C., Rupérez P. (2010), High hydrostatic pressure improves the functionality of dietary fibre in okara by-product from soybean, *Innovative Food Science & Emerging Technologies,* 11(3), pp. 445–450.
2. Golbitz P. (1995), Traditional soyfoods: processing and products, *The Journal of nutrition*, 125(3 suppl), pp. 570–572.
3. Ruan C., Ai K., & Lu L. (2014), Biomass-derived carbon materials for high-performance supercapacitor electrodes, *RSC Advances*, 4(58), pp. 30887–30895.
4. Liu X., Jin J., Wang G., & Herbert S. J. (2008), Soybean yield physiology and development of high-yielding practices in Northeast China, *Field crops research*, 105(3), pp. 157–171.
5. Li B., Qiao M., & Lu F. (2012), Composition, nutrition, and utilization of okara (soybean residue), *Food Reviews International*, 28(3), pp. 231–252.
6. Bowles S., Demiate I. M. (2006), Physicochemical characterization of the soymilk by product-okara, *Food Science and Technology*, 26(3), pp. 652–659.
7. Iskander F. Y. (1987), Maturation stage and mineral content in soybeans, *Food chemistry*, 24(1), pp. 29-35.
8. Wang D. L., Li B., L U. F., & Nan H. J. (2010), Analysis of Nutrient Components of Bean Curd Residue, *Food and Fermentation Technology*, 46(04), pp. 85–87.

9. Xiang Z. N., Ning Z. N. (2006), Technology of superfine grinding and its application in food industry, *Food Research and Development, 17*(10), pp. 991–1009.
10. Liu S. L., Wang H. (2007), Application and Research of Superfine Grinding Technique in Food Industry, *Drying Technology & Equipment*, 5(1), pp. 35–38.
11. 11. Zhang M., Zhang C. J., & Shrestha S. (2005), Study on the preparation technology of superfine ground powder of agrocybe chaxingu huang, *Journal of Food Engineering*, 67(3), pp. 333–337.
12. Rosa N. N., Barron Cécile, Gaiani C., Dufour C. & Micard Valérie. (2013), Ultra-fine grinding increases the antioxidant capacity of wheat bran, *Journal of Cereal Science*, 57(1), pp. 84–90.
13. Cheng J. J., Luo C. X, Liu J. (2018), Optimization of preparation technology and characteristics analysis of soybean dregs ultrafine powder, *Science and Technology of Food Industry* (2), pp. 202–206.
14. Li M. J., Zhang Y. Y,. You,X. R. (2015), Banana biscuit processing technology, *Science and Technology of Food Industry*, 36(3), pp. 204–208.
15. P. Rupérez & Saura-Calixto F. (2001), Dietary fibre and physicochemical properties of edible spanish seaweeds, *European Food Research and Technology*, 212(3), pp. 349–354.
16. Chau C. F., & Huang Y. L. (2003), Comparison of the chemical composition and physicochemical properties of different fibers prepared from the peel of Citrus sinensis L. Cv. Liucheng, *Journal of Agricultural and Food Chemistry*, 51(9), pp. 2615–2618.
17. Turnbull C. M., Baxter A. L., & Johnson S. K. (2005, Water-binding capacity and viscosity of Australian sweet lupin kernel fibre under in vitro conditions simulating the human upper gastrointestinal tract, *International journal of food sciences and nutrition*, 56(2), pp. 87–94.
18. Tu Z. C,. Chen L. L., Wang H. (2014), Effects of Fermentation and Dynamic High Pressure Microfluidization on Physicochemical Properties of Dietary Fiber in Soybean Residue, *Chinese Journal of High Pressure Physics*, 28(1), pp. 113–119.
19. Huang S. Y., He Y. W., Qian B. J. (2015), Modification of Insoluble Dietary Fiber in Okara by High Pressure Homogenization and High Hydrostatic Pressure and Functional Properties of the Modified Product, *Food Science*, 36(15), pp. 81–85.
20. Cheng J. J. (2018), Study on drying method of soybean and its modification technology, *(Master's thesis, Shanxi University of Science & Technology)*, pp. 1–78.
21. Gao C. (2013), Development and research on high oilgosaccharides-containing okara dietary fiber, *(Doctoral dissertation)*, pp. 1–67.
22. Zhu K. X., Huang S., Peng W., Qian H. F., & Zhou H. M. (2010), Effect of ultrafine grinding on hydration and antioxidant properties of wheat bran dietary fiber, *Food Research International,* 43(4), pp. 943–948.
23. Ren S. G., (2009), Studies on the nutrition and physicochemical properties of super-micronized soybean meal powder, *(Doctoral dissertation, Si chuan Agricultural university)*, p. 102.
24. Jin-Xingliu C. (2009), Optimization of dried older stems ultrafine pulverizing of asparagus officinalis, *Food & Machinery*, 25(6), pp. 157–159.
25. Wang L, D., Wang W. H. (2016), Processing Technology of Millet Flour by Fluidized Bed Air Superfine Grinding, *Farm Products Processing*, 11, pp. 30–33.
26. Xie Y. F., Tian S, J., Ma Y. (2014), Effect of ultrafine grinding on functional properties of okara, *Food & Machinery,* 2, pp. 7–11.

Food dispersion systems process stabilization. A review.

Andrii Goralchuk, Olga Grinchenko, Olga Riabets, Oleg Kotlyar

Kharkiv State University of Food Technology and Trade, Kharkiv, Ukraine

Keywords:

Emulsion
Foam
Stabilization
Rheology
Layers

Article history:

Received 28.11.2018
Received in revised form 15.08.2019
Accepted 28.11.2019

Corresponding author:

Andrii Goralchuk
E-mail:
abgora@gmail.com

DOI: 10.24263/2304-974X-2019-8-4-4

Abstract

Introduction. The overview is given to systematize information on the indicators, affecting the production and stabilization of foams and emulsions, for applying the existing regularities for more complex dispersed (polyphase) systems.

Materials and methods. Analytical studies of the production and stabilization of foams and polyphase dispersed systems published over the past 20 years. The research focuses on the foams, emulsions, foam emulsion systems and the systems, being simultaneously foam, emulsion and suspension.

Results and discussion. Though foams and emulsions have similarities and their production differs in the dispersion rate, determined by the rate of surfactants adsorption. Emulsifying is faster than foaming, therefore, the production of foam emulsions can be sequential only. Coalescence, as a destruction indicator, is typical of foams and emulsions alike, and it is determined by the properties of surfactants. Other indicators are determined by the features of the dispersion medium. The study systematized the factors, ensuring the stability of dispersion systems. The structural mechanical factor is effective in stabilizing foams and emulsions. It is implemented by the usage of proteins only, or solids with partial soaking, or a combination of proteins and low-molecular surfactants or a combination of proteins and polysaccharides. The structural mechanical factor for polyphase systems stabilization, in particular, for foam emulsions, is based on selecting surfactants to regulate rheological properties of interface adsorption layers, the sequence of dispersion phases, which ensures their spatial location in the food product.

Conclusions. The rheological properties of interface adsorption layers, containing proteins, surfactants, polysaccharides and high viscosity of the dispersion medium play the vital part in ensuring the stability of food dispersion systems.

Introduction

Many culinary and confectionary products are characterized by the polyphase structure. The phases may differ in content, aggregate state, ingredients, and the degree of dispersion. Food dispersion systems are thermodynamically unstable. These systems require the development of effective solutions to strengthen their process stability. In other words, it is necessary to increase the time during which the food product will not be affected. Extensive pure and applied studies have been discussing the production and stabilization of foams, emulsions, suspensions, and foods. The fundamental research into the production and stabilization of foams and emulsions, which unite the known evidence-based data, determined by the system ingredients and the way of their production, is continuously developing and scientifically expanding. However, fundamental papers that would ensure polyphase foods (systems containing several different phases) production and stability are nearly non-existent. Therefore, the development and intensification of process technologies for heterogeneous polyphase foods are inhibited. Accordingly, it is necessary to analyze scientific data on producing and stabilizing heterogeneous systems with a single continuous phase – foams and emulsions and their further development for polyphase dispersed structure foods.

Materials and methods

The analytical examination of the papers on the production and stabilization of emulsions, foams and polyphase dispersed systems over the past 20 years.

The research focuses on the foams, emulsions, foam emulsion systems and the systems, being simultaneously foam, emulsion and suspension. The study analyzes surfactants and stabilizers, used to provide dispersion systems stability.

Results and Discussion

1. The production foams and emulsions, process differences and similarities

Foams are thermodynamically unstable systems, with a gaseous dispersed phase and a liquid or solid dispersion. No clear size ranges of bubble have been reported in the literature. It is noted that the gas bubble size fluctuates from several micrometers to several centimeters [1]. Depending on the continuous phase content, bubbles have different shapes – from spherical (provided low concentration phase) to dodecahedric (provided high concentration phase). Foam stability is influenced by various factors, in particular: the nature and concentration of the foaming agent, temperature, viscosity and pH of the dispersion medium, the surface tension of solutions, the introduction of electrolytes into the liquid phase, different foods as solid particles, fatty raw materials [2, 3]. However, their impact on the foam stability has been studied insufficiently and further work is to be performed in this respect.

Foams are manufactured in two ways [1]. The first is in air dispersion via frothing, intensive mixing or gas blowing through liquid. The other way is in gas or vapor liberation in liquid as a result of liquid boiling due to fast heating or pressure drop. For this purpose, gas is first dissolved in the liquid under high pressure. This approach is effectively implemented in spray whipping cream.

Emulsions belong to lyophobic colloids, they are also thermodynamically unstable heterogeneous systems, which are two liquids that do not mix, but are distributed in each other. The discontinuous (dispersed) phase size varies from 10 nm to 50 μm. Depending on the discontinuous phase particle size emulsions are divided into nano-emulsions, micro-emulsions and emulsions (or macro emulsions). The specific feature of these emulsions is that micro-emulsions, unlike the others, are formed by themselves due to the ultra-low interfacial tension at about 0.1 mN/m, the discontinuous phase particle size ranging from 10 to 100 nm. Micro-emulsions are thermodynamically stable systems with high content of surfactants. In nano-emulsions particle size varies from 50 to 500 nm. These emulsions are kinetically stable, have low surface tension – 1–10 mN/m and the medium content of surfactants. Emulsions are kinetically stable, have low interfacial tension and the dispersed particle size from 500 nm to 50 μm [4, 5]. Nano-emulsions and emulsions have become practically used in foods.

Emulsions are classified according to two criteria: discontinuous phase concentration – diluted ($C \leq 0.1\%$), concentrated ($0.1\% \leq C \leq 74\%$) and highly concentrated ($C > 74\%$); dispersion medium polarity – direct (the dispersion medium is a polar liquid) and reverse (the dispersion medium is a non-polar liquid) [6].

It is necessary to carry out thorough examination of the processes occurring while forming and destroying foams and emulsions. The processes of forming and destroying foams and emulsions are quite similar. The formation of the dispersed system of a foam (Figure 1, a) or an emulsion (Figure 1, b) [6] is accompanied by three simultaneous processes:

- Discontinuous phase particles are deformed and broken;
- Srfactants are diffused in the newly created phase boundary surfaces and are adsorbed on them;
- Discontinuous phase particles collide, which leads to coalescence or repulsion.

Emulsions are produced using the methods of dispersion in emulsifying machines, rotary pulsers, homogenizers, ultrasound machines or via oil feeding through a network of micro-channels [7]. Emulsifying features availability of two liquids, which are not dissolved in each other, and the availability of surfactants, which ensure formation of the interface adsorption layer. The way of energy supply is important to ensure emulsion dispersion [8, 9].

To produce a dispersed system, it is necessary to put efforts into forming a new phase boundary surface, meaning that it is necessary to put efforts into destroying intermolecular forces (cohesion forces). Thermodynamically, lower degree of dispersion corresponds to the lower values of surface (in the foam) or interfacial (in emulsion) tension, which is ensured by including surfactants [11, 12]. The breakup of drops, bubbles is counteracted by the capillary pressure, which is proportionate to the surface (interfacial) tension and is turned proportionate to the dispersion particle radius [11, 12]. The difference in the capillary pressure of two adjacent bubbles triggers gas diffusion and leads to their coalescence. Surfactants resist coalescence, due to the surface tension gradient [13, 14].

The foam and emulsion production processes are similar, but have certain differences. An important difference between the formation of foams and emulsions is in the dispersion rate. Emulsifying process is much faster than that of foam formation, which determines different rates of adsorption on various phase boundary surfaces. The second difference is the size of dispersion particles, which is normally lower in emulsion. In foams it is hard to separate foam formation from stabilization, since the destruction processes start at the stage of foam formation [15]. In emulsions (such as milk) fat particles can aggregate and coalesce only under the homogenizing pressure of 8-10 MPa after cooling [16, 17].

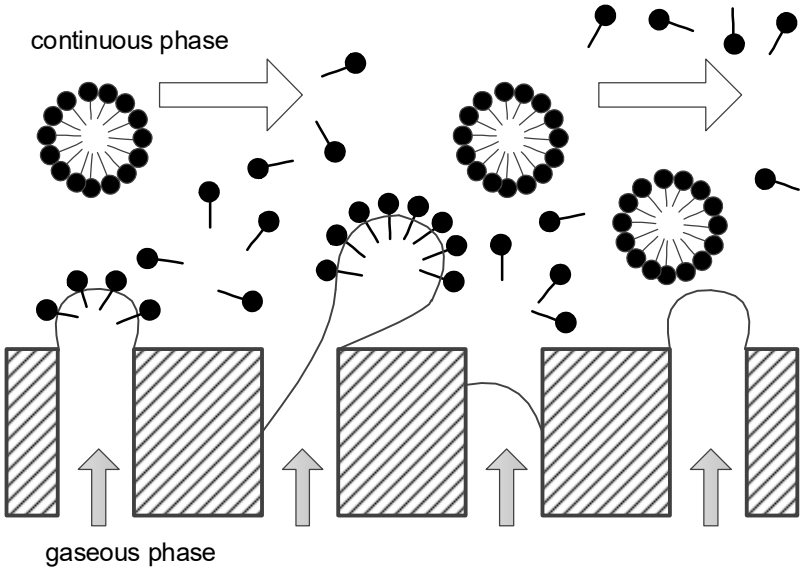

Figure 1, a. Foam formation [1].

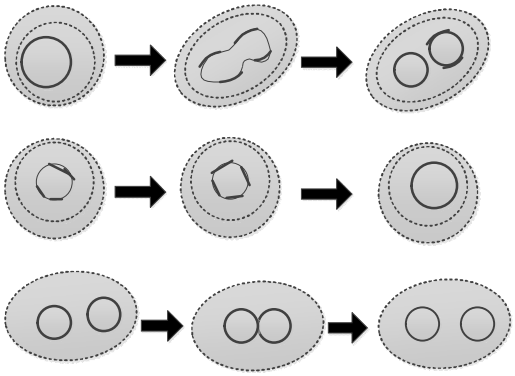

b)

Figure 1, b. Schematic representation of the various processes occurring during emulsion formation. The drops are depicted by thin lines and the surfactant by heavy lines and dots [3].

2. Factors, affecting foam and emulsion destruction

The coalescence rate depends on many factors: the conditions of foam and emulsion formation, size and homogeneity of continuous phase particles, the content of solid fat, crystal shape and size, the content of continuous phase, the kind and content of surfactants, the viscosity of dispersion medium [18, 19].

The temperature impact on the stability of foams is rather complex due to numerous simultaneous competing processes. If the temperature rises, the pressure inside bubbles rises, too, as well as the surfactants solubility, the surface tension decreases, which improves foam stability. However, if the temperature rises, thermal vibrations of adsorbed molecules increase. That leads to the decrease in the mechanical strength of the surface layer, created by surfactant molecules. Furthermore, solution viscosity decreases, which raises the rate of liquid bleeding from the foam, and the conditions of surfactant polar group hydration change, which causes foam stability loss. However, in some foams, received using high-molecular substances (egg white), thermal treatment entails transition from the liquid dispersion medium to solid. The resulting foam becomes stable. The examples of these foams are fruit candy, marshmallow, sponge cake semi-finished product etc. Thus, the temperature effect on the foam stability is to be analyzed on case-by-case basis [20].

Accordingly, the integrated process of forming and destroying dispersed systems becomes obvious. In this respect, one of the main problems in producing dispersed systems is that of their stability, which is in finding the conditions, necessary for long keeping of homogeneously distributed continuous phase in the dispersion medium [21, 22]. The keeping time is determined by process objectives in each case. Therefore, it is generally possible to identify the factors of ensuring the process stability of dispersed systems.

Emulsion destabilization involves six processes: creaming, sedimentation, flocculation (agglomeration), phase inversion, coalescence and Ostwald ripening [22] (Figure 2, a). Foam destruction involves the following processes: syneresis and air bubble coalescence as well as disproportionation (the appearance of much bigger bubbles due to the bubble coalescence (merging)), the film rupture and thinning (Figure 2, b) [23, 24].

The surface tension gradient decreases the intensity of liquid bleeding from films [11, 13]. The motion of liquid in foam leads to the local changes in the liquid and gaseous phase ratio and it occurs due to two forces – the local gradient of capillary pressure and gravity force. It is expected that drainage phenomena are related to liquid bleeding from films, caused by the capillary pressure change, which leads to the liquid flow to thicker areas with lower pressure [26]. When the film thickness is below 10 nm, it loses its integrity. At the same time gas bubbles merge (coalescence occurs), the bubbles volume increases, their quantity decreases and, eventually, foam hardens [26]. Film ruptures near the foam boundary entail the loss of the gaseous phase by the system [27]. Liquid from films gets in Plateau ribs. The channels, formed by these ribs, build a complex network for the liquid to flow out of foam due to the gravity force. The features of “wet foam” syneresis include the period of half-decay – the time for the foam to half in volume [27].

Another important mechanism of foam destruction is disproportionation. Owing to higher capillary pressure in foams a smaller bubble, compared to bugger one, undergoes gas diffusion from the smaller to the bigger bubble through the dividing film [8, 28]. Eventually, larger bubbles grow due to smaller ones. The higher the degree of polydispersion is, the stronger the gas diffusion is. “Wet” foams with thick liquid layers firstly undergo liquid bleeding, which entails film thinning followed by the gas diffusion and film rupture [29].

Emulsions destruction has both similarities and differences. Emulsion creaming is due to the difference between the density between the continuous phase and medium, which leads to bulk separation. In other words, creaming is characterized by continuous phase rise, as oil density is lower than that of water.

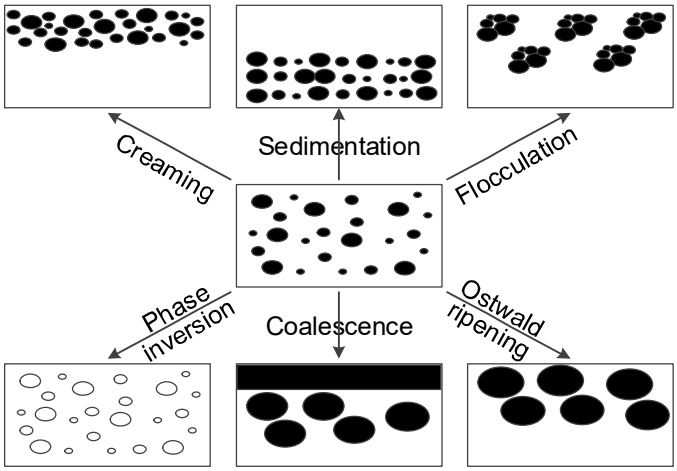

Figure 2, a. Emulsion destruction [3].

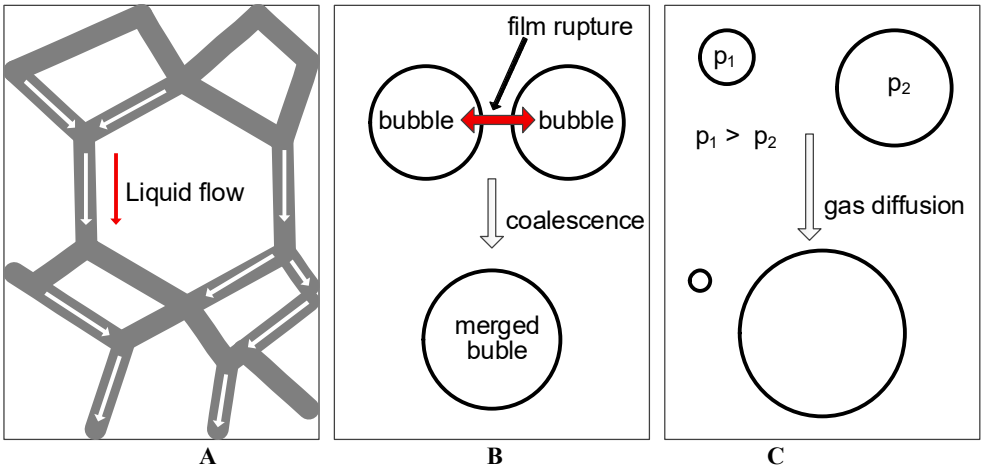

Figure 2, b. Foams [25] Gravitational drainage (A), Coalescence (B), Ostwald ripening (Disproportionation) (C).

Flocculation or agglomeration of the fat phase can occur in emulsion, provided van der Waals energy values are higher than those of the repulsion forces energy. During flocculation several oil droplets unite and form agglomeration, where each droplet stays intact, i.e. the droplet content does not shift. The process of coalescence is generally similar, and the only difference is that the droplet content unites, whereas the capillary pressure makes the resulting drop spherically shaped. In existing food emulsions the above processes are interrelated: creaming accelerates as the drop size increases through coalescence [30]. The effect is explained by the fact [29] that the oil drop lift rate rises proportionately to its squared radius. Flocculation and coalescence processes enlarge the radius of agglomerates or drops.

Studies also attend specifically to partial coalescence as a mechanism of emulsion instability [31, 32]. This process is only between partially crystallized droplets, when a crystal

of one droplet penetrates another. Liquid fat may flow out of the droplet, strengthen molecular binding, and create a bridge between two droplets [33] the mechanical force of the fat crystal binding is sufficient to stand capillary pressure, thus, protecting droplet shape and preventing their merging [31, 32].

Thus, coalescence is inherent in foams and emulsions, which is determined by the surface properties of surfactants. Such emulsion destruction processes as sedimentation, separation, Ostwald ripening and foam destruction processes – syneresis and disproportionation – are determined by the dispersion medium viscosity. The emulsion flocculation and phase inversion is due to surfactants activity.

3. Factors, ensuring foam and emulsion stability

Following the processes, occurring in dispersed systems destruction, three kinds of dispersion systems stability are singled out – aggregate, kinetic and phase. All of them are supported by different factors (Figure 3). The aggregate stability is the ability to keep unchanged size of dispersion particles over time, i.e. to resist coalescence. Kinetic stability is the system ability to keep unchanged continuous phase particle distribution within the system over time, i.e. to resist outflow or sedimentation of particles. Phase stability is the ability to keep unchanged nature of interaction between dispersed particles over time, which is important for the systems, where dispersed particles interact (flocculation) [34].

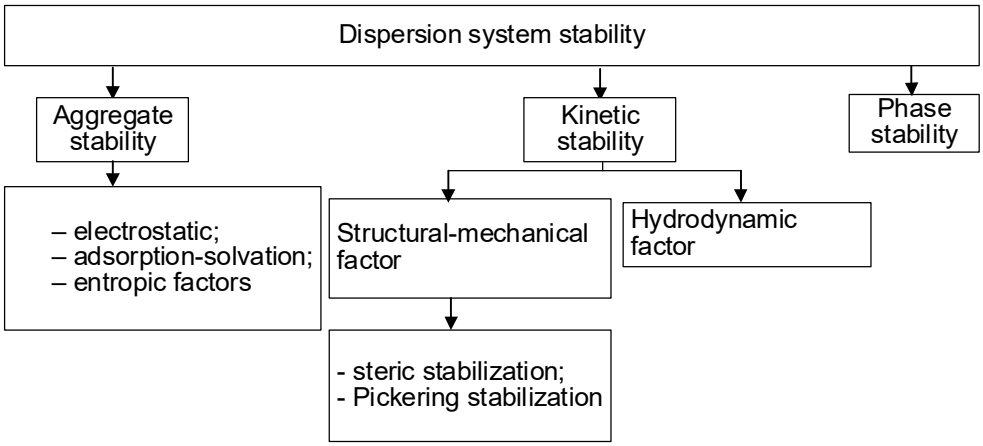

Figure 3. Factors, ensuring dispersion systems stability

The factors, ensuring the aggregate and kinetic stability of dispersed systems, include thermodynamic and kinetic ones. These factors can emerge severally or jointly.

The thermodynamic stabilization factors are [35]:

– Electrostatic;
– Adsorption-solvation;
– Entropic;

The electrostatic factor of stabilization is based on the theory, developed individually by Derjaguin, Landau, Verwey and Overbeek (DLVO). According to this theory, a double

electric layer of ions is formed on the surface of the continuous phase particles, which brings about an electric power (energy) barrier (disjoining pressure). The latter prevents approximation of like-charged particles to the distances with intensive molecular attraction forces. It is not always possible to explain the stability of emulsions and foams, stabilized by nonionic surfactants, using the electrostatic factor. Nevertheless, the application of disjoining pressure models, under the DLVO theory, enables to unite several stabilization factors and forecast system behavior [36, 37].

The adsorption-solvation factor consists in forming a dispersion medium or an adsorbed molecule layer around the dispersed particle of solvation layers. When particles approach each other, solvation (adsorption) layers prevent their coalescence [34].

The stabilization entropic factor is determined by the thermal motion and mutual repulsion of flexible chains of surfactant macromolecules, partially bound to the dispersed particles as a result of adsorbing some of their parts. This mechanism of stabilization is definitely effective in low-concentration systems and in surfactant-containing systems with long flexible chains, oriented on the dispersion medium [34].

Kinetic factors include hydrodynamic and the structurally mechanical factor. The hydrodynamic factor is related to the speed of particles approximation and the speed of medium layer bleeding between them. The slowdown in the destruction of these systems may be achieved due to increasing the density and viscosity of the dispersion medium [34].

The structurally mechanical factor includes the steric stabilization factor and Pickering stabilization. The steric stabilization factor is determined by the formation of protective interface adsorption layers on the surface of dispersion particles, which prevent coagulation of dispersion particles owing to high-molecular substances or low-molecular non-ionic surfactants. Pickering stabilization of dispersion particles is due to the formation of a high-dispersion solid particle protective barrier on their surface [37].

The study has established the effectiveness of stabilizing food dispersion systems (foams and emulsions) with structural-mechanical stabilization factor varieties – steric stabilization, provided the use of proteins, protein mixes [38], proteins with low-molecular surfactants [39, 40], protein complexes with polysaccharides [41, 42], and Pickering stabilization via using solid particles [43, 45], ethylcellulose [44], hydro dairy proteins, corn [46], fat particles [47], mustard flour, ginger flour [48] (Figure 4). The stabilization of foams and emulsions due to the structural-mechanical factor enables to significantly extend the shelf life of these products.

The research into the joint impact of substances with various surface activity rates allowed for emulsion stabilization with a combined emulsifier – protein and lecithin [51], protein and polysaccharide [34, 50]. In this stabilization, provided a specific correlation of two surfactants, the main stabilizer, though being partly replaced from the drop surface with a more active surfactant, but insufficiently to damage mechanical strength of the shell. These adsorption shells are mobile and easily self-restored.

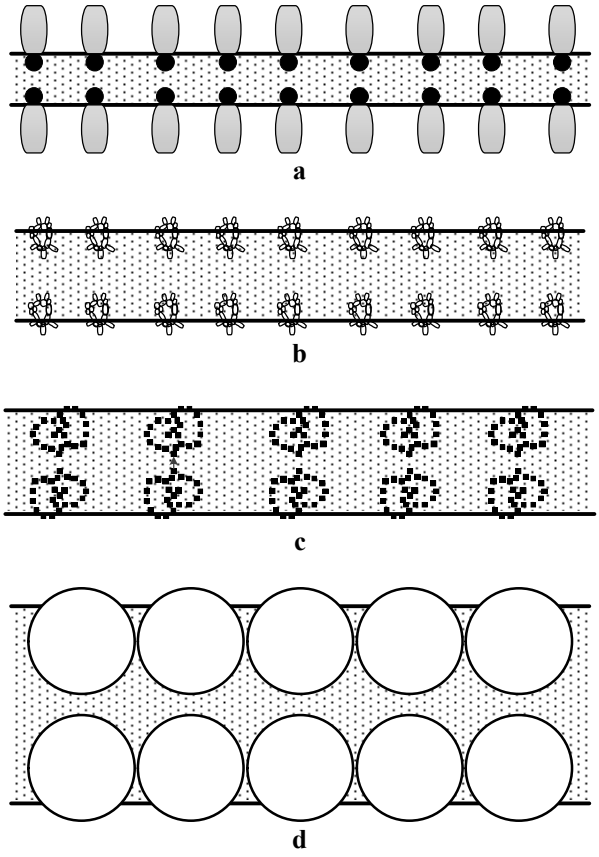

Figure 4. Schematic representation of relative thicknesses of thin films between closely approaching oil droplets stabilized by (a) surfactants, (b) proteins, (c) hydrocolloids (complex protein polysaccharides) and (d) colloidal particles (Pickering stabilization) [49]

Self-restoring emulsion properties are also typical of stabilizers thixotropic solutions, which can create a spatial network in the dispersion medium or form complexes with proteins and stabilize emulsions. The spatial network, on the one hand, binds a stabilizer with an adsorption layer, on the other – with the dispersion medium. The spatial network can be destroyed mechanically and easily restored upon the force loss [52, 53]. There are four kinds of systems, containing two polymers and a solvent:

1. The solution containing two neutral polymers refers to the segregate systems (i.e. formation of two solutions that do not mix).
2. A neutral polymer and a polyelectrolyte, that mix with each other with no creaming or sedimentation, can form associates due to the hydrogen binding, and during the charge neutralization the system may break into phases that do not mix [54].
3. Like-charged polyelectrolytes, thermodynamically incompatible, refer to segregate systems.

4. Oppositely charged polyelectrolytes. The electrostatic attraction between the oppositely charged groups leads to the emergence of complexes with rather strong binding, i.e. these systems refer to associative ones. They are widely spread in living systems and are commonly used in practice. Polyelectrolyte complexes are formed owing to the cooperative reactions of oppositely charged functional grouping. Cooperative reaction implies the emergence of each inter-chain salt binding, facilitating the formation of further bonds between polyelectrolyte complex chains, which makes is highly stable [55, 56].

The simplest way of producing polyelectrolyte complexes is mixing the solutions, where one contains anionic, and the other – cationic polyelectrolyte. There are two types of polyelectrolyte complexes – stoichiometrical and non-stoichiometrical. Stoichiometrical complexes are normally water-insoluble and characterized by high hardness and hydrophobicity. Non-stoichiometrical polyelectrolyte complexes are water-soluble as there are chain segments that were not involved in complex formation. The formation of the complexes features considerable viscosity increase, in some cases even gel formation. All these processes are influenced by pH, solution ionic force and other factors [57]. The production of polyelectrolyte complexes of milk proteins and low-etherified pectin on inter-phase surfaces enables not only to strengthen emulsion, but also to raise destruction resistance under temperature rise [58].

It was found that if the pH value is above the isoelectric point, proteins and anionic polysaccharides form soluble complexes, while if pH is below the isoelectric point, the formed complexes are water-insoluble [59, 60]. Thus, provided the conditions of forming soluble polyelectrolyte complexes between proteins and anionic polysaccharides, according to the structural-mechanical stabilization factor theory, it is possible to produce stable foams and emulsions.

Following the data analysis of the indicators, ensuring the stability of dispersion systems, structural mechanical stabilization factor varieties show high performance.

4. Factors in foam and emulsion stabilization

Food emulsion stabilization frequently involves the increase of dispersion medium viscosity. It was found that the inclusion of k-carrageenan polysaccharide in aqueous phase at 0.4% slightly raised the concentrated drop average size (30% soy oil) in sodium caseinate emulsions [61]. If the k-carrageenan content is below 0.2% there is fast coagulation of oil drops. Under high polysaccharide concentrations emulsion creaming decreases due to the formation of the mesh structure of flocculating drops. Emulsions viscosity rises along with the increase of the k-carrageenan content. The stability of emulsions, their structure and rheological properties directly relate to the quantity of the polysaccharide added to the aqueous phase.

Sodium caseinate-stabilized emulsions with k-carrageenan feature pseudo-plastic behavior, showing the reverse flocculation of oil drops. Similar properties are typical of whey protein isolate emulsions [62]. It was also identified that if pH is <6.0, and, mainly under low shear rates, the emulsion effective viscosity rose, which stabilized emulsions against creaming. This effect referred to creating oil-droplet bridges due to electrostatic interaction between whey protein isolate and k-carrageenan on the drop surface and formation of a netlike framework.

When studying the impact of k-carrageenan on the bovine-serum-albumin-stabilized (BSA) emulsion properties, it was found [63] that under the aqueous phase pH of 6.0 and certain polysaccharide limit concentration there emerges the so-called “binding”

flocculation, which leads to the formation of an oil-drop netlike framework. Provided the above pH value, experimental data on surface tension under the low ionic force show strong electrostatic BSA and k-carrageenan interaction.

It was established that adding low-molecular surfactants or polysaccharides to a protein-containing system causes emulsion flocculation and form destruction [64, 65]. To this end, the examination of the visco-elastic properties of sodium caseinate stabilized 1-Bromohexadecane-in-water emulsions confirmed [65] that under low xantan gum content, the region of emulsions linear visco-elasticity reduces, which, according to the authors, shows drop flocculation. In other words, the stabilizer acts as a flotation agent, which may be caused by charge neutralization on the surface of dispersed particles or by simultaneous adsorption of polysaccharide on different particles, thus intensifying their flotation. However, the rise of polysaccharide concentration is accompanied by the increase of visco-elastic properties – the elasticity module and complex viscosity values grow. As xantan content rises in the emulsion flow curves, there emerges a Newtonian region in the flow. Therewith, the value of the highest Newtonian viscosity grows along with the rise of the polysaccharide content in the system. That points to the formation of a spatial structure, which hinders the emulsion drops motion, and to the lower flocculation of emulsion drops. When analyzing emulsion relaxation properties it was shown that the higher xantan concentration in the stabilizing mix, the longer relaxation is required [65], which also indicates protection against emulsion drops flocculation when polysaccharide is added. The obtained data are quite comparable with findings in [66].

Studies were carried out on the stability of n-tetradecane aqueous emulsions [67, 68], stabilized by sodium caseinate and non-ionic surfactant Tween-20 (Polyethylene glycol sorbitan monolaurate) at 21 °C. In the emulsions with a stable surfactant content, the replacement of Tween-20 with caseinate leads to higher emulsifying, which, in turn, increases protein content. In addition, under lower caseinate concentrations in emulsions, their rheological parameters gradually change from visco-elastic to Newtonian – non-ionic surfactants Tween-20 weakly interact with proteins and reduce sodium caseinate emulsion viscosity. This is determined by the ability of the non-ionic surfactant, in case of adsorption, to replace protein macromolecules from the drop surface.

It was noted in [69] that despite new studies in the rheology of emulsions and interface layers, the data related to the correlation between the rheological properties of protein adsorption layers and protein-surfactant mixes and emulsion stability based on these systems are insufficient due to the missing indicator or quantitative ration between rheological interface properties and emulsion stability. It is noted that without the data on the ingredients, structure of sodium caseinate-surfactant associates and mixed interface adsorption layers it is impossible to identify the emulsion stabilization mechanism.

Thus, the joint use of proteins and polysaccharides or proteins and surfactants enables to regulate the stability of emulsions and foams. However, the mechanisms ensuring the stability (as shown in analyzed literature) may vary even in the systems with identical surfactants, but with different proportions. The situation becomes more complicated provided a polyphase system.

5. The perception and stabilization of foam emulsions

The availability and kind of oil differently influence the process of foaming and foam stability, which depends on the oil content, fat globule size and its aggregate condition [67, 70]. The production of foam emulsion systems using hard oils improves foaming ability and foam stability. This is the way to stabilize ice cream structure [71]. This process is related to foam stabilization due to adhesion of solid fat particles on air bubbles [72] (Figure 5).

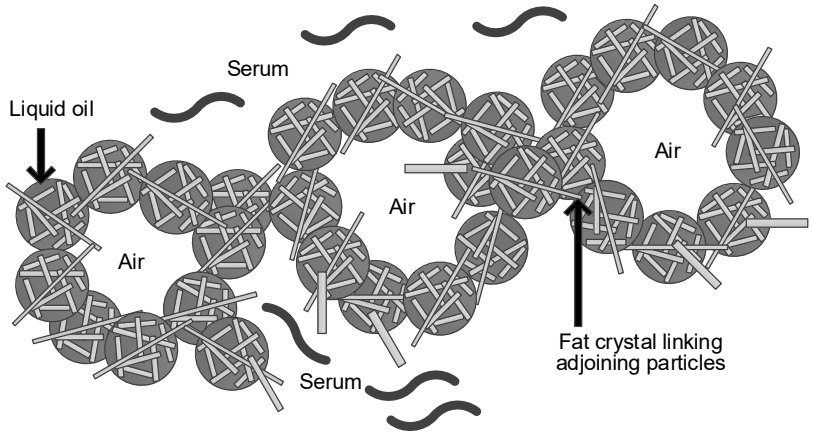

Figure 5. Adhesion of fat particles on air bubbles as a factor of foam emulsion stabilization [73]

The addition of liquid oils to foamy protein-based systems leads to lower foaming capacity and foam stability, which is related to the foam destruction and is in its ability to intensively replace protein from phase boundaries and entail the rupture of interface adsorption layers. Vice versa, the addition of hard oils raises the foaming capacity and mechanical strength of foam emulsion systems [74]. The addition of liquid oils is an effective antifoam [75], which is used in antifoaming technologies. The antifoam mechanism is in the fact that due to the adhesion of oil drops on air bubbles they, depending on the size of the surface tension, either spread on the surface of the bubble, or form a fat bridge between two adjacent bubbles (foam is destroyed anyway) Figure 6.

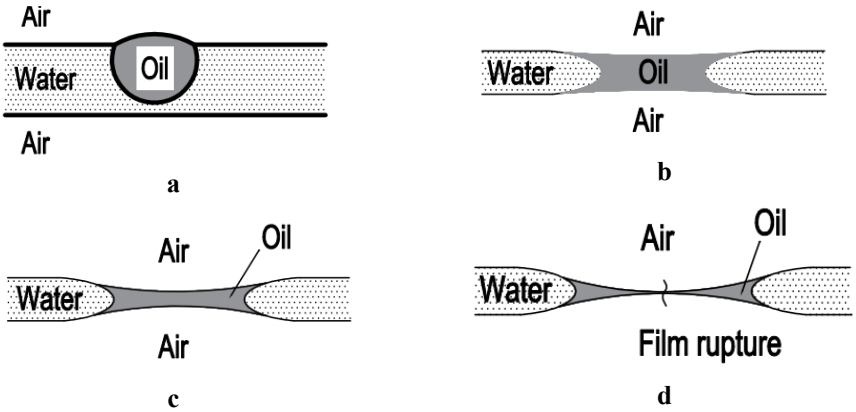

Figure 6. Schematic presentation Bridging-stretching mechanism of foam film rupture. (a-b) Bridging of the foam film surfaces by antifoam globule leads to an oil bridge with non-balanced capillary pressures at the oil-water and air-water interfaces. (c-d) The bridge stretches with time until a thin, unstable oil film is formed in the bridge center. The rupture of this oil film leads to destruction of the entire foam lamella [76].

However, in case of forming a fat bridge the destruction becomes more effective. To describe these processes a theoretical model was developed. Therewith, it involved Dupre equation and the equation of defining Harkinson spreading parameter, which the authors call the input and the spread ratios, respectively. This model describes the foam destruction process. It is noted that provided an input barrier, at the bubble interface foam destruction becomes less effective, which requires inputting non-spherical hydrophobic particles into oil [76, 77]. The input barrier may be created by colloidal surfactants, proteins. If there is an adsorption layer on fat particles and air bubbles, the stability of systems is determined by the behavior of pseudo-emulsion film, surface, interfacial tension and film tension, which create the Neumann's triangle [78].

When studying the impact of oil mixes with different content of liquid triglycerides, it was found that the higher the liquid triglycerides content is, the lower the volume of foam is. That is the result of the oil spreading on the air/water interface [79] Figure 7.

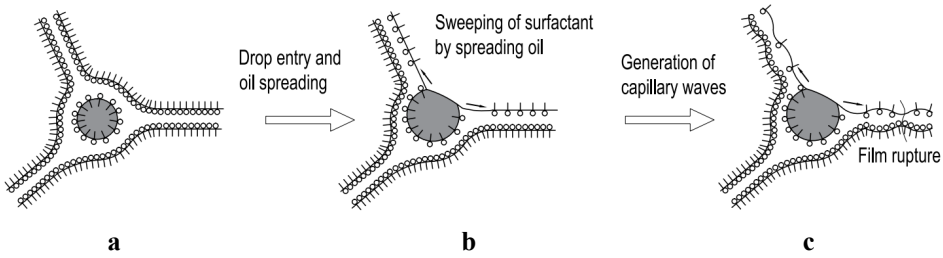

Figure 7. Schematic presentation of the "spreading-wave generation" mechanism, (a, b) Entry of an oil drop in the region of the Plateau channel leads to oil spreading on the surfaces of the neighboring foam films (b, c).

The higher the fat phase content in foam emulsion systems is, the higher the air dispersion general volume becomes, which indirectly points to the fat globules involvement in the air bubble stabilization [80]. There is also a shift of the foaming maximum towards a later whipping stage, which is, probably, related to the increase in the system viscosity. The impact of other factors on the air dispersion volume appears related to the fat dispersion destabilization. Lower destabilization and higher whipping temperature reduce foam volume. Higher destabilization of emulsions due to longer storage of cooled fat-containing emulsion products and higher acidity result in higher foam volume [81].

The air of foam emulsion structured products undergoes considerable changes while being whipped. These changes are cause by mechanical impact of mixing. The average diameter of air bubbles, which is 100–150 μm during the first five minutes, gradually reduces to 50…70 μm by about the mid of the process and further it increases by 20 μm on average till foam destruction [81].

When emulsion products are whipped, individual fat particles aggregate. This process of fat particles aggregation is both on the water/air interface and thoughout the volume of the systems. The initial stage of aggregation is the involvement of hydrophobic fat globules interfaces (flotation). The fat particles aggregation in the volume phase is not normally caused by simple collisions of single particles, but when air bubbles are actively introduced and then used to float fat globules [72].

The conditions of dispersed particles flotation include the creation a non-zero contact angle of the continuous phase and a dispersed particle, low viscosity of dispersion medium, no "protective barrier", which can be formed by high-molecular compounds [82, 83], significant shift rates (a turbulent flow), which raise the probability of air bubbles collision with dispersed particles [84, 85]. Higher hydrophobization (destabilization) of the fat phase raises the contact angle.

The process of fat particles aggregation in the aqueous phase comprises two successive stages: flocculation of fat globules with preserved, though somewhat changed shells and the aggregation of glyceride nuclei of fat globules to form emulsion gels [86, 87]. The aggregation of fat particles and forming emulsions gels might occur due to building the binding hydrophobic or salt bridges between proteins on different fat particles [88] or due to the hydrophobic binding between fat crystals or liquid oil [89, 90]. The value of the structural-mechanic barrier to be overcome by the fat globules aggregation is determined by the degree of shell native structure destruction during the whipping process or another mechanical impact. The first stage of the fat bubbles aggregation at the water/air interface is their flotation by air bubbles. The main pre-condition of this process is the hydrophobicity of the fat particles surface. The hydropobization of fat globules surfaces is ongoing throughout the emulsion production, during products preparation for whipping and while whipping; it is related to the shell loss of the most hydrophilic elements. As they are removed, the shell surface (fat globule surface) grows hydrophobic. Consequently, the shell surface becomes mosaic. Hydrophobic and hydrophilic regions are unstable, and they differently interact with the molecules of the aqueous medium [81, 86]. Accordingly, emulsion whipping process depends on the original size of the fat globules and the enlargement of fat particles while whipping [91, 92].

The foaming capacity and stability of foams in foam emulsion systems depends on the functional process properties of surfactants, namely, on the interface activities between surfactants and proteins, carbohydrates, and fats, which form rheological properties of foodstuffs [93, 94]. Depending on the specifications and texture characteristics it is necessary to regulate spatial distribution of fat particles in the aerated product, which requires different process solutions and recipes. For instance, in creams fat particles need to be distributed on the surface of air bubbles (Figure 8, a) thus providing plastic texture properties. In oil, chocolate and nut sponge cakes and aerated nut semi-finished products they are to be distributed throughout these products (Figure 8, b), since during the thermal treatment fat particles on the bubble surface will destroy and reduce the volume of the foam.

Surfactants in foam emulsion systems can destabilize emulsion, caused by mechanical impact, and lead to fat agglomeration. While whipping, agglomerates form a strong structure around air bubbles and among them, thus stabilizing the foam. To achieve required indicators of foaming capacity, foam stability and finished product texture, the functional and process properties of surfactants are to be considered, as they ensure destabilization and agglomeration of fat particles in foam emulsion systems. The fat phase agglomeration raises foaming capacity and foam stability in foam emulsion systems, though the mechanisms underlying the foaming capacity rise have not been fully clarified [95, 96].

It was found in [97] that the entry of saturated mono-glycerides in the emulsion fat phase enables to form foam emulsion systems with high foaming capacity, high air phase dispersion, dense texture, whereas the use of unsaturated mono-glycerides leads to forming soft foam emulsion systems with few large air bubbles, which sediment faster while being stored.

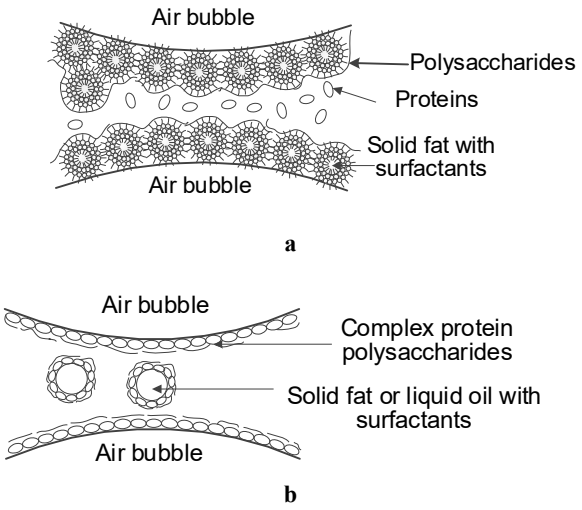

Figure 8. The diagram of foam emulsions with fat particles on air bubbles (a) and throughout the system (b)

The studies in [98, 99] made it evident that during the reconstitution and whipping of fat-containing mix powders, surfactants play an important part in destabilizing the emulsion, while protein is necessary to create the initial emulsion stability. Reconstituted whipped systems are mainly stabilized providing crystal fat at water/air interface [99, 100]. It was proven in [98] that a part of the fat in spray-dried mix powers is overcooled. During the reconstitution of these mix powders at low temperatures by adding water, there are significant changes that determine whipping properties and foam structure. The emulsion becomes unstable due to the rapid recrystallization of overcooled fat [101, 102]. The emulsion destabilization promotes protein desorption from the water-oil surface [103, 104].

Therefore, foam emulsion systems are stabilized due to surfactant properties at various interfaces. It is necessary to consider the interaction of different surfactants in foam emulsions. The sequence of dispersion phase production in foam emulsions specifies their spatial location and different texture properties. Thus, it becomes possible to make products with different textures but identical system ingredients.

6. Interface protein and low molecular surfactant interactions

Interface protein and low molecular surfactant interactions at the water-fat interface play an important role for the emulsion stability, destabilization level control, and for the formation of foam emulsion system texture. Surfactants influence fat crystallization, preventing their recrystallization, which leads to defects in fat-based foodstuffs [95, 106].

Functional and process properties of food surfactants are determined by their chemical composition, which is due to the hydrophilic and hydrophobic properties of molecules [107, 108]. The surfactants that have distinct hydrophilic properties, in particular, anionic surfactants or non-ionic ones with high hydrophilic-lipophilic balance, can disperse in water [109, 110]. These surfactants are adsorbed on the water-oil interface or interact on other phase interfaces with other foodstuff components, e.g. with proteins [111, 112].

In the systems containing several surfactants three kinds of adsorption are singled out: competitive, associative and layered. Schematically, the adsorption kinds are shown in Figure 9.

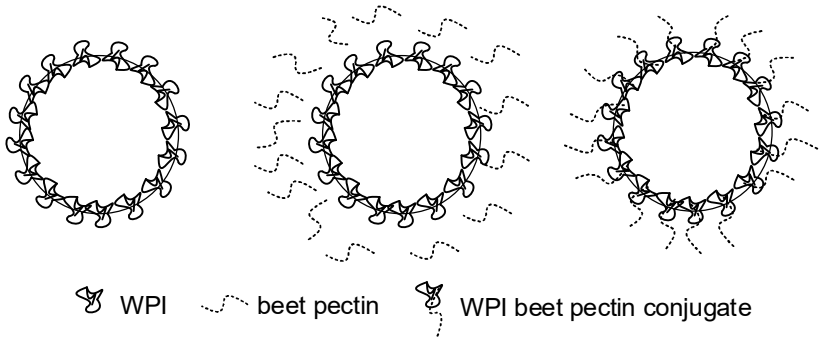

a – Associative [114]

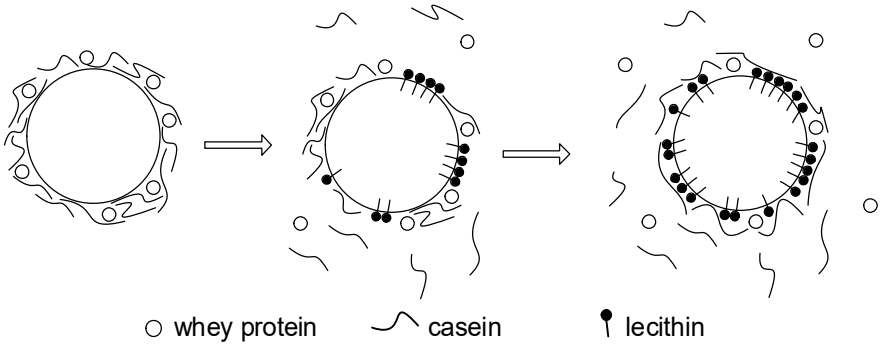

b – Competitive [115]

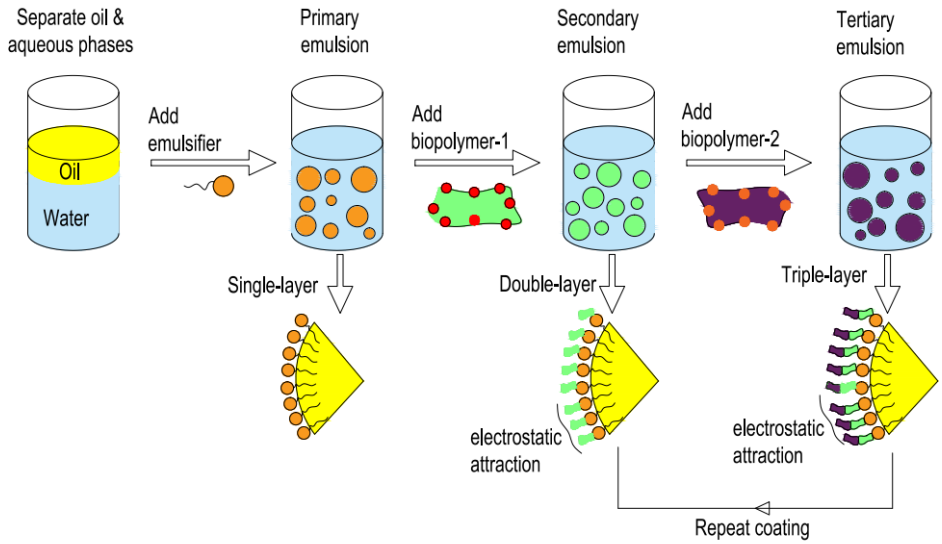

c – Layered [116]

Figure 9. The diagram of adsorption in the systems with several surfactants: a – Associative; b – Competitive; c – Layered

Dairy and many other products, containing proteins, interface adsorption layers are a mix of proteins and surfactants. The actual composition of interface adsorption layers depends on the chemical structure and relative concentrations of proteins and surfactants. During the adsorption of the chaotic protein, e.g. β-casein, rather thick interface adsorption layers with long hydrophilic ends are formed. They exude at phase interfaces, while the molecules of β-lactoglobulin are densely located near the phase interface, forming thinner interface adsorption layers [113]. The availability of surfactants impacts adsorbed proteins, in many cases replacing them from the phase interfaces, which promotes protein foaming in emulsion systems.

Non-ionic surfactants with high hydrophilic-lipophilic balance most effectively replace proteins from the interface at 15–25 ºC compared to non-ionic surfactants with low hydrophilic-lipophilic balance, for example, with mono-glycerides [117, 118]. The impact on the adsorbed protein depends on the surfactant concentration. Providing the concentration is low, the surfactant has nearly no effect on the level of protein, adsorbed on the surface, whereas higher concentration enables almost total replacement of protein from the interface, which significantly destabilizes the emulsion.

Lipophilic surfactants are less effective in replacing the protein from the phase interface. The combined use of lipophilic and hydrophilic surfactants leads to the synergy in the protein replacement [117, 118].

The effectiveness of protein replacement from the phase interface with a specific surfactant is considerably dependent on the closeness of the surfactant to the phase interface. For many lipid surfactants this process depends on temperature. Low-polarity surfactants (mono-glycerides), in small quantities, at high temperature (above 70 °C) increase the content of protein, adsorbed on the surface. Protein adsorption decrease occurs at higher concentrations. Diglycerides (E471) do not affect the adsorption or replacement of proteins [93]. At 10–40 °C saturated and unsaturated mono-glycerides (E471) decrease the interfacial tension more intensively than protein [119]. This is due to the formation of mixed interface surfactant-protein adsorption layers. Provided the temperature is below 10 °C, there appears a distinction between saturated and unsaturated mono-glycerides: saturated ones, unlike the unsaturated, determine significant decrease in the interfacial tension. The difference in the impact of saturated and unsaturated mono-glycerides on the interfacial tension at low temperatures is explained by the surfactant crystallization – saturated mono-glycerides feature higher Krafft point temperatures than the unsaturated ones.

Surfactants with stronger hydrophobic properties (saturated mono- and diglycerides, lecithin and polysorbates) more intensively reduce the interfacial tension owing to their hydrophobicity. Furthermore, their impact on the interfacial tension is less temperature dependent. A more significant decrease of the surface tension is determined by higher adsorption of the surfactant on the phase interface, thus replacing more protein. However, in food emulsions with high protein concentrations, its total replacement is not observed [120, 121].

Similarly to protein and surfactant interaction in simple emulsions, complex food emulsions involve interaction of different proteins. The proteins that are more surface-active may replace less surface-active proteins, for instance, β-casein is more likely to replace α-casein than vice versa. It was also proven that casein is added into a gelatin-stabilized emulsion, the added protein can replace gelatin [122, 123].

Under certain circumstances, the fat phase destabilization, important for foam emulsion systems (creams, ice cream etc.), may be achieved by adding differently polarized surfactants. The destabilization includes several physical changes, occurring in the emulsion, in particular, partial desorption of the interface protein and fat phase crystallization. Both

processes decrease emulsion stability during a mechanical impact. It is known that fat crystallization is required to achieve partial coalescence [124]. The addition of different surfactants can affect the degree of the fat crystallization and the shape of the created fat crystals. With water available, saturated and unsaturated surfactants promote the formation of different fat crystals. In model systems as well as in food foam emulsion ones the use of unsaturated mono-glycerides leads to forming large, multi-faceted fat crystals, while saturated mono-glycerides encourage forming smaller but more evenly structured fat crystals [125, 126].

During the emulsion whipping, protein is partially desorbed. For the beginning of fat globules flocculation protein replacement from the fat globule surface is not required [127]. Thus, for the partial destabilization of the emulsion, which is necessary to produce foam emulsion systems, the impact of surfactants on rheological properties of interface adsorption layers may be more important than their ability to replace protein. It was found that unsaturated mono-glycerides facilitate destabilization more than the unsaturated ones [119]. The control of the interaction among proteins, surfactants and fat particles on the surface of the water-air interface in foam emulsion systems can be considered as the process of air bubbles stabilization [128, 129].

Therefore, the process of forming and stabilizing foam emulsion systems is influenced by a number of factors, which eventually determine not only the stability of these systems but also their rheological properties [130]. However, rheological properties of food foam emulsion systems have been studied insufficiently, and the rheological behavior of these dispersion systems are frequently characterized qualitatively. Despite the fact that the properties of the interacting phases and components of foam emulsion systems during their formation and stabilization are essential factors for their diversity, their relation to the foaming capacity and foam stability has not been fully identified, which is determined by a wide composition of food dispersion systems and the conditions of their production.

The analysis of the above information enables to state controversial as to the stabilization of foam emulsion systems. Obviously, the stability of foam emulsion systems is achieved by raising the viscosity of dispersion medium – adding a stabilizer, higher content of the dispersion phase, ensuring conditions for fat particles agglomeration and forming a three-dimensional grid, the formation of strong interface adsorption layers on the surface of dispersion particles. As to the controversial data, it is necessary to specify the conditions and the need of fat particles flotation by regulating their contact, which, in turn, leads to the need of identifying the conditions of forming interface adsorption layers using proteins, surfactants or their mixes. To ensure flotation, it is necessary to identify the rational dispersion capacity of fat particles. It becomes evident that the key role belongs to the interface adsorption layer formation and the identification of regularities in their control, as well as the mechanisms, underlying their formation and destruction. It is clearly specified what conditions are required for the fat particles to agglomerate, float and adhere to air bubbles and the conditions, under which fat particles can provide process stability to the systems with a polyphaser dispersed structure.

The study allowed us to specify the concentrations of proteins and surfactants as well as the parameters of homogenization and whipping under which there emerge processes of emulsion destabilization, fat particle agglomeration and flotation to produce a foam emulsion system [131]. The role of proteins and surfactants was identified and NaCMC in resistance to fat particle flotation and make the structure of the aerated nut semi-finished product [132]. The process flow parameters and the content of proteins and surfactants in dry fat mixes to produce a foam emulsion system based on them [133].

Thus, interface adsorption layers play an essential role in stabilizing foams, emulsions and dispersion polyphaser systems.

7. The role of interface adsorption layers in process stability of food heterogeneous systems

The structural mechanical barrier is expressed in inhibiting coalescence and is among universal factors of dispersion system stabilization owing to its high viscosity, elasticity and mechanical strength of the interface adsorption layers. The best known interface adsorption layers are based on proteins; they can form quasi-crystal or gel-like structures. The data on the protein adsorption show [34, 134] that the effective stabilization is ensured only provided protein on the phase interface. This ensures the formation of a monomolecular layer. These interface adsorption layers determine dispersion system stability. Structured interface adsorption layers of proteins form 10–100 nm thick layers, which are sometimes are considered as a separate phase, where the protein content in this interface adsorption layer may be 20…40% [34, 35]. The role of the structural mechanical barrier in the stability of direct emulsions, stabilized by high molecular substances, was proven [135, 136].

To enforce the structural mechanical stabilization factor it is important to:

- provide decrease of the surplus free energy at the phase interface [137, 138];
- ensure the Hamaker constant, especially on the outer part of the stabilizing layer, which lowers energy and the force of dispersion particles interaction [139, 140];
- provide high shear stress, elasticity module, the viscosity of an interface adsorption layer (elastoplastic body) [141, 142];
- confirm the need to overcome a high activation barrier to destroy the interface adsorption layer (according to Zhurkov's theory) [136].

The structural mechanical barrier includes thermodynamic (elasticity modules) and kinetic (viscosity) factors, which may guarantee stability of dispersion systems in case of drop interaction [143, 144]. The stabilization of dispersion systems with high molecular substances is usually considered within the steric stabilization model [145, 146]. The steric stabilization can be regarded as a special case of the structural mechanical barrier effect [147].

The study of the structural mechanical barrier role in the stability of foams and emulsions includes the assessment of rheological parameters and the structure of stabilizing layers as well as the study of the peculiarities of losing aggregate stability of bubbles and drops when interacting with each other [34].

Today it is possible to consider a new science – rheology of interface adsorption layers, which emerged at the boundary of biological disciplines (molecular biology, biophysics and cytology), physical chemistry, physical-chemical mechanics of dispersion systems and rheology [148].

To describe the kinetics of pattern structuring in the interface adsorption layers the study in [148] offers a quantitative method, based on the parameter of structure strength growth in the interface layers of polyelectrolytes and their mixes with surfactants. The time of reaching the permanent shear stress P_s (maximum number of contacts) in the layer and the balanced surface tension is measured in hours.

The process of forming adsorption layers by proteins is divided into three stages. At the first stage there is diffusion to the phase interface, at the second – a contact with a phase, resulting in destroying the force balance, stabilizing the globule, and, accordingly, there occur conformation changes, i.e. orientation processes, at the third stage, there is a process of saturating the surface layer and the reduction of surface energy [149].

Adsorbed molecules hamper further adsorption. Depending on the redistribution of components among phases and on the king of protein there are two types of interface adsorption layers: gel-like and quasi-crystal [147, 150]. During the multilayer adsorption the protein-oil binding is replaced by the protein-protein binding, and this adsorption becomes reverse [151, 152]. It is known that proteins with flexible chains (beta-casein) are more surface active that globular proteins (lysozyme, beta-lactoglobulin, alpha-casein) or hard rod-like proteins, which becomes, inter alia, evident when studying the time of forming adsorption layers.

The rheological properties of the interface adsorption layers of high molecular surfactants on the flexible phase boundaries have been studied thoroughly [153, 154]. It was shown that the adsorption layers are characterized by the shear stress, modules of plasticity and elasticity.

As the concentration of the high molecular surfactant in the aqueous solution increases, it is possible to observe the transition from the liquid state of the layer with a low quantity of contacts, which shows Newtonian behavior, to the solid-like, strong low-defect elastoplastic structures.

Significant scope of accumulated data on interface adsorption layers rheological properties enabled to summarize the information and develop models, underlying the interface adsorption layer formation. For example, the models of gel-like and quasi-crystal interface adsorption layers correspond to the structures with coagulation and crystal-condensate contacts [147, 151]. The models of interface adsorption layers formation were developed and their quantification was carried out in the conditions of the combined use of proteins and polysaccharides [155, 156], the combined use of proteins and low-molecular surfactants [159], and the combined use of several proteins [160, 161]. However, there is scarce data on the properties of the interface adsorption layers, formed by proteins and solids [162]. However, the developed models refer to foams or emulsions. As to the models of dispersion system stabilization with two or more phases, these studies are limited, and discuss only foam emulsion systems [79, 90] and creams [73, 163]. These models are based on the principle of surface and interfacial tension and their values, which enables to substantiate the principles of stabilization. Nevertheless, following the values of the surface and interfacial tension it is impossible to explain the processes, occurring when whipping emulsions, and, probably, it is necessary to consider rheological properties of interface adsorption layers [79]. The stability of foams and emulsions greatly depends on the properties of interface adsorption layers [137, 164]. The knowledge limited by the value of surface or interfacial tension is insufficient to understand and forecast their behavior; rheological properties are more useful and informative to assess the behavior of these systems. Rheological properties of interface adsorption layers correlate to the rheological properties of foams [165] and the stability of foams and emulsions [166] as well as theoretical models [167]. Using the rheological properties of interface adsorption layers, theoretical models were developed on the foodstuff patterns with steric-stabilized polyphase dispersion structures [132], foam stabilization with fat particles [131] and their combination [133].

The analysis of literature in the field has confirmed the need to use rheological methods to do research into interface adsorption layers.

8. Methods of studying rheological properties of interface adsorption layers

The overview papers [156, 158] provide the list and features of rheological methods of studying interface adsorption layers. In addition to the torsion viscosimeter with various disk shapes, other devices are applied, but it is remarked that the torsion viscosimeter is the most

universal tool in researching interface adsorption layers with proteins. It was found that depending on the selected theoretical model of interface adsorption layers, different methods are used to study rheological properties of interface adsorption layers [157].

Surface rheological properties measurement results, obtained using the torsion surface viscosimeter [34], brought to the conclusion that there is perfect analogy of surface and volume rheology provided that measurements of surface layer rheological properties are carried out on flat faces and liquid phase interfaces. Thus, the mathematical tools, developed to describe rheological properties of three-dimensional systems, may be applied to studying rheological properties of interface adsorption layers.

To describe the interface adsorption layer behavior, it is possible to use methods with different mechanical impact on the interface adsorption layer (under permanent deformation, continuous stress, waved stress) and thus it is possible to specify such indicators as the yield shear stress [34, 169], viscosity [170], modules of plasticity and elasticity [171, 172]. To assess emulsion stability the Boussinesq number as the correlation of the interface adsorption layer viscosity to the medium viscosity [168]. In case the Boussinesq number is considerably higher than one, the system is stable, and vice versa – if it is below one – stability is low. A dilatational elasticity module is used as the ability of interface adsorption layers to resist external forces and restore interface adsorption layers to the original state after the external force termination [173, 174]. The viscosity and dilatational elasticity module are used in the systems with low protein content (up to 0.5%) or in the systems, containing low molecular substances. For the systems with high protein content (over 0.5%) in the systems, containing proteins and polysaccharides the yield shear stress of interface adsorption layers is found, as well as the elasticity module [33, 34].

Considering the known data and interface adsorption layer models, it is necessary to analyze the main approaches to regulating rheological properties of protein interface adsorption layers, using low molecular surfactants and polysaccharides. As mentioned above, surfactants can either raise or lower the stability of emulsions and foams.

9. Regulation of rheological properties of interface adsorption layers

The research into the rheological properties of gelatin interface adsorption layers showed that the layers feature visco-elastic properties [178]. A model of an interface multilayer pattern was suggested. According to it, the gelatin adsorption layer at the water-air boundary consists of one irreversibly adsorbed monomolecular layer and several reversible adsorbed secondary layers.

The yield shear stress of interface adsorption layers rises along with the protein content rise in the system, reaching the maximum, typical of gelatin для желатини, ovalbumin and casein [34]. It is due to the fact that the maximum shear stress corresponds to the monomolecular layer and strongest binding (cohesion force) of protein-protein. The maximum yield shear stress of protein interface adsorption layers meets all requirements to their coagulation, i.e. under the environment pH value that corresponds to the protein isoelectric point, ovalbumin thermal coagulation temperature (55 °C) the strength of the interface adsorption layer at the water-air interface rises 10 times. The regulation of the solution ionic force and the addition of substances, suppressing the formation of hydrogen bonds, enabled to define that bond formation in interface adsorption layers is due to the hydrogen, electrostatic and hydrophobic interactions. It was found out that regardless of the protein in the yield shear stress of interface adsorption layers at the phase interface with a non-polar solvent is 6–10 times higher compared to the interface adsorption layers at the

phase interface with air. Thus, this opens a way to regulate the yield shear stress of protein interface adsorption layers either with process factors or with addition of substances [34].

The formation of protein-polysaccharide complexes is widely used in dispersion system stabilization [179, 180]. Therewith, electrostatic or chelate coordination compound is used (formation of salt bridges between proteins and polysaccharides [181]. These complexes are characterized by quite a strong binding. Polyelectrolyte complexes are created as a result of cooperative reactions of uniting oppositely charged functional groups. The cooperative nature of reactions implies the emergence of each inter-chain salt bond, facilitating the formation of other bonds between chains of the polyelectrolyte complex, which makes it highly stable. There are two types of polyelectrolyte complexes – stoichiometrical and non-stoichiometrical [182, 183]. Stoichiometrical complexes are normally not water-soluble and feature high hardness and hydrophobic level. Non-stoichiometrical polyelectrolyte complexes are water-soluble, which is determined by the presence of chain segments, which were not involved in complex formation [55, 56]. Being formed, these complexes have high viscosity, in some cases gels are formed, which is influenced by the pH value, solution ionic force and other factors. The complexes can be formed throughout the volume and further adsorbed, or be built directly at the phase interface [58, 184].

The rheological parameters of interface layers, e.g. their viscosity, elasticity module, and shear stress can be controlled, using surfactant mixes. The strength of mixed interface adsorption layers in the considered systems is always higher than in the conditions, when proteins and surfactants are taken separately, which is determined by the formation of additional hydrogen and hydrophobic bonds between polar groups of both surfactants [142, 144].

The best and systematically known surface properties of protein-surfactants binary systems, as well as their role in forming the structure and ensuring the stability of colloidal systems are those of emulsions or foam. At the same time a special focus is on searching a possible synergetic interaction of proteins and surfactants. The combination of hydrophilic and hydrophobic segments enables the protein to form complexes with ionic and non-ionic surfactants, which is due to different physical-chemical mechanisms. In particular, owing to the electrostatic attraction between oppositely charged functional groups of ionic surfactants and proteins, or owing to the interaction between hydrophobic spots on the protein surface and non-ionic surfactants [165, 174]. Depending on the concentration, surfactants can interact with protein as individual molecules or as micelle-like aggregates. However, joining the protein, molecules of the surfactants can either stabilize or destabilize the protein structure, while acceleration or inhibiting self-association of protein molecules depending on the type of surfactants (hydrophilic-lipophilic balance, availability of charge), its concentration and environmental conditions (temperature, pH, ionic force) [185, 186].

It was established that the addition of phospholipids results in the protein interface layers losing their hardness [187], lower shear stress value [188, 189]. On the other hand, it is possible to strengthen interface layers by forming at the phase interface of inter-polymer associates, using gelatin and water-soluble surfactants (with a high hydrophilic-lipophilic balance) [189] as well as oil-soluble surfactants (with a low hydrophilic-lipophilic balance) [190].

It was stated that proteins, being adsorbed on the fat phase surface, form separate sites covered with protein [191, 192]. At low concentration of surfactants, mixed interface adsorption layers are formed. They comprise adsorbed surfactants and proteins. Surfactants can be adsorbed, being built in between the hydrophobic parts of protein molecules. That explains low correlation of surfactants: a protein does not entail protein desorption. Moreover, low concentrations of mono-glycerides can intensify protein adsorption at phase

interfaces. Adsorbed surfactants create a rather high surface pressure, interface adsorption layers aggregate, which leads to protein layer thickening. Then the regions of interface adsorption layers are finally removed into the aqueous phase as protein aggregates [193].

Rheological properties of emulsions, containing β-lactoglobulin and anionic surfactants sodium dodecylbenzenesulfonate (SDS) (at 30 °C), are defined by the molar surfactant-protein ratio [194]. A ratio, which enables emulsion elasticity modules to reach maximum values, was found. At the low and high SDS concentration the boundary of emulsion fluidity decreases compared to protein emulsions without surfactants. The results are explained by the specifics of the associated surfactant structures and the interactions between protein and SDS at the phase interface. The addition of SDS to sodium caseinate emulsions [195] raises the stability and viscosity of emulsions, which is explained by binding SDS with protein throughout the aqueous phase and by forming layers with surfactant complexes. The milk protein and iota-carrageenan correlation, under which the shear stress of the interface adsorption layers at the water-air and water-oil phases interface increases, was found [196]. Further, the sodium caseinate and k-carrageenan correlation was identified, too [133]. In both cases the increase of the maximum shear stress of interface adsorption layers is due to the formation of milk protein-carrageenans complexes.

Combined availability of a certain quantitative ration of proteins and surfactants can lead to the formation of mixed adsorption layers or to the competitive replacement of a less surface active component from the adsorption layer [67, 197].

There may emerge thermodynamic incompatibility between proteins and surfactants when exceeding the critical micelle concentration at the phase interface, thus allowing for replacement of one component with another [198, 199]. In addition, two more mechanisms were suggested to replace proteins from the surfactants phase interface [200]. The first is the mechanism of solubilization meaning the increase of the protein water solubility as a result of forming a more hydrophilic protein-surfactant complex and adding water-soluble surfactants; the other is the replacement mechanism, under which, the surfactant is stronger bound to the surface of the phase interface compared to protein (or a protein-surfactant complex) and replaces the latter.

The stability of foams, based on protein-surfactant mixes, depends on the kind of phase interface of proteins and surfactants under competitive or associative adsorption [201, 202]. In the first case, the protein interface adsorption layer is destroyed (i.e. foam stability falls), while in the other case rheological properties of interface adsorption layers strengthen (foam stability rises). For instance, the addition of Tween 20 led to the destruction of foams based on β-lactoglobulin and α-lactoalbumin [203].

The addition of non-ionic surfactants (e.g. Tween-80) to protein aqueous solutions leads to the weak interaction among components [66, 204]. The formation of complexes between bovine serum albumin (BSA) and Tween-80, is due to hydrogen bonds [205]. It was marked that the surface activity of the created complexes, is nearly 5 times higher than protein surface activity and twice as high as the Tween-80 surface activity.

The interaction between proteins was considered: β-casein, β-lactoglobulin, BSA, human serum albumin (HSA) and ionic and non-ionic surfactants throughout the aqueous phase [186]. The models of protein-ionic surfactant complexes were offered. They are formed under low concentrations of surfactants, and under electrostatic interaction between the protein and surfactants, resulting in a hydrophobic complex (associate). The complex has much lower solubility than protein, but higher surface activity. As the surfactant concentration rises throughout the aqueous phase, electrostatic interactions are complemented by hydrophobic ones. Thus, the complex becomes hydrophilic, and, accordingly, more water-soluble, and loses its surface activity.

Summing up, it is to be noted that the analysis of the literature on rheological properties shows their important role in ensuring the stability of dispersion systems. It was found that the additional entry of polysaccharides or surfactants with different hydrophilic-lipophilic balance values to protein solutions enables to regulate adsorption of proteins and surfactants in the system, change the surface activity by forming protein-polysaccharide or protein-surfactants complexes. It was established that in the literary sources most results are related to the use of non-food surfactants (sodium dodecylbenzenesulfonate) or those, restricted in their application – Tween-20, Tween-80, and also proteins as separate fractions. This approach allows for précising molecular interactions. However, to transfer them into foodstuffs, even to model systems requires some systematic experimental research.

Conclusion

1. The differences in the production of foams and emulsions are in the speed of dispersion. Emulsifying is faster than that of foaming, and the size of fat particles is smaller than that of air bubbles. Therefore, the production of foam emulsions food products, where emulsifying and foaming are simultaneous is impossible thermodynamically. The production must be performed sequentially.
2. The work systematized the factors, determining foam and emulsion destruction. The destruction factors are due to the properties and viscosity of the dispersion medium. Providing food products include both airy and fat phases, destruction will run faster.
3. The study systematized the factors, ensuring the stability of foams and emulsions. Multi-component food systems may feature several factors. The most considerable includes the varieties of the structural mechanical stabilization factor. It is implemented by the formation of a protection barrier on the dispersion particles via using only proteins, or solids with partial soaking (according to the Pickering stabilization), or combined use of proteins with low-molecular surfactants or the combined use of proteins and polysaccharides.
4. The production and stabilization of foam emulsions is to be based on the required spatial location of phases in the system, which is decisive for the foods textural properties. It is necessary to consider that this system contains phase boundaries of water-air and water-oil with varied difference of polarity. Thus, when selecting the kind and concentration of surfactants it is required to comply with the rheological properties of interface adsorption layers.
5. Interface properties of proteins and low-molecular surfactants specify rheological properties of interface adsorption layers, due to their kinds of adsorption (competitive, associative or layered), and their temperature-dependent surface activity. The rheological properties of interface adsorption layers play the leading role in the stability of foam emulsions, and foam emulsion suspensions.
6. The paper analyzed the methods of studying the rheological properties of interface adsorption layers. The values of viscosity, yield stress shear, and the elasticity modules correlate with the stability of foams and emulsions, and can be effectively used to forecast the stability of polyphase dispersion systems.
7. The rheological properties of interface adsorption layers are regulated by the addition of low-molecular surfactants with different hydrophilic-lipophilic балансу to the protein-containing systems, thus regulating adsorption, and the addition of polysaccharides, forming complexes throughout or at the boundaries of phases.

References

1. Gilka-Bötzow A., Ukrainczyk N., Koenders E.A.B. Modelling Mineral Foam Morphology Dynamics for Stability and Insulation Properties, Conference: 4th Workshop on The New Boundaries of Structural Concrete – ACI Italy Chapter At: Anacapri, Italy, September 2016, Available at: https://www.researchgate.net/publication/313248828_Modelling_Mineral_Foam_Morphology_Dynamics_for_Stability_and_Insulation_Properties.
2. Murray B.S., Ettelaie R. (2004), Foam stability: Proteins and nanoparticles, *Current Opinion in Colloid and Interface Science*, 9(5), pp. 314–320.
3. Tadros, T.F. (2013), *Emulsion formation and stability*. John Wiley & Sons, New York.
4. Burguera J. L., Burguera M. (2012) Analytical applications of emulsions and microemulsions, *Talanta,* Vol. 96, pp. 11–20.
5. Koroleva M. Iu., Iurtov E. V. (2012), Nanoemulsii: svoistva, metody polucheniia i perspektivnye oblasti primeneniia, *Uspekhi khimii*, 81(1), pp. 21–43.
6. Schramm L.L. (2006), E*mulsions, Foams, and Suspensions: Fundamentals and Applications*, WILEY-VCH Verlag GmbH & Co, New York.
7. Kawakatsu T., Tragardh G., Tragardh C. (2001), The formation of oil droplets in a pectin solution and the viscosity of the oil-in-pectin solution emulsion, Journal of *Food Engineering*, 50, pp. 247–254.
8. Damodaran S., Paraf A. (1997), Protein-Stabilized Foams and Emulsions. *In Food proteins and their applications*, Marcel Dekker, New York.
9. Perrier-Comet J. M., Marie P., Gervais P. (2005), Comparison of emulsification efficiency of protein-stabilized oil-in-water emulsions using jet, high pressure and colloid mill homogenization, *Journal of Food Engineering*, 66, pp. 211–217.
10. Walstra P. (1993), Principles of emulsion formation, *Chem. Eng. Sci.,* 48, pp. 333–349.
11. Prins A. (1999), Stagnant surface behaviour and its effect on foam and film stability, *Colloids Surf,* 149, pp. 467 – 473.
12. Van Kalsbeek H.K.A.I., Prins A., Dickinson E., Rodriguez J.M. (1999), Foam formation by food proteins in relation to their dynamic surface behavior. In Food emulsions and foams: Interfaces, interactions and stability, *Royal Society of Chemistry: Cambridge,* pp. 91–103.
13. Velikov K.P., Velev O. D., Marinova K.G., Constantinides G. N., (1997), Effect of the surfactant concentration on the kinetic stability of thin foam and emulsion films, *J. Chem. Soc., Faraday Trans,* 93, pp. 2069–2075.
14. Xu W., Nikolov A., Wasan D.T. (2005), Shear-induced fat particle structure variation and the stability of food emulsions: II. Effects of surfactants, protein, and fat substitutes, Journal ofFood Engineering, 66, pp. 107–116.
15. Walstra P., Fennema O.R. (1996), *Dispersed Systems: Basic Considerations. In Food Chemistry,* Marcel Dekker: New York.
16. Kielczewska K., Kruk A., Czerniewicz M., Warmi*ƒ*ska M., Haponiuk E. (2003), The effect of high-pressure homogenization on changes in milk colloidal and emulsifying systems, *Polish Journal of Food and Nutrition Sciences,* 12(1), pp. 43–46.
17. Cano-Ruiz M. E., Richter R. L. (1996), Effect of homogenization pressure on the milk fat globule membrane proteins, *J. Dairy Sci,* 80, pp. 2732–2739.
18. Boode K., Walstra P. (1993), Kinetics of partial coalescence in oil-in-water emulsions. In: *Food Colloids and Polymers: Stability and Mechanical Properties*, R. Soc. Chem., Cambridge, UK.
19. Boode K., Walstra P. (1993) Partial coalescence in oil-in-water emulsions 1. Nature of the aggregation, *Colloids and Surfaces a-Physicochemical and Engineering Aspects*, 81, pp. 121–137.
20. Boode K., Walstra P., Degrootmostert A. E. A. (1993) Partial coalescence in oil- in-water emulsions 2. Influence of the properties of the fat, *Colloids and Surfaces a-Physicochemical and Engineering Aspects,* 81, pp. 139–151.
21. Wierenga P.A., Gruppen H. (2010) New views on foams from protein solutions, *Current Opinion in Colloid {&} Interface Science*, 15(5), pp. 365–373.

22. Kochetkova A.A. (2002), Pishchevye emulsii i emulgatory: nekotorye nauchnye obobshcheniia i prakticheskie podrobnosti, *Pishchevye ingredienty. Syre i dobavki*, 2, pp. 8–13.
23. Bhakta A., Ruckenstein E. (1997), Decay of standing foams: drainage, coalescence and collapse, *Advances in Colloid and Interface Science*, 70, pp. 1–124.
24. Cox S.J., Alonso M.D., Weaire D., Hutzler S. (2006), Drainage induced convection rolls in foams, *The European Physical Journal*, 19, pp. 17–22.
25. Volkert M. (2009), High pressure-low temperature induced structures in dairy foams and protein model systems. Diss. Technische Universität Berlin.
26. Weaire D., Hutzler S., Cox S., Kern N., Alonso M. D., Drenckhan W. (2003), The fluid dynamics of foams, Journal of Physics: Condensed Matter, 15, pp. S65–S73.
27. Weaire D., Vaza M. F., Teixeira P.I.C., Fortes M. A. (2007), Instabilities in liquid foams, *Soft Matter*, 3(1), pp. 47–57.
28. Pugh R.J. (1996) Foaming, foam films, antifoaming and defoaming, *Advances Colloid and Interface Science*, 64, pp. 67–142.
29. Santos S. F., Zanette D., Fischer H., Itri R. (2003), A systematic study of bovine serum albumin (BSA) and sodium dodecyl sulfate (SDS) interactions by surface tension and small angle X-ray scattering, *J. Colloid Interface Science*, 262, pp. 400–408.
30. Muller D., Malmsten M., Bergcnstahl B., Hessing J., Olijve J. Mori F. (1998), Competitive Adsorption of Gelatin and Sodium Dodecylbenzenesulfonate at Hydrophobic Surfaces, *Langmuir*, 14, pp. 3107–3114.
31. McClements, D. J. (2016), *Food Emulsion Principle, Practices, and Techniques*, CRC, Boca Roton.
32. Walstra P. (1996), *Emulsion stability. In: Encyclopedia of emulsion technology* /Ed. By Becher P. New-York-Basel-Hong Kong: Marcel Dekker, 4, pp. 1–62.
33. Jackson N.E., Tucker Ch.L. (2003), A model for large deformation of an ellipsoidal droplet with interfacial tension, *J. Rheol,* 47, pp. 659–682.
34. Izmailova V.P., Iampolieskaia G.P, Summ B.D. (1988), *Poverkhnostnye iavleniia v belkovykh sistemakh*, Khimiia, Moskov.
35. Izmailova V.N, Rebinder P.A. (1974), *Strukturoobrazovanie v belkovykh sistemakh*, Nauka, Moskva.
36. Mishchuk N.A. (2011), The model of hydrophobic attraction in the framework of classical DLVO forces, *Adv. Colloid Interface Sci*, 168(1–2), pp. 149–166.
37. Babak V. G. (1992), Lineinoe natiazhenie v termodinamike tonkikh zhidkikh plenok, *Uspekhi khimii*, 61(10), pp. 1777–1804.
38. Wouters Arno GB, Rombouts I., Fierens E., Brijs K., Blecker C., Delcour J.A., Murray B.S. (2018) Foaming and air-water interfacial characteristics of solutions containing both gluten hydrolysate and egg white protein *Food Hydrocolloids,* 77, pp. 176–186.
39. Day L., Golding M., Xu M., Keogh J., Clifton P., Wooster T. J. (2014), Tailoring the digestion of structured emulsions using mixed monoglyceride-caseinate interfaces, *Food Hydrocolloids,* 36, pp. 151–161.
40. Tadros T. (2015), Viscoelastic properties of sterically stabilised emulsions and their stability, *Advances in colloid and interface science*, 222, pp. 692–708.
41. Wierenga P.A., L. van Norél, Basheva E.S. (2009), Reconsidering the importance of interfacial properties in foam stability, *Colloids and Surfaces A: Physicochemical and Engineering Aspects*, 344(1–3), pp. 72–78.
42. Cottrell T., J. Van Peij (2014), *Emulsifiers in Food Technology*, Blackwell Publishing Ltd, New Jersey.
43. Ettelaie R., Murray B.S. (2014), Effect of particle adsorption rates on the disproportionation process in pickering stabilised bubbles, *Journal of Chemical Physics*, 140(20), pp. 204713.
44. Jin H., Zhou, Cao J., Stoyanov S. D., Blijdenstein T.B. J, Groot P. W. N., Arnaudov L. N., Pelan E. W. G. (2012), Super stable foams stabilized by colloidal ethyl cellulose particles, *Soft Matter*, 8(7), pp. 2194–2205.

45. Miller R., Fainerman V. B., Kovalchuk V. I., Grigoriev D. O., Leser M. E., Michel M. (2006) Composite interfacial layers containing micro-size and nano-size particles, *Advances in colloid and interface science*, 128–130, pp. 17–26.
46. Deshmukh O.S., D. van den Ende, M. C. Stuart, F. Mugele, M. H. G. Duits (2014), Hard and soft colloids at fluid interfaces: Adsorption, interactions, assembly {&} rheology, *Advances in Colloid and Interface* Science, 222, pp. 215–227.
47. Sagis L.M.C., Scholten E. (2014), Complex interfaces in food: Structure and mechanical properties, *Trends in Food Science and Technology*, 37(1), pp. 59–71.
48. Nushtaeva A.V. (2015), Pishchevye tverdye emulgatory, Universum: Khimiia i biologiia, 7(15), Available at: http://7universum.com/ru/nature/archive/item/2337.
49. Dickinson E. Hydrocolloids as emulsifiers and emulsion stabilizers, *Food Hydrocolloids*, 23(6), pp. 1473–1482.
50. YuanY., Oberholzer M.R., Lenhoff A.M. (2000), Size does matter: electrostatically determined surfacecoverage trends in protein and colloid adsorption, *Colloids and Surfaces a-Physicochemical and Engineering Aspects*, 165(1–3), pp. 125–141.
51. Diakina T.A., Derkach S.R., Levachev S.M. (2004), Kontsentrirovannye emulsii na osnove smesei zhelatiny s letsitinom: reologicheskie svoistva, *Vesnik moskovskogo universiteta. Seriia 2. Khimiia*, 45(1), pp. 58–63.
52. Laneuville S.I., Paquin, P., Turgeon, S.L. (2000), Effect of preparation conditions on the characteristics of whey protein–xanthan gum complexes, *Food Hydrocolloids*, 14, pp. 305–314.
53. Lii C.Y., Liaw S.C., Lai V.F., Tomasik T. (2002), Xanthan gum – gelatin complexes, *European Polymer Journal*, 38, pp. 1377–1381.
54. Nikolaeva O.V., Budtova T.V., Kaliuzhnaia L.M., Belkevich N.G., Vlasova E.N., Frenzel S.Ia. (1999), Mezhmolekuliarnye vzaimodeistviia v smesiakh polurazbavlenykh rastvorov poliakrilovoi kisloty i efirov tselliulozy, *Vysokomolek. Soedineniia*, 41(7), pp. 1176–1182.
55. Azarikia F., Abbasi S. (2016), Efficacy of whey protein–tragacanth on stabilization of oil-in-water emulsions: Comparison of mixed and layer by layer methods, *Food Hydrocoll*, 59, pp. 26–34.
56. Patino J.M.R., Pilosof A.M.R. (2011), Protein-polysaccharide interactions at fluid interfaces, *Hydrocoll.*, 25(8), pp. 1925–1937.
57. Izumrudov V.A., Zenin A.B., Kabanov V.A. (1983), Reaktsii obrazovaniia nestekhiometrichnykh polieletrolitnykh kompleksov, *Vysokomolek. soedineniia*, 25(9), pp. 1972-1978.
58. Goralchuk A.B., Pivovarov P.P. (2010), *Tekhnologiia termostabilnikh emulsiinikh sousiv na osnovi ovochevoï sirovini*, KhDUKhT, Kharkiv.
59. Tolstoguzov V.B. (1987), *Nove formy belkovoi pishchi (Tekhnologicheskie problemy i perpektivy proizvodstva)*, Agropromizdat Moskov.
60. Maklakova A. A., Voronko N. G., Derkach S. R., Kadyrova G. I. (2014), Zotova Vzaimodeistvie zhelatiny s κ-karraginanom po dannym IK-spektroskopii, *Vestnik MGTU*, 17(1), pp. 53–60.
61. Singh H., Tamehana M., Hemar Y., Munro P. A. (2003), Interfacial compositions, microstructures and properties of oil-in-water emulsions formed with mixtures of milk proteins and k-carrageenan: 1. Sodium caseinate, *Food Hydrocolloids*, 17(4), pp. 539–548.
62. Singh H., Tamehana M., Hemar Y., Munro P. A. (2003), Interfacial compositions, microstructures and properties of oil-in-water emulsions formed with mixtures of milk proteins and k-carrageenan: 2. Whey protein isolate (WPI), *Food Hydrocolloids*, 17(4), pp. 549–561.
63. Dickinson E., Pavvlowsky K. (1998), Influence of k-carrageenan on the properties of a protein-stabilized emulsion, *Food Hydrocolloids*, 12(4), pp. 417–423.
64. Dickinson E., in: P.A. Williams, G.O. Phillips (Eds.) (2004), *Gums and Stabilisers for the Food Industry*, Royal Society of Chemistry, Cambridge, UK.
65. Murray, B.S. (1998), Interfacial rheology of mixed food proteins and surfactant adsorption layers with respect to emulsion and foam stability, *In Proteins and Liquid Interfaces, in "Studies of Interface Science"*, 7, pp. 179–220.
66. Das K.P., Kinsclla J. E. (1990), Stability of food emulsions: physicochemical role of protein and nonprotein emulsifiers, *Adv Food Nutr Res*, 34, pp. 81.

67. Dickinson E. (1998), Proteins at interfaces and in emulsion. Stability, rheology and interactions, *J. Chem. Soc., Faraday Trans*, 94(12), pp. 1657–1669.
68. Dickinson E., Ritzoulis C., Povey M.J.W. (1999), Stability of emulsions containing both sodium caseinate and Tween 20, *J. Colloid Interface Sci*, 212(2), pp. 515–529.
69. Dickinson E., Rad-ford S.J., Golding M. (2003), Stability and rheology of emulsions containing sodium caseinate: combined effects of ionic calcium and non-ionic surfactant, *Food Hydrocolloids*, 17(2), pp. 211–220.
70. Guzey D., McClements D. J. (2006), Formation, stability and properties of multilayer emulsions for application in the food industry, *Advances in Colloid and Interface Science*, pp. 227–248.
71. Rybak O. (2016) Milk fat in structure formation of dairy products: a review, *Ukrainian food journal,* 5(3), pp. 499–514.
72. Pareyt B., Finnie S. M., Putseys J. A., Delcour J. A. (2011), Lipids in bread making: Sources, interactions, and impact on bread quality, *Journal of Cereal Science*, 54, pp. 266–279.
73. Carr, N.O., Hogg W. F. (2005), A manufacturer's perspective on selected palm-based products, *Asia Pac J Clin Nutr*, 14(4), pp. 381–386.
74. Allen K.E., Murray B.S., Dickinson E. (2008), Development of a model whipped cream: Effects of emulsion droplet liquid/solid character and added hydrocolloid*, Food Hydrocolloids*, 22(4), pp. 690–699.
75. Denkov N. D., Marinova K. G., Tcholakova S. S. (2014), Mechanistic understanding of the modes of action of foam control agents, *Adv. Colloid Interface Sci.,* 206, pp. 57–67.
76. Denkov N. D. (2004), Mechanisms of foam destruction by oil-bases antifoam, Langmuir, 20, pp. 9463–9505.
77. Hadjiiski A., Denkov N. D., Tcholakova S., Ivanov, I. B. (2002), *Role of entry barriers in the foam destruction by oil drops*, Marcel Dekker, New York.
78. Garrett P. R. (2014), *The Science of Defoaming: Theory, Experiment and Applications* , *CRC Press*, New York.
79. Hotrum N.E., Cohen Stuart M. A., Van Vliet T., Van Aken G. A. (2004), Spreading of partially crystallized oil droplets on an air/water interface*, Colloids and Surfaces A: Physicochemical and Engineering Aspects*, 240(1-3), pp. 83–92.
80. The Foam, (2009) IHC News, 4, Available at: http://www.clariant.com/C12575E4001FB2B8/vwLookupDownloads/2009_01_IHC_Newsletter_Defoaming.pdf/$FILE/2009_01_IHC_Newsletter_Defoaming.pdf.
81. Arkhipov A. N. (2009), Primenenie strukturoobrazovatelei v proizvodstve molochnykh produktov, *Tekhnika i tekhnologiia pishchevykh proizvodstv*, 4. pp. 16–19.
82. Kaltsa O., Paximada P., Mandala I., Scholten E. (2014), Physical characteristics of submicron emulsions upon partial displacement of whey protein by a small molecular weight surfactant and pectin addition, *Food Research International*, 66, pp. 401–408.
83. Ralston J., Dukhin S.S., Mishchuk N.A. (2002), Wetting film stability and flotation kinetics, *Advances in Colloid and Interface Science*, 95(2–3), pp. 145–236.
84. Shahbazi B., Rezai B. (2015), The Effect of Micro Turbulence on Quartz Flotation Rate, *Iran. J. Chem. {&} Chem. Eng. English Ed*, 34(3), pp. 79–89.
85. Albijanic B., Ozdemir O., Hampton M. A., Nguyen P.T., Nguyen A. V, Bradshaw D. (2014), Fundamental aspects of bubble-particle attachment mechanism in flotation separation, *Miner. Eng*, 65, pp. 187–195.
86. Rodionova N. S., Pashchenko L. P., Klimova E. A. (2009), Svoistva razlichnykh penoobrazovatelei v tekhnologii kislorodnykh kokteilei, *Pivo i napitki*, 5, pp. 20–21.
87. Dickinson E. (2012) Emulsion gels: The structuring of soft solids with protein-stabilized oil droplets. *Food hydrocolloids*, 28, pp. 224–241.
88. Dickinson E. (2019), Strategies to control and inhibit the flocculation of protein-stabilized oil-in-water emulsions. *Food Hydrocolloids,* 96, pp. 209–223.
89. Arboleya J-C., Ridout M. J., Wilde P. J. (2009), Rheological behaviour of aerated palm kernel oil/water emulsions. *Food hydrocolloids*, 23, pp. 1358–1365.

90. Fredrick E., Heyman B., Moens K., Fischer S., Verwijlen T., Moldenaers P., Van der Meeren P., Dewettinck K. (2013), Monoacylglycerols in dairy recombined cream: II. The effect on partial coalescence and whipping properties, *Food Res. Int*, 51(2), pp. 936–945.
91. Prosekov A. Iu. (2005), Vliianie tekhnicheskikh kharakteristik rotorno-pulsatsionnogo apparata na strukturu vzbitogo produkta, *Khranenie i pererabotka selskokhoziaistvennoi produktsii*, 5, pp. 61–63.
92. Kakimov A. K., Kakimova Zh. Kh., Gaibalino G. M. (2008), Stabilizatsiia slivochnogo deserta, *Molochnaia promyshlennost*, 10, pp. 83–84.
93. Borcherding K., Lorenzen P., Offmann W. (2009), Effect of protein content, casein-whey protein ratio and pH value on the foaming properties of skimmed milk, *International Journal of Dairy Technology*, 62 (2), pp. 161–169
94. Erni P., Windhab E. J., Gunde R. (2007), Interfacial rheology of surface-active biopolymers: Acacia senegal versus hydrophobicallymodified starch, *Biomacromolecules*, 8, pp. 458–466.
95. Perez (2010), Interfacial and foaming characteristics of milk whey protein and polysaccharide mixed systems, *AIChE Journal*, 56(4), pp. 1107–1117.
96. Rodriguez Patino J. M., Rodriguez Nino M. R. , Sanchez C. C. (2002), Static and dynamic properties of a whey protein isolate and monoglyceride mixed films at the air-water interface, *Ind. Eng. Chem. Res*, 41, pp. 297–303.
97. Kotlyar, O., Goralchuk A., Grynchenko O., Riabets O**.** (2014), Discourse of the form and concentration of surfactants to ensure the sustainability foam-emulsive products, *Ukrainian food journal,* 3(3), pp. 361–371.
98. Zhaoa Q. (2014), Frozen, chilled and spray dried emulsions for whipped cream: Influence of emulsion preservation approaches on product functionality, *LWT – Food Science and Technology*, 62(1), pp. 287–293.
99. Munka M., Erichsenb H., Andersen M. (2014), The effects of low-molecular-weight emulsifiers in O/W-emulsions on microviscosity of non-solidified oil in fat globules and the mobility of emulsifiers at the globule surfaces, *Journal of Colloid and Interface Science*, 419, pp. 134–141.
100. Méndez-Velasco C., Douglas Goff H. (2012), Fat structures as affected by unsaturated or saturated monoglyceride and their effect on ice cream structure, texture and stability, *International Dairy Journal*, 24(1), pp. 33–39.
101. Murray B. (2009), Bubble stability in the presence of oil-in-water emulsion droplets: Influence of surface shear versus dilatational rheology, *Food Hydrocolloids*, 23(4), pp. 1198–1208.
102. Xu R., Dickinson E. , Murray B. (2008), Morphological Changes in Adsorbed Protein Films at the Oil−Water Interface Subjected to Compression, Expansion, and Heat Processing, *Langmuir*, 24(5), pp. 1979–1988.
103. Fischer P., Windhab E. (2011), Rheology of food materials, *Current Opinion in Colloid & Interface Science*, 16(1), pp. 36–40.
104. Horozov T. (2008), Foams and foam films stabilised by solid particles, *Current Opinion in Colloid & Interface Science*, 13(3), pp. 134–140.
105. Kamath S. (2008), The influence of temperature on the foaming of milk, *International Dairy Journal*, 18(10-11), pp. 994–1002.
106. Chanamai R., Clements D. J. (2001), Prediction of emulsion colour from droplet characteristics: Monodisperse oil-in-water emulsions, *Food Hydrocolloids*, 15, pp. 83–92.
107. Müller-Fischer N., Windhab E. J. (2005), In fluence of process parameters on microstructure of food foam whipped in arotor-stator device with in awidestatic pressurerange, *Colloids and Surfaces: Physicochemical and Engineering Aspects*, 263, pp. 353–362.
108. Narchi I., Vial Ch., Labbafi M. (2011), Comparative study of the design of continuous aeration equipment for the production of food foams, *Journal of Food Engineering*, 102, pp. 105–114.
109. Sonntag N. (1982), *Reactions of fats and fatty acids, Bailey's Industrial Oil and Fat Products*, John Wiley & Sons, New York.
110. Goh J., Kravchuk O., Deeth H. C. (2009), Comparison of mechanical agitation, steam injection andairbubbling for foaming milk of different types, *Milch wissens chaft. Milk science international*, 64, pp. 121–124.

111. Indrawati L., Wang Z., Narsimhan G. (2008), Effect of processing parameters on foam formation using acontinuous system with amechanical whipper, *Journal of food engineering*, 88, pp.65–74.
112. Kreu M., Krauseb I., Kulozik U. (2009), Influence of glycosylation on foaming properties of bovine caseinomacropeptide, *International Dairy Journal*, 19(12), pp. 715–720.
113. Truong T., Bansal N., Bhandari B. (2014), Effect of emulsion droplet size on foaming properties of milk fat emulsions, *Food and Bioprocess Technology*, 7(12), pp. 3416–3428.
114. Xu D., Wang Xi., Jiang Ju., Yuan F., Gaoet Ya. (2012), Impact of whey protein–Beet pectin conjugation on the physicochemical stability of β-carotene emulsions. *Food Hydrocolloids*, 28(2), pp. 258–266.
115. Zhou Xi., Chen Li., Han J., Shi M., Wang Yu., Zhang L., Li Ya., Wu W. (2017), Stability and physical properties of recombined dairy cream: Effects of soybean lecithin. *International Journal of Food Properties*, 20(10), pp. 2223–2233.
116. Bai, Long, and McClements D. (2016), Extending emulsion functionality: post-homogenization modification of droplet properties. *Processes*, 4(17), pp.1–18.
117. Fameaua A., Salonen A. (2014), Effect of particles and aggregated structures on the foam stability and aging, *Comptes Rendus Physique*, 15(8–9), pp. 748–760.
118. Zhaoa Q. (2013), Effect of sorbitan monostearate on the physical characteristics and whipping properties of whipped cream, *Food Chemistry*, 141(3), pp. 1834–1840.
119. Creux P., (2009), Strong specific hydroxide ion binding at the pristine oil/water and air/water interfaces, *J. Phys. Chem*, 113(43), pp. 14146–14150.
120. Akartuna I. (2008), Stabilization of oil-in-water emulsions by colloidal particles modified with short amphiphiles, *Langmuir*, 24(14), pp. 7161–7168.
121. Cervantes Martinez A. (2008), On the origin of the remarkable stability of aqueous foams stabilised by nanoparticles: link with microscopic surface properties, *Soft Matter*, 4, pp. 1531–1535.
122. Fredricka E., Walstrab P., Dewettinck K. (2010), Factors governing partial coalescence in oil-in-water emulsions, *Advances in Colloid and Interface Science*, 153(1–2), pp. 30–42.
123. Yuan B. (2012), Effects of limited enzymatic hydrolysis with pepsin and high-pressure homogenization on the functional properties of soybean protein isolate, *LWT – Food Science and Technology*, 46(2), pp. 453–459.
124. Borcherding K., Lorenzen P., Hoffmann W. (2008), Effect of foaming temperature and varying time/temperature-conditions of preheating on the foaming properties of skimmed milk, *International Dairy Journal*, 18(4), pp. 349–358.
125. Nicorescu I. Influence of protein heat treatment on the continuous production of food foams, *Food Res. Int*, 43, pp. 1585–1593.
126. Barfod N. M., Schrader K., Buchheim W. (2000), *Water continuous fat crystal networks in ice cream mix with unsaturated monoglyceridcs*, Proceedings of the 2nd international Symposium on Food Rheology and Structur, Zurich, pp. 104–121.
127. Davies E., Dickinson E., Bee R. D. (2001), Orthokinetic destabilization of emulsions by saturated and unsaturated monoglycerides, *Inc. Dairy Journal*, 11, pp. 827–836.
128. Dickinson E. (2011), Food colloids research: Historical perspective and outlook, *Advances in Colloid and Interface Science*, 165(1), pp. 7–13.
129. Middelberg A. A., Dimitrijev-Dwyer M. (2011), Designed Biosurfactant Protein for Switchable Foam Control, *ChemPhysChem*, 12(8), pp. 1426–1429.
130. Huppertz T., (2010), Foaming properties of milk: A review of the influence of composition and processing. *International Journal of Dairy Technology,* 63(4), pp. 477–488.
131. Goralchuk A., Omel'chenko S., Grinchenko O., Mikhaylov V. (2016), Developing a model of the foam emulsion system and onfirming the role of the yield stress shear of interfacial adsorption layers to provide its formation and stability, *Eastern-European Journal of Enterprise Technologies*, 3(11), pp. 11–19.
132. Goralchuk A., Grinchenko O., Gubsky S., Tovma L., Zhuravl'ov S. (2017), Development of a model of steric stabilization of the air-nut semi-finished product structure, *Eastern-European Journal of Enterprise Technologies*, 3(11), pp. 11–17.

133. Goralchuk A., Gubsky S., Tereshkin O., Kotlyar O., Omel'chenko S., Tovma L. (2017), Development of a theoretical model for obtaining the whipped emulsions from a dry fat-containing mixture and its experimental verification, *Eastern-European Journal of Enterprise Technologies*, 2(10), pp. 12–19.
134. Izmailova V.N., Derkach S.R., Levachev S.M., Iampolskaia G.P., Tulovskaia Z.D., Kharlov A.E., Diakina T.A., Tarasevich B.N. (2002), Ustoichivost priamykh emulsii (maslo/voda), stabilizirovannykh zhelatinoi, *Zhurnal prikladnoi fotografii*, 47(6), pp. 38–73.
135. Dickinson, E. (1997) Floculation and competitive adsorption in a mixed polymer system. Relevance to casein-stabilized emulsions, *J. Chem. Soc., Faraday Trans*, 93(13), pp. 2297–2301.
136. Izmailova V.N., Yampolskaya G.P. (1998), Concentrated emulsions stabilized by macromolecules and the contributions of Hans Sonntag to this scientific field, *Colloid & Surfaces A*, 142, pp. 125–134.
137. Langevin D. (2000), Influence of interfacial rheology on foam and emulsion properties, *Advances in Colloid and Interface Science*, 88(1-2), pp. 209–222.
138. Langevin D. (2011), Surface shear rheology of monolayers at the surface of water, *Advances in Colloid and Interface Science*, 207(1), pp. 121–130.
139. Langevin D., Monroy F. (2010), Interfacial rheology of polyelectrolytes and polymer monolayers at the air–water interface, *Current Opinion in Colloid {&} Interface Science*, 15(4), pp. 283–293.
140. Miller R., Fainerman V.B., Leser M.E., Michel A. (2004), Surface tension of mixed non-ionic surfactant/protein solution: comparison of a simple theoretical model with experiments, *Colloids & Surfaces. A, Physicochemical and Engineering Aspects*, 233, pp. 39–42.
141. Kovalchuk V.I., Miller R., Fainerman, Loglio G. (2005), Dilational rheology of adsorbed surfactant layers-role of the intrinsic two-dimensional compressibility, *Advances in Colloid and Interface Science*, 114–115, pp. 303–312.
142. Krägel J., Derkach S.R., Miller R. (2008) Interfacial shear rheology of protein-surfactant layers, *Advances in colloid and interface science*, 144(1–2), pp. 38–53.
143. Maldonado-Valderrama J., Fainerman V. B., Gálvez-Ruiz M. J., Martín-Rodriguez A., Cabrerizo-Vílchez M. A., Miller R. (2005), Dilatational Rheology of β-Casein Adsorbed Layers at Liquid−Fluid Interfaces, *The Journal of Physical Chemistry B*, 109(37), pp. 17608–17616.
144. Maldonado-Valderrama J., Patino J.M.R. (2010), Interfacial rheology of protein-surfactant mixtures, *Current Opinion in Colloid and Interface Science*, 15(4), pp. 271–282.
145. Miller R., Javadi A., Bastani D., Miller R., Kragel J., Javadi A., Bastani D., Miller R. (2010), Rheology of interfacial layers, *Colloid and Polymer Science*, 288(9), pp. 937–950.
146. Babak V.G. (1994), Stericheskaia stabilizatsiia zhidkikh plenok adsorbtsionnymi sloiami makromolekul, *Uspekhi khimii*, 63(3), c. 228–242.
147. Izmailova V.N, Iampolskaia G.P., Tulovskaia Z.D. (1998), Razvitie predstavlenii o roli strukturno-mekhanicheskogo barera po Rebinderu v ustoichivosti dispersii stabilizirovannykh belkami, *Kolloidnyi zhurnal*, 60(5), pp. 598–612.
148. Musabekov K.B., Zhubanov B.A., Izmailova V.K, Summ B.D. (1987), *Mezhfaznye sloi polielektrolitov*, Nauka, Alma-Ata.
149. Beverung C.J., Radke C.J., Blanch H.W. (1999), Protein adsorption at the oilrwater interface: characterization of adsorption kinetics by dynamic interfacial tension measurements, Biophysical Chemistry, 81, pp. 59–80.
150. Izmailova V.N., Malkova D. A., Iampolskaia G.P. (1987), Ustoichivost emulsii, stabilizirovannykh kazeinom, Kolloidnyi zhurnal, 49(1), pp. 151–153.
151. Dickinson E. (1992) Structure and composition of adsorbed protein layers and the relationship to emulsion stability, *J. Chem. Soc. Faraday Trans*, 88, pp. 2973–2983.
152. Dickinson E., Matsumura Y. (1991), Time-dependent polymerization of beta-lactoglobulin through disulphide bonds at the oil/water interface in emulsions, *J. Biol. Macromol*, 88(13), pp. 26–30.
153. Izmailova V. N., Yampolskaya G. P. (1999), Rheological behavior of protein interfacial layers in emulsion stability, *Applied Mechanics and Engineering*, 4, pp. 141–144.

154. Izmailova V.N., Yampolskaya G. P. (2000), Rheological parameters of protein interfacial layers as acriterion of the transition from stable emulsions to microemulsions, *Adv. Colloid and Interface Sci*, 88(1), pp. 99–128.
155. Derkach, S. R., Krägel J., R. Miller (2009), Methods of measuring rheological properties of interfacial layers (Experimental methods of 2D rheology), *Colloid J.*, 71(1), pp. 1–17.
156. Pelipenko J., Kristl J., Rošic R., Baumgartner S., Kocbek P. (2012), Interfacial rheology: an overview of measuring techniques and its role in dispersions and electrospinning, *Acta Pharm*, 62(2), pp. 123–140.
157. Danov, K. D., Kralchevsky P. A., Radulova G. M., Basheva E. S., Stoyanov S. D., Pelan E. G. (2015), Shear rheology of mixed protein adsorption layers vs their structure studied by surface force measurements, *Adv. Colloid Interface Sci*, 222(8), pp. 148–161.
158. Martin A., Bos M., Stuart M. C., Van Vliet T. (2002), Stress-strain curves of adsorbed protein layers at the air/water interface measured with surface shear rheology, *Langmuir*, 18(4), pp. 1238–1243.
159. Stanimirova R.D., Marinova K. G., Danov K. D., Kralchevsky P. A., Basheva E. S., Stoyanov S. D., Pelan E. G. (2014), Competitive adsorption of the protein hydrophobin and an ionic surfactant: Parallel vs sequential adsorption and dilatational rheology, *Colloids and Surfaces A: Physicochemical and Engineering Aspects*, 457(1), pp. 307–317.
160. Radulova G.M., Golemanov K., Danov K. D., Kralchevsky P. A., Stoyanov S. D., Arnaudov L. N., Blijdenstein T. B. J., Pelan E. G., Lips A. (2012), Surface shear rheology of adsorption layers from the protein HFBII hydrophobin: Effect of added β-casein, *Langmuir*, 28(9), pp. 4168–4177.
161. Marinova K.G., Basheva E. S., Nenova B., Temelska M., Mirarefi A. Y., Campbell B. E., Ivanov I. B. (2009), Physico-chemical factors controlling the foamability and foam stability of milk proteins: Sodium caseinate and whey protein concentrates, *Food Hydrocolloids*, 23(7), pp. 1864–1876.
162. Murray B.S., Durga K., Yusoff A., Stoyanov S. D. (2011), Stabilization of foams and emulsions by mixtures of surface active food-grade particles and proteins, *Food Hydrocolloids*, 25(4), pp. 627–638.
163. Rousseau D. (2000), Fat crystals and emulsion stability — a review, *Food Research International*, 33(1), pp. 3–14.
164. Santini E., Ravera F., Ferrari M., Stubenrauch C., Makievski A., Krägel J. (2007), A surface rheological study of non-ionic surfactants at the water–air interface and the stability of the corresponding thin foam films, *Colloids Surfaces A Physicochem. Eng. Asp.*, 298(1–2), pp. 12–21.
165. Lexis M., Willenbacher N. (2014), Yield stress and elasticity of aqueous foams from protein and surfactant solutions – The role of continuous phase viscosity and interfacial properties, *Colloids Surfaces A Physicochem. Eng. Asp*., 459, pp. 177–185.
166. Maldonado-Valderrama J. , Martín-Rodriguez A., Gálvez-Ruiz M. J., Miller R., Langevin D., Cabrerizo-Vílchez M. A. (2008), Foams and emulsions of β-casein examined by interfacial rheology, *Surfaces A Physicochem. Eng. Asp.*, 323(1–3), pp. 116–122.
167. Aksenenko E. V., Kovalchuk V. I., Fainerman V. B., Miller R. (2006), Surface dilational rheology of mixed adsorption layers at liquid interfaces, *Adv. Colloid Interface Sci.*, 122(1–3), pp. 57–66.
168. Carrillo-Navas H., Vernon-Carter E.J., Alvarez-Ramírez J. (2014), Viscoelastic retardation spectra of interfaces formed by water/glycerol monostearate crystals in canola oil dispersions, *Colloids and Surfaces A: Physicochemical and Engineering Aspects*, 441, pp. 1–7.
169. Goralchuk A.B., Pivovarov P.P., Prasol D.Iu. (2008), Doslidzhennia reologichnikh vlastivostei mizhfaznikh adsorbtsiinikh shariv dlia obghruntuvannja parametriv virobnitstva gariachikh emulsiinikh sousiv, *Obladnannia ta tekhnologhiji kharchovikh virobnitstv*, 18, pp. 234–240.
170. Golemanov K., Tcholakova S. S., Denkov N. D., Pelan E., Stoyanov S. D. (2014), The role of the hydrophobic phase in the unique rheological properties of saponin adsorption layers, *Soft matter*, 10, pp. 7034–7044.
171. Golemanov K., Tcholakova S. S., N. D. Denkov, Pelan E., Stoyanov S. D. (2013), Remarkably high surface visco-elasticity of adsorption layers of triterpenoid saponins, *Soft Matter*, 9(24), pp. 5738–5752.

172. L´opez-Castejon M.L., FACuente J., Ruiz M., Guerrero A. (2012), Influence of the presence of monoglyceride on interfacial properties of soy protein isolate, *Journal of the Science of Food and Agriculture*, 92(13), pp. 2618–2623.
173. Fainerman V.B., Aksenenko E. V., Lylyk S. V., Lotfi M., Miller R. (2015), Adsorption of proteins at the solution/air interface influenced by added nonionic surfactants at very low concentrations for both components. 3. Dilational surface rheology, *The Journal of Physical Chemistry B*, 119(9), pp. 3768–3775.
174. Dan A., Gochev G., Miller R. (2015), Tensiometry and dilational rheology of mixed β-lactoglobulin/ionic surfactant adsorption layers at water/air and water/hexane interfaces, *Journal of Colloid and Interface Science*, 449, pp. 383–391.
175. Noskov B.A. (2010), Dilational surface rheology of polymer and polymer/surfactant solutions, *Curr. Opin. Colloid {&} Interface Sci*, 15(4), pp. 229–236.
176. Diez-Pascual A.M., Monroy F., Ortega F., Rubio R. G., Miller R., Noskov B. A. (2007), Adsorption of water-soluble polymers with surfactant character. Dilational viscoelasticity, *Langmuir*, 23(7), pp. 3802–3808.
177. Mucic N., Javadi A., Kovalchuk N. M., Aksenenko E. V., Miller R. (2011), Dynamics of interfacial layers-Experimental feasibilities of adsorption kinetics and dilational rheology, *Advances in Colloid and Interface Science*, 168(1-2), pp. 167–178.
178. Wustneck R., Kragel J. (1998) Proteins and Liquid Interfaces*, Studies of Interface Science*, 7, pp. 433–490.
179. Cheng J., Ma Y., Li X., Yan T., Cui J. (2015), Effects of milk protein-polysaccharide interactions on the stability of ice cream mix model systems, *Food Hydrocolloids*, 45, pp. 327–336.
180. Ganzevles R.A., Zinoviadou K., Van Vliet T., Stuart M. C., De Jongh H. H. J. (2006), Modulating surface rheology by electrostatic protein/polysaccharide interactions, *Langmuir*, 22(24), pp. 10089–10096.
181. Ghosh A.K. Polysaccharide-Protein Interactions and Their Relevance in Food Colloids, *Bandyopadhyay in The Complex World of Polysaccharides*, 14, pp. 395–408.
182. Chang Y., Hu Y., McClements D.J. (2016), Competitive adsorption and displacement of anionic polysaccharides (fucoidan and gum arabic) on the surface of protein-coated lipid droplets, *Food Hydrocolloids*, 52, pp. 820–826.
183. Liang Y., Gillies G., Patel H., Matia-Merino L., Ye A., Golding M. (2014), Physical stability, microstructure and rheology of sodium-caseinate-stabilized emulsions as influenced by protein concentration and non-adsorbing polysaccharides, *Food Hydrocolloids*, 36, pp. 245–255.
184. Miquelim J.N., Lannes S.C.S., Mezzenga R. (2010), pH Influence on the stability of foams with protein–polysaccharide complexes at at their interfaces, *Food Hydrocolloids*, 24(4), pp. 398–405.
185. Kelley D., McClements D.J. (2003), Interactions of bovine serum albumin with ionic surfacatants in aqueous solutions, *Food Hydrocolloids*, 17, pp. 73–85.
186. Miller R., Fainerman V. B., Makievski A. V., Krägel J., Grigoriev D. O., Kazakov V. N., Sinyachenko O. V. (2000), Dynamics of protein and mixed protein/surfactant adsorption layers at the water/fluid interface, *Advances in Colloid and Interface Science*, 86(1–2), pp. 39–82.
187. Levachev S. M., Izmailova V. N. (1994), Nekotorye svoistva assotsiatov bychego syvorotochnogo albumina i lipidov (letsitin, kholesterin), *Kolloid, zhurnal*, 56(2), pp. 193–196.
188. Kotlyar O., Goralchuk A., Grinchenko O. (2014) The study of surface-activ agents impact on the strength of interfacial adsorption layers, *The Advanced Science Journal*, 10, pp. 37–42.
189. Omelchenko S. B., Goralchuk A. B. (2014), Vivchennia mizhfaznikh adsorbtsiinikh shariv z metoiu rozrobki tekhnologhiji molochnoji produkciji, *Skhidno-Jevropejsjkyj zhurnal peredovikh tekhnologii*, 5/11(71), pp. 46–51.
190. Izmailova V. N., Levachev S. M., Iampolskaia G. P., Gratskova I. A., Kapustina A.A., Nuss P. V., Martynova E. V., Adebaio G. (2000), Reologicheskie kharakteristiki adsorbtsionnykh sloev interpolimernykh assotsiatov syvorotochnogo albumina i polistirola na granitse faz voda/ksilol, *Kolloidnyi Zhurnal*, 62(1), pp. 70–77.
191. Kralovaa I., Sjöbloma J. (2009) Surfactants used in food industry: A review, *Journal of Dispersion Science and Technology*, 30(9), pp. 1363–1383.

192. Dickinson E. (2001), Milk protein interfacial layers and the relationship to emulsion stability and rheology, *Coll. Surf. B: Biointerfaces*, 20, pp. 354–363.
193. Maldonado-Valderrama J., Langevin D. (2008), On the difference between foams stabilized by surfactants and whole casein or β-casein. Comparison of foams, foam Films, and liquid surfaces studies, *J. Phys. Chem*, 112 (13), pp. 3989–3996.
194. Dickinson E., Ritzoulis C. (2000), Creaming and rheology of oil-in-water emulsions containing sodium dodecyl sulfate and sodium caseinate, *J. Colloid and Interface Sci*, 224, pp. 148–154.
195. Dickinson E., S. T. Hong (1997), Influence of an anionic surfactant on the rheology of heat-set β-lactoglobulin-stabilized emulsion gels, *Colloid and Surfaces A.*, 127, pp. 1–10.
196. Sabadosh G. O., Goralchuk A. B. (2009), Doslidzhennia mizhfaznikh vlastivostei bilkiv moloka u tekhnologhiji otrimannia molochnikh desertiv, *Proghresyvni tekhnika ta tekhnologhiji kharchovykh vyrobnyctv restorannogho ghospodarstva i torghivli*, 2(10), pp. 191–197.
197. Courthaudon J-L., Dickinson E., Christie W.W. (1991), Competitive adsorption of lecithin and p-casein in oil in water emulsions, *Journal of Agriculture and Food Chemistry*, 39, pp. 1365–1368.
198. Murray B.S., Cros L. (1998), Adsorption of β-lactoglobulin and β-casein to metal surfaces and their removal by a non-ionic surfactant, as monitored via a quartz crystal microbalance, *Colloids and Surfaces B: Biointerfaces*, 10(4), pp. 227–241.
199. Roth S. Dickinson E. (2000), Interfacial shear rheology of aged and heat-treated β-lactoglobulin films: displacement by nonionic surfactant, *J. Agric. Food Chem.*, 48, pp. 1491-1497.
200. Semenova M. G., Antipova A. S., Belyakova L. E., Dickinson E., Brown R., Pelan E.G., Norton I. T. (1999), Effect of pectinate on properties of oil-in-water emulsions stabilized by α_{s1}-casein and β-casein. *In Food emulsions and foams: interfaces, interactions and stability*, Cambridge: The Royal Society of Chemistry, pp. 163–175.
201. Patino J., Nino R., Gomez J. (1997), Interfacial and foaming characteristics of protein-lipid systems, *Food Hydrocolloids*, 11, pp. 49–58.
202. Rouimi S., Schorsch C., Valentini C., Vaslin S. (2005), Foam stability and interfacial properties of milk protein-surfactant systems, *Food Hydrocolloids*, 19, pp. 467–478.
203. Clark D.C., Wilde P.J., Bergink-Martens D.J.M., Kokelaar A.J.J., Prins A. (1993), Surface dilatational behavior of aqueous solutions of β-lactoglobulin and Tween 20, *In Food Colloids and Polymers: Stability and Mechanical Properties*, pp. 354–364.
204. Maria E. F, Silva Da, Meirelies N. C. (2004), Interaction of non-ionic surfactants with hepatic CYP in *Prochilodus scrofa, Toxicology in Vitro*, 18, pp. 859–867.
205. Zadymova N.M., Iampolskaia T.P., Filatova L.Iu. (2006), Vzaimodeistvie bychego syvorotochnogo albumina s neionogennym PAV Tvin-80 v vodnykh rastvorakh: kompleksoobrazovanie i assotsiatsiia, *Kolloidnyi Zhurnal*, 68(2), pp. 187–197.

Influence of maturity stages and variety on viscoelastic properties and mechanical toughness of the strawberries

Sergiu Pădureţ

Faculty of Food Engineering,"Stefan cel Mare" University of Suceava, Suceava, Romania

Keywords:

Burger model
Creep
Retardation
Strawberries
Strain

Article history:

Received 16.03.2019
Received in revised form 18.06.2019
Accepted 28.11.2019

Corresponding author:

SergiuPădureţ
E-mail:
sergiu.paduret@fia.usv.ro

DOI: 10.24263/2304-974X-2019-8-4-5

Abstract

Introduction. This study aims to determine the influence of maturity stages and variety on the strawberries viscoelastic properties and to evaluate their mechanical toughness.

Materials and methods. The fresh strawberry samples (*Vibrant, Elsanta and Magic* variety) were subjected to a creep test and the Burger model with four Kelvin Voigt elements was used to determine the viscoelastic parameters. The strawberry samples were divided on three maturity stages: almost ripe (S1), ripe (S2) and overripe (S3).

Results and discussion. The strawberries samples were analyzed in terms of moisture content, soluble substances concentration, pH and total acidity. The moisture content ranged between 87.38 and 89.67%, the overripe maturity stage (S3) showing higher values of moisture compared to nearly ripe ones (S1), $p<0.05$. The highest concentration of soluble substances was recorded by *Elsanta* variety overripe maturity stage and followed by *Magic* (11.91) and *Vibrant* (11.57) varieties.

The instantaneous elastic strain of strawberries ranged between 1.057–3.135 mm and the retardation time, which is correlated with storage period, varies from 10.92 to 140.83 s. The Pearson correlation matrix between physicochemical (moisture content, Brix concentration, pH and total acidity) and viscoelastic parameters (retarded and instantaneous elastic strain, retardation time, viscous strain, creep strain and area under the creep curves) highlighted a significant positive correlation between retarded elastic strain (ε2) and the creep strain ($p<0.01$).

Conclusions. The *Vibrant* strawberry variety had the highest resistance to mechanical impact and also a high mechanical resistance to compression due to the fact that showed the lowest values of instantaneous and retarded elastic strain

Introduction

Strawberries (*Fragaria* x *ananassa* Duch.) are fragile, nonclimacteric fruits, consumed by worldwide people due to the nutrients presence (dietary fibers, vitamin C, sugars, organic acids and minerals), bioactive compounds (phenols, anthocyanins) and for their organoleptic characteristics including texture properties [1, 2].

According to *Kim, 2013,* [3] strawberries have an initial growing and enlarging stage followed by a maturation stage. The ripening process of strawberries stops when the fruits are harvested, this biochemical process being a very complex one influenced by the hormones, pigments synthesis, the sugars metabolism and their action; thus the ripening process changes the fruits color, aroma, flavor and texture [4, 5].

Over the years a large number of strawberry varieties have been created by the breeding programs over the world, in Romania the most cultivated varieties were*: Premial, Elsanta, Magic, Senga Sengana, Elegance, Real, Elsignore, Darselect*; on an area of about 2,500 ha and with a production of approximately 9 t/ha [6].

A major aspect of strawberry fruits it is represented by their firmness, which is the result of both the fruit pulp firmness and fruit skin strength; the information about strawberries mechanical properties being of great importance. The firmness measurement of strawberries is valuable in quality assurance, ripening evaluation, toughness damage evaluation during handling or differences between varieties [7].

The fruits mechanical properties (firmness or toughness) are measured most commonly by various types of penetrometers (Magness Taylor test), which are less acceptable for softer fruits such as strawberries [8].

A relatively simple test for viscoelastic properties evaluation of food products and to obtain a rheological model is the creep test, which implies a constant stress application on a sample and the deformation or strain is measured as a function of time [9, 10].

The viscoelastic properties measurements by rheological tests were applied for: apples [11], frankfurters [12], potato [13], bread dough [14]and gels [15]. To date no other study related to the viscoelastic properties of strawberries has been reported.

Therefore, the objective of this study is to evaluate the viscoelastic properties and quality characteristics of three strawberry varieties based on compression creep test and Burger mechanical model.

Materials and methods

Materials. The fresh strawberry samples were purchased from a local producer (Suceava, Romania) and they are of the *Vibrant, Elsanta and Magic* variety. Each strawberry variety was divided on three maturity stages: almost ripe (S1), ripe (S2) and overripe (S3), having about the same weight (18±0.35 g) and volume (20±0.55 cm^3).

Physicochemical parameters. The soluble substances concentration (°Brix) was measured with a Leica Mark II Plus refractometer, the moisture content was performed by oven method [16], the pH was measured using a Hach pH-meter (HQ11d), [17] and total acidity were determined too and express as cm^3NaOH/100g sample [18].

Texture properties measurement. For strawberries texture properties (toughness) evaluation a creep test was performed using an electronic device (Mitutoyo, USA), [19], the stress force was held constant at 200 g and the stress time was 1200 s. The compression probe

was flat with a diameter of 70 mm, larger than the cross-sectional area of the sample, thus eliminating the shear stress effect [20].

To determine the viscoelastic properties of strawberries samples, the strain versus time data (creep curves) were interpreted using Burger model with 4 KelvinVoigt elements (eq.1).

$$\varepsilon(t) = \varepsilon_1 + \varepsilon_2 + \varepsilon_3 = \frac{\sigma_0}{G_0} + \frac{\sigma_0}{G_1} \cdot \left(1 - \exp\frac{-t}{\lambda_{ret}}\right) + \frac{\sigma_0 \cdot t}{\mu_0} \quad (1)$$

where ε(t) represents the strain at retardation time (t), ε_1 – the instantaneous elasticstrain, ε_2 –the retardedelastic strain, ε_3 – viscous strain, G_0 – the instantaneous elastic modulus (Pa); G_1 – the retarded elastic modulus (Pa); λ_{ret} – the retardation time for the Kelvin part of the model (s); μ_0 – the Newtonian viscosity of the free dashpot (Pa s) and σ_0 represents the constant stress (Pa), [21, 22].

The Burger model shown in Fig.1 is the series combination of a Kelvin-Voigt and Maxwell elements, dividing the creep curve into three parts: instantaneous deformation (Maxwell spring), viscoelastic deformation (Kelvin element) and viscous deformation (Maxwell dashpot) [11].

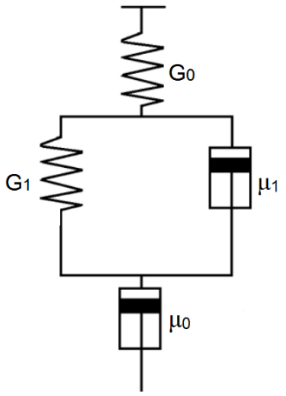

Figure 1. Burger model

As a measure of the Burger mechanical model's fit to the experimental data the coefficient of determination (R^2) and the absolute average deviation (AAD) were calculated by the following equations [23]:

$$R^2 = 1 - \frac{\sum_{i=1}^{n}\left(Y_{CAL} - Y_{EXP}\right)^2}{\sum_{i=1}^{n}\left(Y_{EXP} - Y_{MEDIU}\right)^2} \quad (2)$$

$$AAD = \frac{1}{T} \cdot \sum_{i=1}^{n}\left|\frac{Y_{EXP} - Y_{CAL}}{Y_{EXP}}\right| \cdot 100 \quad (3)$$

where Y_{EXP} and Y_{CAL} are the experimental and calculated values data and *T* is the number of the experimental run [24].

Statistical analysis. The results were subjected to one factor analysis of variance (ANOVA) by STATGRAPHICS CENTURION XVI, the statistical significance being set at $\alpha = 0.05$. The Burger model predicted data was obtained by nonlinear regression analysis. Pearson correlation was performed by SPSS (SPSS Inc., Chicago, IL, USA) and Principal Component Analysis (PCA) by UNSCRAMBLER 9.7 (Trial Version).

Results and discussion

Physicochemical properties

In Table 1 are presented the ANOVA results of physicochemical parameters of strawberry samples. The *Vibrant, Elsanta and Magic* strawberries varieties were analyzed in terms of moisture content, soluble substances concentration, pH and total acidity. The strawberries moisture content ranged between 87.38 and 89.67%, the overripe maturity stage showing higher values of moisture compared to nearly ripe ones; the results of one factor analysis of variance ANOVA showed that the differences is statically significant at $p<0.05$. The concentration of soluble substances express as º Brix varies from 8.11 (almost ripe) to 13.89 (overripe), the highest concentration being recorded by *Elsanta* variety overripe maturity stage and followed by *Magic* (11.91) and *Vibrant* (11.57) varieties.The moisture and soluble substances contents being similar to those reported in other studies [25, 26].

Table 1

ANOVA physicochemical parameters of strawberry samples

Strawberry samples – mean (SD)		Moisture [%]	° Brix concentration	pH	Total Acidity [cm³NaOH/ 100g]
Vibrant	Almost ripe	87.51^{b} (0.34)	8.11^{a} (0.34)	3.88^{a} (0.09)	10.65^{a} (0.32)
	Ripe	88.96^{ab} (0.41)	9.21^{a} (0.12)	3.90^{a} (0.08)	10.59^{ab} (0.25)
	Over ripe	89.67^{a} (0.25)	11.57^{b} (0.30)	4.08^{a} (0.05)	9.37^{b} (0.54)
Elsanta	Almost ripe	88.63^{b} (0.31)	8.95^{a} (0.12)	3.80^{a} (0.08)	11.01^{a} (0.15)
	Ripe	89.01^{ab} (0.21)	9.93^{a} (0.10)	3.85^{a} (0.11)	10.78^{ab} (0.19)
	Overripe	89.58^{a} (0.22)	13.89^{b} (0.20)	3.99^{a} (0.05)	9.29^{b} (0.21)
Magic	Almost ripe	87.38^{b} (0.11)	8.89^{a} (0.11)	3.92^{a} (0.05)	10.51^{a} (0.88)
	Ripe	87.90^{ab} (0.20)	9.23^{a} (0.10)	4.10^{a} (0.06)	9.01^{ab} (0.10)
	Overripe	89.28^{a} (0.09)	11.91^{b} (0.21)	4.01^{a} (0.02)	9.32^{b} (0.56)
F-Ratio		6.93	17.50	2.46	4.37
P – value		0.027	0.003	0.166	0.067

Note: NS – not significant ($p > 0.05$), * $p < 0.05$, ** $p < 0.01$, *** $p < 0.001$; Different lowercase letters in a column show significant differences between the groups ($p < 0.05$).

One way ANOVA analysis highlighted the soluble substancesdifference between thematurity stages of strawberries samples at a level of $p < 0.01$. The strawberries pH values were close to each other (3.80–4.10); the statistical differences being insignificant ($p > 0.05$). Total acidity content measurement is important in strawberries quality evaluation since less acidic strawberries are preferred to be consumed fresh, while more acidic strawberries are processed by food industry [27].

The total acidity of *Vibrant, Elsanta and Magic* varieties was between 9.29–11.01 cm^3NaOH/100g, decreasing with the strawberries ripening process; which is in agreement with the study of *da Silva Pinto 2008*, [28], who sustain also that the fruit acid content is consumed in the respiratory process.

Texture properties measurement

Mechanical properties evaluation is very important especially when it comes to fragile perishable food products susceptible to mechanical damage and it is also of great importance in measuring their viscoelastic properties. Strawberries are highly perishable fruits with a short shelf life due to the fact that they are predisposed to microbiological contamination and mechanical damage during harvesting, transport and storage; the fruit's resistance evaluation to mechanical shocks representing a very important aspect for both producers and consumers.

Figure 2 (a, b and c) presents the *Vibrant*, *Elsanta* and *Magic* strawberries toughness evaluation to mechanical stress by creep test and as we can see the strawberries deformation resistance depends on the fruit variety and also of the maturity stages. The most toughness strawberries to compression stress belong to the *Vibrant* variety followed by *Elsanta* and *Magic*. The creep curves of analyzed strawberries can be also characterized by two very important determinants – the strain and the area under the curve (W), this values being presented in Table 2.

The strawberries strain range from 1.96 mm to 6.62 mm, the greatest deformation being recorded by the *Magic* variety (5.79-6.62) which shows also the greatest area under the curve (75.65-81.45). In contrast with *Magic* variety, which shows a low resistance to deformation, the *Vibrant* variety strawberries have a greater resistance to deformation (1.96-2.67), being more resistant to mechanical shocks during the harvest and postharvest handling like sorting, packing, cleaning or to transport. As regarding the maturity stages, the overripe strawberries are softer than the ripe ones, the loss of deformation resistance being due to the ripening process, when the fruits turn redder, accumulate more sugars, the moisture content increases and lose some of their firmness [3].

Strawberries viscoelastic parameters prediction using Burger model

Another important aspect stated by *Vergara 2018,* [27] is that smaller strawberries (third category) have a higher resistance to deformation due to a more compact cellular arrangement. Also in Table 2 are presented the mathematical equations of Burger model, which were applied to describe the viscoelastic properties of analyzed strawberry samples; Figure 2 shows the Burger model's fit (predicted data) to the experimental data and it can be observed that the four elements mechanical model can be successfully used to predict the viscoelastic properties of strawberries samples.

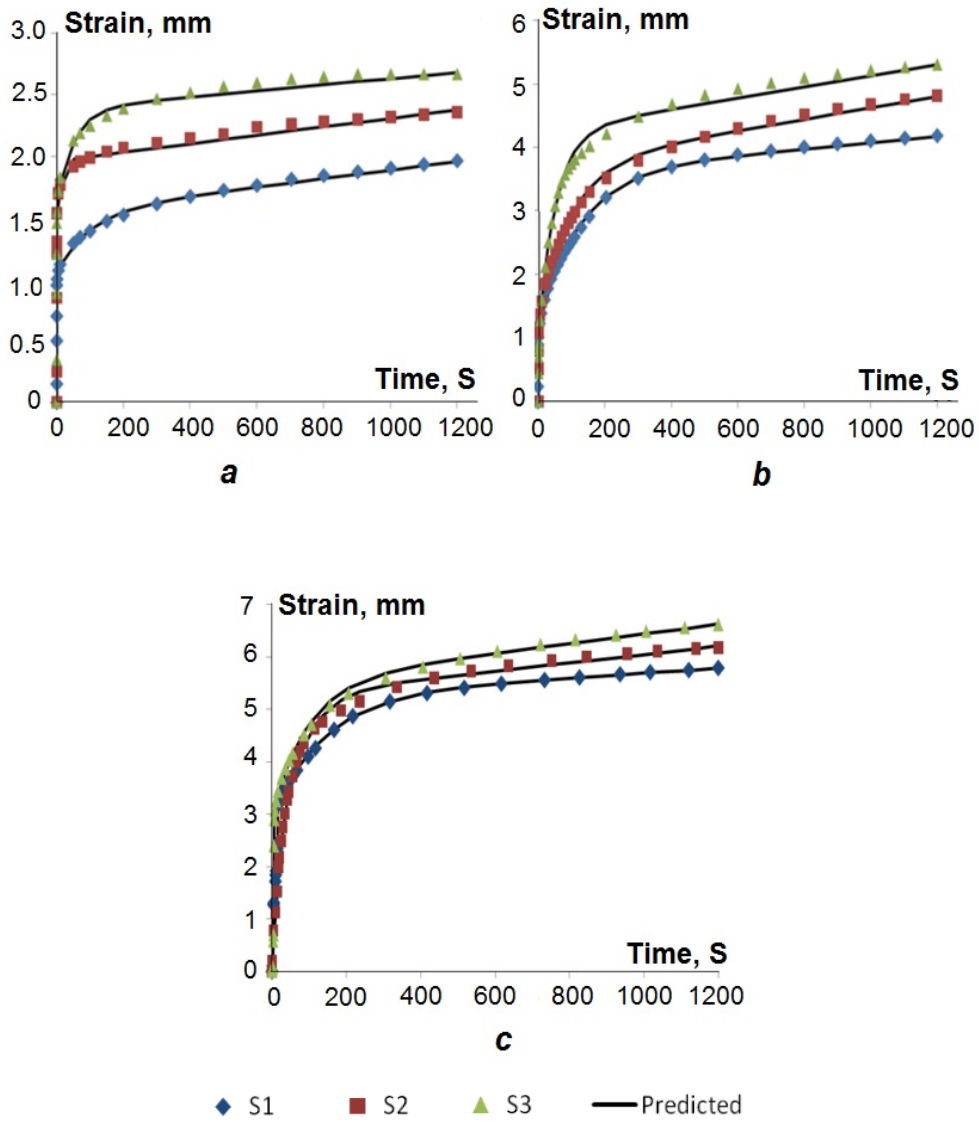

Figure 2. Creep curves of strawberry samples – experimental vs. predicted data:
***a – Vibrant*, *b – Elsanta*, *c – Magic*.**
S1 – almost ripe, S2 – ripe, S3 – overripe.

Table 2

Equations of Burger mechanical model and the strawberries creep curves characteristics

Sample		Burger model with four Kelvin Voigt elements	R^2	AAD	Strain [mm]	W [mm·min]
Vibrant	S1	$\gamma = 1.057 + 0.483 \cdot \left(1 - \exp\frac{-t}{98.649}\right) + \frac{t}{2897.678}$	0.952	1.75	1.96	26.58
	S2	$\gamma = 1.374 + 0.588 \cdot \left(1 - \exp\frac{-t}{10.920}\right) + \frac{t}{2906.185}$	0.926	2.35	2.36	35.78
	S3	$\gamma = 1.647 + 0.738 \cdot \left(1 - \exp\frac{-t}{52.898}\right) + \frac{t}{4057.171}$	0.943	2.47	2.67	40.36
Elsanta	S1	$\gamma = 1.108 + 2.473 \cdot \left(1 - \exp\frac{-t}{120.032}\right) + \frac{t}{2025.271}$	0.982	2.95	4.18	50.11
	S2	$\gamma = 1.248 + 2.476 \cdot \left(1 - \exp\frac{-t}{97.301}\right) + \frac{t}{1112.259}$	0.983	2.61	4.82	56.96
	S3	$\gamma = 1.321 + 3.113 \cdot \left(1 - \exp\frac{-t}{56.056}\right) + \frac{t}{1336.073}$	0.971	4.26	5.30	66.60
Magic	S1	$\gamma = 3.029 + 2.052 \cdot \left(1 - \exp\frac{-t}{140.830}\right) + \frac{t}{2290.884}$	0.965	1.34	5.79	75.65
	S2	$\gamma = 3.114 + 2.168 \cdot \left(1 - \exp\frac{-t}{66.543}\right) + \frac{t}{1282..330}$	0.944	1.31	6.18	77.93
	S3	$\gamma = 3.135 + 2.377 \cdot \left(1 - \exp\frac{-t}{95.825}\right) + \frac{t}{1079.789}$	0.972	0.30	6.62	81.45

S1-almost ripe, S2- ripe, S3- overripe, W- area under the creep curves.

The instantaneous elastic strain varied between 1.057 mm and 3.135 mm, the highest values of this parameter being recorded by *Magic* variety; for *Vibrant* and *Elsanta* varieties it can be observed that this parameter presents smaller and close values which imply that these two varieties have a high resistance to mechanical impact. In addition the *Elsanta* strawberries had the highest values of retarded elastic strain (2.473-3.113 mm) predicted by the Burger model, followed by *Magic* variety (2.052-2.377 mm), while the *Vibrant* strawberries had the lowest values of retarded elastic strain (0.483-0.738 mm), these being also the most resistant strawberries to mechanical damage which involves a longer compression and not just mechanical impact. Both the instantaneous and the retarded elastic strain increase with the maturation stages, the highest values being recorded by overripe strawberries (S3 stage) and the lowest by almost ripe ones (S1 stage) which means that fruits resistance decreases during ripening process. According to *Chakespari 2010,* [11] the retardation time (λ_{ret}) represents an important factor in fruits storage period and as Burger model predicted the higher retardation time was recorded by the almost ripe strawberries (98.949-140.83 s), the almost ripe *Magic* variety being characterized by an higher storage time. The absolute average deviation -AAD and the coefficient of determination -R^2 represents a measure of how much the Burger model predicted data deviates from the experimental data.

The ADD values for the Burger model with four Kelvin Voigt elements range between 0.30 and 4.26, whereas the R^2 values range between 0.926 and 0.983. Considering the above mentioned values it seems that Burger model with four Kelvin Voigt elements can be used successfully for the interpretation of strawberries creep curves and to determine the viscoelastic parameters.

Table 3 presents the Pearson correlation of viscoelastic and physicochemical parameters of strawberries. It seems that some viscoelastic parameters are positively correlated with creep strain (S) and area under the curves (W). A significant positive correlation was recorded between the instantaneous elastic strain (ε_1) and area under the curves ($p<0.01$, $r=0.805^{**}$); another significant positive correlation being between retarded elastic strain (ε_2) and the creep strain ($p<0.01$, $r=0.827^{**}$). Regarding the chemical composition, moisture content was positively correlated with the soluble substances concentration ($p<0.05$), the values of this two parameters increasing during the ripening process. The retarded elastic strain and viscous strain are positively influenced one by the other ($p<0.05$).

Table 3

Pearson correlation of viscoelastic and physicochemical parameters of strawberries

	S	**W**	**ε_1**	**ε_2**	**ε_3**	**λ_{ret}**	**M**	**B**	**pH**	**TA**
S	1	0.989^{**}	0.740^{*}	0.827^{**}	0.792^{*}	0.391	-0.027	0.326	0.302	-0.439
W		1	0.805^{**}	0.765^{*}	0.721^{*}	0.332	-0.027	0.345	0.394	-0.504
ε_1			1	0.244	0.356	0.244	-0.281	0.031	0.575	-0.529
ε_2				1	0.779^{*}	0.374	0.188	0.457	-0.023	-0.208
ε_3					1	0.160	0.210	0.385	0.129	-0.333
λ_{ret}						1	-0.529	-0.322	-0.397	0.370
M							1	0.794^{*}	0.230	-0.355
B								1	0.473	-0.657
pH								.	1	-0.949^{**}
TA										1

S – strain, W – area under the creep curves, ε_1 – instantaneous elastic strain, ε_2 – retardedelastic strain, ε_3 – viscous strain, λ_{ret} – retardation time; M – moisture, B – Brix concentration, TA – total acidity.

Principal component analysis (PCA)

Principal Component Analysis (PCA) carried out on strawberry samples explains all the data variation; first component (PC1) explains 81% while second one (PC2) explains 19% of the variance in the obtain data. The results of correlations loadings and scores of PCA are presented in Figure 3 and Figure 4 based on this statistical analysis the strawberry samples are distributed in different quadrants. From PCA score, Figure 3, we can observe that PC1 separates the almost ripe strawberry samples (S1) from the other samples (S2 and S3), while the PC2 separates the samples based on strawberry variety.

In Figure 4 – PCA loadings, the parameters distributed in the center of the ellipse (the instantaneous elastic strain and the viscous strain) have an insignificant influence in samples differentiation, while the parameters from outside ellipse (the creep curve characteristic, retardation time, retarded elastic strain, moisture, pH, Brix concentration and total acidity) present a strong influence in samples differentiation.

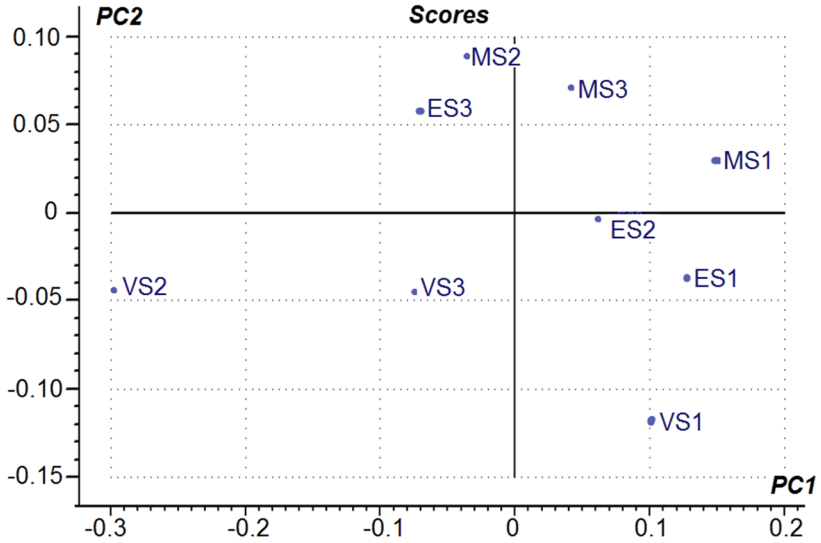

Figure 3. PCA scores of strawberry samples:
M – *Magic*, E – *Elsanta*, V – *Vibrant*, S1 – almost ripe, S2 – ripe, S3 – overripe.

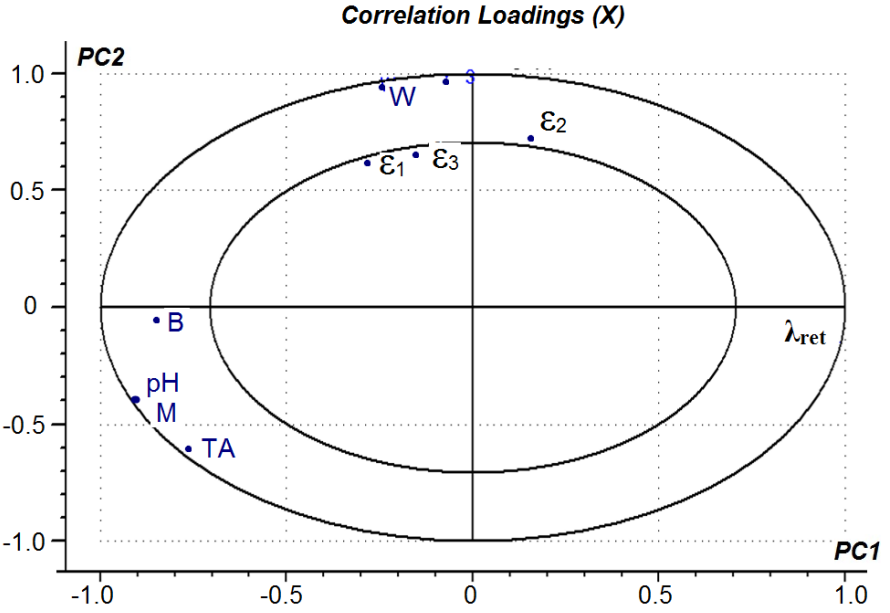

Figure 4. PCA loadings of strawberry samples parameters:
S – strain, W – area under the creep curves, ε_1– instantaneous elasticstrain, ε_2 – retardedelastic strain, ε_3 – viscous strain, λ_{ret}–the retardation time; M – moisture, B – Brix concentration, TA –total acidity.

The Burger model retardation time is strongly correlated with first component (PC1) and consequently with almost ripe strawberry samples, which showed the lowest values of Brix concentration and the highest total acidity and retardation time. The creep strain (S) influences the *Magic* strawberry projection, this variety being characterized by high values of Burger instantaneous elastic strain.

Conclusions

The compression creep test conducted in this study highlighted that all strawberries samples presents viscoelastic properties influenced by the variety and by the maturity stages.The strawberries from *Vibrant* variety have the highest resistance to mechanical impact and also a high mechanical resistance to compression due to the fact that showed the lowest values of instantaneous and retarded elastic strain. Keeping into account the R^2 and ADD values, the mechanical Burger model with four Kelvin Voigt elements can be successful used to determine the viscoelastic properties of strawberries samples such as instantaneous elastic strain, retarded elastic strain or retardation time. The PCA statistical analysis revealed that creep curves characteristic and Burger viscoelastic properties have a great impact in strawberry samples projection based on variety and maturity stages.

Acknowledgement. This work was supported by "DECIDE – Dezvoltare prin educație antreprenorială și cercetare inovativă doctorală și postdoctorală", Cod proiect POCU/380/6/13/125031, proiect cofinanțat din Fondul Social European prin Programul Operațional Capital Uman 2014 – 2020"

References

1. López-Valencia D., Sánchez-Gómez M., Acuña-Caita J. F., Fischer G. (2018), Physicochemical properties of seven outstanding strawberry (Fragaria x ananassaDuch.) varieties cultivated in Cundinamarca (Colombia) during maturation, *CorpoicaCiencia y TecnologíaAgropecuaria*, 19(1), pp. 147–162.
2. Zeliou K., Papasotiropoulos V., Manoussopoulos Y., Lamari F. N. (2018), Physical and chemical quality characteristics and antioxidant properties of strawberry cultivars (Fragaria× ananassaDuch.) in Greece: assessment of their sensory impact, *Journal of the Science of Food and Agriculture*, *98*(11), pp. 4065–4073.
3. Kim S. K., Bae R.N., Na H., Dal Ko K., Chun C. (2013), Changes in physicochemical characteristics during fruit development in June-bearing strawberry cultivars, Horticulture, Environment, and Biotechnology, 54(1), pp. 44–51.
4. Azodanlou R., Darbellay C., Luisier J.L., Villettaz J. C., Amadò R. (2004), Changes in flavour and texture during the ripening of strawberries, *European Food Research and Technology*, 218(2), pp. 167–172.
5. Jia H., Wang Y., Sun M., Li B., Han Y., Zhao Y., Jia W. (2013), Sucrose functions as a signal involved in the regulation of strawberry fruit development and ripening, *New Phytologist*, *198*(2), pp. 453–465.

6. Temocico G., Sturzeanu M., Ion V. (2017), Choice of strawberry varieties by the Romanian growers, *Scientific Papers: Management, Economic Engineering in Agriculture & Rural Development*, pp. 17(1).
7. Døving A., Måge F., Vestrheim S. (2005), Methods for testing strawberry fruit firmness: a review, *Small Fruits Review*, *4*(2), pp. 11–34.
8. Duprat F., Grotte M. G., Pietri E., Studman C. J. (1995), A multi-purpose firmness tester for fruits and vegetables, *Computers and electronics in agriculture*, *12*(3), 211–223.
9. Sirisomboon P., & Posom J. (2018), A new creep model for studying the non-linear viscoelastic behavior of cooked white, brown and germinated brown Thai jasmine rice by large deformation testing, *Heliyon*, *4*(8), e00745.
10. Lazaridou A., Vouris D.G., Zoumpoulakis P., Biliaderis C.G. (2018), Physicochemical properties of jet milled wheat flours and doughs, *Food hydrocolloids*, *80*, pp. 111–121.
11. Chakespari A. G., Rajabipour, A., Mobli H. (2010), Anisotropic relaxation and creep properties of apple (cv. ShafiAbadi and GolabKohanz), *Advanced Journal of Food Science and Technology*, 2, pp. 200–205.
12. Dzadz Ł., Markowski M., Sadowski P., Jakóbczak A., Janulin M. (2015), Creep and recovery characteristics of chicken meat Frankfurters, *Journal of Agricultural Science and Technology*, *17*(4), pp. 827–835.
13. Álvarez M.D., Canet W., Cuesta F., Lamua M. (1998), Viscoelastic characterization of solid foods from creep compliance data: application to potato tissues, *ZeitschriftfürLebensmitteluntersuchung und-Forschung A*, *207*(5), pp. 356–362.
14. Mohammed M. A. P., Tarleton E., Charalambides M. N., Williams J. G. (2013), Mechanical characterization and micromechanical modeling of bread dough, *Journal of Rheology*, *57*(1), pp. 249–272.
15. Nussinovitch A.M. M. A., Ak M. M., Normand M. D., Peleg M. (1990), Characterization of gellan gels by uniaxial compression, stress relaxation and creep, *Journal of Texture Studies*, *21*(1), pp. 37–50.
16. Pădureț S., Oroian M., Gutt G., Amariei S. (2017), Evaluation of strawberry texture in close relation with their anisotropy, *International Journal of Food Properties*, 20(2), pp. 247–259.
17. ISO 1842:1991, Fruit and vegetable products – Determination of pH
18. ISO 750:1998, Fruit and vegetable products determination of titratable acidity
19. Paduret S., & Gutt G., (2016), The Use of Texture Destructive Methods to Assess the State of Pork Freshness, *Food and Environment Safety Journal*, pp. 14(2).
20. Bourne C., M., (2002), Food Texture and Viscosity: Concept and Measurement, An Elsevier Science Imprint, London.
21. Xu Y. L., Xiong S. B., Li Y. B., Zhao S. M. (2008), Study on creep properties of indica rice gel, *Journal of Food Engineering*, *86*(1), pp. 10–16.
22. Sahin S., & Sumnu S. G. (2006), *Physical properties of foods*, Springer Science & Business Media
23. Moghaddam M. G., Ahmad F. B. H., Basri M., Rahman M. B. A., (2010), Artificial neural network modeling studies to predict the yield of enzymatic synthesis of betulinic acid ester. Electronic Journal of Biotechnology, 13(3), pp. 3–4
24. Oroian M., Paduret S., Amariei S., Gutt G. (2016), Chemical composition and temperature influence on honey texture properties, *Journal of food science and technology*, 53(1), pp. 431–440.
25. Nunes M. C. N., Brecht J. K., Morais A. M., Sargent S. A. (2006), Physicochemical changes during strawberry development in the field compared with those that occur in

harvested fruit during storage, *Journal of the Science of Food and Agriculture*, 86(2), pp. 180–190.
26. Khan M. N., Sarwar A., Bhutto S., Wahab M. F. (2010), Physicochemical characterization of the strawberry samples on regional basis using multivariate analysis, *International Journal of Food Properties*, 13(4), pp. 789–799.
27. Vergara M., Vargas J., Acuña J. (2018), Physicochemical characteristics of strawberry (Fragaria χ ananassaDuch.) fruits from four production zones in Cundinamarca, Colombia. *Agronomía Colombiana*, 36(3), pp. 227–236
28. da Silva Pinto M., Lajolo F. M., Genovese M. I. (2008), Bioactive compounds and quantification of total ellagic acid in strawberries (Fragaria x ananassaDuch.), *Food Chemistry*, 107(4), pp. 1629–1635.

Polyphenolic compounds transition into protein-plant concentrates during the deposition of milk proteins by *Plantago major L.*

Olena Grek[1], Larisa Chubenko[1], Amit Kumar[2], Volodymyr Khareba[3], Alla Tymchuk[1], Olena Onopriichuk[1]

1 – National University of Food Technologies, Kyiv, Ukraine
2 – Integral University, Lucknow, India
3 – Department of Agricultural Economics and Food of the National Academy of Agrarian Sciences of Ukraine

Keywords:

Milk
Plantago major L.
Coagulation
Protein
Polyphenolic

Article history:

Received 24.05.2019
Received in revised form 29.09.2019
Accepted 28.11.2019

Corresponding author:

Olena Onopriichuk
E-mail: olena.onopriychuk@gmail.com

DOI:
10.24263/2304-974X-2019-8-4-6

Abstract

Introduction. Implementation of scientifically sound use principles of dairy and plant raw materials with functional-technological properties is relevant.

Materials and methods. Normalized milk was used as the raw material to obtain protein concentrates. As a coagulant in the deposition of proteins used juice of direct extraction from the terrestrial part of *Plantago major L*. Identification and quantification of polyphenols and flavanoids in the samples of the plantain juice and the obtained whey was performed by high-performance liquid chromatography using system Prominence LC-20 Shimadzu (Japan). Comparisons were made with external standard samples.

Results and discussion. The study of the qualitative composition and quantitative content of polyphenols and flavonoids in protein-plant concentrates obtained by deposition of milk proteins with the juice of direct extraction of the terrestrial part of Plantago major L were presented. The process took place at elevated temperatures. According to the analysis of absorption spectra of the experimental samples of juice from the plantain found that the maximum is at wavelengths of 225-350 nm. This result is correlated with the fact that of the 22 isolated flavonoids, 9 substances are 6-oxyflavones, characterized by a maximum within the range of 255-285 nm.

The difference between the content of polyphenols in *Plantago major L.* juice and whey indicates the degree of transition of polyphenolic compounds into protein-plant concentrates. The total content of flavonoids in all tested samples was equal to the content of substances that were similar to the standards of flavonoids (phenolic acids, catechins, flavonols, flavonones and flavones) with the exception of catechin-like substances. Flavonols are represented by the glycosides of myricetin. Naringin and hesperidin are part of flavonones. The flavones in the quantitative sense are of the lowest weight and are represented by luteolin and its glycosides and glycosides of apigenin. Phenolic acids content ranged from 12.36 mg/l for plantain juice and 0.07 mg/l for colored whey.

Conclusions. The degree of polyphenolic compounds transition in protein-plant concentrate was determined at the level – 77% of the total amount, of which 74% are flavonoids.

Introduction

The actual direction is the implementation of the scientifically sound use principles of dairy and plant raw materials with functional-technological properties. Such modifications, under the conditions of the traditional technological process, are able to give the products new qualities other than simple mixing of raw materials [1].

It is advisable to determine the technological action of plant raw materials with biologically active substances in dairy products. First of all, it concerns the process of milk proteins deposition using wild plant, namely *Plantago major L.* This plant is widely distributed worldwide, used as a medicinal raw material, and has a positive effect on health [2, 3]. In addition, the plantain is a carrier of mammalian enzymes – proteases and organic acids. Thus, the acid complex of plantain leaves is represented by: fumaric, oxalic (31–103 mg%) [4], tartaric (1.60–1.87%), citric (1.22–1.53%), malic (0,20–0.51%), malonic (0.11–0.35%) and succinic (0.25–0.55%) acids. The total content of organic acids is 10–12%, of which up to 60% are related [5].

Due to the availability of sources and the relative ease of obtaining, such plant coagulants with different mechanism of action are the subject of growing scientific and practical interest of specialists in the production of milk-protein products enriched with polyphenolic compounds. It is necessary to provide technological modes and methods of treatment that will allow to preserve biologically active substances as much as possible.

The harmful effects on the body of "free radicals" can be reduced by the systematic use of some herbal preparations, with high antioxidant activity, or by adjusting diets towards the consumption of the corresponding products.

It is known from literature sources [6] that the highest antioxidant activity has a vegetable raw material with a high content of phenolic and polyphenolic compounds, as well as vitamins A, E, K and C. In addition, such compounds – such as phenolic terpenoids, carnosol – have similar activity, chamazulene, coumarin, quercitin and others.

Flavonoids are physiologically active substances that are involved in many biochemical processes in the body. More than 200 natural flavonoid substances have been identified and more than 40 species have been identified [7].

In view of the above, more research is needed on the use in the technologies of milk-protein concentrates of plant raw materials, namely juice from the ground part of the plantain, as a coagulant. Unlike food ingredients synthesized by the industrial process, natural raw materials components can be a valuable source of various biologically active substances for the human body, including polyphenolic compounds necessary to maintain normal homeostasis, meet energy, plastic needs, and others.

The aim of this work was to determine the degree of polyphenolic compounds transition into protein-plant concentrates under precipitation of milk proteins by *Plantago major L. juice.*

Materials and methods

Materials

The raw material for protein concentrates was normalized milk with a solids mass fraction of (12.3±0.62)%, fat – (2.6±0.13)%, protein – (2.8±0.14)%, with active acidity – (6.9±0.35) units of pH, density – 1027 kg/m^3.

As a coagulant, the juice of direct extraction from the ground part of Plantago major was used with the following parameters: quantity of solids – (4.5±0.23)%, active acidity – (5.85±0.18) units of pH.

From the leaves of *Plantago major* by various researchers were isolated 15 compounds from the class of flavonoids [8]. They are all derivatives of the flavon. The first compounds that have been isolated are Baikalin and Scootarein [9]. The presence of apigenin, luteolin, luteolin-7-glycoside and some other flavonoids was also found in the composition of large plantain leaves [8]. The leaves of a large plantain contain most of Routine (40.3%) [10].

A modified method for complex deposition of protein substances of milk with the juice of plantain large has been developed. Plantago major juice was introduced into the heated to 96–98 °C milk, stirred slightly and kept until the formation of a clot. The maximum precipitation of milk protein substances was observed with the introduction of 8±1% coagulant and the duration of the process – 2 min. Then the clot was pressed for 15 min to separate the whey, which was picked to determine the content of polyphenolic compounds [11].

Methods

In the obtained milk-protein concentrate, the polyphenol content was determined by the calculation method. Previously, their contents and composition were investigated in plantain juice and whey obtained by high-performance liquid chromatography (HPLC) using system Prominence LC-20 Shimadzu (Japan). 96% ethanol in a 1:1 ratio was added to the liquid samples, then filtered using a Supelco Iso-Disc Filters PTFE 25-4 syringe filter (25 mm x 0.45 μm) [12, 13]. The initial ratio of eluent components is 1: 9. The methanol content of the eluent during the experiment was varied according to the following scheme:

- first 13 min – increase from 10 to 40%;
- from 13 min to 20 min – from 40 to 53%;
- from 20 min to 26 min – from 53 to 55%;
- from 26 min to 40 min – holding 55%;
- from 40 min to 41 min – reduction to 10%;
- from 41 min to 56 min – holding 10%.

The speed of the eluent is 0.5 ml/min. The column temperature is 40 ºC. The volume of the entered sample – 5 μl.

Identification of the substances in the extract was performed by comparing the retention time and spectral characteristics of the test substances with similar characteristics of the standards according to the method [14] identification of polyphenols. Chromatography was performed at 225, 255, 286 and 350 nm [14, 15, 16]. For accurate identification of the test substances to specific groups of polyphenols, the following regulatory documents were used: chlorogenic and caffeic acids (phenolic acids), catechin (catechins), flavonols myricetin, quercetin and rutin, flavanones naringenin, naringin, hesperinidin, and protestin cyanidine (anthocyanins) (Sigma-Aldrich, Germany). The identification characteristics of these standards were obtained under the above conditions of chromatography. The "peak area – content of the standard " calibration dependences were linear with an accuracy of at least $r^2 = 0.994$.

Substances whose similarity level according to any standard was below 70% were classified as a group of unidentified substances and their content was determined by the standards with the highest similarity level.

Results and discussion

Determination of biologically active substances in *Plantago major* juice and whey

To determine the degree of transition of biologically active substances into protein-plant concentrates, the polyphenolic composition of the coagulant – the juice from the ground part of the plantain and the serum obtained during the deposition of milk proteins, was analyzed. The colloidal state destabilization of sol of casein micelles occurs under the action of proteolytic enzymes and changes in pH value. Milk gel is a structure consisting of a gel frame filled with whey. A characteristic feature of the gel is syneresis – a decrease in water-binding capacity under the influence of temperature, pH value and mechanical action [17]. In the classic embodiment, the concentrates contain only the casein fraction of milk proteins or manufactured with the addition of various chemicals of artificial origin (lactic, ascorbic, acetic and other acids) during precipitation. Traditional methods of concentration have several disadvantages – the lack of complex precipitation of proteins, the use of animal coagulants, high processing temperatures, providing a clot of foreign taste and odor, obtaining a bunch with a dense consistency, and more. For research, coagulation of milk proteins with proteases and organic acids of Plantago major was performed.

The absorption spectra characteristic of these compounds were measured for the qualitative determination of biologically active substances. Flavonoids are completely released from the test samples of the alcohol solution, and the absorption spectra of the solutions have bands corresponding to phenolic compounds (225–350 nm).

The content of the test substances in the alcohol extract (C_{ex} mg/l) and in the juice of the plantain (C mg/l_{juice}), which were identified as flavonoids, are presented in Table 1.

The content of substances in the whey sample obtained by deposition of milk proteins with *Plantago major juice*, which were identified as flavonoids, are presented in Table 2.

Identification was performed by the similarity of maintenance time (T maintenance) of the test substances and the similarity index (Is), indicating the similarity between the substance and the spectral characteristics standard to which the substance is more similar.

A greater number of flavanoids were identified at a wavelength (λ) of 225 nm, which was used to calibrate the dependency "the peak area – content" (S) for a particular standard.

The design of the species – Quercetin – refers to accurately identified substances. Design of the rutin-L (routine) form – a substance belongs to the same group of polyphenols as rutin, ie in this case it is flavonol, and is a glycoside (or an aglycone depending on the name of the standard, for example, rutin is a glycoside, quercetin is an aglycone, daidzin is a glycoside, daidzein is an aglycone).

In the course of the study, substances (not included in Table 1, 2) were identified that were not identified due to the low index of similarity with the standards. Their content is set to the standard with the highest similarity.

Substances belonging to the polyphenols were determined by peaks on the chromatograms (Figure 1, 2) of plantain juice and whey after precipitation of the proteins by the plant coagulant.

The results obtained are presented on the chromatograms on Figure 1, 2.

Table 1

Flavonoid content in plantain juice

Peak	T maintenance	Match index, I_L	Identification	λ, nm	S (y.e.)	$C_{extract}$, mg/l	C, mg/l_{juice}
20	10.052	0.787	catechin-L	225	569483	11.92	23.85
21	10.645	0.673	catechin-L	225	221883	4.65	9.29
22	11.021	0.658	catechin-L	225	12590	0.26	0.53
23	11.494	0.719	catechin-L	225	78780	1.65	3.30
25	12.240	0.891	naringin-L	286	25290	1.21	2.42
26	12.502	0.650	hesperidin-L	286	10619	0.69	1.38
27	12.769	0.844	catechin-L	225	464447	9.73	19.45
30	14.036	0.843	catechin-L	225	24309	0.51	1.02
31	14.258	0.747	catechin-L	225	344752	7.22	14.44
32	14.524	0.685	myricetin-L	255	23669	0.73	1.47
37	16.096	0.934	catechin-L	225	44374	0.93	1.86
38	16.267	0.843	catechin-L	225	248952	5.21	10.43
39	16.865	0.875	catechin-L	225	145150	3.04	6.08
40	17.125	0.938	Naringin	286	31679	2.06	4.12
44	18.461	0.807	Hesperidin	286	95157	4.55	9.10
50	20.256	0.933	rutin-L	255	268823	15.25	30.50
51	20.567	0.672	apigenin-L	350	2348	0.07	0.14
55	21.876	0.823	naringin-L	286	27823	1.33	2.66
56	22.201	0.713	rutin-L	286	2519	0.11	0.22
57	22.534	0.624	apigenin-L	350	3904	0.12	0.23
58	22.899	0.739	Luteolin	350	8030	0.15	0.29
61	25.639	0.854	quercetin-L	255	34893	0.90	1.79

Table 2

Content of flavanoids in whey obtained by the juice deposition of milk proteins *Plantago major*

Peak	T maintenance	Match index, I_L	Identification	λ, nm	S (y.e.)	$C_{extract}$, mg/l	C, mg/l_{sample}
15	9.151	0.863	Catechin	225	162942	3.41	6.82
17	10.000	0.881	catechin-L	225	84781	1.78	3.55
19	11.480	0.759	catechin-L	225	20216	0.42	0.85
21	12.874	0.872	catechin-L	225	28707	0.60	1.20
23	14.310	0.898	catechin-L	225	485960	10.18	20.35
24	14.711	0.613	myricetin-L	255	16290	0.50	1.01
27	16.140	0.954	catechin-L	225	12055	0.25	0.50
28	16.407	0.843	catechin-L	225	9944	0.21	0.42
30	17.049	0.954	Naringin	286	1333	0.06	0.13
33	18.436	0.836	Hesperidin	286	6972	0.45	0.91
38	19.787	0.642	rutin-L	255	4058	0.23	0.46
39	20.253	0.820	luteolin-L	350	25057	0.45	0.91

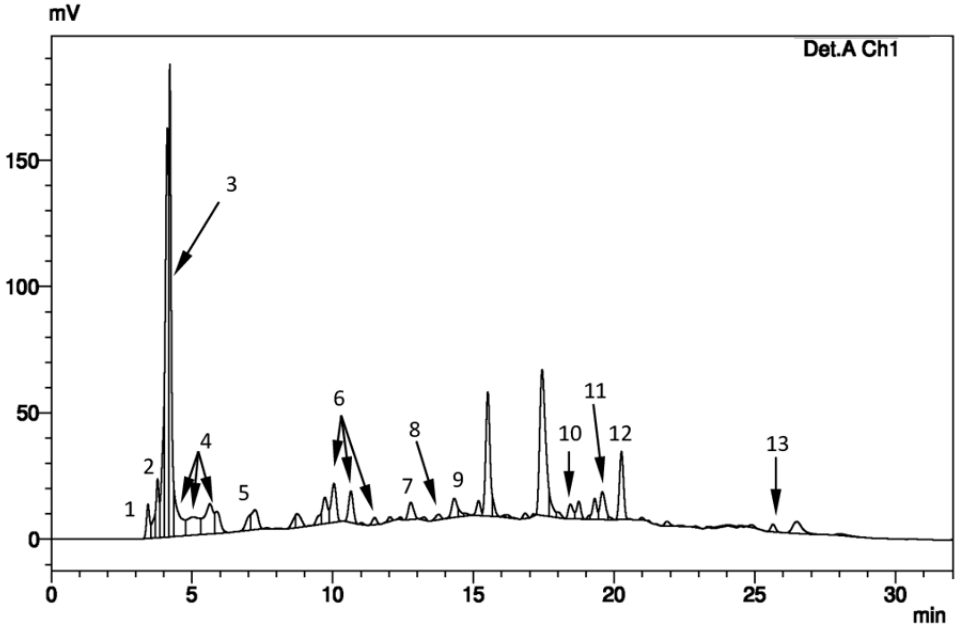

Figure 1. Chromatogram of plantain juice: catechin-like (1-5), catechins (6-7, 9), phenolic acids (8, 11), hesperidin (10), flavonol (glycoside) (12), flavonol (aglycone) (13).

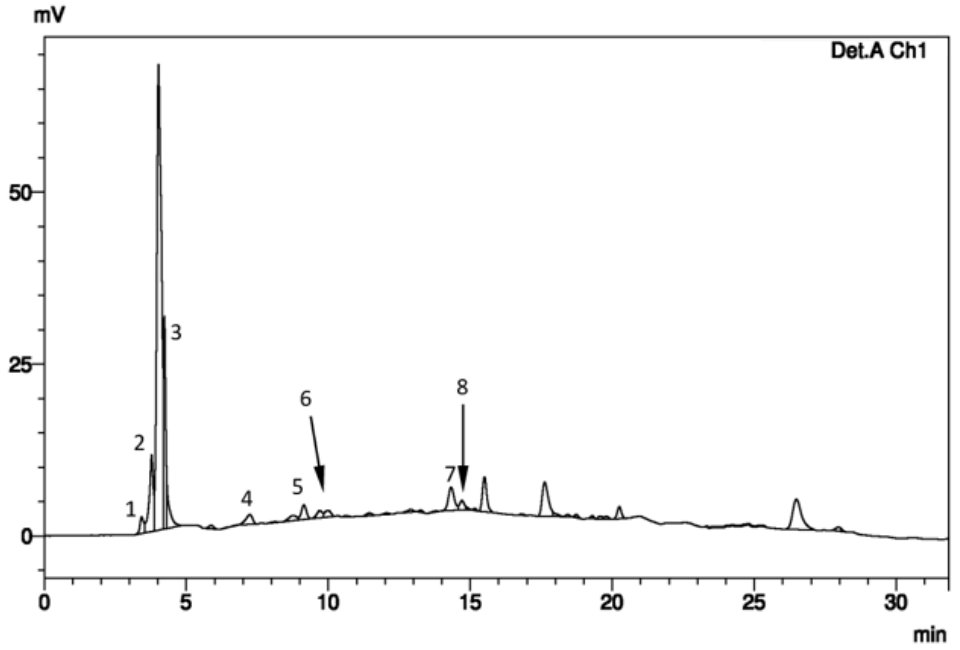

Figure 2. Chromatogram of whey after precipitation of milk proteins by plant coagulant: catechin-like (1-4), catechin (5), catechins (6, 7), myricetin glycosides (8).

Plantago major juice flavonoid composition is multicomponent. In the study of the type of absorption spectrum of alcohol extraction from the juice of the ground part of the plantain large found that the maximum is at a wavelength of 225-350 nm. Of the 22 given flavonoids, 9 substances are 6-oxyflavones, characterized by a maximum within the range of 255–285 nm.

In total, 12 flavonoid-class compounds were identified in the colored whey that was removed after precipitation of milk proteins by plant coagulant, which is 10 fewer compared to their content in plantain juice. This is probably due to the fact that a considerable amount of the polyphenolic compounds from the juice have passed to the milk protein concentrate during denaturation.

Determination of total content of polyphenols and flavonoids

The total content of polyphenols in all samples was determined by summing the content of substances found in the range of peaks of flavonoids, neflavanoids and phenolic acids on the chromatograms. The polyphenols, whose peaks were located outside the area of the catechin peaks, but with the spectral characteristics of the catechins, were assigned to the catechin-like group and were not considered flavonoids. Their contents were 1036.72 and 166.53 mg/l, respectively, in plantain juice and whey. The total content of flavonoids in all samples tested was equal to the content of substances that were similar to the standards of flavonoids (phenolic acids, catechins, flavonols, flavonones and flavones) with the exception of catechin-like substances. Flavonols are represented by the glycosides of myricin; naringin and hesperidin are part of flavonones; the flavones in the quantitative sense are the smallest and are represented by luteolin and its glycosides and glycosides of apigenin. Phenol acids content ranged from 12.36 mg/l for plantain juice and 0.07 mg/l for colored whey. The results of the study are presented in Table 3.

Table 3

Total composition and content of polyphenols in samples of plantain juice and whey

A group of polyphenols	Content, mg/l	
	Plantain juice	Whey
Phenolic acids	12.36	0.07
Catechins, including certain substances:	90.25	33.69
- catechin		6.82
Catechin-like *	1036.72	166,53
Flavonols, including certain substances:	33.98	1.47
- glycosides of myricin	1.47	1.01
Flavanones, including certain substances:	19.68	1.04
- naringin	4.12	0.13
- hesperidin	9.1	0.91
Flavones, including certain substances:	0.52	0.31
- luteolin	0.29	
- glycosides of apigenin	0.23	
- glycosides of luteolin		0,31
Unidentified	217.62	120.72
The sum of polyphenols	1411.13	324.43

* – catechin-like – polyphenols whose peaks are located outside the area of the catechin peaks, but with the spectral characteristics of catechins.

The interaction of polyphenols with proteins depends on the structure of both polyphenol and protein, as well as the pH of the solution, ionic strength, temperature, polyphenol – protein ratio [18]. When binding, hydrophobic interplanar interactions of aromatic groups of amino acid residues of protein and polyphenols and (or) hydroxyl groups of polyphenols with a protein chain take place [19]. According to studies [20], the binding of polyphenols to different protein chains leads to the full or partial "unfolding" of the latter.

Therefore, the change of the native state of the protein is accompanied by the loss of the organized structure of the protein molecule without disruption of covalent bonds in them. In this case, the denaturation of both casein and serum proteins contributes to the increase of temperature and the process in the presence of the active complex Plantago major. During denaturation of proteins, hydrogen bonds and disulfide bridges that determine the spatial structure of their molecules are destroyed, which is accompanied by a change in the configuration, hydration, and aggregate state of the particles. The breaking of intramolecular bonds increases the reactivity of molecules, resulting in complexes between peptides and phenolic compounds.

The mechanism of polyphenols adsorption is to attach them to the protein globule surface at the time of deployment of the polypeptide chain due to the formation of a hydrogen bond between the hydroxyl group of the polyphenol and the carbonyl group of the protein molecule.

In the second stage, "Coagulational", destabilized protein molecule micelles by molecular interaction forces and calcium "bridges" are combined into aggregates, then into chains that are subsequently longitudinally and transversely structured into a spatial grid. In this case, the molecules of polyphenolic compounds are captured. There is a gelation process. At the final stage there is a structure formation and strengthening of a clot of protein-polyphenoliphenol complexes. The quantitative reflection of this mechanism is presented in table. 3, where the difference between the values of the polyphenols content in juice and whey indicates the degree of their transition to protein-plant concentrate.

Conclusions

Thus, the amount of polyphenols in the plantain juice was 1411.13 mg/l, and in the whey – 324.43 mg/l, the content of flavonoids was fixed at 144.57 mg/l and 37.11 mg/l, respectively. Having analyzed the results, we can conclude that the degree of transition of polyphenolic compounds into milk protein concentrate is 77% of the total number, including 74% of flavonoids.

Therefore, the binding of polyphenols by proteins depends on the structure of the protein molecule, the spatial distribution of amino acid residues responsible for the binding of polyphenols, and the number of conditions for such interaction. In addition, this relationship can cause a change in the spatial structure of the protein and affect the bioavailability of both components.

References

1. Slashcheva A. V., Nykyforov R. P., Popova S. Yu. (2016), Obgruntuvannia dotsilnosti vykorystannia bilkovo-vuhlevodnoho napivfabrykatu v tekhnolohii produktsii z

dyspersnoiu strukturoiu, *Vostochno-Evropeiskii zhurnal peredovykh tekhnolohii*, 2/11(80), pp. 24–32.

2. Elena M., Emim J.,Souccar C., Lapa A. (1997), Analgesic and Anti-inflammatory Activities of the Aqueous Extract of Plantago major L., *International Journal of Pharmacognosy*, 35(2), pp. 99–104, DOI: 10.1076/phbi.35.2.99.13288
3. Najafian Y., Hamedi S., Farshchi M., Feyzabadi Z. (2018), Plantago major in Traditional Persian Medicine and modern phytotherapy: a narrative review. *Electronic Physician*, 10 (2), pp. 6390-6399, DOI: 10.19082/6390.
4. Guil, J.L., Torija, M.E., Gimenez, J.J., Rodríguez, I. (1996), Identification of Fatty Acids in Edible Wild Plants by Gas Chromatography. *Journal of Chromatography,* 719 (1), pp. 229–235, DOI: 10.1016/0021-9673(95)00414-9.
5. Olennikov, D.N., Tanhaieva, L.M., Mykhailova, T.M. Samuelsen, A.B. (2005), Organic acids of herbal plants 1. Plantago major L. *Chemistry of Natural Connections*, 41(4), 354–355, DOI: 10.1007/s10600-005-0180-1.
6. Holovko M.P., Penkina N.M., Kolesnyk V.V. (2011), Antioxidant properties of some kinds of vegetable raw material, *Eastern-European Journal of Enterprise Technologies*, 4,6(52), pp. 9–11.
7. Kamiyama V., Harakawa M., Otoguno C, Ozawa S. (2007), Iap. Soc. *Food Sci. Technoi.,*25, 1, pp. 36-40.
8. Olennikov D.N. (2007), Podorozhnik bolshoi. Khimicheskii sostav i primenenie, *Khimiia rastitelnogo syria*, 2, pp. 37–50.
9. Samuelsen A.B. (2000), The traditional uses, chemical constituents and biological activities of Plantago major. A review, *Journal of Ethnopharmacology*, 71, pp. 1–21.
10. Janković T., Zdunić G., Beara I., Balog K., Pljevljakušić D., Stešević D. Šavikin K. (2012), Comparative study of some polyphenols in Plantago species. *Biochemical Systematics and Ecology*, 42, pp. 69–74, DOI: 10.1016/j.bse.2012.02.013.
11. Grek O., Krasulya O., Chubenko L., Tymchuk A. (2018), The investigation of the potentional complex from plantago major to coagulate milk proteins, *Food and Environment Safety*, XVII(2), pp. 165–175.
12. Choma I., Olszowy M., Studziński M., Gnat S. (2019), Determination of chlorogenic acid, polyphenols and antioxidants in green coffee by thin-layer chromatography, effect-directed analysis and dot blot – comparison to HPLC and spectrophotometry methods, *Journal of Separation Science*, 42(8), pp. 1542–1549, DOI: 10.1002/jssc.201801174.
13. Malenčić D., Cvejić J., Miladinović J. (2012), Polyphenol Content and Antioxidant Properties of Colored Soybean Seeds from Central Europe, *Journal of Medicinal Food,* 15(1), pp. 89–95, DOI: 10.1089/jmf.2010.0329.
14. Khodakov I.V. (2013), Sposob identifikatsii polifenolov v rastitelnykh ekstraktakh pripomoshchi VEZhKh. Opredelenie sostava izoflavonov soi, *Metody i obieekty khimicheskogo analiza*, 8(3), pp. 132–142.
15. Khodakov I.V. (2012), Sposob identifikatsii polifenolov v rastitelnykh ekstraktakh, *Visnik stomatologii*, 80(7), pp. 42.
16. Khodakov I.V., Makarenko O.A. (2010), Vysokoeffektivnaia zhidkostnaia khromatografiia vissledovanii rastitelnykh polifenolov, *Visnik stomatologii*, 73(5), pp. 59–60.

17. Ostroumov L.A., Khusnullina N.V. (2010), Izuchenie kislotno-sychuzhnogo svertyvaniia moloka s primesiu SOM, *Tekhnika i tekhnologiia pishchevykh proizvodstv*, 1, pp. 1–5.
18. Wang Sh, Liu Ff, Dong XY, Sun Y. (2010), Thermodynamic analysis of the molecular interactions between amyloid beta-peptide 42 and (–)– epigallocatechin-3-gallate, *J Phys Chem B.;*114(35), pp. 11576–11583, DOI: 10.1021/jp1001435.
19. Bandyopadhyay P., Ghosh A.K, Ghosh C. (2012), Recent developments on polyphenol-protein interactions: effects on tea and coffee taste, antioxidant properties and the digestive system, *Food Funct,* 3(6), pp. 592–605, DOI: 10.1039/c2fo00006g.
20. Rawel H.M, Rohn S, Kroll J. (2003), Influence of a sugar moiety (rhamnosylglucoside) at 3-o position on the reactivity of quercetin with whey proteins, *Int J Biol Macromol*., 32(3–5), pp. 109–120, DOI: 10.1016/S0141-8130(03)00044-8.

Comparative study on chemical composition and antibacterial activity of fenugreek (*Trigonella Foenum graecum* L.) and cumin (*Cuminum cyminum* L.) seeds

Hasna Bouhenni[1], Koula Doukani[1], Nazım Şekeroğlu[2], Sevgi Gezici[2], Souhila Tabak[1]

1 – University of Ibn Khaldoun, Tiaret, Algeria
2 – Kilis 7 Aralık University, Kilis, Turkey

Keywords:

Cumin
Fenugreek
Seed
Antibacterial

Article history:

Received 27.02.2019
Received in revised form 14.06.2019
Accepted 28.11.2019

Corresponding author:

Koula Doukani
E-mail: kouladoukani@gmail.com

DOI:
10.24263/2304-974X-2019-8-4-7

Abstract

Introduction. The objective of this study was determination of the physico-chemical characteristics of fenugreek (*Trigonella Foenum graecum* L.) and cumin (*Cuminum cyminum* L.) and evaluation of their antibacterial properties against *Staphylococcus aureus* ATCC25923*, Escherichia coli* ATCC 25922 and *Bacillus subtilis* ATCC 6633.

Materials and Methods. Different varieties of fenugreek and cumin were analyzed for their weight of 1000 seeds and germination rate. The physico-chemical analysis carried out was pH, titratable acidity, moisture, ash, total soluble solids, electrical conductivity, viscosity, proteins, fats, crude fibers, pectins, total and reducing sugars and minerals. The antibacterial activity of the extracts was evaluated by disc diffusion method against tested bacterial strains.

Results and discussion. The obtained results showed that the Algerian variety of fenugreek and Syrian one of cumin seeds gave the highest weight with a value of 16.8 and 13.9 g respectively and the better germination rate with a percentage of 70%. The pH and titratable acidity of fenugreek and cumin seeds ranged from 5.6 to 6.5 and 2.8 to 3% respectively. The moisture and ash content varied from 3 to 2.8% and 3 to 7% respectively. Total soluble solids, electrical conductivity, viscosity varied from 2.8 to 5.5 °Brix, 18.1 to 42.8 mvs and 2.4 to 2.8 m/pa/s respectively. The analysis showed that fenugreek and cumin contained a high amount of proteins which was between 23.1 and 26.8%. On the other hand, fats ranged from 8.8 to 21%. While crude fibers, pectins varied from 5.1 to 7.9% and 1.9 to 2.8% respectively. Total and reducing sugars varied from 5.2 to 6.7%, and 0.5 to 1% respectively. According to the present data, mineral and heavy metals profile of fenugreek and cumin showed that they contain potassium as a major mineral in a maximum quantity followed by sulphur, phosphorus, calcium, magnesium, iron, zinc and boron, copper, lead, nickel, chromium, molybdenum, cobalt and cadmium. The results of antibacterial activity of methanol extract plants against three bacterial strains revealed the sensitivity of these strains to the extracts plants with DZI (Diameter Zone of Inhibition) of 21 mm, 12 mm, 18 mm for cumin and 10 mm, 08 mm, 09 mm for fenugreek respectively for *S. aureus, E. coli* and *B. subtilis.*

Conclusion. The overall evaluation of this study concludes that both spices fenugreek and cumin have good chemical composition and revealed their sensitivity on the tested bacterial strains.

Introduction

The World Health Organization [WHO] estimates that 80 percent of the world population use medicinal plants for some aspect of primary health care [1]. Plants showed large spectre of pharmacological activities including anticancer, antimicrobial, cardiovascular, antioxidant, anti-inflammatory, immunological, analgesic and many other pharmacological effects [2]. Spices and herbs have been used for thousands of centuries by many cultures and scientific experiments have documented the antimicrobial properties of spices, many spices are also used for purposes of medicine and in cosmetics, perfumery and liquorices in many parts of the world [3]. Fenugreek and cumin are commonly used spices in very small quantities as a food additive for flavor, color, or as a preservative and therapeutic agent [4].

Fenugreek seed (*Trigonella Foenum graecum* L.) is an annual herb of the Leguminosae family indigenous to western Asia and South Eastern Europe. It has long been cultivated in the Mediterranean area, in India and in North Africa, and consumed in many forms, it has wide range of characteristics such as aromatic smell, bitter taste, carminative properties, antioxidant and antibacterial benefits, major constituent of fenugreek seed is carbohydrate that accounts for 50%. Other chemical constituents of seed are 3 to 4% ash, 3 to 5% moisture, 25 to 30% protein, 7 to 9% lipids, 20 to 25% insoluble fibre [5]. Seeds have 7.5% lipids that are usually in the form of triglycerides 6.3% and 450 mg/100g phospholipids [6]. Fenugreek is used traditionally as a demulcent, laxative, lactation stimulant and exhibits hypocholesterolemic, hypolipidemic and hypoglycemic activity in healthy and diabetic animals and humans, the defatted seeds material of fenugreek may reduce gastrointestinal absorption of glucose and cholesterol and increase bile acid secretion [7].

Cumin is a strong aromatic dried ripe fruit seed of *Cuminum cyminum* L. It belongs to the Apiaceae family (parsley family), cumin seeds are ancient spices with a strong aromatic smell and warm, bitterish taste. It is widely used as a condiment, it has great medicinal value, is used in traditional medicine to treat flatulence, digestive disorders, and diarrhea and in the treatment of wounds. It is valuable in dyspepsia, diarrhea and hoarseness, and as remedy against indigestion and colic [8]. Physicochemical analysis showed that *Cuminum cyminum* contained 8% Moisture, 7.5% total ash:, 18.4±0.16% crude proteins, 21.8±0.13% crude fibers and 55.6% total carbohydrates [9]. The previous pharmacological studies revealed that *Cuminum cyminum* exerted antimicrobial, insecticidal, anti-inflammatory, analgesic, antioxidant, anticancer, antidiabetic, antiplatelet aggregation, hypotensive, bronchodilatory, immunological, contraceptive, anti-amyloidogenic, anti-osteoporotic, protective and central nervous effects [3].

Therefore, the present study was lunched to highlight some chemical, nutritional properties and health benefits of fenugreek (*Trigonella Foenum graecum* L.) and cumin (*Cuminum cyminum* L.) seeds and to investigate the bacteriological characteristics of these plants. In this context, a research work was undertaken to elucidate physico-chemical and minerals analysis of fenugreek and cumin, and to estimate the antibacterial activity of their extracts against three bacterial strains (*S. aureus, E. coli* and *B. subtilis*) in order to compare the proximate composition and the inhibitory effects of these plants.

Materials and methods

Selection of varieties

Different varieties of fenugreek (*Trigonella foenum-graecum L.*) and cumin (*Cuminum cyminum L.*) from Algeria, Egypt, India, Morocco and Syria were purchased from a local market and analyzed for their weight of 1000 seeds and germination rate in order to select the best ones.

Weight of 1000 seeds. The number of seeds taken into by hand count on 100 and 1000 seed weight was measured in (g/mg) and used to estimate the seed rate based on fixed number of seeds and test weight [10].

Germination Rate. Seeds were treated with dry heat at 50 °C for 4 days to eliminate residual dormancy that might interfere with germination rate. Two sets of 25 seeds for each cultivar [one from each replication] were placed on Whatman no. 1 filter paper inside a 9 cm Petri dish. The filter paper was moistened with 2.5 ml of distilled water, and the seeds were germinated in the dark at 25 °C and >97% relative humidity (RH) inside a germinator. Seeds showing 2 mm of radicle growth or more were considered germinated. Germination rate was calculated using the following formula and designated as RG index : [11]

$$\text{Rate of germination}\left(\text{RG}\right)=\frac{\text{no. of seeds germinated at}48\text{ h}}{\text{no. of seeds germinated at}168\text{ h}}\times 100$$

Sample preparation

The selected samples were sorted, peeled, washed, dried at room temperature, then powdered and screened at 200μm.

Physico-chemical analyses

Physico-chemical analyses: pH, titrable acidity, ash, moisture, viscosity, electrical conductivity, total soluble solids, fibers, fats, proteins, pectins, total and reducing sugars and minerals were estimated according to the following methods:

pH. 10 g of each fresh sample was added to 100 ml of distilled water, shaking for 10 min and immersing the pH electrode in the solution [12].

Titratable acidity. 5 g of each sample was diluted in 25 ml of distilled water and titrated with NaOH (0.1N) until pH 8.1. [12].

Ash. 10 g of powder sample was weighed and incinerated at 550 °C for 6 h in an ashing muffle furnace until ash was obtained. The ash was cooled and reweighed [12].

Moisture. 10 g sample was dried at a temperature of 105 °C±5 until weight was constant [12].

Viscosity. The viscosity was estimated using viscometer at 20 rpm and 25 °C [13].

Electrical conductivity. Electrical conductivity expresses the ability of the aqueous solution to conduct an electric current. The conductivity meter electrode was immersed in a 20% solid solution [14].

Total soluble solids. Total soluble solids [TSS] were directly recorded by digital refractometer and the results were expressed as percent soluble solids (°Brix) [14].

Crude fat. The crude fat was determined using Soxhlet extraction for 6 hrs, using n-hexane as a solvent [12].

Crude fibers. 1 g of powdered sample was digested with H_2SO_4 (1.25%) followed by NaOH [1.25%] solution. After filtration and washing with distilled water and acetone, remaining residues were weighed and putted in muffle furnace at a temperature of 550-650 °C till grey or white ash was obtained [12].

Crude proteins. The powdered samples of fenugreek and cumin were tested for crude protein content according to the Kjeldahl's method as described in AOAC [12]. Briefly, 2 g of each sample were digested with H_2SO_4 by using digestion mixture (catalyst). The digested material was diluted up to 250 ml in volumetric flask. 10 ml of NaOH 40% as well as 10 ml of digested sample was taken in distillation apparatus where liberated ammonia was collected in beaker containing 4% boric acid solution using methyl red as an indicator. The percentage of nitrogen in the samples was assessed by titrating distillate against 0.1N H_2SO_4 solution. Crude protein content was calculated by multiplying nitrogen percent (N%) with factor (6.25).

Pectins. The extraction of the pectins was estimated by a treatment of samples with high temperature using hydrochloric acid as described by Multon [15]. Pectins were separated from the residue by centrifugation and precipitation with alcohol, the obtained precipitate was filtered to remove soluble impurities, then dried and weighed.

Total sugars. Totals sugars were determined using a colorimetric test according to Dubois [16], using phenol and concentrated sulfuric acid. In brief, 1 ml of sugar solution was added to 1 ml of phenol 5% and 5 ml of concentrated sulfuric acid, then shaked and placed for 10 to 20 min in a water bath at 25 to30 °C. The absorbance was measured at 490 nm. The amount of sugars was determined by reference to a standard curve established with glucose.

Reducing sugars. 1ml of the sugar solution was removed and 1ml of DNSA reagent was added after 5 min of heating in a water at 100 °C, the absorbance reading was made at 540 nm, the results were expressed in relation to a standard curve using glucose as reference [17].

Mineral content. The plant samples were analyzed for their macronutrients (P, Ca, K, Mg and S), micronutrients (Fe, Cu, B and Zn) and heavy metals (Cd, Co, Cr, Mo, Ni and Pb) by using ICP-AES [18]. Briefly, 0.2 g of samples were put into burning cup and 5 ml HNO3 65% and 2 ml $H_2O_2$30% were added. After burning in a HP-500 CEM MARS 5 microwave at 200 ºC, the solution was cooled at room temperature for 45 min, filtrated by Whatman 42 filter paper. The extracts were cooled by high-deionized water in a 20 ml polyethylene bottles and kept at 4ºC for ICP-AES analyses.

Antibacterial analysis

Preparation of extracts. The extracts were prepared using maceration method [19].100 ml of methanol 70% was added to 10 g of each sample, the solutions were shaked for 24 h at room temperature, the mixtures were then filtered using Whatman paper N°01 and evaporated using rotary evaporator. Dried extract was stored in the refrigerator at 4 °C for further analyses.

Antibacterial activity. The antibacterial activity of the extracts was evaluated by disc diffusion method against three bacterial strains *S. aureus* ATCC25923*, E. coli* ATCC 25922 and *B. subtilis* ATCC 6633 [20]. Bacterial strains were inoculated with Muller Hinton broth for 24 h at 37 °C. The suspensions were standardized using U.V spectrophotometer in order to provide initial cell counts of about 10^6 CFU/ml, Sterile discs (diameter 6 mm) were impregnated with 10 µl of fenugreek and cumin extracts of different concentrations (50 and 100 mg/ml). Metronidazol was used as standard antibiotic and methanol as negative control. The diameter of the clear zone around the disc was measured and expressed in millimeters as antibacterial activity [21].

Statistical analysis

The data from chemical composition and antibacterial effect were analyzed with a statistical software program (SPSS version 20). Differences between plants were compared at $P < 0.05$ with ANOVA 1 in order to find the statistically significant differences. The assays were carried out with four repetitions and the results were expressed as mean values and standard deviation.

Results and discussion

Selection of varieties

As shown in Table 1, there are significant differences between the weight of 1000 seeds (g) and germination rate of the different varieties.

Table 1

Weight of 1000 seeds and germination rate of different varieties of cumin and fenugreek seeds

Variety		Algeria	Egypt	India	Morocco	Syria
Fenugreek	Weight of 1000 seeds (g)	16.8±0.25	11.6±0.2	10.2±0.03	10±0.2	10±0.000
	Germination Rate (%)	70±0.000	40±0.066	30±0.25	20±0.75	20±0.045
Cumin	Weight of 1000 seeds (g)	10.1±0.033	09.8±0.1	13.6±0.04	10.2±0.00	13.9±0.111
	Germination Rate (%)	40±0.05	20±0.3	60±0.05	40±0.05	70±0.025

Physicochemical analysis

Table 2 showed the proximate chemical composition of fenugreek and cumin seeds; No significant differences ($p>0.05$) were observed between the parameters.

Table 2

Results of physicochemical analysis of fenugreek and cumin seeds

Parameters	Fenugreek	Cumin
pH	5.6±0.0075	6.5 ±0.0075
Titrable acidity (%)	3 ±0.00	2.8 ±0.00
Moisture (%)	3 ±0.0005	5.6±0.00
Ash (%)	3±0.00	7±0.00
TSS (°Brix)	2.8 ±0.82	5.5±0.00
Electrical conductivity (mvs)	18.1±0.005	42.8±0.00
Viscosity (m/pa/s)	2.8 ±0.0003	2.4±0.0009
Proteins (%)	26.8±0.063	23,1 ±0.25
Fats (%)	8.8±0.34	21±0.00
Fibers (%)	5.1±0.00	7.9±0.00
Pectins (%)	1.9 ±0.00	2.8 ±0.0033
Total sugars (%)	6.7 ±0.0066	5.3 ±0.00
Reducing sugars (%)	0.5±0.00	1 ±0.0033

The macronutrients, micronutrients and heavy metal contents of cumin and fenugreek seeds were given in Table3. Analysis of the mineral contents showed no significant differences between cumin and fenugreek.

Table 3

Results of minerals analysis of fenugreek and cumin

		Plant	
Minerals (mg/kg)		**Fenugreek**	**Cumin**
Macronutrient	Ca	1445±68	8077±89
	K	10605±555	14647±501
	Mg	1229±88	2610±111
	P	5143±366	3817±321
	S	2648±135	3423±211
Micronutrient	B	11.8±0.06	22.1±0.14
	Cu	9.9±0.4	10±0.5
	Fe	91±6	133±8
	Zn	30.9±1.5	37.8±1.8
Heavy metal	Cd	0.03±0.002	0.1±0.008
	Co	0.2±0.004	0.2±0.000
	Cr	0.2±0.007	1±0.009
	Mo	2±0.900	0.3±0.009
	Ni	1.3±0.90	1.5±0.11
	Pb	0.4±0.00	1.4±0.10

Antibacterial activity

The results of antibacterial activity of fenugreek and cumin extract against three bacterial strains (*S. aureus, E. coli* and *B. subtilis*) revealed the sensitivity of these strains to the plants extracts as shown in Table 04. In the dose response study, the inhibition zone increased with increasing concentration of the extracts.

Table 4

Results of antibacterial analysis of fenugreek and cumin

Plant	DZI (mm)		
	Strains / Concentration	50 mg/ml	100mg/ml
Fenugreek	*S. aureus*	07±0.003	10±0.004
	E. coli	06±0.05	08±0.0075
	B. subtilis	07±0.4	09±0.05
Cumin	*S. aureus*	11±0.06	21±0.333
	E. coli	07±0.08	12±0.66
	B. subtilis	10±0.0002	18±0.075

Our results illustrate that cumin extracts displayed the highest inhibitory effects compared to fenugreek.

Discussion

Physicochemical composition

The choose of varieties depended on the results of weight of 1000 seeds (g) and germination rate (%) of different varieties of fenugreek and cumin, the results showed that the Algerian variety of fenugreek was the best one comparing to the other varieties with a weight of 16.8±0.25g and germination rate of 70±0.000%, while the Syrian variety of cumin present the higher weight with an amount of 13.9±0.111g and germination rate with percentage of 70±0.025%.

The result of pH in fenugreek was lower in comparison with the results of Ahmed Dilshad [22] which were in the range of 6.8 and 6.9, however our pH value of cumin was significantly lower to the earlier research of Al-Snafi [3] which was 7.3 and higher than results of Monojit [23] which were 3. The pH determined for the two spices taken into consideration is in the range of 6-7, which shown slight acidic character. Otherwise differences on pH can be due to the diversity of the variety, the growing conditions, the degree of ripening and climate [24].

Concerning Titratable acidity, Tabaestani [25] found that cumin posses a lower value of titratable acidity in confrontation with our results which was 0.7±0.09. The differences on pH and titratable acidity could be due to the lower water content as well as to different growing conditions [24].

The percentage of moisture content in fenugreek was similar to those of Abdelmoneim [26] which were 4% and significantly higher than the results of Udayasekhara [27] which

were 2.4%. However, cumin revealed very low percentage of moisture compared to the results of Al-Snafi [3] which were 8%. The variations in moisture content reported by various investigators could be attributed to the differences in the environmental conditions, the time of harvesting and the storage conditions [28].

Awais [29] showed a similar amount of ash in fenugreek with our results; 3.4%, and lower than those of Abdelhamid [30], with a value of 7.6%. Concerning cumin, it was observed that it presents a high content of ash in contrast to Al-Snafi [3] results which were 6.5, while the present result was similar to those presented by Monojit [23] which were 7.5% and lower than the maximum limits indicated by the Egyptian Specification Standards [ES: 1930/2008] and by the International Standards Organisation [ISO 9301/2003] which was 8.5% and 12% respectively. The variation in the ash content could be due to the soil conditions [28].

Total Soluble Solids contents in cumin was higher than fenugreek, regarding fenugreek our results was lower than those of Abdelnabey [31] which were 3.5 °Brix, while Tabaestani [25] found that cumin TSS contents was higher with 7.7°Brix. No significant difference was detected on TSS between fenugreek and cumin ($p=0.000$).

For the viscosity, Brummer [32] found that fenugreek viscosity was significantly higher than the present result 9.6 m/pa/s. while cumin viscosity value was lower than Nazima [33] result 0.3 ±0.009 m/pa/s, Juszczak [34] experiments show that the values of viscosity depend strongly on soluble solids content, the viscosity changed with higher soluble solids content.

Electrical conductivity of cumin was higher than fenugreek, Fred [35] found that cumin present a higher value than the present study 35.1 mvs. The results of specific conductivity indicate that the ash alone was not the cause of the conductivity, but that the organic compounds were concerned [35].

The crude proteins level of fenugreek was approximately comparable to those of Mullaicharam [36] with a value of 25.9%, however our result was significantly higher than those of Fahad [37] with values of 12.9%.

The found protein content amount in cumin seeds were higher compared to those reported in literature of Al-Snafi [3], Monojit [23] which was 18.4%±0.16 and 18.4% respectively. The difference on crude protein content between plants may be due to different cultural practices, soil and environmental conditions [28].

Suleiman [28] evaluated the chemical composition of fenugreek and concluded that crude fats contents were similar to the presented result with an amount of 8.1%, Also our result was higher than those of Abdelmoneim [26] with a percentage of 4%. While, fats contents in cumin found by Muhammad Sultan [38] was higher with percentage of 31.2%, in the present data the level of fats was approximately similar to the studies of Mengmei [39] with an amount of 22.7%. According to Abdelmoneim [26] the percentage of total lipids of plants differs according to the location and conditions of cultivation.

Many studies have been carried out to estimate the amount of fibers present in fenugreek. Haram [40] present a higher percentage of fibers 13%. while pectins content in fenugreek was lower than Anita [41] result which was 3%. Fiber contents in cumin were significantly lower in comparison with other studies of Peter [8] with an amount of 30%, however pectins percentage was higher than Mengmei [39] result which was 1.7%. There is evidence that crude fibers has a number of beneficial effects related to its indigestibility in the small intestine [42].

Sugars analysis expressed that the percentage of total sugars in fenugreek was significantly higher than that showed by Elmahdy and Elsebaiy [43] which was 4.2%. On the other hand, it was lower than the results presented by Anita [41] with an amount of 8.8%, While reducing sugars in fenugreek were similar to the result of Rajini [44] which were 0.5%

and lower than Anita [41] result; 0.8%. Concerning cumin, significant differences in total sugars content were also observed compared to previous studies of Kumar [45] which were 2.4%. Reducing sugars contents in cumin was similar to those found by Kumar [45] which were 1.2%. The nutritional composition of plants depends on climatic conditions, geographic origin of seeds and cultural practices [46].

According to the present data, mineral and heavy metals profile of fenugreek showed that it contains potassium as a major mineral in a maximum quantity followed by sulphur, phosphorus, calcium, magnesium, iron, zinc and boron, for the heavy metals the higher percentage was their of copper followed by lead, nickel, chromium, molybdenum, cobalt and cadmium. Extensive research has been carried out to determine the amount of mineral elements in fenugreek, and results of Magboul [47] were higher than our results with a value of calcium (158 mg/100g), phosphorous (415mg/100g), iron (22.5 mg/100g), sodium (493 mg/100g), magnesium (1550 mg/100g), potassium (1306 mg/100g), copper (331 mg/100g) and zinc (9.9 mg/100g).The levels of Cu, Fe, Mn and Zn were higher than the levels given by Ozkutlu [48] (9±0.6mg/kg), (36±3.6mg/kg), (8±1mg/kg) and (19±0.9mg/kg) respectively except Cd which was higher than our result (0.1±1.6 mg/kg). Fenugreek seeds are good source of minerals that helped in a number of physiological functions of body and maintains health status [7]. Although they are required in very low quantities because some trace elements heavy metals including iron, copper, zinc and manganese are essential micronutrients with one or more structural or functional roles for living organisms [49]. The present study showed that cumin contains potassium as major mineral followed by calcium, phosphorus, sulphur, magnesium, iron, zinc, boron, copper, lead, chromium, nickel, cobalt, cadmium, molybdenum respectively. Al-Snafi [3] reported a very lower value compared to our results, potassium (35.8mg/100g) was being the most abundant element in cumin followed by calcium (18.6 mg/100g), phosphates (10 mg/100g), magnesium (7.3 mg/100g), sodium (3.4 mg/100g), iron (1.3mg/100g), manganese (0.1mg/100g), copper (0.1mg/100g), selenium (0.1mg/100g) and Zinc (0.1mg/100g). The amounts of Cu, Fe, Mn and Zn in cumin reported by Ozkutlu [48] was lower with an amount of (8±0.3 mg/kg), (129±2.1 mg/kg), (14±0.8mg/kg) and (22±0.5 mg/kg) respectively except Cd which was higher (77±1.3 mg/kg). Januz [50] indicated that the plants collected from rural areas or grown in less industrialized regions had lower contents of heavy metals than those growing in industrialized regions.

Statistically, there is no significant difference between fenugreek and cumin in term of all parameters ($P>0.05$) except cobalt ($P= 0.345$), Significant differences might be due to the great heterogeneity in the species studied, plant parts used and growing regions [48].

Antibacterial activity

In the present study, antibacterial activities of methanolic plants were based on the concentration of the extracts. while 100 mg/ml of methanolic fenugreek extract inhibited *E.coli* with DZI of 09 mm±0.05, the same concentration inhibited *B.subtilis* with 08mm±0.0075 and *S.aureus* with10 mm±0.004. No significant difference was observed between the two plants [p=0.003]. Dash [51] found that methanol fenugreek extract was effective in inhibiting the growth of *E.coli* with DZI of 7±0.23 mm. However, Ramya Premanath [52] examined the antibacterial activity of fenugreek against *E.coli and S.aureus*, the strongest antibacterial effect was showed against *S.aureus* compared to *E.coli* with DZI of 12±0.7 and 9±0.4 respectively. It was clear from the present results that methanolic extracts exhibited pronounced activity against all the tested bacteria. The highest antibacterial activity may due to the presence of polyphenols because the phenol content was more in the methanolic extract than in any other solvent extracts. A study by Field [53] has shown that

antimicrobial properties exhibited by plants could be due to the presence of phenols and flavonoids, while fenugreek seeds may contain higher amount of active components which resulted in higher antibacterial property.

Our obtained results demonstrated that methanolic cumin extract at a concentration of 100mg/ml present inhibitory effect on the growth of all tested bacteria with diameter of 21 mm±0.333for *S.aureus,* 12 mm±0.66 for *E.coli* and 18 mm±0.075 for *B. subtilis,* Sagdic [54] investigated the antibacterial effects of cumin against three strains *E.coli, S.aureus* and *B. subtilis,* the results showed that cumin extract don't affect the growth of *S.aureus* and *B. subtilis* on the other hand it produced bactericidal effect on *E. coli* [19mm]. Nazia Masood [55] found that extracts of cumin *i*nhibited the growth of *S. aureus, E.coli w*ith a diameter of 8.9±5.6 and 23.8±1.2 respectively. Nazia Masood [55] results suggest that the use of some spice as antimicrobial agents may be exploitable to prevent the deterioration of stored foods by bacteria, as long as the taste impact is acceptable in the targeted foods. The extracts of fenugreek and cumin were found to be effective antibacterial agents against human pathogens. This study paves the way for further attention and research to identify the active compounds responsible for the plant biological activity. Further studies should be undertaken to elucidate the exact mechanism of action by which extracts exert their antimicrobial effect.

Conclusion

The analytical study of fenugreek and cumin seeds showed that these two plants develop a particular composition including nutrients such as proteins, fats, fibers, sugars and minerals. This work represents the first attempt to compare the chemical composition and biological activities of fenugreek and cumin especially to study their antibacterial effect against *S. aureus, E.coli* and *B. subtilis* strains. In this context, cumin extracts gave interesting results in terms of theses strains comparing to fenugreek extracts. As a whole, these findings confirm the interesting potential of these two spices as a valuable source of nutriments and energy and as antibacterial agents.

Acknowledgments. The authors would like to sincerely thank the staff of Medicinal and Aromatic Plants Laboratory, Advanced Technology Application and Research Center, Kilis 7 Aralik University (Turkey) for their collaboration, and Dr. Samia Meliani (Faculty of Nature and Life Sciences, University of Ibn Khaldoun –Algeria) for her statistical analysis and continuous help.

References

1. WHO (2002), WHO Traditional Medicine Strategy 2002–2005, World Health Organization, Geneva.
2. Al-Snafi A.E. (2015), The chemical constituents and pharmacological effects of *Chenopodium album* – An overview, *International Journal of Pharmacological Screening Methods*, 5, pp. 10–17.
3. Al–Snafi A.E. (2016), The pharmacological activities of *Cuminum cyminum* – A review, *IOSR Journal of Pharmacy*, 6(6), pp. 46–65.

4. Anupam S., Sunil K., Kiran K., Deepti S. (2018), Medicinal uses of spices used in our traditional culture, *Worldwide Journal of Medicinal Plants Studies*, 6(3), pp. 116–122.
5. Shankaracharya N.B., Natarajan C.P. (1972), Fenugreek chemical composition and use, *Indian Spices,* 9, pp. 2–12.
6. Nayak A.K., Pal D., Santra K. (2015), Screening of polysaccharides from tamarind, fenugreek and jackfruit seeds as pharmaceutical excipients, *International Journal of Biological Macromolecules*, 79, pp. 756–760.
7. Im K.K., Maliakel B. (2008), Fenugreek dietary fibre a novel class of functional food ingredient, *Agro Food Ind. Hi-tech,* 19,pp. 18–21.
8. Peter K.V. (2001), *Handbook of herbs and spices*, Woodhead Publishing Limited Abington Hall, Abington Cambridge, England Vol. 1. pp. 1–332.
9. Moawad S., El-Ghorab A., Hassan M., Nour-Eldin H., El-Gharabli M. (2015), Chemical and microbiological characterization of Egyptian cultivars for some spices and herbs commonly exported abroad, *Food and Nutrition Sciences*, 6, pp. 643–659.
10. Deivasigamani S., Swaminathan C., (2018), Evaluation of seed test weight on major field crops, *International Journal of Research Studies in Agricultural Sciences*, 4(1), pp. 8–11.
11. Krishnasamy V., Seshu D.V. (1989), Seed germination rate and associated characters in rice, *Crop Sci.,* 29, pp. 904–908.
12. AOAC. (2000), Official method of analysis. Association of Official Analytical Chemists,17th Ed. Maryland. U.S.A.
13. NF EN 12092: Adhesives – Determination of viscosity, (2002).
14. AOAC (2002), Official Methods of Analysis. Association of Official Analytical Chemists, 17th Ed. Gaithersburg.
15. Multon J.L. (1991). Techniques d'analyses et de contrôle dans les industries agroalimentaires, Ed. *Tech et Doc* –Lavoisier. France, pp. 121–137.
16. Dubois M., Gilles K.A., Hamilton J.K., Rebers P.A., Smith F. (1956), Colorometric method for determination of sugars and related substances, *Analytical Chemistry*, 28(3), pp. 350–356.
17. Miller G.L. (1972), Use of dinitrosalicylic acid reagent for determination of reducing sugars, *Analytical Chemistry,* 31, pp. 426–428.
18. Sekeroglu N., Meraler S. A., Ozkutlu F., Kulak M. (2012), Variation of mineral composition in different parts of Mahaleb, *Asian Journal of Chemistry,* 24(12), pp. 5824–5828.
19. Gezici S., Sekeroglu N. (2019), Current perspectives in the application of medicinal plants against cancer: novel therapeutic agents, *Anti–Cancer Agent Med. Chem.,* 19(1), pp. 101–111.
20. Kim J.W., Huh J.E., Kyung S.H., Kyung K.H. (2004), Antimicrobial activity of alk(en)yl sulfides found in essential oils of garlic and onion, *Food Sci. Biotechnology*, 13, pp. 235–239.
21. Bauer A. W., Kirby W. M., Sherris J. C., Turck M. (1966), Antibiotic susceptibility testing by a standardized single disk method, *Am J Clin*. 45, pp. 493–496.
22. Ahmad Dilshad (2017), Physicochemical properties of chemurgic–fenugreek (*Trigonella foenum–graecum*) herb of different origin, *Der Pharma Chemica*,9(1), pp. 102–106.
23. Monojit D., Samyak C., Amalesh N., Moulisha B., Pallab K.H. (2017), Pharmacognostic and preliminary physicochemical study of vidangadilouham– an ayurvedic antidiabetic herbomineral preparation, *Journal of Ayurvedic and Herbal Medicine*, 3(1),pp. 15–26.
24. Ariyama K., Nishida T., Noda T., Kadokura M., Yasui A. (2006), Effects of fertilization, crop year, variety, and provenance factors on mineral concentrations in onions, *Journal of Agricultural and Food Chemistry,* 54(9), pp. 3341–3350.
25. Tabaestani H., Sedaghat N., Saeedi Pooya E., Alipour A. (2013), Shelf life improvement and postharvest quality of cherry tomato (*Solanum lycopersicum* L.) fruit using basil

mucilage edible coating and cumin essential oil, *International Journal of Agronomy and Plant Production*, 4(9), pp. 2346–2353.
26. Abdel Moneim E., Sulieman Heba E., Ahmed Awad M., Abdelrahim A. (2008),The chemical composition of fenugreek (*Trigonella foenum graceum* L) and the antimicrobial properties of its seed oil, *J. of Eng. & Applied Sci,* 3(2), pp. 52– 71.
27. Udayasekhara Rao P., Sesikeran M.D.P., Srinivasa R., .Nadamuni Naidu V., Vikas R. (1996), Short term nutritional and safety evaluation of fenugreek, *Nutrition Research Nutrition Research*, 16(9), pp. 1495–1505.
28. Sulieman A. Elhadi. (1995), Fenugreek supplemented backed products, quality aspects. M. Sc. Thesis, University of Gezira, Wad Medani, Sudan.
29. Awais A, Salem S, A., Kaiser M., Muhammad A. (2015), Fenugreek a multipurpose crop: Potentialities and improvements, *Saudi Journal of Biological Sciences*, 23, pp. 1–11.
30. Abdel–Hamid M.R., Alalla R.K., Moue Z.N. (1984), Chemical studies on Egyptian fenugreek seed, *Ann. Agric. Sc.,* 29(1), pp. 43–60.
31. Abdel–Nabey A.A., Damir A.A. (1990), Changes in some nutrients of fenugreek (*Trigonella Foenum graecum* L.) seeds during water boiling, *Plant Foods for Human Nutrition,* 40 (26), pp. 72–74
32. Brummer Y., Cui W., Wang Q. (2003), Extraction, purification and physicochemical characterization of fenugreek gum, *Food Hydrocolloids*, 17, pp. 229– 236.
33. Nazima S., Adeel A. (2013), A study on viscosity, surface tension and volume flow rate of some edible and medicinal oils, *International Journal of Science, Environment and Technology,* 2(6), pp. 1318–1326.
34. Juszczak L., Fortuna T., Kosla A. (2003), Sensory and rheological properties of Polish commercial mayonnaise, *Nahrung /Food,* 47 (4), pp. 232–235.
35. Fred D. (1902), The electrical conductivity of plant juices; Botanical Gazette, *The University of Chicago Press journals,* 34(2), pp. 81–92.
36. Mullaicharam A.R., Geetali D., Uma M. (2013), Weight serum cholesterol levels and the nitrogen medicinal values of fenugreek, *Biol. Chem. Sci.,* 4, pp. 130– 134.
37. Fahad Mohammed J., Al–Jasser MS. (2012), Chemical composition and fatty acid content of some spices and herbs under Saudi Arabia conditions, *Sci World J.*, 20(12), pp. 1–5.
38. Muhammad T S., Masood S B., Faqir M A., Amer J. (2009), Influence of black cumin fixed and essential oil supplementation on markers of myocardial necrosis in normal and diabetic rats, *Pakistan Journal of Nutrition,* 8, pp. 1450–1455.
39. Mengmei M., Taihua M., Hongnan S.,Miao Z., Jingwang C., Zhibin Y.(2015), Optimization of extraction efficiency by shear emulsifying assisted enzymatic hydrolysis and functional properties of dietary fiber from deoiled cumin (*Cuminum cyminum* L.), *Food chemistry*, 179, pp. 270–277.
40. Haram M.A. (1991), The protein quality of Sudanese fenugreek seeds. M. Sc.Thesis, University of Khartoum, Sudan.
41. Anita K., Malkit N., Rajbir S. (2006), Proximate composition, available carbohydrates, dietary fibre and anti nutritional factors of selected traditional medicinal plants, *J. Hum. Ecol.,* 19(3), pp. 195–199
42. Aremu M., Olaleke O., Olorunfemi A., Emmanuel T. (2006), A Comparative study on the chemical and amino acid composition of some Nigerian under–utilized legume flours, *Pakistan Journal of Nutrition*, 5, pp. 34–38.
43. Rafik El–Mahdy A., El–Sebaiy L.A (1982), Effect of germination on the nitrogenous constituents, protein fractions, in vitro digestibility and antinutritional factors of fenugreek seeds (*Trigonella foenum graecum* L.), *Food Chemistry*, 8(4), pp. 253–262.
44. Rajni M., Joshi R., Beenu T. (2016), Effect of domestic processing on physico chemical and nutritional quality of fenugreek cultivars, *Asian. J. Dairy & Food Res*, 35 (4), pp. 338–344.

45. Kumar Amit N., Dilipkumar P., Kousik S. (2015), Screening of polysaccharides from tamarind, fenugreek and jack fruit seeds as pharmaceutical excipients*, International Journal of Biological Macromolecules,* 79, pp. 756–760.
46. Demarne F.E. (1985), Le Geranium rosat, *Parfums, Cosmétiques et Aromes*, 62, pp. 85–92.
47. Magboul B. I. (1986), Chemical and amino acid composition of fenugreek Seeds grown in Sudan, *Food Chemistry*, 22, pp. 1–5.
48. Özkutlu F., Kara S.M., Şekeroğlu N. (2007), Determination of mineral and trace elements in some spices cultivated in Turkey, *Acta Hortic*, 756, pp. 321–328.
49. WHO. (1999), Monographs on selected medicinal plants, World Health Organization, Geneva.
50. National Research Council. (1989), Dietary fiber, in committee on diet and health, Food and Nutrition Board, Commission Life Sciences (Eds.),Diet and health implications for reducing chronic disease risk (pp. 291–309), National Academy Press, Washington.
51. Dash B K., Sultana S., Sultana N. (2011), Antibacterial activities of methanol and acetone extracts of fenugreek (*Trigonella foenum)* and coriander (*Coriandrum sativum*), *Life Sciences and Medicine Research,* 27, pp. 65–72.
52. Ramya Premanath J., Sudisha N.,Lakshmi D., Aradhya S.M. (2011), Antibacterial and antioxidant activities of fenugreek (*Trigonella foenum graecum* L.) leaves, *Research Journal of Medicinal Plants,* 5, pp. 695–705.
53. Field JA., Lettinga G. (1992), Toxicity of tannic compounds to microorganisms. In: Hemingway RW, Laks PE, Eds. Plant Polyphenols, Plenum Press, New York, pp. 673–689.
54. Sagdıc O., Kuscu A., Ozcan M., Ozcelik S. (2002), Effects of Turkish spice extracts at various concentrations on the growth of *Escherichia coli* O157:H7, *Food Microbiology*, 19, pp. 473–480.
55. Nazia M., Ahmed C., Perween T. (2006), Anti–microbial activity of *Cinnamomum cassia* against diverse microbial flora with its nutritional and medicinal impacts, *Pak. J. Bot.*, 38(1), pp. 1–9.

Investigation of oxygen scavengers influence on cooked sausages stability

Anatoliy Ukrainets, Vasyl Pasichniy, Andrii Marynin, Yulia Zheludenko

National University of Food Technologies, Kyiv, Ukraine

Keywords:
Sausage
Stability
Oxygen scavengers
Storage

Article history:

Received 15.05.2019
Received in revised form 16.10.2019
Accepted 28.11.2019

Corresponding author:

Vasyl Pasichniy
E-mail:
pasww1@ukr.net

DOI: 10.24263/2304-974X-2019-8-4-8

Abstract

Introduction. The effect of packing ukrainian and chinese oxygen scavengers on microbiological stability and oxidation stability of a cooked sausages during storage was investigated.

Materials and methods. Cooked sausages packing with different oxygen scavengers were examined. Microbiological attributes, such as Quantity of Mesophilic Aerobic and Facultative Anaerobic Microorganisms (QMAFAnM), yeasts and molds were determined Pasteur method. The acid and peroxide values were determined by the titration method.

Results and discussion. The oxygen complete removal time in the packed sample is reduced with reduce volume from which oxygen is removed. From the minimum oxygen content renewal dynamics in the packaged samples it can be seen that the ability to recover MAP only works when the packaging were opened once. The QMAFAnM of unpacking samples was $4,5\times10^2$ cfu/g. On the 8th day of storage QMAFAnM for samples with chinese oxygen scavengers and control stored at 0+6 °C were not significantly different ($5,0\times10^3$ cfu/g and $6,5\times10^3$ cfu/g, respectively) and were was significantly lower than the sample with ukrainian oxygen scavenger ($1,9\times10^4$ cfu/g). On the 13th day of storage, QMAFAnM for sample 3 were lower than sample 2 ($1,2\times10^4$ cfu/g and $6,9\times10^4$ cfu/g, respectively). At the same time, this parameter was much higher for control. Sample 2 and Sample 3 demonstrated stable meaning of moulds during entire research (<10 cfu/g) and were lower than counts from control ($3,0\times10^1$ cfu/g on 13th day). All samples demonstrated yeasts increase during storage and no significant differences between were observed compared to control ($7,0\times10^1$ – $4,8\times10^2$ cfu/g and $5,0\times10^2$ cfu/g respectively). The initial acid value for unpacking sausages on 1 storage day was 1,41 mg KOH/g. On the 13th day of storage the sausages packed with oxygen scavengers stored at 0+6 °C showed the slightest increase compared to the control (3,57-3,76 mg KOH/g and 3,98 mg KOH/g respectively). Peroxide value for samples 2 and 3 did not differ after 13 d of storage, but were significantly lower than control (3,14 ½Ommol/kg, 3,36 ½Ommol/kg and 4,05 ½Ommol/kg).

Conclusions. Packaging with oxygen scavenger slows down the microbiological spoilage and oxidation processes for cooked sausages compared to the control. This allows recommend the use of oxygen scavenger for the cooked sausages packaging.

Introduction

The selection of the packaging solution plays an important role: it has to guarantee the safety of the product during storage.

The object of the present research was to study the ukrainian and chinese oxygen scavengers effect on the microbiological stability and oxidation stability of a cooked sausages during storage.

Active packaging application for food products. Packaging of food extends beyond the original function of product protection and provides many functions for and about the packaged product. Packaging and packaging-related product traits influence purchase intentions and decisions by consumers [1, 2]. The major packaging options are airpermeable, vacuum, and modified atmosphere (MAP) with low levels of oxygen or high levels of oxygen [3, 4].

Active packaging is a novel technology designed to incorporate components in the packaging material that release substances to the food or to the environment surrounding the food in order to extend shelf-life. The protection or shelf life of the product in response to interactions of the product, package and environment are often the functions of active packaging technologies, but other functions may also be employed [5].

The development of a whole range of active packaging systems, some of which may have applications in both new and existing food products, is fairly new.

Active packaging types were categorized into moisture absorbers, antimicrobial packaging, CO_2 emitters, O_2 scavengers, antioxidant, and other groups [6].

EU regulations (№ 1935/2004 and 450/2009) give specific rules on new types of materials and compounds to actively maintain or improve condition of the food, encompassing antioxidant, preservative, and flavor components. The approaches for active packaging are to incorporate the active compounds into a sachet for use with the packaging, to disperse active compounds, usually of nanometric size, into the polymer matrix or to imbed the inorganic particles into the package surface for controlled release. The EU guidance also includes the function of package absorption of chemicals from the food or package environment [7, 8].

High levels of oxygen present in food packages may facilitate microbial growth, off flavours and off odours development, colour changes and nutritional losses thereby causing significant reduction in the shelf life of foods. Oxygen absorbing systems provide an alternative to vacuum and gas flushing technologies as a means of improving product quality and shelf life [9].

To reduce the access of oxygen, foods are packaged with barrier materials and the headspace of packagings is flushed with nitrogen or nitrogen/carbon dioxide mixtures [10].

However, residual oxygen can remain in the headspace, it can permeate from the environment into the packaging or it is gotten into packagings as solved oxygen in food [11]. A strategy to reduce the oxygen permeability of plastic packagings and to absorb oxygen from packaged food and from packaging headspace is the application of oxygen scavengers. Oxygen scavengers remove oxygen from the inner package environment and thus, in turn, from the food product itself through partial pressure actions.

Although oxygen sensitive foods can be packaged accordingly using MAP or vacuum packaging, such techniques do not always facilitate complete removal of oxygen. Using an oxygen scavenger, which absorbs the residual oxygen after packaging, quality changes in oxygen sensitive foods can often be minimised [12].

The oxygen scavenging component of a package can take the form of a sachet, label, film (incorporation of scavenging agent into the packaging film), card, closure liner or concentrate [13]. Absorbent pads may absorb liquids or gases and be impregnated with silver, copper, or copper oxide nanoparticles [14].

Oxygen scavengers are most commonly iron or ferrous oxide fine powders, although ascorbic acid, sulphites, catechol, ligands, and enzymes like glucose oxidase may also be used [15, 16, 17, 18].

The most commonly used oxygen scavenger for commercial purposes are iron powder satchets. These scavengers are based on the principle of oxidation in presence of moisture or lewis acids like $FeCl_3$ [19].

Materials and methods

The present study focused on the monitoring of Quantity of Mesophilic Aerobic and Facultative Anaerobic Microorganisms (QMAFAnM), yeasts, molds, acid value and peroxide value in cooked sausages.

Experimental design

Studies of oxygen scavenger were conducted to determine their impact on the final product during storage.

Industrial production «Austrian» cooked sausages of the first chop were investigated. Ingredients: meat 65% (pork, chicken meat), animal protein stabilizer, mechanically deboned poultry, whey powder, potato starch, egg powder, water, salt, spices and their extracts (nutmeg, black pepper, garlic, juniper, coriander, chilli, bay leaf), flavor enhancer, color retainer. Shelf life at temperature 0+ 6ºC, and relative humidity 75% – 78% – 3 days in the case of open packaging.

«Austrian» sausages were packaged with the following systems:

Sample 1 – control sample packed without oxygen scavengers, stored at 0+6 °C,

Sample 2 – sausage packed with ukrainian oxygen scavengers stored at 0+6 °C,

Sample 3 – sausage packed with chinese oxygen scavengers stored at 0+6 °C,

Sample 4 – sausage packed with chinese oxygen scavengers stored at +24+26 °C.

The sausages were stored at 0+6 ºC and +24+26 °C for 13 days. Analysis of unpacked cooked sausages was carried out on day 1, packed cooked sausages – on days 8 and 13 of storage.

Determination of the microbiological attributes

10 g of each sample were aseptically placed into a stomacher bag. Afterward, 90 cm^3 of Peptone Saline Solution (PSS) was added and homogenized using a stomacher for 60 s at room temperature. Serial 10-fold dilutions were prepared by diluting 1 cm^3 of homogenate in 9 cm^3 of PSS [20].

Serial decimal dilutions were inoculated (1 cm^3) onto nutrient agar for QMAFAnM and onto Sabouraud agar for yeasts and molds. Plates were incubated at 30±1 °C for 72 h for QMAFAnM and 24±1 °C for 120 h for yeasts and molds.

After incubation, two plates with nutrient agar and Sabouraud agar for each sampling point were counted. Results were expressed as a number of colony forming units per gram (cfu/g). All plates were examined visually for typical colony types and morphological characteristics that were associated with each growth medium.

Determination of the lipid oxidation

The method for determining the peroxide value is based on the reaction of the fat oxidation (peroxides and hydroperoxides) primary products interaction with potassium iodide in an acidic medium, followed by titration with a sodium thiosulfate solution and quantitative determination of the released iodine [21].

The method for determining the acid value is based on free fatty acids titration with a potassium hydroxide solution.

Results and discussion

Oxygen scavengers caracteristics

Oxygen scavengers active component is the iron activated form, which is standardized for its reactivity with oxygen in the moisture presence.

The oxygen scavenger functional ability to remove oxygen present in packaged sausages was examined. This ability characterized the oxygen scavenger effectiveness to modify the MAP by oxygen content in the system.

The decrease of oxygen concentration dynamics in different volumes (0,001 m^3 and 0,002 m^3) was investigated.

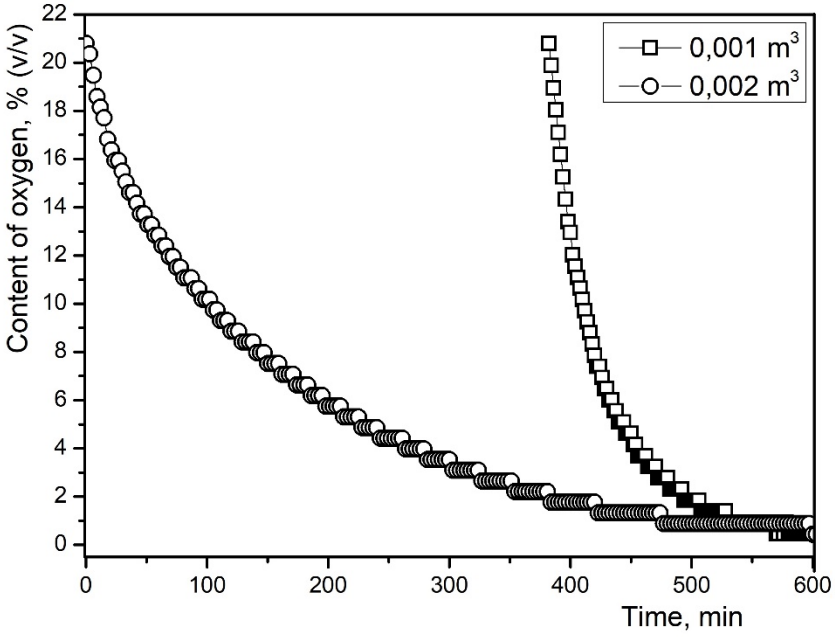

Figure 1. Oxygen concentration dynamics in different volumes with oxygen scavenger

Figure 1 shows that the oxygen complete removal time in the packed sample is reduced with reduce the volume from which oxygen is removed. In this case, this dependence is exponential. The oxygen concentration dynamics in this study is in accordance with previous studies [22].

In order to ensure the viability of the active packaging elements in the process of technological use, its ability to maximum oxygen removal with package partial depressurization was studied.

The studies were performed by measuring the oxygen concentration in a closed volume with the container subsequent opening.

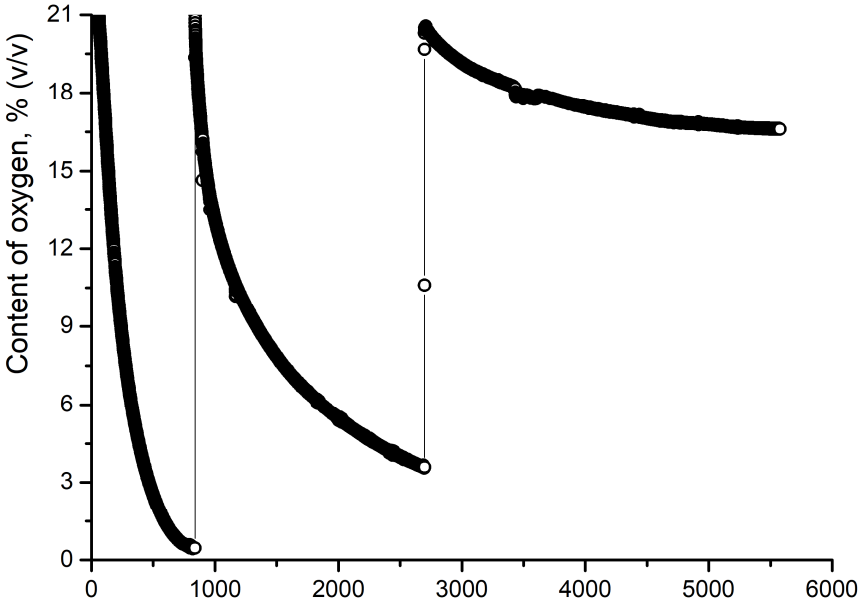

Figure 2. The action of ukrainian oxygen scavenger to restore MAP with package depressurization

From the minimum oxygen content renewal dynamics in the packaged samples shown in Figure 2, it can be seen that the ability to recover MAP only works when the packaging were opened once.

Figure 3 presents the oxygen removal kinetics in packaged sausages samples. The experimental packaging system contained the sausages sample with the oxygen scavenger had a 0,0005 m^3 volume.

The MAP modification kinetics of packaged sample (Figure 3) was consistent with the oxygen removal kinetics in a pressurization volume, which allows us to state that the sausages storage process is regulated.

Cooked sausage samples microbiological attributes

The changes in the cooked sausage QMAFAnM during storage are shown in Figure 4.

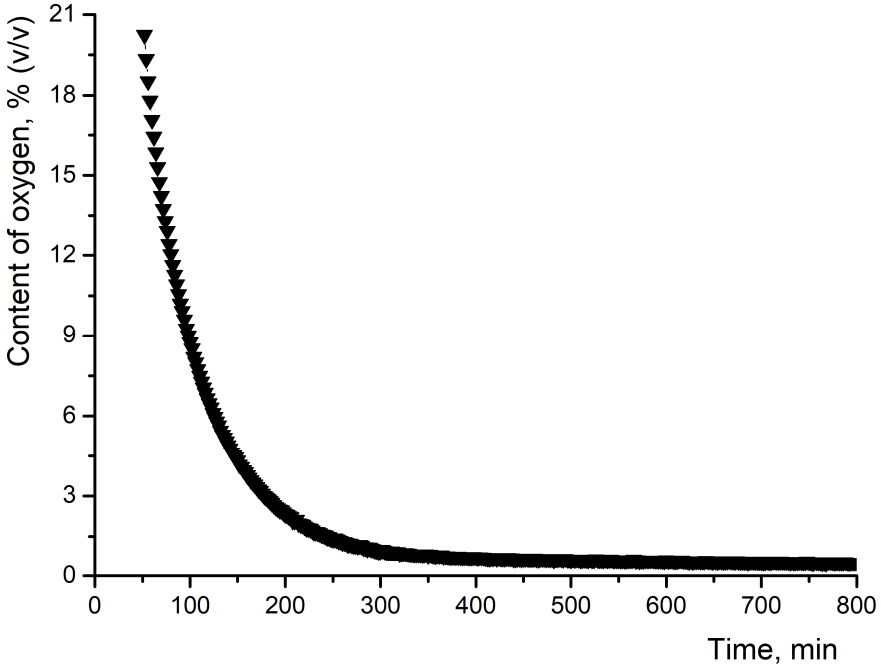

Figure 3. Oxygen removal kinetics in packaged sausages sample with oxygen scavenger

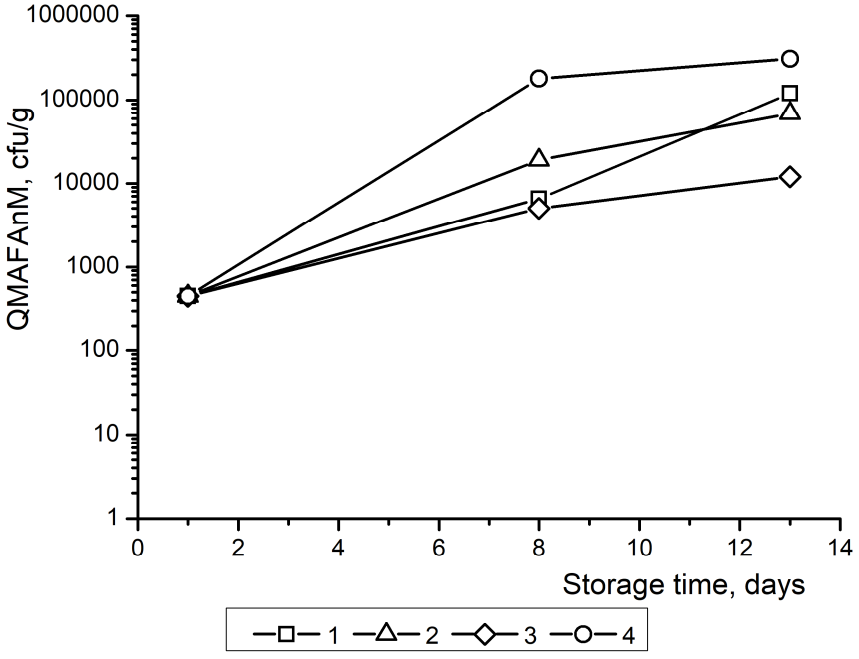

Figure 4. QMAFAnM changes in cooked sausage with different packaging d uring 13 days of storage

The QMAFAnM of unpacking samples was $4,5\times10^2$ cfu/g.

On the 8th day of storage QMAFAnM for samples with chinese oxygen scavengers and control stored at 0+6 °C were not significantly different ($5,0\times10^3$ cfu/g and $6,5\times10^3$ cfu/g, respectively) and were was significantly lower than the sample with ukrainian oxygen scavenger ($1,9\times10^4$ cfu/g). The maximum value was for sample 4 – $1,8\times10^5$ cfu/g.

On the 13th day of storage, QMAFAnM for sample 3 were lower than sample 2 ($1,2\times10^4$ cfu/g and $6,9\times10^4$ cfu/g, respectively). At the same time, this parameter was much higher for control and sample with oxygen scavenger stored at + 24 + 26 °C.

The initial population of moulds for unpacked sample was <10 cfu/g, initial population of yeasts for unpacked sample was 10 cfu/g.

The results of further studies are presented in Table 1.

Table 1

Changes of moulds in packed cooked sausage during storage

Days of storage	Moulds, cfu/g			
	Sample 1	Sample 2	Sample 3	Sample 4
8	$2,0\times10^1$	<10	<10	$5,0\times10^1$
13	$3,0\times10^1$	<10	<10	$5,0\times10^1$

Sample 2 and Sample 3 demonstrated stable meaning of moulds during entire research and were lower than counts from control. It can be concluded that use of oxygen scavengers effective for the inhibition of moulds.

The development of the yeasts for the samples is shown in Table 2.

Table 2

Changes of yeasts in packed cooked sausage during storage

Days of storage	Yeasts, cfu/g			
	Sample 1	Sample 2	Sample 3	Sample 4
8	$3,3\times10^2$	$2,0\times10^2$	$3,0\times10^2$	$3,0\times10^1$
13	$5,0\times10^2$	$4,6\times10^2$	$4,8\times10^2$	$7,0\times10^1$

All samples demonstrated yeasts increase during storage and no significant differences between were observed compared to control. So use of oxygen scavengers did not inhibit yeasts.

Oxygen is responsible for oxidation of food constituents and proliferation of aerobic bacteria and moulds resulting in quality losses due to changes in flavour, colour, texture and nutritive value, and therefore in a reduction of meat shelf life [23]. Those results clearly demonstrated the inhibitory effect on microbial growth of oxygen scavengers in accordance with previous reports [24].

Cooked sausage samples acid value and peroxide value

The kinetics of fat oxidation during the sausages storage was characterized by acid and peroxide values. The depth of the fat hydrolytic changes was determined use an acid value that shows the amount of free fatty acids formed during the fat hydrolysis.

The initial acid value for unpacking sausages on 1 storage day was 1,41 mg KOH/g.
The results of further studies are presented in Table 3.

Table 3

Changes of acid value in cooked sausage during storage

Days of storage	Acid value, mg KOH/g			
	Sample 1	Sample 2	Sample 3	Sample 4
8	2,91	3,11	3,09	4,11
13	3,98	3,57	3,76	4,46

The increase of acid value rate for the samples packed with oxygen scavenger stored at +24+26 °C was highest. At the same time, the sausages packed with oxygen scavengers stored at 0+6 °C acid value dynamics for 13 days of storage showed the slightest increase compared to the control, indicating the inhibition of the hydrolysis process.

To determine the primary oxidation products of sausages was evaluated peroxide value, with which you can determine the damage degree of fat, which affects the product shelf life.

For unpackaged sausages, the peroxide value was 1,98 ½Ommol/kg immediately.
The results of further studies are presented in Table 4.

Table 4

Changes of peroxide value in cooked sausage during storage

Days of storage	Peroxide value, ½Ommol/kg			
	Sample 1	Sample 2	Sample 3	Sample 4
8	2,42	2,58	2,34	3,41
13	4,05	3,14	3,36	4,72

The results obtained show that peroxide value increased more intensively for the samples packed with oxygen scavenger stored at + 24 + 26 °C. At the same time the oxygen scavengers use in samples stored at 0+6 °C slowed the oxidation processes.

These results are in line with the study of L. Martinez et al. in which samples with O_2 scavenger had the lowest values of pork sausages lipid oxidation and led to extension of shelf life due to low oxidation rates [25].

Conclusions

It has been found that with the reduced volume, the time of oxygen complete removal in the packed sample is reduced. In this case, this dependence is exponential.

The MAP modification kinetics of packaged sample was consistent with the oxygen removal kinetics in a pressurization volume, which allows us to state that the sausages storage process is regulated.

The QMAFAnM samples packed using oxygen scavenger stored at 0+6 °C increased more slowly compared to the control regardless of the origin of the scavenger. These samples also showed stable values of molds and yeasts at all control points.

Packaging with oxygen scavenger slows down the oxidation processes for cooked sausages compared to the control.

This allows recommend the use of oxygen scavenger for the cooked sausages packaging.

At the same time, the use of oxygen scavengers does not inhibit the development of yeast for cooked sausages, which needs further investigation.

References

1. Verbeke W., De Smet S., Vackier I., Van Oeckel M. J., Warnats N., Van Kenhove P., (2005), Role of intrinsic search cues in the formation of consumer preferences and choice for pork chops, *Meat Science*, 69(2), pp. 343–354.
2. Grobbel J. P., Dikeman M. E., Hunt M.C., Milliken G. A., (2008), Effects of packaging atmospheres on beef instrumental tenderness, fresh color stability, and internal cooked color, *Journal of Animal Science*, 86, pp. 1191–1199.
3. McMillin K. W. (2008), Where is MAP going? A review and future potential of modified atmosphere packaging for meat, *Meat Science*, 80, pp. 43–65.
4. Pasichnyj VM, Ukrainec AI, Khrapachov OV, Marynin AI (2017), Perspektyvy vykorystannja pakuval'nyh materialiv dlja termichnoi'obrobky m'jasa ta m'jasoproduktiv, *Tekhnika, energhetyka, transport APK*, 2(97), pp. 71–75.
5. Yam K. L., Takhistov P. T., Miltz J., (2005), Intelligent packaging: Concepts and applications, *Journal of Food Science*, 70(1), pp. 1–10.
6. Realini C. E. Marcos B. (2014), Active and intelligent packaging systems for a modern society, *Meat Science*, 98, pp. 404–419.
7. Fang Z., Zhao Y., WarnerR. D., Johnson S. K., (2017), Active and intelligent packaging in meat industry, *Trends in Food Science Technology*, 61, pp. 60–71.
8. de Kruijf N., van Beest M., Rijk R., Sipiläinen-Malm Losada P. P., De Meulenaer B., (2002), Active and intelligent packaging: applications and regulatory aspects, *Food Additives and Contaminants*, 19, Supplement, pp. 144–162.
9. Ozdemir M., Floros J. D. (2004), Active food packaging technologies, *Critical Reviews in Food Science and Nutrition*, 44(3), pp. 185–193.
10. Lange J., Wyser Y. (2003), Recent innovations in barrier technologies for plastic packaging-a review, *Packaging Technology and Science*, 16(4), pp. 149–158.
11. Chaix E., Guillaume C., Guillard V. (2014), Oxygen and carbon dioxide solubility and diffusivity in solid food matrices: A review of past and current knowledge, *Comprehensive Reviews in Food Science and Food Safety*, 13(3), pp. 261–286.
12. Vermeiren L., Devlieghere F., Van Beest M., de Kruijf N., Debevere J. (1999), Developments in the active packaging of foods, *Trends in Food Science and Technology*, 10, pp. 77–86.
13. Suppakul P., Miltz J., Sonneveld K., Bigger S.W. (2003), Active packaging technologies with an emphasis on antimicrobial packaging and its applications, *Journal of Food Science*, 68, pp. 408–420.
14. Otoni C. G., Espitia P. J. P., Avena-Bustillos R. J., McHugh T. H., (2016), Trends in antimicrobial food packaging systems: Emitting sachets and absorbent pads, *Food Research International*, 83, pp. 60–73.
15. Brody A. L., Bugusu B., Han J. H., Sand C. K., McHugh T. H. (2008), Innovative food packaging solutions, *Journal of Food Science*, 73, pp. 107–116.

16. Yu J., Liu R. Y. F., Poon B., Nazarenko S., Koloski T., Vargo T., (2004), Polymers with palladium nanoparticles as active membrane materials, *Journal of Applied Polymer Science, 92*(2), pp. 749–756.
17. Hamilton R. J., Kalu C., Prisk E., Padley F. B., Pierce H. (1997), Chemistry of free radicals in lipids, *Food Chemistry, 60*(2), pp. 193–199.
18. Sangatash M. M., NiazmandR., Jamab M. S., Modaressi A. S., (2016), Development of antioxidant active films containing sodium ascorbate (SA) and ethylene vinyl alcohol (EVOH) to extend the shelf life of peanut, *Journal of Food Science Technology, 53*(4), pp. 1766–1783.
19. Cruz R. S., Soares N. D. F. F., Andrade N. J. D. (2006), Evaluation of oxygen absorber on antimicrobial preservation of lasagna–type fresh pasta under vacuum packed, *Ciencia E Agrotecnologia,* 30(6), pp. 1135–1138.
20. Ukrainets A., Pasichniy V., Zheludenko Yu., Zadkova S. (2016), Oleoresins effect on cooked poultry sausages microbiological stability, *Ukrainian Food Journal*, 5 (1), pp. 124–134.
21. Bozhko N., Tischenko V., Baidak L., Pasichnyi V. (2018), Evaluation of rosemary extract effectiveness in the technology of meat–containing sausages with duck meat *Ukrainian Food Journal*, 7 (1), pp. 54–64.
22. Hutter S., Ruegg N., Yildirim S. (2016), Use of palladium based oxygen scavenger to prevent discoloration of ham, *Food Packaging and Shelf Life*, 8, pp. 56–62.
23. Brody A.L., Strupinsky E.R., Kline L.R. (2001), *Active packaging for food applications*, Technomic Publishing Company, Lancaster.
24. Kerry J.P., O'Grady M.N., Hogan S.A. (2006), Past, current and potential utilisation of active and intelligent packaging systems for meat and muscle–based products: A review, *Meat Science*, 74, pp. 113–130.
25. Martinez L., Djenane D., Cilla I., Beltran J. A., Roncales P., (2006), Effect of varying oxygen concentrations on the shelf–life of fresh pork sausages packaged in modified atmosphere, *Food Chemistry*, 94, pp. 219–225.

Physicochemical composition and FTIR characterization of castor seed oil

Tarique Panhwar[1], Sarfaraz Ahmed Mahesar[1], Aftab Ahmed Kandhro[2], Syed Tufial Hussain Sheerazi[1], Abdul Hameed Kori[1], Zahid Hussain Laghari[1], Jamil-ur-Rehman Memon[2]

1 – National Centre of Excellence in Analytical Chemistry, University of Sindh, Pakistan
2 – Dr. M. A. Kazi Institute of Chemistry, University of Sindh, Pakistan

Keywords:

Oil
Castor
Seed
FTIR

Article history:

Received 14.02.2019
Received in revised form 25.08.2019
Accepted 28.11.2019

Corresponding author:

Tarique Panhwar
E-mail: panhwertarique@gmail.com

DOI: 10.24263/2304-974X-2019-8-4-9

Abstract

Introduction. This paper provides the complete profile of physicochemical properties and fatty acid composition of local castor varieties from Sindh, Pakistan. Initially, physical characteristics of seeds were studied followed by detailed examination of oil.

Materials and methods. Oil was extracted through Soxhlet extraction method followed by physico–chemical examination of necessary parameters (iodine value, peroxide value, saponification value, viscosity and moisture). For qualitative analysis of castor oil GCMS and FTIR instruments were used.

Results and discussions. Oil content was observed in the range of 44–48%. Moisture and ash content of castor seeds were found to be 4.22–5.16% and 5.66–6.49%, respectively. Compositional analysis by GCMS has shown ricinoleic acid (88.5–93.1%) as a prominent fatty acid in all local varieties. Other fatty acids present were palmitic (0.4–0.8%), stearic (0.8–1.0%), linoleic (2.8–3.3%), and ecosenoic (0.2–1.5%). Free fatty acid value of all castor oil varieties was found to be in the range of 0.16–0.53%. Other quality parameters such as IV, PV and SV of different castor oil varieties were determined in the range of 79.16–90.03 gI_2/100g, 1.62–1.89 meq/Kg, and 188.12–204.76 mgKOH/g, respectively. The FTIR spectra of castor seed oil varieties were nearly similar. On careful examination of the intensity values of each functional group present in the oil showed some variations in castor seed varieties.

Conclusion. Indigenous local varieties of castor with sufficient oil content (> 40%) were explored and examined for some important parameters. FTIR band intensities of some functional groups highly correlated with important parameters of castor oil.

Introduction

Castor is one of the most promising non-edible oil seed crop with great industrial importance, grown all over the world in warm temperate, tropical and subtropical regions [1]. Castor belongs to Eurphorbiaceae family and botanically known as *Ricinus Communis* L. [2]. The purpose of cultivation of castor plant is because of its seeds that have high oil content. The oil is pale yellow in color, viscous in nature with a lot of applications in industrial and medicinal fields [3].

Since the fatty acid composition consists of about 90% ricinoleic acid and other fatty acids include oleic acid 2.8%, palmitic acid 0.7%, stearic acid 0.9%, linoleic acid 4.4%, and linolenic acid 0.2% [4]. The unique properties of castor oil among other vegetable oils are due to the ricinoleic acid (a unique fatty acid $C_{18}H_{34}O_3$) known as cis-12-hydroxyoctadeca-9-enoic acid. Castor oil has relatively high viscosity, specific gravity and solubility in alcohols due to high hydroxyl value in the nature [5].

Castor oil is widely used as a raw ingredient in the manufacture of pharmaceuticals, cosmetics, coatings, soap, nylon, lubricants, dyes, inks, and waxes [6]. More over castor oil is used in various industrial fields as a potential by product [7]. Castor oil has limited food value and do not compete with food crops [3]. It is mainly cultivated for trading purpose in more than 30 countries of the world in the area of 1.525 million hectares, which produce 1.58 million tons of seed. Major castor growing countries are India, Brazil, China, Thailand, Russia, Ethiopia and Philippines [8]. India has major contribution of 65% of castor oil all over the world, thus fulfils 80 to 90% of world's requirement of ricinus oil [1].

Pakistan is agricultural country with 70% population belongs to an agriculture sector [9]. Pakistan has total area of 79.6 million hectares, 70% of which is arid to semi-arid. The total unused land is about 28 million hectares, due to shortage of water, severe heat and saline nature of soil, the large area of land is unproductive [9, 10, 11] and therefore castor plant has potential to grow on marginal lands as compared to other non-edible oil yielding plants [12].

A sufficient research work has been reported on physicochemical characteristics of castor oil [2,13] and its fatty acid composition [5]. However, a limited work is done on searching new varieties of castor seed for complete profiling. The current study presents some more aspects to study new castor varieties, which include complete profiling of castor seed in the light of environmental factors such as light, altitude, latitude and soil type. Furthermore, FTIR study was also carried out to characterize castor oil and correlated with the physiochemical properties.

Materials and methods

Reagents and sample collection

All the chemicals and reagents used in the present work were purchased from E-Merck (Darmstadt, Germany). Castor beans were collected from fifteen different locations of Sindh province. Some harvesting sites had different environmental conditions and soil types. Five locations were selected within the same environmental conditions. The plants at different sites showed variability in their height. Branch distribution in castor plant was ramified. Sites 1-5 belong to middle region of Sindh province, where luminosity exposure was observed. The region has low humidity with temperature of 40–50 °C throughout the growing season and type of soil was non-sodic, non-saline and alluvium in nature having more ratios of silt and clay with moderate level of water observed at sites. Sites 6–10 belong to downstream of

Sindh province with the temperature of 35 °C with humidity of about 60%. Soil was rocky, slightly saline with little water present in the area. Sites 11–15 also come in downstream with the temperature of 35 °C. Soil was fertile, non-sodic, non-saline. The collected castor seeds were broken off and packed in clean sampling bags until analysis.

Classification

Castor seeds were classified on the basis of color, plant characteristics, and seed weight. On the basis of classification, the collected castor seeds generated three new local varieties. These newer local varieties were coded as S-1, S-2 and S-3. All castor varieties were dried and cleaned in order to remove some foreign materials and stored at room temperature in the absence of light.

Oil extraction

Crude oil from castor beans was extracted by Soxhlet extraction method using n-hexane as a solvent with slight modification as reported by Akpan *et al.,* 2006 [13]. Finely ground 10g of sample were put into thimble and carefully placed inside the Soxhlet extractor, then 300 mL of n-hexane was added to round bottom flask. The process continued for about 6 h at 65 °C. After complete extraction hexane was evaporated using rotary evaporator (Buchi, Switzerland). For total oil content, weight of the extracted oil was measured using electronic balance. The oil was kept at low temperature for further physicochemical analysis.

Physicochemical analysis of seed and oil

Seed characteristics. Some physical characteristics of castor seeds of different varieties were analyzed such as seed color, weight, thickness, length and weight of 100-seeds. Specific gravity and refractive index were measured according to reported method [13].Viscosity of oil samples was measured using a viscometer (VM 3000 stabinger Anton Park, Austria) at 40 $^{\circ C}$ using 5 mL of sample. Ash content was determined by AOCS (method Ba 5a-49) [14]. Moisture content measurement was done by drying up to constant weight at 105 $^{\circ C}$ [15].

Chemical analysis. For the chemical characteristics official methods of AOCS were used for the determination of iodine value (IV method- Cd 1-25), peroxide value (PV method-Cd 8-53), saponification value (SV method-Cd 3-25) and free fatty acids (FFA method- Aa 6-38)[14].

FTIR analysis of castor oil. For the qualitative analysis of castor oil, infrared (IR) spectra were recorded using FTIR spectrometer (Thermo Nicolet Avatar 330) with a DTGS detector (Thermo Nicolet Analytical Instruments, Madison, WI). The removable (ZnSe crystal) single bounce-attenuated total reflection (ATR) accessory was used for oil analysis with the conditions as follows: resolution 4 cm^{-1}, scans 32, IR range 4000–650 cm^{-1}. The background spectrum was recorded before the sample analysis. After recording the spectra ZnSe crystal was carefully cleaned with hexane to remove any residue of the previous sample.

Determination of fatty acid composition. Fatty acid methyl esters (FAMEs) were prepared according to official IUPAC method No: 2.30 [16]. A complete profile of fatty acid composition including major and minor fatty acids was studied using GC-MS (Agilent 5975 GC-MSD) with chemstation 6890 Scale mode software. FAMEs were analyzed using Agilent autosampler 7683-B injector (Agilent Technologies, Little Fall, NY, USA), a HP-5MS (5% phenyl methylsiloxane) capillary column with dimension of 30 m, i.d 0.25 mm. The initial temperature was set as 150 $^{\circ C}$ and maintained for 2 min then raised to 220 °C at a ramp of 3

°C/min and finally held for 15 minutes. Carrier gas used was helium at a flow rate of 1.5 mL/min. About 2-µL of FAMEs were injected into the column using split mode injection system. The mass spectrometer was operated using electron impact mode at 70eV in the scan range of 50-550 m/z. GC-MS chromatograms were compared with two libraries (NIST and Wily) which provided much information about major and minor fatty acids in castor oil.

Statistical analysis

Two samples of each variety (1 kg each) were collected and every sample was analyzed thrice and the obtained results were reported as mean±standard deviation, by using Microsoft® excel 2003 software.

Results and discussion

Table 1A shows the geographical locations of three different castor seed harvesting sites. S-1 variety was collected from sites 1–5, S-2 variety from sites 6-10 and S-3 variety from sites 11–15. Table 1B represents physical characteristics of three different castor seed varieties. Some variations among different varieties were found; this might be due to different environmental conditions and soil types [17]. Moisture and ash content of castor seeds showed little variability as shown in Table 1B. Moisture and ash content of castor seeds were found to be 4.22–5.16% and 5.66–6.49%, respectively.

Table 2 shows the proximate composition along with some quality attributes of different castor varieties. A significant variability was found in the oil content of studied castor seed varieties that ranged from 44–48%. The obtained values showed less oil content than indigenous variety reported earlier [18]. Observed variations in the seed oil content may be due to castor seed genotypes, harvesting time, environmental and cultural aspects.

Refractive index, specific gravity and viscosity in castor varieties were found in the range of 1.4321–1.4532, 0.9531–0.9576 g/cm^{-3} and 663–713 *m*Pas.s, respectively. The high viscosity of castor oil is due to the presence of long chain carbon atoms which mainly consist of ricinoleic acid; a mono-saturated, 18-carbon fatty acid having hydroxyl group at 12th carbon, a very uncommon property for a biological fatty acids which makes it unique oil from other vegetable oils.

The chemical parameters such as IV, PV and SV of different varieties were determined in the range of 79.16–90.03 gI_2/100g, 1.62–1.89 meq/Kg, and 188.12–204.76 mgKOH/g, respectively. The quality of oil depends on the presence of FFA. Generally these values are calculated as percentage of oleic acid. In current study, the range of FFA in castor varieties was determined as 0.16–0.53%. These values are almost comparable to freshly processed vegetable oils [19].

Table 1A

Site coordinates where the castor beans were harvested

Site	Elevation (m)	Latitude	Longitude
1	24	26.73° N	67.78° E
2	42	26.41° N	67.37° E
3	43	26.56° N	67.71° E
4	43	26.86° N	67.78° E
5	41	26.42°N	67.86°E
6	38	25.41°N	68.27°E
7	29	25.90°N	68.24°E
8	39	25.35°N	68.26°E
9	39	26.03°N	68.13°E
10	38	25.28°N	68.15°E
11	24	25.38°N	68.36°E
12	25	25.42°N	68.54°E
13	21	25.52°N	69.01°E
14	22	25.45°N	68.72°E
15	26	25.76°N	68.66°E

Table 1B

Physical characteristics of castor seeds

Mean±SD								
Seed Variety	**Qualitative description**	**Moisture (%)**	**Ash (%)**	**Length (mm)**	**Thickness (mm)**	**Width (mm)**	**Seed weight (g)**	**100-seed weight (g)**
S-1	Brownish	4.22 ±0.21	5.88 ±0.23	11.55 ±0.39	5.47 ±0.40	7.62 ±0.31	0.40 ±0.08	38.86 ±0.14
S-2	Light brown	5.16 ±0.15	6.49 ±0.19	12.19 ±1.02	5.20 ±0.50	7.21 ±0.96	0.34 ±0.04	35.18 ±0.20
S-3	Reddish brown	4.46 ±0.12	5.66 ±0.12	12.55 ±1.49	6.10 ±0.75	7.88 ±0.58	0.48 ±0.12	39.60 ±0.10

Table 2

Proximate composition and quality attributes of castor varieties

Variety	Oil content %	Specific gravity at 28 °C (g/cm^{-3})	Viscosity at 28 °C (*m*Pas.s)	RI at 28 °C	FFA %	IV gI_2/100g	PV meq/Kg	SV mgKOH/g
S-1	48 ±1.21	0.9531 ±0.02	681 ±9.11	1.4321 ±0.05	0.16 ±0.006	80.34 ±1.55	1.89 ±0.05	197.35 ±1.81
S-2	44 ±1.38	0.9576 ±0.03	713 ±8.59	1.4385 ±0.04	0.27 ±0.01	90.03 ±1.33	1.87 ±0.06	204.76 ±2.13
S-3	46 ±1.22	0.9563± 0.01	663 ±8.87	1.4532 ±0.06	0.53 ±0.02	79.16 ±1.12	1.62 ±0.03	188.12 ±1.93

Knowledge of fatty acid profile is much essential for industrial sectors including energy, cosmetic and soap making industries [20]. Table 3 represents the fatty acid composition of extracted oil of castor seed varieties. Analysis showed that the most abundant fatty acid in each variety was ricinoleic acid; found as 88.5%, 90.9% and 93.1% respectively in S-1, S-2 and S-3. Other fatty acids present were palmitic (0.4-0.8%), stearic (0.8–1.0%), linoleic (2.8-3.3%), and ecosenoic (0.2–1.5%). Three different isomers of oleic acid were also detected in castor varieties such as oleic n-9 (2.6–4.3%), oleic n-10 (0.4–0.5%), and isomeric oleic n-11 was also found at 0.2%. Ricinoleic acid is the prominent fatty acid found in castor varieties. The obtained values of this unique fatty acid are even higher than Malaysian (84.2%), Egyptian (81.9%), and Brazilian (90.2%) castor varieties. Whereas all studied varieties showed lower recinoleic acid content than Indian castor varieties. Presence of high content of ricinoleic acid represents good quality of oil.

Table 3

Fatty acid composition of extracted castor seed oil from three varieties of Sindh Pakistan

Variety	$C_{16:0}$	$C_{18:0}$	$C_{18:1\ n9}$	$C_{18:1\ n10}$	$C_{18:1\ n11}$	$C_{18:2\ n9,\ 12}$	$C_{20:1\ n11}$	$C_{18:1\ n9,12\text{-}OH}$
S-1	0.8±0.02	0.9±0.01	4.3±0.1	0.5±0.02	-	3.3±0.1	1.5±0.05	88.5±3.1
S-2	0.7±0.01	1.0±0.03	3.8±0.09	0.4±0.01	-	3.2±0.1	-	90.9±2.9
S-3	0.4±0.01	0.8±0.02	2.6±0.1	-	0.2±0.01	2.8±0.09	0.2±0.01	93.1±3.3

Table 4 represents the comparative data of fatty acid profile of current varieties with Malaysian, Indian, Brazilian, Egyptian and indigenous castor variety from this region. The two fatty acids including isomers of oleic acid (C18:1 n10) and ecosenoic acid (C20:1 n11) were present in indigenous varieties but both were absent in varieties of other countries. The total unsaturated fatty acid content was higher than Malaysian, Brazilian, Indian and Egyptian varieties.

Table 4

Comparison of fatty acid composition of castor varieties with world varieties

Fatty acid (%)	Current Study	Indigineous[a]	Malaysia[b]	Brazil[c]	India[d]	Egypt[e]
Palmitic; $C_{16:0}$	0.4-0.8	0.31	1.3	0.7	-	1.6
Stearic; $C_{18:0}$	0.8-1.0	0.45	1.2	0.9	1.0	3.4
Oleic; $C_{18:1\ n9}$	2.6-4.3	2.05	5.5	2.8	-	8.3
Oleic; $C_{18:1\ n10}$	0.4-0.5	0.22	-	-	-	-
Oleic; $C_{18:1\ n11}$	0.2	-	-	-	-	-
Linoleic; $C_{18:2\ n9,12}$	2.8-3.3	1.84	7.3	4.4	4.3	4.7
Linolenic; $C_{18:3}$	-	-	0.5	0.2	-	-
Ricinoleic; $C_{18:1\ n9,\ 12\text{-}OH}$	88.1-93.1	94.59	84.2	90.2	94.0	81.9
Ecosenoic; $C_{20:1\ n11}$	0.2-1.5	0.53	-	-	-	-
Saturated fatty acids (SFA)	1.5-1.7	0.76	2.5	1.6	1.0	5.0
Unsaturated fatty acids (UFA)	98.1-98.9	99.23	97.5	97.6	98.3	94.9

[a]Panhwar *et al.* (2016) [18], [b]Salimon *et al.* (2010) [2], [c]Conceicao *et al*. (2007) [4], [d]Gupta *et al*. (1951) [23], [e]Algharib and Kotb (2013) [24].

FTIR Analysis of Castor Seed Oil

The FTIR spectra of castor varieties were nearly similar and no significant difference served as shown in Figure 1. For the identification of functional groups and bands corresponding to various stretching and bending vibrations, which clearly indicates the different characteristic bands of the expected functional groups. The band at 3424 cm^{-1} represents the O-H stretching vibrations which clearly indicate the presence of hydroxylated ricinolic acid (prominent peak of castor oil). The band at 3007 cm^{-1} represents -C-H stretching vibrations of cis- double bond of unsaturation, whereas the band at 2922 and 2855cm^{-1} are characteristics of assymetrical and symmetrical vibrations of aliphatic $–CH_2$ fatty acid hydrocarbon chain [21,22]. The ester carbonyl (C=O) functional group shows characteristic stretching band of triglyceride at 1739 cm^{-1}. The bending vibrations of $–CH_2$ scissoring aliphatic groups observed at 1455 cm^{-1}, while the band at 1366 and 1235 cm-1 are due to bending vibration of $–CH_2$ groups. The bands at 1235, 1160, 1089 and 1040 cm^{-1} belongs to bending vibrations of ester carbonyl group. The band at 971 cm^{-1} reveal the presence of–HC=CH-(*trans*) bending out of plane. The band at 858 cm^{-1} is for $=CH_2$ wagging vibrations. However the band at 719 cm^{-1} is due to overlapping of $–CH_2$ rocking out of plane vibration of cis-disubstituted olefins, characteristics of long chain fatty acids.

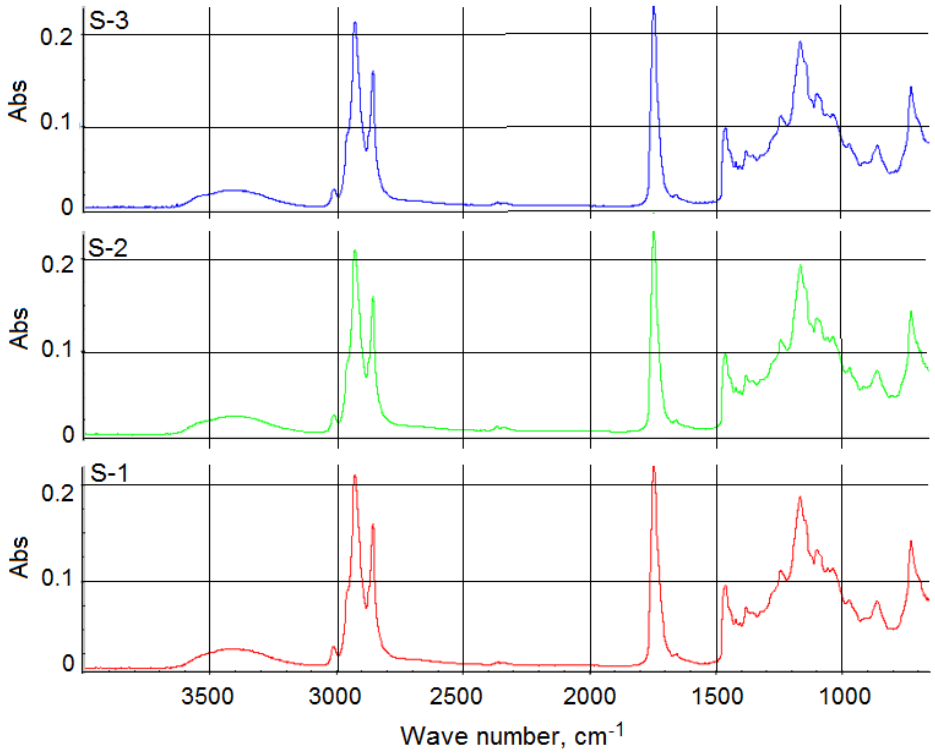

Figure 1. FTR Spectra of three castor seed oil varieties

Correlation of IR band intensity with physicochemical properties of castor oil

As mentioned earlier that no significant differences was observed in the spectra of castor seed varieties. On careful examination of the intensity values of each functional group present in the oil showed some variations in castor seed varieties as shown in Table 5. Therefore, attempt was made to correlate the intensities of different functional groups with the physiochemical properties of castor oil. The band at 3421cm^{-1} showed correlation with the values of specific gravity as it can be seen from Table 2. The highest specific gravity was observed in S-2 and lowest in S-1, similarly higher intensity was observed in S-2 and lower in S-1. FFA showed correlation with the intensity of band at 3007cm^{-1} as it can be seen from Table 2, the highest FFA was noted in S-3 and lower in S-1. Usually band at 1709 cm^{-1} has been reported for FFA determination. As this band is completely absent in all castor varieties, therefore band at 3007 cm^{-1} was selected. The band at 1742 cm^{-1} was linked with the SV of castor oil. Higher and lower SV was observed in S-2 and S-3 variety, similarly higher and lower intensities were also observed in S-2 and S-3, respectively. Table 2 further shows highest values of IV in S-2 variety and lowest IV in S-3, likewise IV was correlated with the intensity of band at 1652 cm^{-1}. It is well known fact that castor oil show high values of viscosity. Among three varieties, highest viscosity was observed in S-2, while lowest in S-3 variety. These viscosity values highly correlated with the intensity of band at 1457 cm^{-1}, which showed similar trend. The band at 1377 cm^{-1} showed correlation with the values of refractive index. The highest and lowest refractive index value was observed in S-3 and S-1, similarly higher intensity was observed in S-2 and lower in S-1, respectively. PV also showed correlation with two infrared bands at 1161 cm^{-1} and 1096 cm^{-1}. As it can be seen from Table 2, that highest PV was observed in S-1 and lowest in S-3. Similar trend in higher and lower intensity was observed in S-1 and S-3.

Table 5

FTIR spectral intensity of functional groups of castor seed oil

S.No.	Frequency (cm^{-1})	Intensity			Observation
		S1	S2	S3	
1	3421	0.0273	0.0279	0.0276	O─H stretching
2	3007	0.0288	0.0293	0.0297	C-H stretching vibration of the *cis*-double bond (=CH)
3	2923	0.212	0.213	0.210	CH_2 Asymmetrical stretching
4	2853	0.159	0.159	0.158	CH_2 Symmetrical stretching
5	1742	0.232	0.233	0.221	C=O stretching
6	1652	0.0232	0.0240	0.0226	C=C Stretching
7	1457	0.0958	0.0972	0.0945	CH_2 Scissors
8	1377	0.0714	0.0716	0.0718	Bending vibration of CH_2 groups
9	1239	0.109	0.110	0.110	Vibrations of the C─O ester groups
10	1161	0.193	0.192	0.188	
11	1096	0.136	0.135	0.131	
12	1031	0.112	0.111	0.112	
13	965	0.0784	0.0789	0.0789	CH=CH (*trans*) bending out of plane
14	858	0.0765	0.0771	0.0777	=CH_2 Wagging
15	723	0.140	0.141	0.141	Overlapping of the CH_2 rocking vibration and the out-of-plane vibration of *cis*-disubstituted olefins

Conclusion

The current investigation on indigenous local castor seed varieties encourages their commercialization to increase economic growth at national level. A complete profile of local varieties showed sufficient oil content (44–48%). Fatty acid examination by GCMS has shown ricinoleic acid in high percentage. Some unusual fatty acids like isomers of oleic acid and eicosenoic acid were also determined and reported in local varieties from this region. FTIR study revealed the correlation of band intensities with physiochemical characteristics of castor seed oil such as specific gravity, free fatty acids, saponification value, iodine value, viscosity, refractive index and peroxide value.

Acknowledgments. The National Centre of Excellence in Analytical Chemistry, University of Sindh, Jamshoro, Pakistan is gratefully acknowledged for the financial support. The authors also would like to thank Higher Education Commission (HEC), Pakistan.

References

1. Ramanjaneyulu A.V., Reddy A.V., Madhavi A. (2013), The impact of sowing date and irrigation regime on castor (Ricinuscommunis L.) seed yield, oil quality characteristics and fatty acid composition during post rainy season in South India, *Ind. Crops Prod,* 44, pp. 25–31.
2. Salimon J., Noor D.A.M., Nazrizawati A.T., Firdaus M.Y.M., Noraishah A. (2010), Fatty Acid Composition and Physicochemical Properties of Malaysian Castor Bean Ricinuscommunis L. Seed Oil, *Sains Malaysiana*, 39(5), pp. 761–764.
3. Ogunniyi D.S. (2006), Castor oil: A vital industrial raw material, *Biores. Technol,* 97, pp. 1086–1091.
4. Conceição M.M., Candeia R.A., Silva F.C., Bezerra A.F., Fernandes, Jr V.J., Souza A.G. (2007), Thermoanalytical characterization of castor oil biodiesel, *Renew. Sust. Energ. Rev,* 11, pp. 964–975.
5. Perdomo F.A., Acosta-Osorio A.A., Herrera G., Vasco-Leal J.F., Mosquera-Artamonov J.D., Millan-Malo B., Rodriguez-Garcia M.E. (2013), Physicochemical characterization of seven Mexican Ricinuscommunis L. seeds & oil contents, *Biomass Bioenerg,* 48, pp. 17–24.
6. Berman P., Nizri S., Wiesman Z. (2011), Castor oil biodiesel and its blends as alternative fuel, *Biomass Bioenerg,* 35, pp. 2861–2866.
7. Amara A.A., Salem S.R. (2009), Dehydration of castor oil and lipase production by pseudomonas aeruginosa, *American-Eurasian J. Agric. Environ. Sci,* 5(4), pp. 556–563.
8. Damodaram T., Hegde D.M. (2011), Oilseeds Situation: A Statistical Compendium, Directorate of Oilseeds Research, Hyderabad.
9. Khan N.A., Dessouky H. (2009), Prospect of biodiesel in Pakistan, *Renew. Sust. Energy Rev,* 13, pp. 1576–1583.
10. Cheema N.A., Farooq U., Shabbir G., Shah M.K.N., Musa M. (2013), Prospects of castor bean cultivation in rainfed tract of Pakistan, *Pak. J. Bot,* 45(1), pp. 219–224.
11. Soil Survey of Pakistan, Available at: www.pakistan.gov.pk/divisions/food-division.

12. Chakrabarti M.H., Ahmad R. (2008), Transesterification studies on castor oil as a first step towards its use in Bio Diesel production, *Pak. J. Bot,* 40(3), pp. 1153–1157.
13. Akpan U.G., Jimoh A., Mohammed A.D. (2006), Extraction, Characterization and Modification of Castor Seed Oil, *Leonardo J. Sci*, 8, pp. 43–52.
14. AOCS. (2013), *Firestone D. 6th Edition. Official Methods of Analysis*, Association of Analytical Chemistry, Inc. Arlington, USA.
15. Nikovska K., Stefanova S., Stefanov L., Damyanova S., Stoyanova A., Gubenia O. (2017), Influence of adding of laurel essential oil extracts on salad dressings properties, *Ukrainian Food Journal*, 6(3), pp. 433–442.
16. International Union of Pure and Applied Chemistry. (1992), Standards methods for the analysis of oils, fats and derivatives, 7th edition. Alden Press, Oxford.
17. Cheema N.M. (2011), *Yield and chemical composition of castor bean (Ricinuscommunis L.) as influenced by environment, Ph.D. thesis UAAR*, Rawlpindi, Pakistan.
18. Panhwar T., Mahesar S.A., Mahesar A.W., Kandhro A.A., Talpur F.N., Laghari Z.H., Chang A.S., Sherazi S.T.H. (2016), Characteristics and composition of high oil yielding castor variety from Pakistan, *J. Oleo Sci,* 65(6) pp. 471–476.
19. Kandhro A., Sherazi S.T.H., Mahesar S.A., Bhanger M.I., Talpur M.Y., Arain S. (2008), Monitoring of Fat Content, Free Fatty Acid and Fatty Acid Profile Including trans Fat in Pakistani Biscuits, *J. Am. Oil Chem. Soc,* 85, pp. 1057–1061.
20. Nangbes J.G., Nvau J.B., Buba W.M., Zukdimma A.N. (2013), Extraction and Characterization of Castor (RicinusCommunis) Seed Oil, *Int. J. Eng. Sci,* 2, pp. 105–109.
21. Mahesar S.A., Sherazi S.T.H., Kandhro A.A., Bhanger M.I., Khaskheli A.R., Talpur M.Y. (2011), Evaluation of important fatty acid ratios in poultry feed lipids by ATR FTIR–spectroscopy, *Vibr. Spectrosc,* 57.
22. Sherazi S.T.H., Kandhro A., Mahesar S.A., Bhanger M.I., Talpur M.Y., Arain S. (2009), Application of transmission FT-IR spectroscopy for the trans fat determination in the industrially processed edible oils, *Food Chem,* 114, pp. 323–327.
23. Gupta S.S., Hilditch T.P., Riley J.P. (1951), The Fatty Acids and Glycerides of Castor Oil, *J. Sci. Food Agric,* 2(6), pp. 245–251.
24. Algharib A.M., Kotb E.A. (2013), Biodiversity of castor bean in Egypt for the potential possibility of using as a bioenergy crop, *The 3rd International Conference on: Neglected and Underutilized Species (NUS): for a Food–Secure Africa Accra, Ghana, 25–27 September 2013.*

Obtaining of β-LG, α-LA and BSA protein fractions from milk whey

Volodymyr Yukalo[1], Kateryna Datsyshyn[1], Olga Krupa[1], Natalia Pavlistova[2]

1 – Ternopil Ivan Puluj National Technical University, Ternopil, Ukraine
2 – Mogilev State University of Food Technologies, Mahilyow, Republic of Belarus

Keywords:

Milk
Whey
Proteins,
Disc-electrophoresis

Article history:

Received 14.12.2018
Received in revised form 20.05.2019
Accepted 28.11.2019

Corresponding author:

Olga Krupa
E-mail:
cmakota@ukr.net

DOI: 10.24263/2304-974X-2019-8-4-10

Abstract

Introduction. The purpose of the work is to obtain the protein fractions β-LG, α-LA and BSA from the milk whey by preparative disc-electrophoresis.

Materials and methods. The whey was obtained from the fresh cow's milk after isoelectric precipitation of casein complex proteins. The concentration of whey proteins was determined on a spectrophotometer by the absorption at λ = 280 nm. Gel filtration was carried out on liquid chromatography columns. Sephadexes G-25 and G-100 were used for the gel filtration. The fractional composition and homogeneity of whey proteins were analyzed by disc-electrophoresis in the polyacrylamide gel slabs.

Results and discussion. A system of disc-electrophoresis in native conditions for acidic and neutral proteins has been selected for the preparative isolation of homogeneous fractions of bioactive peptides proteins-precursors from milk whey taking into account the effectivety and existence of denaturation factors. A sample of whey proteins, for preparative fractionation purified, from low molecular weight compounds had been obtained at the result of the gel filtration.

An optimal whey proteins sample amount should not exceed 10 ml to provide an effective separation in a modified electrophoretic chamber of Studier type apparatus. Too large sample amount does not allow to separate the whey proteins effectively and obtain the homogeneous fractions extraction. The duration of the extraction process of individual protein fractions after preparative disc-electrophoresis was about 55–60 min.

The degree of homogeneity of the obtained protein fractions was established with the help of analytical disc-electrophoresis. It was 95–97% for β-LG and BSA fractions and 89–91% for α-LA fractions. It has been calculated that the total yield of homogeneous milk whey protein fractions was nearly 49–61% (from milk whey proteins taken for separation).

Conclusions. The proposed variant of the disc-electrophoresis allows to isolate from milk whey the electrophoretically homogeneous fractions of β-LG, α-LA and BSA in native conditions. The duration of electrophoresis and proteins extraction is about 4 hours. The average yield of homogeneous fractions from whey proteins is 55±6%.

Introduction

The main function of the milk proteins (caseins and whey proteins) is to provide mammals by the amino acid nutrition. Also, milk whey proteins perform a number of other important functions. Thus, *β*-lactoglobulin *(β*-LG) is involved in the transport of fatty acids and retinol, exhibits antioxidant effect. For *α*-lactoalbumin (*α*-LA) it is typical to take part in the synthesis of lactose and calcium transport, also it shows immunomodulatory and anticancirogenic effects. Serum albumin (SA) performs the transport function. Lactoferrin (LF) is binding iron ions, shows antimicrobial and antioxidant effects [1]. In addition, in recent years it was found that part of milk whey proteins, like caseins, are precursors of bioactive peptides that can be created during the process of proteolysis [1, 2]. According to our calculations, 50% of amino acid residues of *β*-LG and more than 40% of *α*-LA are included to the composition of the bioactive peptides. To a lesser extent this concerns to lactoferrin (9.4%) and serum albumin (2.6%) [3]. Antihypertensive peptides, antagonists of opioid receptors, regulators of intestinal motility, immunomodulatory and antimicrobial peptides can be formed from different proteins of milk serum. New types of bioactive peptides that exhibit anticancirogenic and antioxidant effect, reduce the level of cholesterol in the blood, regulate the appetite, affect on the calcium assimilation are intensively investigated [3,4].

Taken into attention the expressive fractional specificity of the formation of bioactive peptides, the actual for the research and for using this phenomenon is the obtaining of purified fractions of milk whey proteins. Today there are several laboratory and industrial techniques to obtain the main milk whey proteins: *α*-LA, *β*-LG, immunoglobulins (IG), LF. They are isolated from whey proteins concentrate and purified by the differential precipitation, filtration through the gel or membranes as well as by ion exchange chromatography [1,2,5]. By the combination of ultrafiltration, processing of permeate with trypsin and diafiltration, *α*-LA with a degree of purity about 90% was obtained [6]. *β*-LG (with degree of purification more than 95%) was obtained by Lozano et al [7] using differential ammonium sulfate precipitation and ion exchange chromatography. The main disadvantages of these methods are many stages, duration of procedure as well as the use of extreme pH, high concentrations of salts that can affect on the structure and chemical composition of serum proteins and reduce their yield. In addition, these methods do not always provide a high degree of protein fractions homogeneity.

Taking in to account the growing interest to the homogeneous milk whey proteins, their purification due to differences in electrophoretic mobility in a neutral environment may be promising [8]. This makes it attractive to use electrophoresis for milk whey proteins fractionation. Earlier in our laboratory, it was shown that a promising variant of electrophoresis for this may be disc-electrophoresis in PAG slabs in native conditions [9]. The influence of individual parameters of electrophoresis on the efficiency of proteins fractions separation [10] was established.

The purpose of this work is to isolate the homogeneous protein fractions β-LG, α-LA and BSA from milk whey by disc-electrophoresis in native conditions.

Materials and methods

Materials

Whey proteins were isolated from the cow's fresh skimmed milk. The whey was separated by repeated isoelectric point precipitation of casein complex proteins. Reagents from the "Reanal" (Hungary) company and high-purity domestic production reagents were used in this work.

Determination of the milk whey protein concentration

The concentration of the milk whey proteins, as well as the concentration of individual milk protein fractions, were determined spectrophotometrically by absorption at λ = 280 nm on a spectrophotometer SF-46. In this case, previously used absorption coefficients ($D_{cm}^{1\%}$) were used: 12.3 – for the total milk whey protein; 9.6 – for β-LG; 20.1 – for α-LA; 6.7 for the BSA and 13.6 for the IG [8].

Gel filtration

Gel filtration of milk whey was carried out on columns (2 × 35 cm) from the liquid chromatography kit of «Reanal» (Hungary) company. Sephadex G-25 from «Pharmacia» (Sweden) was used for gel filtration [11]. Sephadex was equilibrated with the electrode buffer for disc-elctrophoresis before the application into the column. Whey samples before the application into the column were centrifugated (centrifuge T-24 10000 g, 20 minutes) to remove insoluble components. 5 cm^3 of supernatant was taken for gel filtration and applied on sephadex. The elution speed was set on 20 cm^3/h. 5 cm^3 of eluate was taken. The optical density in chromatographic fractions was determined at λ = 280 nm for constructing the chromatogram.

Homogenous β-LG fractions and the IG fraction obtained by repeated gel filtration of the milk whey on Sephadex G-100, as previously described, were used to identify the electrophoretic fractions [12].

Disc-electrophoresis

The fractional composition and homogeneity of milk whey proteins were analyzed by disc-electrophoresis in the slabs of polyacrylamide gel (PAG). The analytical system of disc-electrophoresis for acidic and neutral proteins in native conditions was used as the basis [13]. Gels were stained and fixed by conventional methods. Electrophoresis was performed on a modified Studier type apparatus [14]. Stacking and separating PAG were prepared as shown in Tables 1 and 2.

Table 1

Composition of the separating PAG

Solutions	Part of the solution in the PAG (volume)	Component	Amount
Gel components	2	Acrylamide	15 g
		N,N'methylenebisacrylamide	0,4 g
		water	to 50 cm^3
Buffer for gel and catalyst	1	1 H HCl	24 cm^3
		Tris (hydroxymethyl) aminomethane	18,3 g
		N,N,N',N' tetramethylethylenediamine	0,115 cm^3
		Water	to 50 cm
Initiator solution	5	Ammonium persulphate	are selected experimentally
		Water	to 25 cm^3

Table 2

Composition of the stacking PAG

Solutions	Part of the solution in the PAG (volume)	Component	Amount
Gel components	2	Acrylamide	5 g
		N,N'methylenebisacrylamide	1,25 g
		Water	to 50 cm^3
Buffer for gel	1	1H H_3PO_4	12,8 cm^3
		Tris (hydroxymethyl) aminomethane	2,85 g
		Water	to 50 cm^3
Initiator and catalyst solution	1	Ammonium persulphate	are selected experimentally
		N,N,N',N' tetramethylethylenediamine	0,115 cm^3
		Water	to 5 cm^3
Sucrose solution	4	Saccharose	20 g
		Water	to 50 cm^3

Also, an electrode buffer was prepared as shown in Table 3. Before use, the buffer was diluted 10 times with distilled water.

Table 3

Composition of the electrode buffer

Solution	Buffer components	Amount
Electrode buffer (pH 8,3)	tris (hydroxymethyl) methylamine	6 g
	glycine	28,8 g
	Water	to 1000 cm^3

Statistical analysis

The statistical analysis of the obtained results and the graphical representation of the experimental data were carried out using the Microsoft Excel 2007 program. The accuracy of the obtained results was provided by triple repetition of the experiments.

Results and discussion

Whey protein fractions separating in disc-electrophoresis system

For analytical fractionation of whey proteins, the most commonly used are two types of disc-electrophoresis. This is disc-electrophoresis recommended by the American Dairy Science Association Committee on the Nomenclature, Classification, and Methodology of

Milk Proteins in the sodium dodecylsulfate (SDS) [8]. Also, disc-electrophoresis in native conditions for acidic and neutral proteins is used [13]. Taking into account, that the denaturation of proteins occurs in the presence of SDS, the disc-electrophoresis system in the native conditions (Figure 1) have been taken as the basis for whey protein fractions separating. As can be seen from the electrophoregram, the system allows effective separation of the main milk whey proteins fractions. These are β-LG (A and B variants), α-LA, BSA, as well as the heterogeneous group of immunoglobulins (IG) and proteose-peptone fraction (PPF).

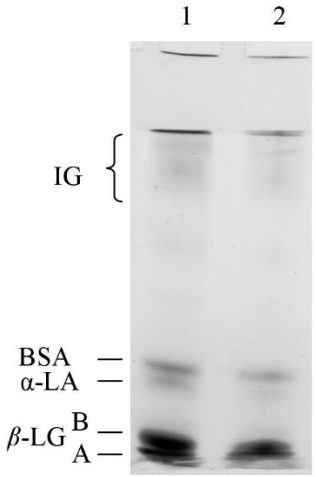

Figure 1. Analytical disc-electrophoresis of milk whey proteins (1) and chromatographic fraction I after whey gel filtration on sephadex G-25 (2)

Before preparative electrophoretic fractionation low molecular weight compounds were separated from the milk whey by gel filtration on a column with Sephadex G-25 [11]. Sephadex was equilibrated with the electrode buffer for disc-elctrophoresis. The results of gel filtration are shown in Figure 2. The combined fractions of the chromatographic peak I were selected for the preparative electrophoresis. The analytical disc-electrophoresis of this peak testifies that the proteins composition does not change at the result of gel filtration comparing with the milk whey (Figure 2).

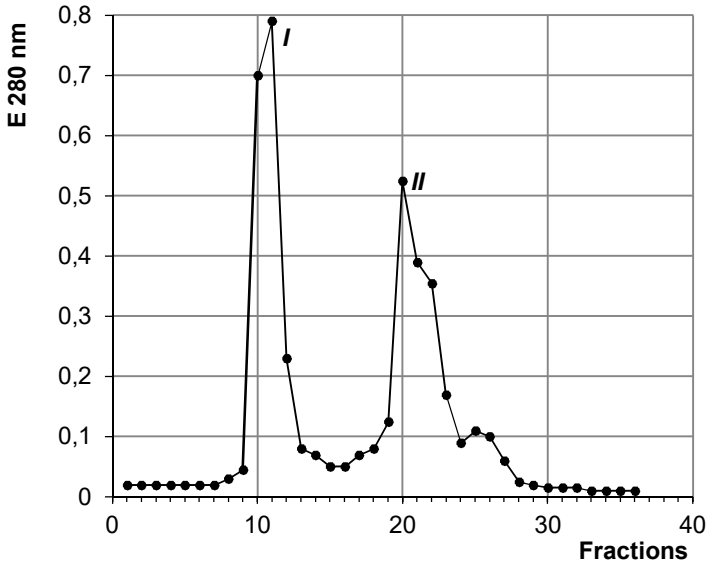

Figure 2. Chromatogram of milk whey after gel filtration on Sephadex G-25

The concentration of PAG was reduced by 0.5%, in order to reduce the electrophoresis duration and the extraction process alleviation. Preparative electrophoresis testing was performed on a modified Stadier type apparatus [13]. The design of the electrophoretic chamber and former were modified in such way that they can provide an effective separation of the milk whey sample. The electrophoresis duration has been reduced up to 2 hours and the volume of whey can be increased to 10 cm^3 as a result of these modifications.

The amount of whey in the sample for each electrophoretic chamber was determined experimentally. Too large sample amount does not allow to separate the whey proteins effectively. In this case, the electrophoregram has the following form (Figure 3a). Densitogram (Figure 3b) testifies about the impossibility of homogeneous fractions extraction from such gel. While using the optimal amounts of milk whey, the electropherogram has such form (Figure 4). Comparing with the analytical variant (Figure 1) there are no significant differences. It may be noted only the union of two fractions of β-LG-A and β-LG-B into a single line.

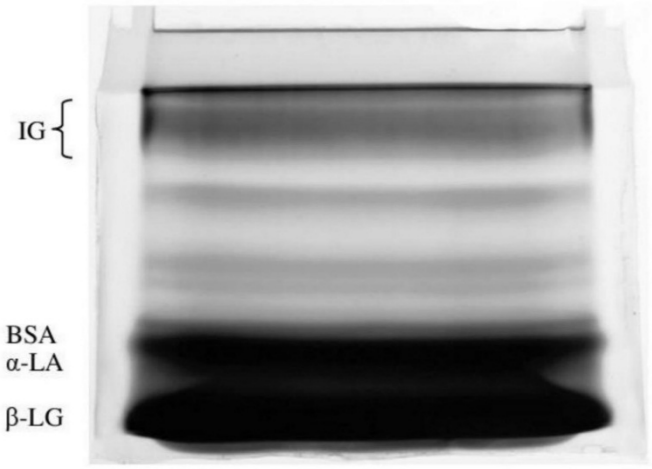

a

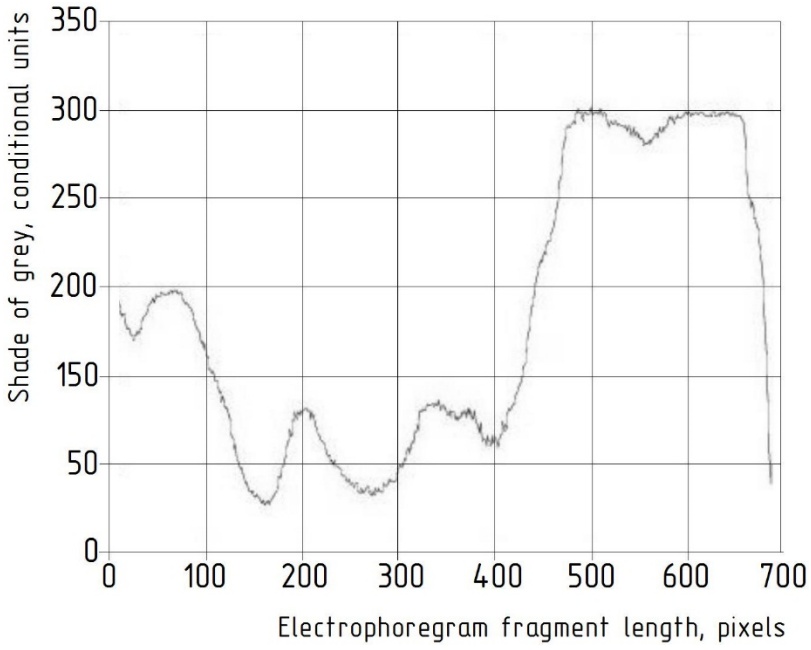

b

Figure 3. Electrophoregram (a) and densitogram (b) of milk whey proteins in the preparative variant of disc-electrophoresis. Excessive amount of milk whey.

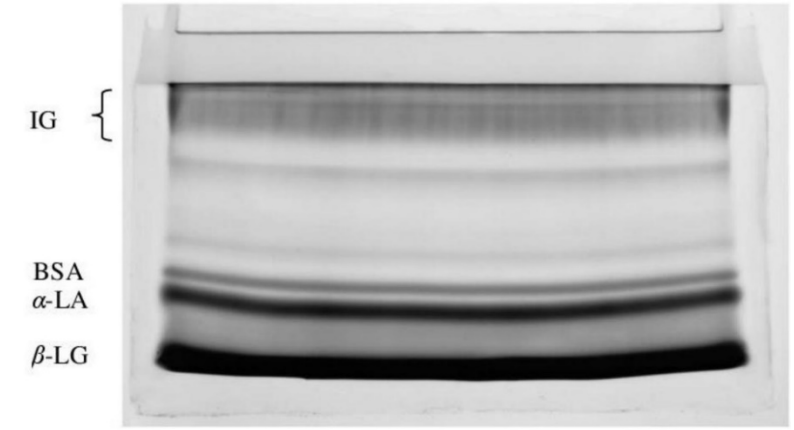

a

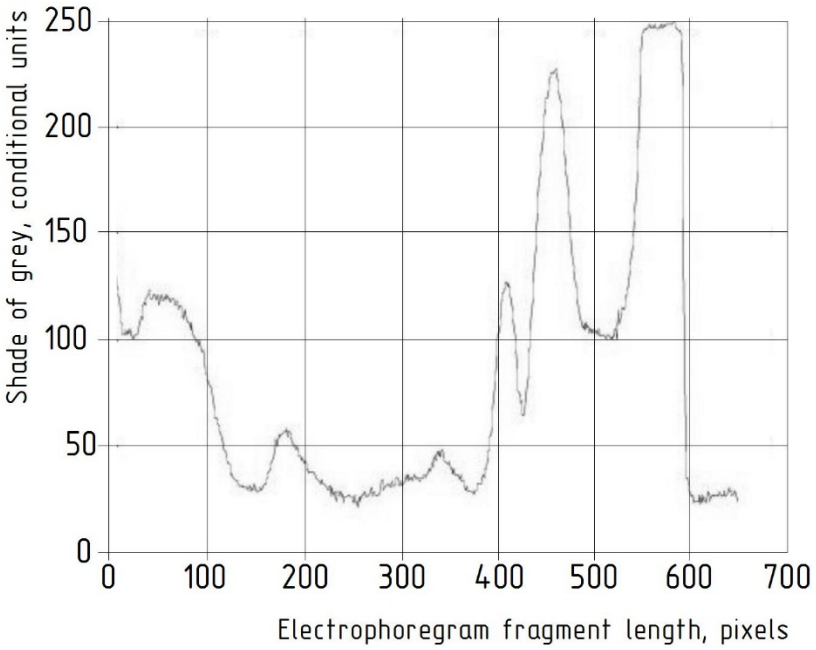

b

Figure 4. Electrophoregram (a) and densitogram (b) of milk whey proteins in the preparative variant of the disc-electrophoresis. The optimal amount of milk whey.

Identification and extraction of main fractions of the milk whey proteins

After completion of the electrophoresis, we remove the gel slab from the chamber and cut the side strips with a width of about 1 cm and place them in a solution of fresh dye for 1 minute. After intense destaining during 15 min, the main fractions of the milk whey proteins can be identified on the strips. Then, the strips were applied to the unstained part of the gel plate for the identification and cutting out areas with certain fractions [15]. In this case, we remove gel fragments that contain β-LG, α-LA, BSA and IG. The duration of the gel strip staining process, identification of fractions and cutting of the main plate of the gel was less than 30 minutes. In special studies, we have shown that for such period in the gel without fixation, the milk whey proteins do not mix due to diffusion. Next, obtained gel fragments with the appropriate fractions were crushed and protein extraction with an electrode buffer (1:5) was performed. During the extraction the samples were selected and the yield of proteins was controlled by the absorption at $\lambda = 280$ nm. The results are shown in Figure 5. Each point on the chart is the average value of the three definitions. According to the results presented in Figure 5, we can conclude that extraction is mostly completed after 60 min.

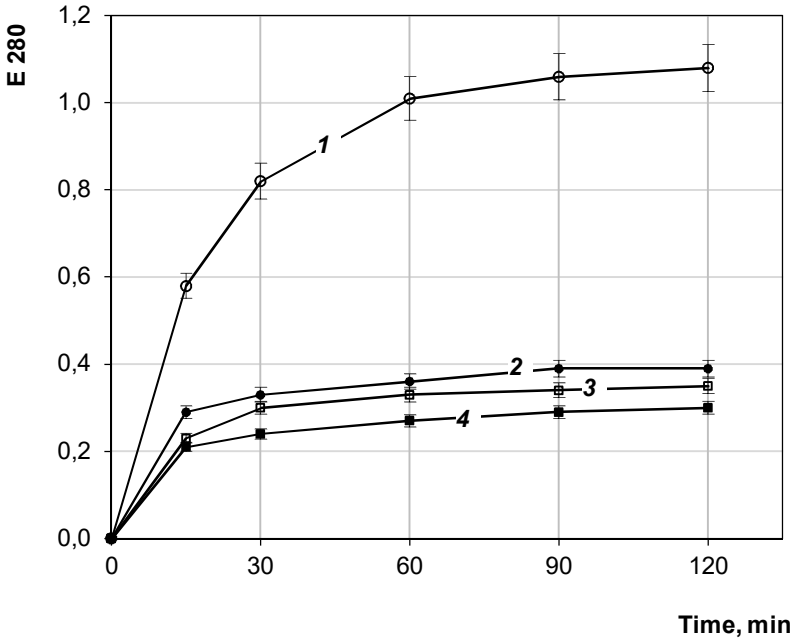

Figure 5. The course of extraction of separate fractions of milk serum proteins from polyacrylamide gel:
1 – β-lactoglobulin, 2 – immunoglobulins, 3 – α-lactalbumin, 4 – serum albumin

Degree of homogeneity of whey protein fractions

The fractions obtained after extraction were analyzed in the same electrophoretic system (analytical version) for homogeneity (Figure 6) [13]. It is visible on the electrophoregram,

that β-LG, BSA and IG fractions are electrophoretically pure and only α-LA fractions content β-LG bands. A heterogeneous fraction of IG is also separately isolated. The total protein yield was determined in the obtained electrophoretically pure fractions based on the three preparative electrophoresis results. The concentration of the proteins in whey and individual fractions was determined spectrophotometrically [8]. The yield of purified fractions was nearly 55±6% (from milk whey proteins taken for separation). Losses can be explained by incomplete extraction for 60 minutes, as well as by the fact that only separate sectors were taken for the extraction, and not the whole gel.

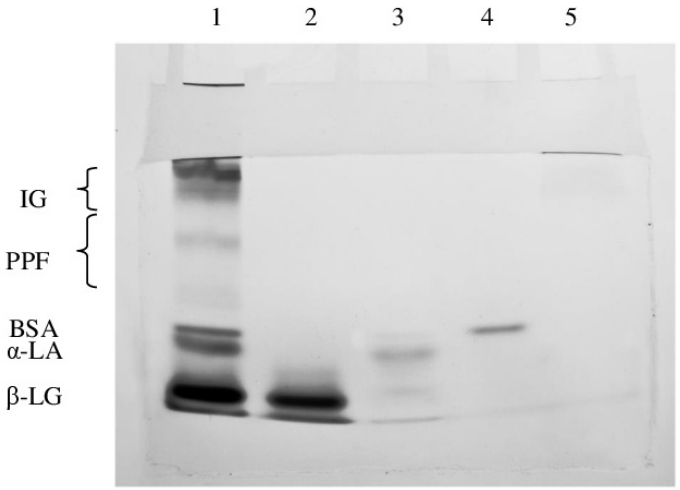

Figure 6. Electrophoregram of milk whey proteins and obtained fractions. 1 – proteins of milk whey , 2 – β-lactoglobulin, 3 – α-lactalbumin, 4 – serum albumin, 5 – immunoglobulins

Conlusion

1. The proposed version of the disc-electrophoresis in the PAG slabs allows isolating the electrophoretically homogeneous fractions of β-LG, α-LA and BSA from milk whey in native conditions.
2. The duration of electrophoresis and proteins extraction is about 4 hours.
3. The average yield of homogeneous fractions from proteins is 55±6%. The obtained fractions are the major precursors of BAP amount the serum proteins and can be used to study the ways of their formation.

References

1. Fox P.F., Uniacke T., Mc Sweeney P.L.H., O'Mahony J.A. (2015), *Dairy chemistry and Biochemistry (Second Edition)*, Springer, New York.

2. ParkY.W. (2009), *Bioactive components in milk and dairy products*, Wiley-Blackwell, Boston.
3. Iukalo A.V, Datsyshyn K.Ye., Yukalo V.G. (2013), Bioaktyvni peptydy proteiniv syrovatky moloka koriv (Bos Taurus), *Biotechnolohiia Acta*, 6, pp. 49–61.
4. Corredig M. (2009), *Dairy-derived ingredients: food and nutraceutical uses,* CRC Press, USA.
5. Konrad G., Klenschmidt T. (2008), A new method for isolation of native α-lactalbumin from sweet whey, *International Dairy Journal*, 18, pp. 47–54.
6. Konrad G., Klenschmidt T. (2008), A new method for isolation of native α-lactalbumin from sweet whey, *International Dairy Journal*, 18, pp. 47–54.
7. Lozano J., Giraldo G., Romero C. (2008), An improved method for isolation of β-lactoglobulin. *International Dairy Journal*, 18, pp. 55–63.
8. Farrell H.M., Jimenez-Flores R., Bleck G.T., Brown E.M.,Butler J.E.,Creamer L.K.,Hicks C.L.,Hollar C.M.,Ng-Kwai-Hang K.F., Swaisgood H.E. (2004), Nomenclature of the proteins of cows' milk – sixth revision, *Journal of Dairy Science,* 87(6), pp. 1641–1674.
9. Yukalo V.G., Storozh L.A., Datsyshyn K.Ye., Krupa O.M. (2018), Electrophoretic systems for the preparative fractionation of proteins-precursors of bioactive peptides from cow milk, *Food science and technology*, 12(2), pp. 26–32.
10. YukaloV.G., Datsyshyn K.Ye. (2017), Pidbir umov dlia preparatyvnoho elektroforezu proteiniv syrovatky moloka u natyvnykh umovakh, *Naukovyi visnyk LNUVMB imeni S.Z. Gzhytskoho*, 17(80), pp. 13–17.
11. Pharmacia Fine Chemicals (1985), *Gel Filtration. Theory and practice*, Uppsala, Sweden.
12. Yukalo V.G., Datsyshyn K. Ye. (2018), Gel filtration of cow milk serum proteins, *Food science and technology*, 12(4), pp. 72–78.
13. Yukalo A., Yukalo V., Shynkaryk M. (2009), Electrophoresis separation of the Milk Protein, *Proceedings of the International Conference on Bio and Food Electrotechnologies,* Compiegne, France, pp. 227–231.
14. Studier F.W. (1973), Analysis of bacteriophage T7 early RNAs and proteins on slab gels, *Journal of Molecular Biology*, 79, pp. 237–248.
15. Osterman L.A. (1981). Metody issledovaniya belkov i nukleinovykh kislot : Elektroforez i ultratsentrifugirovaniye, Nauka, Moscow.

Grape seeds effect on refined wheat flour dough rheology: optimal amount and particle size

Mădălina Iuga, Silvia Mironeasa

Ştefan cel Mare University of Suceava, Faculty of Food Engineering, Suceava, Romania

Keywords:

Wheat flour
Grape
Seed
Dough
Rheology

Article history:

Received 22.04.2019
Received in revised form 30.09.2019
Accepted 28.11.2019

Corresponding author:

Silvia Mironeasa
E-mail: silviam@fia.usv.ro

DOI:
10.24263/2304-974X-2019-8-4-11

Abstract

Introduction. When developing grape seed enriched-bread, it is important to know the changes that may occur in the bread making process.

Materials and methods. The addition of different amount of grape seed flour (from 3 to 9%) and particle size changes (large, L>500 μm, medium, 200 μm>M<500 μm and small fractions, S<200 μm) on the physico-chemical characteristics of the grape seeds-wheat composite flours and dough rheological behavior were investigated.

Results and discussion. The protein and ash contents increased after GSF incorporation, while the moisture and the falling number decreased depending on the particle size and addition level. The decrease of falling number values with the decrease of GSF particle size and increase the addition level indicates an increase of alpha-amylase activity in the composite flour. The storage (G'), loss (G"), complex modulus (G*) and loss tangent (tan δ) of dough increased with the particle size and addition level increase. A decrease of dough maxim height (Hm), maximum height of gaseous production (H'm) and total carbon dioxide volume production (Vt) with the increase of GSF level in refined wheat flour was obtained. Gas retention coefficient (Rc) increases with the decrease of GSF particle size. Dough fermentation parameters and dynamic rheological properties were adequately predicted by the regression models achieved. The result of optimization process showed that small particle sizes of GSF from white grape variety in an amount of 3.01% are desired to substitute refined wheat flour bread in order to ensure good rheological characteristics. Under these optimal conditions, dough fermentation characteristics and dynamic rheological properties was found to be as follows: H'm of 55.98 mm, Vt of 1274.11 mL, Rc of 81.22%, G' of 28.54 · 10^3 Pa, G" of 9.79 · 10^3 Pa, G* of 30.17 · 10^3 Pa and tan δ of 345.50·10^{-3}.

Conclusions. This study highlights the opportunity to use grape seeds from local wine producers in order to add value to this by-product and to develop new enriched-bakery products.

Introduction

Bakery products, especially bread are consumed all around the world. Nowadays, people turned their attention on functional foods. These are an important source of antioxidants and dietary fibers known as having benefits on human health, including cancer prevention, good cardiovascular and digestive systems functionality [1]. Manufacture of enriched fibers products is challenging since increasing the fiber content can have unfavorable effects on the product quality and consequently on the consumer acceptance. Therefore, producers need to find fiber-rich recipe with the least negative impact on the quality of the final product. Previous studies have documented the incorporation of functional ingredients from different fruit by-products, like grape pomace in bread making in order to improve nutritional value of wheat bread and to develop new functional foods [2, 3, 4]. Among grape pomace components, grape seeds represent 38-52% of grape pomace, on a dry matter basis, depending of the grape varieties [5]. Grape seeds, produced in large amounts as wine industry by-products, are more and more used to create food ingredients [6]. They contain about 10-20% lipid, 10% protein, 40% dietary fibers, sugars, minerals, polyphenolic compounds with high antioxidant activity, which may vary significantly depending on the variety of grape, location, fertilization and pedoclimatic conditions [7, 8, 9]. Grape seeds represent a valuable source of oil, characterized by higher levels of hydrophilic constituents, such as phenolic compounds, and lipophilic constituents, such as vitamin E, unsaturated fatty acids and phytosterols [10]. The amino acid composition and properties of grape seeds proteins are very similar to that of cereals. Grape seed protein is rich in glycine, glutamic acid and aspartic acid and, deficient in tryptophan and sulfur containing amino acids [11, 12].

Due to their chemical composition, grape seeds can be used as ingredients in various food products such as dairy [13], meat products [14], biscuits [15] and others, including wheat bread [3, 4]. As wheat flour replacement in the baking industry, the amount of GSF has a remarkable effect on bread dough. The increase of the addition level of GSF can led to an increased α-amylase activity in the composite flour influencing dough rheological properties [16, 17, 18]. The dough behavior is also influenced by the GSF particle size which substituted wheat flour [19, 20]. GSF reduces gluten content of wheat flour resulting in technological parameters changes. Composite flour dough viscoelastic properties are different because there are some interactions of GSF components in the gluten network. There are various studies that showed the particle size influence on the chemical and physical properties of dough and on the final product quality. Higher particle size can negatively influence the bread quality because of the water absorption change and gluten network dilution by non-wheat additions [21]. The water holding capacity is higher at lower particle sizes due to the surface area augmentation [22]. The volume and the hardness of bread is strongly affected by the particle size of fibers added, so higher particle sizes leads to lower hardness and higher volume [23]. In our previous works we investigated the influence of GSF as a source of dietary fiber on the empirical and dynamic rheological characteristics of dough [19, 20, 24]. The use of large particle sizes of GSF led to significant changes of dough rheological behaviour and consequently, of the final product quality, depending of the GSF substitution level and also, on the grape variety [20]. Smaller particle sizes can be responsible for water-holding capacity increase which may enhance the starch gelatinization, protein denaturation processes, flavor and color of the product [25]. Thus, finding the appropriate addition level and particle size of GSF that can be substitute refined wheat flour (RWF) is important, in order to obtain adequate physico-chemical and rheological characteristics of composite flour and dough which would result in an acceptable bread technological quality.

Dough stretchability and gas retention capacity, important characteristics for the final bread volume [26] can be achieved by using empirical rheological measurements conducted by means of rheofermentometer. In addition, to inform on behaviour of dough systems, the use of fundamental rheological measurements is required. The dynamic rheological properties of dough can be achieved easily using a dynamic oscillatory rheometer which simultaneously measures the elastic as well as the viscous components of dough by the application of sinusoidal oscillating strain or stress with time. This technique is useful for explaining the quality of cereal foods as well as for simulating and predicting responses to the deformation conditions that are present in practical processing but inaccessible to normal rheological measurement. Dynamic oscillatory measurements requires small amounts of sample to measure small deformational rheological changes in polymers at low strains and provides information about the fundamental structural behaviour of the material [27]. Rheological testing in the linear viscoelastic region (LVR) in order to follow the structure and properties of dough and to study the functions of dough's ingredients has been applied in various studies. The storage modulus (G') describes the elastic character and it is in phase with the strain during oscillation. G' values of gluten dough can be a good indicator of loaf volume [28]. Dough from poor quality bread-making flour had G' values of greater magnitude then those of the good quality bread-making flour [29]. The loss modulus (G") that describes the viscous properties is out of phase [17]. The loss tangent (tan δ), defined as the ratio of the viscous to elastic component of tested dough can be an indicator of dough elasticity, a lower value indicating a higher elasticity [30]. Complex modulus (G*) is a factor which represent the dough strength [31], lower G* corresponding to lower dough strength, and vice versa [32].

The aim of the present study was to investigate the influence of different GSF particle size additions at different levels in refined wheat flour on the physicochemical composition of blends, rheofermentometer characteristics and dynamic oscillatory rheological characteristics of dough and to determine the optimal formulation of GSF level-particle size addition which will give the adequate dough rheological behaviour. This information can be helpful for both bakery processors and researchers in order to predict quality of GSF enriched-bread products and to develop novel products by using locally produced grape wine pomace.

Materials and methods

Basic materials

The refined wheat flour (RWF) of 480 type (2016 harvest) was provided from S.C. Dizing S.R.L. (Brusturi, Neamt, Romania) and the grape seeds were obtained from white pomace from the viticulture center Jaristea, Odobesti ecosystem. To separate grape seeds from dried pomace the manually method was applied. Grape seed flour (GSF) resulted from seeds grinding in a domestic blender, and sieving through a Retsch Vibratory Sieve Shaker AS 200 basic (Haan, Germany) to obtain three different particle sizes: large, L > 500 μm, medium, 200 μm > M < 500 μm and small fractions, S < 200 μm.

The grape seeds presented the following analytical characteristics: moisture content 7.70% (SR EN ISO 665:2003), fat content 18.32% (SR EN ISO 659:2009), protein content 9.79% (SR EN ISO 20483:2007), and ash content 2.79% (SR ISO 2171:2009). Fiber content (40.80%) was determined by Near Infrared Reflectance Spectroscopy (NIR).

The flour samples were formulated from RWF and different levels of GSF (3, 5, 7, 9%) for each of the three particle sizes (L, M, S). The control sample was made only of RWF (0% GSF).

Physico-chemical analysis

The composite flours physico-chemical characteristics were determined according to the International Cereal Chemistry methods. The moisture content was performed according to ICC methods 110/1, the ash content according to ICC 104/1 method, the protein content by using the ICC 105/2 method, and the falling number was performed according to the ICC 107/1 method.

Rheological properties of wheat dough

Dough fermentation characteristics. Dough rheological characteristic during fermentation were assessed by using the Chopin Rheofermentometer F3 (Chopin Rheo, Villeneuve-La-Garenne Cedex, France). Mixing was performed in a Brabender Farinograph for 8 min at 30ºC from 250 g flour blend, 7 g compressed yeast, 5 g salt and water according to the Farinograph water absorption. The dough (315 g) was tested at 30ºC for 3 h under a 2000 g cylindrical weight constraint. The fermentation characteristics of dough development determined for the formulated samples (Table 1) shows maximum dough maximum height (Hm), maximum height of gaseous production (H'm), total carbon dioxide volume production (Vt) and gas retention coefficient (Rc).

Dynamic rheological measurement. Dough dynamical rheological properties were achieved using MARS 40 rheometer (Thermo-Haake, Karlsruhe, Germany) equipped with titanium parallel plate geometry (diameter 40 mm). The water needed for dough formulation at optimum consistency was previously established by the farinographic method, based on the water absorption value, for each composite flour formulation. The samples were placed between the parallel plates at 2 mm gap and the excess dough was removed. A thin layer of vaseline was spread to the exposed dough side to prevent water evaporation during measurement. A period of 5 min of rest between plates was established for each sample before test to allow relaxation and stabilize temperature. All the measurements were performed at 20.0±0.1ºC. Before to perform the frequency sweep test, the linear viscoelastic region of the sample was established based on the strain sweep tests, increasing strain from 0.01 to 100 Pa, at constant oscillation frequency of 1 Hz. Frequency sweep tests were conducted in the oscillation frequency of 1 to 20 Hz and at shear stress of 15 Pa. The rheological behavior was evaluated by the storage modulus G' (Eq. 1), the loss modulus G" (Eq. 2), loss tangent (Eq. 3) and complex shear modulus G* (Eq. 4) variation with frequency [33]:

$$G' = \left(\frac{\sigma_0}{\gamma_0}\right)\cos(\delta) \tag{1}$$

$$G'' = \left(\frac{\sigma_0}{\gamma_0}\right)\sin(\delta) \tag{2}$$

$$\tan\delta = \frac{G''}{G'} \tag{3}$$

$$G^* = \sqrt{(G')^2 + (G'')^2} \tag{4}$$

where σ_0 is constant shear stress (Pa), γ_0 is constant shear strain and δ is phase angle (rad).

Experimental design and statistical analysis

The combination effects of two factors, addition level (A) in RWF at five levels (0, 3, 5, 7, 9%) and particle size (B) at 3 levels (L, M, S) for the GSF on the rheofermentometer characteristics (Hm, H'm, Vt and Rc) and the dynamic rheological characteristics (G', G", G*, tan δ) of the composite flour dough as responses were investigated using response surface methodology (RSM) by means of general factorial design. The experimental design with real and coded factors values which led to 15 runs of experiments is shown in Table 1.

Table 1

Coded and real values of formulations factors

Run	Coded values		Real values	
	A	B	GSF (%)	Particle size (μm)
1	0.111	-1.000	5.000	200
2	1.000	1.000	9.000	600
3	1.000	0.000	9.000	400
4	0.556	-1.000	7.000	200
5	0.111	1.000	5.000	600
6	-1.000	0.000	0.000	400
7	0.556	0.000	7.000	400
8	-0.333	1.000	3.000	600
9	-1.000	1.000	0.000	600
10	-1.000	-1.000	0.000	200
11	-0.333	-1.000	3.000	200
12	1.000	-1.000	9.000	200
13	-0.333	0.000	3.000	400
14	0.111	0.000	5.000	400
15	0.556	1.000	7.000	600

To the established predictive models for rheological characteristics, experimental results for each response variable were fitted to polynomial quadratic regression equation (Eq. 1):

$$Y=b_o+b_1\times X_1+b_2\times X_2+b_{11}\times X_1^2+b_{22}\times X_2^2+b_{12}\times X_1\times X_2 \quad (1)$$

where, Y is the response variable, b_o, b_1, b_2, b_{11}, b_{22} and b_{12} – regression coefficients for intercept, linear, quadratic and interaction effects respectively of X_1 and X_2 independent variables (addition level and particle size of grape seeds flour).

The multiple linear regression analysis was applied to fit the results obtained for each response to linear, quadratic and cubic models and the most adequately predictive model was chosen through sequential *F*-test, coefficients of determination (R^2), adjusted coefficients of determination ($Adj.\text{-}R^2$), and significant probabilities. In order to determine the validity of the model for each response, the experimental and predictive values were compared by paired t-test ($p < 0.05$). Analysis of variance (ANOVA) was carried out to evaluate the statistical significance of the coefficients in each model. The polynomial response surfaces were generates showing the combined effect of the factors, addition level and particle size of the

GSF on the response variables, dough rheological characteristics during fermentation and dynamic rheological characteristics.

Stat-Ease Design-Expert 7.1 software (trial version) was employed to carry out the experimental design, the model adequacy testing, response surface plots generation and the optimum level of formulation factors finding. In order to find the optimal value of the factors, level and particle size for the GSF added in RWF, the multiple responses analysis was applied to predictive models fitted. For the optimization, each predicted response is transform into an individual desirability function, d_n which comprise the desired and researcher's priorities when building the optimization procedure for each of the factors. The individual desirability functions are then combined into a single composite response, named overall desirability function, D computed as the geometric mean of the individual desirability function, d_n which varies from 0 to 1 [34]. For the numerical optimization, the minimum particle size of grape seeds flour, as factor, maximum for dough maximum height, maximum gas retention coefficient, minimum for complex viscosity and loss tangent, as responses were selected.

The statistical analysis of data reported for physico-chemical characteristics was performed by using SPSS software (13.0 version) and the results were expressed as mean value with the standard deviation. The multivariate analysis and the *post-hoc* multiple comparisons with Tukey test at a 95% confidence level was used in order to detect statistical difference. Observed factors were addition level and particle size.

Results and discussion

Physico-chemical characteristics

The size reduction of GSF has a significant influence on the physico-chemical characteristics of the composite flours (Table 2). The moisture, ash and protein contents were significantly different ($p < 0.05$) among the samples with different addition levels of GSF and particle sizes. The moisture level decreased after GSF addition compared to the control and increased with the decrease of the particle size, except for 3% addition level. A similar decreasing trend of the moisture content with the size reduction has been reported for the rye and barley flours [35]. The ash content increase with the addition level increase and with the particle size decrease can be related to the mineral content of GSF [36, 67], significant differences ($p < 0.05$) being observed among all the analyzed samples (Table 2).

An increase of the protein content of the samples with GSF was observed with the increase of the addition level and the particle size decrease, as a result of the protein content of GSF [8] which is substantially influenced by the sieving. The highest protein content of composite flour with small particle size (S) could indicate that some parts of the grape seeds, richer in proteins, were broken into small particles. A similar increase of the protein content with the particle size decrease has been reported for soy flour [38].

The falling number value inform on the alpha-amylase activity of the composite flour [39]. The addition of GSF decreased the falling number values compared to the control which means an increase of the alpha-amylase activity as a result of the calcium content increase induced by GSF which is mineral-rich [8, 37]. It is known that alpha-amylase is a metallo-enzyme which depends on the presence of metal ions calcium in its molecule for its activity [40].

Table 2

Influence of the formulation factors on the physico-chemical characteristics of the composite flours

Factor		Moisture	Ash	Protein	Falling number
GSF (%)	Particle size	(%)	(%)	(%)	(s)
0	0	14.10±0.00^{a}	0.47±0.00^{a}	10.80±0.00^{a}	370.50±11.50^{a}
3	L	13.25±0.05^{bx}	0.68±0.00^{bx}	10.90±0.00^{bx}	369.00±10.00^{cy}
3	M	13.06±0.01^{bz}	0.75±0.00^{by}	10.95±0.05^{by}	351.50±12.50^{cx}
3	S	12.98±0.02^{by}	0.80±0.00^{bz}	11.05±0.05^{bz}	346.00±14.00^{cx}
5	L	12.87±0.03^{cx}	0.71±0.00^{cx}	10.93±0.03^{cx}	368.00±6.00^{bcy}
5	M	12.98±0.02^{cz}	0.86±0.01^{cy}	11.10±0.10^{cy}	346.00±4.00^{bcx}
5	S	13.10±0.01^{cy}	0.95±0.01^{cz}	11.30±0.00^{cz}	343.00±13.00^{bcx}
7	L	12.85±0.01^{dx}	0.72±0.00^{dx}	11.00±0.01^{dx}	365.00±7.00^{bcy}
7	M	12.98±0.02^{dz}	0.95±0.02^{dy}	11.15±0.05^{dy}	345.50±5.50^{bcx}
7	S	12.86±0.04^{dy}	1.08±0.00^{dz}	11.50±0.04^{dz}	341.00±15.00^{bcx}
9	L	12.39±0.03^{ex}	1.05±0.01^{ex}	11.25±0.07^{ex}	349.00±7.00^{by}
9	M	12.85±0.02^{ez}	1.07±0.01^{ey}	11.35±0.05^{ey}	336.50±8.50^{bx}
9	S	12.72±0.06^{ey}	1.26±0.00^{ez}	11.69±0.05^{ez}	334.00±11.00^{bx}

GSF particle sizes: Large, L > 500 μm, Medium, 200 μm > M < 500 μm and Small fractions, S < 200 μm. The results are expressed as mean values of triplicates (± standard deviation). Mean values are followed by different superscript (a-e) in the same column (GSF at 0, 3, 5, 7, 9% addition levels) if there are significantly different, according to Turkey's test ($p < 0.05$); x-z for the same addition level of GSF and different particle sizes (L, M and S), means in the same column with different superscript were significantly different ($p < 0.05$).

High alpha-amylase activity leads to an improved bread quality in terms of color, volume and texture [41]. Significant differences ($p < 0.05$) of the falling number values were observed between the control and all samples and between sample with 3% GSF and all others. Similar results were obtained when wheat flour was replaced with grape seed flour from two varieties at different levels [20]. Significant differences ($p < 0.05$) of the falling number values were also obtained between the large (L) particle size and control, small (S) and medium (M) particle size, respectively (Table 2).

Effects of GSF addition level and particle size on dough fermentation characteristics

As shown in Table 3, the quadratic model was found to represent adequately the data for the dough maximum height (Hm) as a function of the formulation factors, the R^2 value (0.92) confirming the adequacy of the model. The linear coefficient of the addition level of GSF indicates a significant negative influence on the Hm, while the linear term of particle size has a significant positive effect. Hm was significantly correlated ($p < 0.05$) with the interaction effect of GSF addition level in RWF and particle size. The effect of GSF addition level and particle size can be seen in Figure 1a, indicating an increase in Hm with particle size increase. The negative coefficient of GSF addition level indicated that the Hm of the composite flour decreased with the increase of GSF addition level in RWF. This decrease may be attributed to the gluten dilution as a result of an addition of non-gluten flour [42]. The high level of GSF added in the gluten matrix may introduce physical interruption which can cause dough weakening. Lower Hm indicates that the gas resulted from the fermentation process and the microstructure of a system were not able to sustain the macrostructure of the proofed dough piece. Unfavorable, final product volume is expected when the gas retention is not efficient. Hm decreased as the level increased (Figure 1a) and the GSF level effect was higher than the one of particle size (Table 3).

Table 3

Effects of formulation factors, expressed as their corresponding coefficients in the predictive models for dough fermentation characteristics and dynamic rheological characteristics [a]

Factors [b]	Characteristics							
	Rheofermentometer				Dynamic rheological			
	Hm (mm)	**H'm (mm)**	**Vt (mL)**	**Rc (%)**	**G'(10^3) (Pa)**	**G''(10^3) (Pa)**	**G*(10^3) (Pa)**	**tan δ (10^{-3})**
Constant	38.86	56.74	1252.00	81.22	25.89	8.69	27.31	340.00
A	-6.66***	-6.34***	-57.93***	-0.44*	11.37***	3.66***	11.94***	-8.29***
B	5.12***	4.27***	2.83	0.52	-6.15***	-2.12***	-6.51***	-3.44*
A x B	4.07**	3.07**	17.61*	0.75*	-9.46***	-3.14***	-9.97***	-
A^2	0.79	0.84	-	-2.13**	1.94	0.73*	2.08	-
B^2	-0.23	0.34	-	0.35	3.16*	1.14*	3.36*	-
R^2	0.92	0.92	0.51	0.78	0.88	0.89	0.89	0.44
Adj.-R^2	0.88	0.87	0.38	0.65	0.82	0.83	0.82	0.35
p-value	< 0.0001	< 0.0001	< 0.05	< 0.01	< 0.001	< 0.001	< 0.001	< 0.05

[a] * $p < 0.5$; ** $p < 0.05$; *** $p < 0.005$

[b] *A*, grape seeds flour level added in white wheat flour (%); *B*, grape seeds flour particle size (μm); R^2, *Adj.*-R^2 are measures of model fit; *Hm*, dough maximum height; *H'm*, maximum height of gaseous production; *Vt*, total carbon dioxide volume production; *Rc*, gas retention coefficient; *G'*, storage modulus; *G''*, viscous modulus; *G**, complex modulus; *tan δ*, loss tangent

The maximum height of gaseous production (H'm), a critical parameter of the fermentation process was significantly ($p < 0.0001$) influenced by the particle size and the level of GSF addition in RWF (Table 3). The R^2 (0.92) and *Adj.*-R^2 (0.87) values showed that the quadratic regression model fitted to the experimental results of H'm characteristics showed higher R^2 value (0.92). The linear term of GSF level, particle size and the interaction term showed a significant effect on H'm. The addition level has a negative effect on H'm, whereas particle size has a positive effect. A negative effect on H'm can be due to the disruption of the starch-gluten matrix from the composite flour which restricts and forces gas cells to expand in a particular dimension influencing gassing power of dough. The effect of GSF level and particle size added in RWF on the H'm is shown in Figure 1b. Response surface plot showed that an increased level of GSF added in RWF increased the maximum height of gaseous production. The H'm was mostly affected by the addition level. The high level of GSF does not allow the increase of the gas production during dough fermentation.

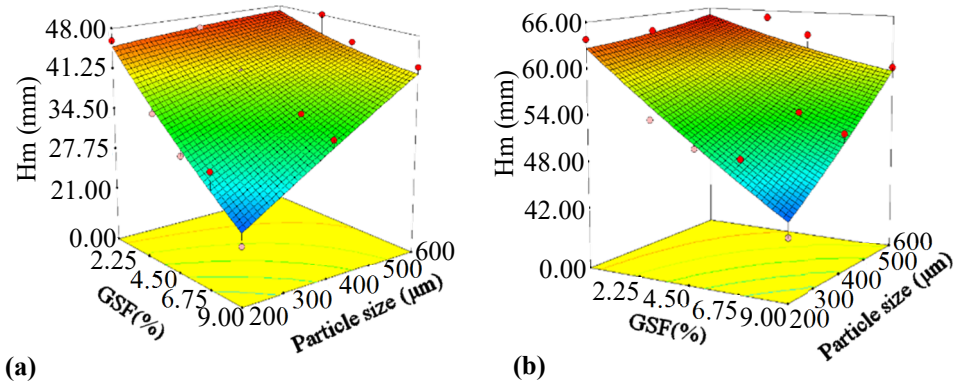

Figure 1. Response surface plot showing the combined effects of grape seeds flour (GPF) level and particle size of GPF on: (a) dough maximum height (Hm) and (b) maximum height of gaseous production (H'm)

The factors GSF addition level in RWF and the particle size affected the total carbon dioxide volume production (Vt) significantly ($p < 0.05$) (Table 3). A two-factor interaction (2FI) regression model for Vt showed a significant effect ($p < 0.05$) in linear term of GSF level, while the linear term of particle size was non-significant ($p > 0.05$). The ANOVA results showed that the regression model obtained was an adequately one with a good R^2 value of 0.51. The negative effect of GSF addition level on Vt can be related to the disruption of the gluten network when the GSF are incorporated in dough matrix. At the large particle size, Vt increased as the particle size increased, but the particle size effect was lower than the one of the level of GSF added in RWF. This effect can be explained by the bioactive compounds from GSF which influenced yeast activity, having an essential effect on CO_2 production. The effect of GSF level and particle size added in RWF on Vt is shown in Figure 2a. The response surface obtained showed that the increase of GSF level decreased Vt parameter.

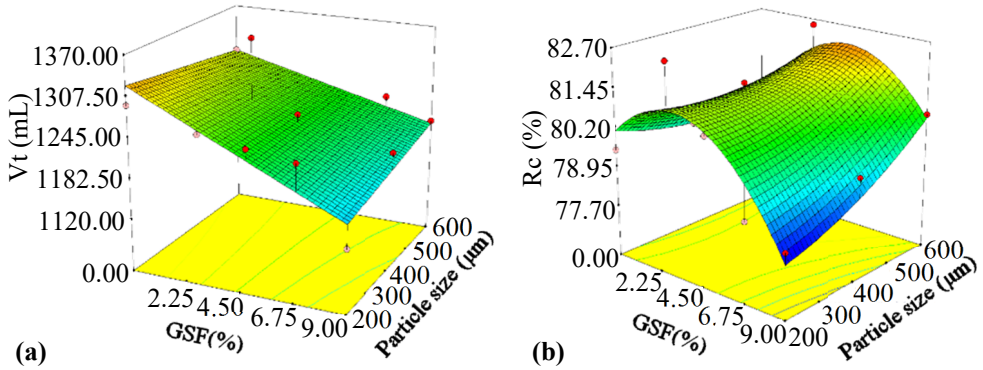

Figure 2. Response surface plot showing the combined effects of grape seeds flour (GPF) level and particle size of GPF on: (a) total carbon dioxide volume production (Vt) and (b) gas retention coefficient (Rc)

The gas retention coefficient (Rc) defined as the retention volume divided by the total gaseous release, was significantly ($p < 0.01$) influenced by the level of GSF addition in RWF. The high value of R^2 (0.78) indicates that the quadratic model is a good prediction model of Rc using the significant factors shown in Table 3. GSF level shows negative influences on Rc while the particle size was non-significant ($p > 0.05$). Also, the quadratic term of GSF addition level was found to have a significant negative effect on Rc. A response surface plot, showing the effect of GSF level and particle size on Rc, is represented in Figure 2b. As it can be seen, the Rc significantly decreased as the GSF addition level increased. This behaviour is probably due to the increase of the osmotic pressure on the yeast cells, which can lead to an inhibitory effect on the yeast metabolism. In addition, the interactions between gluten and the fraction from GSF, especially fibrous, may prevent the free expansion of dough during proofing. Furthermore, fibers can cause a breakdown of the gluten protein matrix, acting as points of weakness within the expanding dough cell walls [19].

Effects of GSF addition level and particle size on dough dynamic rheological characteristics

The effect of GSF addition level and particle size as structural ingredients can be revealed through oscillatory measurements. By measuring the storage or elastic modulus (G') different resistance to the rupture by the action of stress on the dough formulation structures can be assessed. GSF addition level has significant effect on the G' through the linear positive effect. The effect of GSF addition level on G' was counteracted by the negative linear term of particle size (Table 3). The interaction between both factors have a negative significant ($p < 0.01$) effect on G' modulus. The regression model fitted to the experimental results o dough elastic modulus showed higher coefficient of determination ($R^2 = 0.88$). The F-value for G' was significant ($p < 0.001$). The effects of the addition level and particle size on G' are shown in Figure 3a. Response surface plot showed that an increase of GSF level added in RWF increases G' modulus. The increase could be explained by the GSF compounds which can act in dough as filler that reinforces the gluten and produces strong bonds to give higher modulus. Similar results were obtained by Sivaramakrishnan et al. [43] for rice-wheat composite dough.

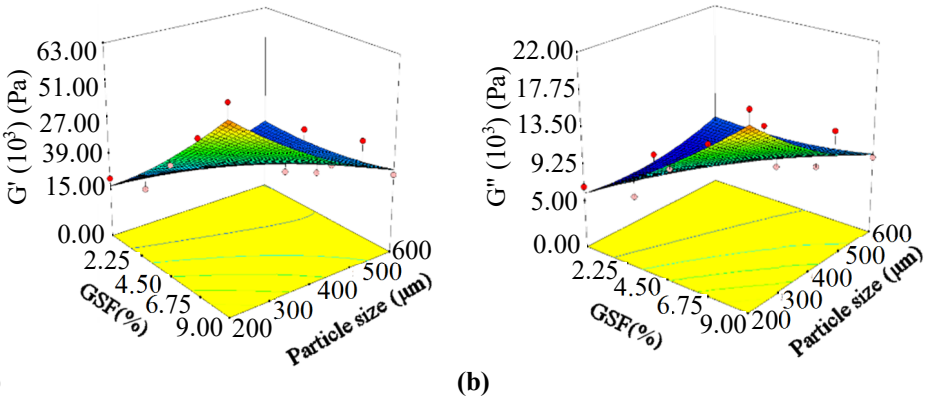

(a) **(b)**

Figure 3. Response surface plot showing the combined effects of grape seeds flour (GPF) level and particle size of GPF on: (a) storage modulus (G') and (b) viscous modulus (G'')

The viscous modulus (G'') was influenced by the presence of GSF levels and particle sizes added in RWF, which had a significant ($p < 0.005$) effect (Table 3). G'' was positively influenced by the addition level and negatively by the particle size and the interaction between them. The quadratic regression model obtained for G'' indicates high correlation coefficient (0.89), statistically significant at $p < 0.001$, revealed that this model is a predictive one. As it can be seen in Figure 3b, the response surface plot showed a decrease of G'' as the level of GSF added in RWF increased. These variations could be attributed to the differences of lipid, protein, fiber constituents of grape seeds flour, shape and size of starch granules of wheat flour [44]. The proportionality of G'' increase with the addition level is probably due to the different soluble and insoluble fractions ratio, higher water absorption can be linked to the higher amount of fibers from GSF [45], which leads to an increased viscosity. The viscous modulus, G'' values are smaller than those of the elastic modulus, G', indicating that the composite flours formulations have a good quality which can lead to higher bread loaf volume [46].

The complex modulus (G^*), as a good indicator of total resistance to deformation of dough, was significantly influenced ($p < 0.001$) by the level and particle size of GSF added in RWF. The ANOVA results showed that the addition level had a significant positive influence ($p < 0.005$) on G^*, but the particle size and the interaction between them have a negative one ($p < 0.005$) (Table 3). The quadratic model is statistically significant ($p < 0.001$) and the value of the determination coefficient ($R^2 = 0.89$) indicates that only 11% of the total variations in the response is not explained by the model. The factors effects are shown in Figure 4a). GSF addition level increase and particle size decrease determined an increase of G^*, showing an increase of dough consistency, probably as a result of GSF water absorption capacity. The amount of insoluble fibers from GSF may be responsible for this increase because the addition of fibers in dough makes his structure stiffer. Similar results were reported by Ahmed [47] who evaluated dough with β glucan addition.

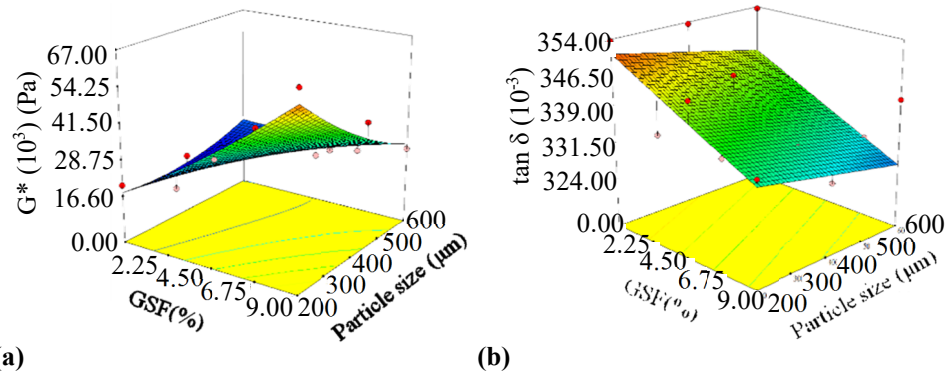

Figure 4. Response surface plot showing the combined effects of grape seeds flour (GPF) level and particle size of GPF on: (a) complex modulus (G*) and (b) loss tangent (tan δ)

The loss tangent or phase angle (tan δ) inform on the phase shift between the stress and strain in oscillation. This characteristics, determined as the ratio of the viscous to the elastic properties of the material, at frequency of 1 Hz, was significantly ($p < 0.005$) influenced by GSF level added in RWF, but the linear coefficient of particle size has not significant effect on tan δ (Table 3). The response surface plot (Figure 3b) indicated an increase of the total resistance to deformation of dough with GSF level increase in RWF. These increase, can be

due to the high content of fiber of GSF, especially insoluble fibre, which substitute RWF, knowing that the dough with fiber enrichment formed stiffer structure than the wheat sample [48]. Insoluble fiber compounds of GSF can interact with the gluten matrix trough hydrogen bonds rising dough stiffness or acting as filler in the viscoelastic matrix.

Optimal particle size and grape seeds flour addition level in refined wheat flour

The optimization was based on the models fitted above for each response and was made by applying the desirability function. In order to improve dough machinability, especially in composite flour dough with different GSF of different particle size, dough rheology is essential. In order to perform simultaneously optimization of multiple responses, some constrains such as Vt and Rc were desired maximal, whereas G* and tan δ were specified as minimum. The results for the optimization revealed that composite flour based on RWF containing 3.01% of GSF of 200 μm particle size could be a good one to achieve the best grape seed-wheat composite flour bread quality. The interactions between dough system's components can change his characteristics due to the macromolecular organization, thus smaller GSF quantity and smaller particle size can lead to better bread quality. The desirability ramp developed for the optimized conditions is shown in Figure 5, revealing an overall desirability value of 0.54.

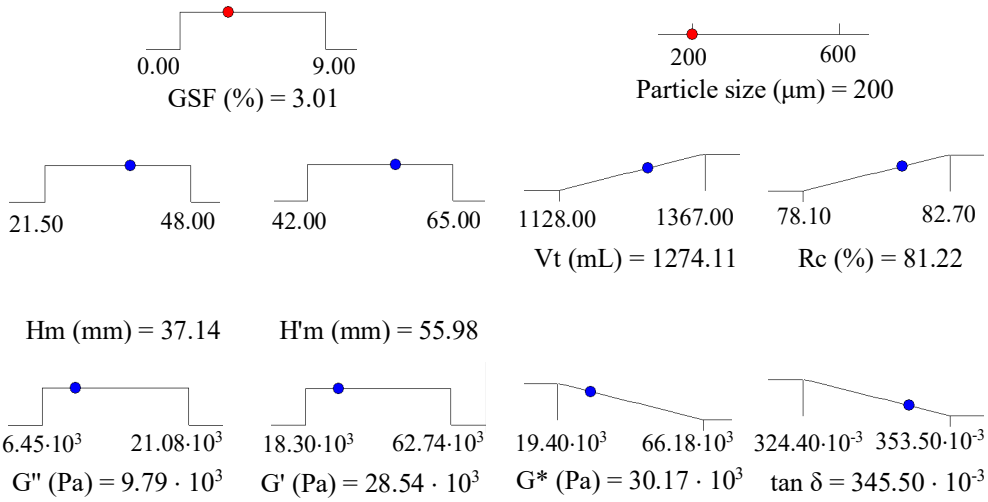

Figure 5. Desirability ramp for optimization process

Under these optimal amount and particle size of grape seed flour addition in refined wheat flour, the values predicted for each response in terms of dough fermentation characteristics and dynamic rheological properties was found to be as follows: dough maximum height, Hm of 37.14 mm, maximum height of gaseous production, H'm of 55.98 mm, total carbon dioxide volume production, Vt of 1274.11 mL, gas retention coefficient, Rc of 81.22%, elastic modulus G' of 28.54 · 10^3 Pa, viscous modulus, G" of 9.79 · 10^3 Pa, complex modulus, G* of 30.17 · 10^3 Pa and loss tangent, tan δ of 345.50·10^{-3}.

Model validation

The obtained models of dough fermentation characteristics and dynamic rheological properties were verified by comparing the predicted data with the experimental data. The data obtained at the optimal value of factors, the amount of GSF added (3.01%) and particle size (small) for each response studied confirms that the optimization was made accurately being close to the predicted values (Table 4).

Table 4

Predicted *versus* experimental values at the optimal amount and particle size of grape seeds flour addition in refined wheat flour

Parameters	Values		
	Predicted	Experimental	SE Mean
Hm (mm)	37.14	37.17	1.37
H'm (mm)	55.98	56.01	1.25
Vt (mL)	1274.11	1274.35	21.98
Rc (%)	81.22	81.22	0.44
G' (Pa)	$28.54 \cdot 10^3$	$28.48 \cdot 10^3$	$2.81 \cdot 10^3$
G" (Pa)	$9.79 \cdot 10^3$	$9.77 \cdot 10^3$	$0.90 \cdot 10^3$
G* (Pa)	$30.17 \cdot 10^3$	$30.11 \cdot 10^3$	$2.95 \cdot 10^3$
tan δ	$345.50 \cdot 10^{-3}$	$345.50 \cdot 10^{-3}$	$3.44 \cdot 10^{-3}$

As it can be seen from Table 5, experimentally, the values obtained for dough rheological characteristics are in good agreement with the predicted values, revealing a satisfactory result.

Conclusion

The physico-chemical characteristics of the refined wheat flour are changed by the addition of GSF at different levels and particle sizes. The increase of the protein and ash contents and higher alpha-amylase activities found in the composite flours can lead to improved chemical characteristics of bread.

Response surface methodology represents an adequate tool to reveal the mechanism remarked in the composite flour dough as well as to optimize the amount of grape seed flour and particle size in the recipe based on refined wheat flour.

This study highlighted that the small particle size at 3.01% GSF replacement level in refined wheat flour could be used in order to obtain grape seeds-wheat composite flour with the best dough rheological properties. Further studies are needed to evaluate the sensorial acceptance of this novel product.

Acknowledgements. This work was supported by a grant of the Romanian National Authority for Scientific Research and Innovation, CNCS/CCCDI – UEFISCDI, project number PN-III-P2-2.1-BG-2016-0136, within PNCDI III.

References

1. Quiles A., Campbell G.M., Struck S., Rohm,H., Hernando I. (2018), Fiber from fruit pomace: A review of applications in cereal-based products, *Food Reviews International*, 34(2), pp.162–181.
2. Šporin M., Avbelj M., Kovač B., Možina S.S. (2018), Quality characteristics of wheat flour dough and bread containing grape pomace flour, *Food Science and Technology International*, 24(3), pp. 251–263.
3. Meral R., Doğan I.S. (2013), Grape seed as a functional food ingredient in bread-making, *International Journal of Food Sciences and Nutrition*, 64, pp. 372–379.
4. Boudová Pečivová P., Kráčmar S., Kubáň V., Mlček J., Juríková T., Sochor J. (2014), Effect of Addition of Grape Seed Flour on Chemical, Textural and Sensory Properties of Bread Dough, *Mitteilungen Klosterneuburg*, 64, pp. 114–119.
5. Brenes A., Viveros A., Chamorro S., Arija, I. (2016), Use of polyphenol-rich grape by-products in monogastric nutrition. A review, *Animal Feed Science and Technology*, 211, pp. 1–17.
6. Gubsky S., Labazov M., Samokhvalova O., Grevtseva N., Gorodyska O. (2018), Optimization of extraction parameters of phenolic antioxidants from defatted grape seeds flour by response surface methodology, *Ukrainian Food Journal*, 7(4), pp. 627–639.
7. Iuga M., Ropciuc S., Mironeasa S. (2017), Antioxidant activity and total phenolic content of grape seeds and peels from Romanian varieties, *Food and Environment Safety Journal*, 16(4), pp. 276–281.
8. Mironeasa S. (2017), *Valorization of secondary products from wine making*, Performantica Publishing House, Iasi, Romania.
9. Rockenbach I.I., Jungfer E., Ritter C., Santiago-Schübel B., Thiele B., Fett R., Galensa R. (2012), Characterization of flavan-3-ols in seeds of grape pomace by CE, HPLC-DAD-MSn and LC-ESI-FTICR-MS, *Food Research International*, 48(2), pp. 848–855.
10. Karaman S., Karasu S., Tornuk F., Toker O.S., Geçgel U., Sagdic O., Ozcan N., Gül O. (2015), Recovery potential of cold press byproducts obtained from the edible oil industry: physicochemical, bioactive, and antimicrobial properties, *Journal of Agricultural and Food Chemistry*, 63(8), pp. 2305–2313.
11. Zhou T., Li Q., Zhang J., Bai Y., Zhao, G. (2010), Purification and characterization of a new 11S globulin-like protein from grape (Vitis vinifera L.) seeds, *European Food Research and Technology*, 230, pp. 693–699.
12. Iuga M., Codină G.G., Mironeasa S., Oroian M. (2017), Amino acid composition of grape seed and peels from grape pomace, *The 16th International Symposium prospects for the 30th Millennium Agriculture*, Cluj–Napoca, Romania, September 28–30, published in *Book of abstracts,* 4, pp. 381.
13. Tseng, A., Zhao, Y., (2013), Wine grape pomace as antioxidant dietary fibre for enhancing nutritional value and improving storability of yogurt and salad dressing, *Food Chemistry*, 138(1), pp. 356–365.
14. Amariei S., Norocel L., Pădureț S., Gutt G., (2018), Effect of grape seed flour on the quality of summer salami, *Journal of Food Processing and Preservation*, 42(5), pp. e13601.
15. Aksoylu Z., Çağindi Ö., Köse E. (2015), Effects of blueberry, grape seed powder and poppy seed incorporation on physicochemical and sensory properties of biscuit, *Journal of Food Quality*, 38, pp. 164–174.
16. Mironeasa S., Codină G. G., Mironeasa C. (2016), Optimization of wheat-grape seed composite flour to improve alpha-amylase activity and dough rheological behavior, *International Journal of Food Properties*, 19(4), pp. 859–872.
17. Tietze S., Jekle M., Becker T. (2016), Possibilities to derive empirical dough characteristics from fundamental rheology, *Trends in Food Science & Technology*, 57, pp. 1–10.

18. Mironeasa S., Codină G.G., Mironeasa C. (2012), The effects of wheat flour substitution with grape seed flour on the rheological parameters of the dough assessed by Mixolab, *Journal of Texture Studies*, 43, pp. 40–48.
19. Iuga M., Mironeasa S., Zaharia D., Ropciuc S., Mironeasa C. (2017), Effects of grape seeds flour addition on wheat flour dough rheological properties, *International Multidisciplinary Scientific GeoConference: SGEM: Surveying Geology & mining Ecology Management*, 17, pp. 209–216.
20. Iuga M., Mironeasa C., Mironeasa S. (2019), Oscillatory rheology and creep-recovery behaviour of grape seed-wheat flour dough: effect of grape seed particle size, variety and addition level, *Bulletin of University of Agricultural Sciences and Veterinary Medicine Cluj-Napoca. Food Science and Technology*, 76(1), pp. 40–51.
21. Sanz-Penella J.M., Tamayo-Ramos J.A., Sanz Y., Haros M. (2009), Phytate reduction in bran-enriched bread by phytase-producing bifidobacteria, *Journal of Agricultural and Food Chemistry,* 57(21), pp. 10239–10244.
22. Kurek M., Wyrwisz J., Piwińska M., Wierzbicka A., (2016), The effect of oat fibre powder particle size on the physical properties of wheat bread rolls, *Food Technology and Biotechnology*, 54(1), pp. 45–51.
23. Martínez M.M., Díaz Á., Gómez M. (2014), Effect of different microstructural features of soluble and insoluble fibres on gluten–free dough rheology and bread–making, *Journal of Food Engineering*, 142, pp. 49–56.
24. Mironeasa S., Iuga M., Zaharia D., Dabija A., Mironeasa C., (2017), Influence of particle sizes and addition level of grape seeds on wheat flour dough rheological properties, *International Multidisciplinary Scientific GeoConference: SGEM: Surveying Geology & mining Ecology Management*, 17, pp. 265–272.
25. Dhingra D., Mona M., Rajput H., Patil R.T. (2012), Dietary fibre in foods: a review, *Journal of Food Science and Technoogy*, 49, pp. 255–266.
26. Hadnadev T.D., Torbica A., Hadnađev M. (2011), Rheological properties of wheat flour substitutes/alternative crops assessed by Mixolab, *Procedia Food Science*, 1, pp. 328–334.
27. Tronsmo K.M., Magnus E.M., Baardseth P., Schofield J.D., Aamodt A., Færgestad E.M. (2003), Comparison of small and large deformation rheological properties of wheat dough and gluten, *Cereal Chemistry*, 80(5), pp. 587–595.
28. Khatkar B.S., Schofield J.D. (2002), Dynamic rheology of wheat flour dough. II. Assessment of dough strength and bread-making quality, *Journal of the Science of Food and Agriculture*, 82, pp. 823–826.
29. Skendi A., Papageorgiou M., Biliaderis C.G. (2009), Effect of barley β-glucan molecular size and level on wheat dough rheological properties, *Journal of Food Engineering*, 91, pp. 594–601.
30. Martínez M.M., Díaz Á., Gómez M. (2014), Effect of different microstructural features of soluble and insoluble fibres on gluten–free dough rheology and bread–making, *Journal of Food Engineering*, 142, pp. 49–56.
31. Mirsaeedghazi H., Emam–Djomeh Z., Mousavi S.M.A. (2008), Rheometric measurement of dough rheological characteristics and factors affecting it, *International Journal of Agriculture and Biology*, 10, pp. 112–119.
32. Tuncil Y.E., Jondiko T., Castell-Perez M.E., Puerta-Gomez A.F., Awika J.M. (2016), Small deformation rheological properties of dough are useful tool to predict the effects of modest sodium reduction on flour tortilla quality, *LWT-Food Science and Technology*, 68, pp. 329–333.
33. Steffe J. (1996), *Rheological methods in food process engineering*, Freeman Press, Michigan, USA.
34. Wu C.J., Hamada M.S. (2011), Experiments: Planning, analysis, and optimization (Vol. 552), Hoboken, New Jersey: John Wiley & Sons.

35. Drakos A., Kyriakakis G., Evageliou V., Protonotariou S., Mandala I., Ritzoulis C. (2017), Influence of jet milling and particle size on the composition, physicochemical and mechanical properties of barley and rye flours, *Food Chemistry*, 215, pp. 326–332.
36. Mironeasa S. (2013), Grape seeds: studies and research, PIM Publishing House, Iasi, Romania.
37. Mironeasa S., Mironeasa C., Codină G.G. (2010), Evaluation of Mineral Element Content in Grape Seed and Defatted Grape Seed, *Food and Environment Safety*, IX, pp. 53–60.
38. Dhen N., Román L., Ben I., Mario R., Martínez M., Garogouri M., Gómez M. (2016), Particle size distribution of soy flour affecting the quality of enriched gluten-free cakes, *LWT-Food Science & Technology*, 66, pp. 179–185.
39. Kiszonas A. M., Engle D.A., Pierantoni L.A., Morris C.F. (2018), Relationships between Falling Number, α - amylase activity, milling, cookie, and sponge cake quality of soft white wheat, *Cereal Chemistry*, 95(3), pp. 373-385.
40. Sundarram A., Murthy T.P.K. (2014), α-amylase production and applications: a review, *Journal of Applied & Environmental Microbiology*, 2(4), pp. 166–175.
41. Păucean A., Man S.M., Socaci S.A. (2016), Wheat germ bread quality and dough rheology as influenced by added enzymes and ascorbic acid, *Studia Universitatis Babes-Bolyai, Chemia*, 2(61), pp. 103–118.
42. Mohammed I., Ahmed A.R., Senge B. (2014), Effects of chickpea flour on wheat pasting properties and bread making quality, *Journal of Food Science and Technology*, 51 (9), pp. 1902–1910.
43. Sivaramakrishnan H.P., Senge B., Chattopadhyay P.K. (2004), Rheological properties of rice dough for making rice bread, *Journal of Food Engineering,* 62(1), pp. 37–45.
44. Abebe W., Ronda F. (2014), Rheological and textural properties of tef [Eragrostis tef (Zucc.) Trotter] grain flour gels, *Journal of Cereal Science*, 60(1), pp. 122–130.
45. Brockmole C.L., Zabik M.E. (1976), Wheat bran and middlings in white layer cakes, *Journal of Food Science,* 41, pp. 357–360.
46. Song Y., Zheng Q. (2007), Dynamic rheological properties of wheat flour dough and proteins, *Trends in Food Science & Technology*, 18(3), pp. 132–138.
47. Ahmed J. (2014), Effect of particle size and temperature on rheology and creep behavior of barley β–d–glucan concentrate dough, *Carbohydrates and Polymers*, 111, pp. 89–100.
48. Mironeasa S., Iuga M., Zaharia D., Mironeasa C. (2019), Rheological analysis of wheat flour dough as influenced by grape peels of different particle sizes and addition levels, *Food and Bioprocess Technology*, 12(2), pp. 228–245.

Physico-chemical and sensory properties of functional confectionery products with Rosa Canina powder

Violina Popovici[1], Oxana Radu[1], Viacheslav Hubenia[2], Eugenia Covaliov[1], Tatiana Capcanari[1], Cristina Popovici[1]

1 – Technical University of Moldova, Faculty of Food Technology, Chisinau, Republic of Moldova
2 – National University of Food Technologies, Kyiv, Ukraine

Keywords:

Rosehip
Confectionery
Candies
Functionality

Article history:

Received 30.01.2019
Received in revised form 17.05.2019
Accepted 28.11.2019

Corresponding author:

Cristina Popovici
E-mail: cristina.popovici@toap.utm.md

DOI:
10.24263/2304-974X-2019-8-4-12

Abstract

Introduction. The purpose of research was to evaluate the physico-chemical and sensory paramenters of functional confectionery products with rosehip powder.

Material and methods. In research *Rosa Canina* harvested in the Republic of Moldova (Central region) was analized. Physico-chemical methods and sensory evaluation of the elaborated functional confectionery products and DPPH antioxidant activity of the roseship extract were used.

Results and discusisions. It was established that rosehip powder can be used as an antioxidant and natural colorant in the preparation of BIO candies enriched with vitamins, natural antioxidants. The acidity index of this products in camparison with the control sample it is within the permissible limits 0,12± 0,01%, and the high content of caratenoids gives the products the red-orange color, so the rosehip powder can be used to obtain functional products. The elaborated functional candies are characterized by positively rated sensory and physico-chemical indices, the value of the acidity index constituting 1.15±0.01 mg KOH/l and the humidity mass fraction of 24.19±0.01%. The results showed that higher concentration of rosehip powder give orange color and the acid value of the product increases, which represent a disadvantage of the rosehip extract, this provides the opportunity to open a new research direction. From a sensory point of view, the product with small content of rosehip power was positively appreciated, which confirms that food products based on natural dye of plan origin is a good alternative for obtaining safe and natural products for consumer health. A relevant aspect of this paper is the fact that an additive and natural dye extracted from the rosehip fruits was obtained. According to the recipe, the obtained natural additive has replaced the synthetic one, giving the prepared candies a pleasant taste and a specific smell of rosehip flowers.

Conclusion. It is justified functional properties and high quality of the confectionery products in which the synthetic food additives were replaced with the natural dyes extracted from plant products.

Introduction

Rosehip or Wild Rose (*Rosa Canina*) is a shrub of the Rosaceae family. It includes over 400 species, widespread in temperate and subtropical areas. Physico-chemical composition, amount of vitamins, pigments etc. of rosehip fruits depends on the climatic conditions, also varying according to the species and the intensity of their growth. The most valuable part of the fruit is the outer shell, which makes up 54–87% of the total mass.

Carotenoid intake with β-carotene, lycopene and rubixantine isomers, as protavitamin A, is one of the main strengths of rosehip fruit. In addition, vitamins B1, B2, B3, B5, K, P, PP, ά-, β-tocopherol (vitamin E), nicotinic acid are found. A specific feature of rosehip fruit is the lack of the ascorbinase enzyme, which destroys vitamin C [1]. Fresh rosehip fruits contain vitamin C – 4,000 mg/%, bioflavonoids up to 3,500 mg/%, carotene from 3 to 8 mg/%, folic acid up to 0.88 mg/%, tocopherols up to 0, 69 mg /%. Polyphenolic compounds of rosehip are represented by catechins, leicoanthocyanins, anthocyanins, flavonols. The content of catechins in most species is 856 – 2712 mg%, of leicoanthocyanins of 72–1296 mg%. The sum of these two polyphenols correlates with the sum of the dyes and tannins content [2]. The rosehip fruits are also a powerful mineralizer, containing magnesium (Mg), calcium (Ca), iron (Fe), manganese (Mn), phosphorus (P), potassium (K), selenium (Se), sulfur (S).), zinc (Zn). Also important is their content of polyphenols, anthocyanins, pectin, citrates, malic acid and citric acid, terpenoids and glycosides [3]. Fruit sugar is sucrose, invert sugars (glucose and fructose). At maturity the fruits contain a larger quantity of starch, which in the phase of ripening turns into sugar. In addition, in the pulp, there are fibers and pentosanes. Of the organic acids, the rosehip fruits contain only citric acid. The fruits are relatively rich in pectic substances.

The administration in the pastry products of a small dose of dried rosehip powder (0.5-1.0%) has a positive influence on the physico-chemical and sensory properties of the pastry products. The administration of rose-hip increases the solubility of iron in foods up to 0.3-0.35 mg Fe/100 g product [5].

Rosehip powder presents an organic product, which is a source of concentrated active ingredients and improves the nutritional and sensory properties of manufactured products. This product has a good reducing capacity and can be used in the manufacture of pastry products as an ingredient to give the dough color, taste and aroma, as well as fillings.

One of the components used in the production of functional foods is the rosehip powder that contributes to the vitaminization and increasing the resistance of the body. Due to the high concentration of caratenoids it is used as a natural dye giving the products red-orange color [3].

The antioxidant properties of the rosehip processing product are known, which positively affect the shelf life of confectionery [15].

The research topic addressed is quite current because the confectionery products require a substantial correction of their chemical composition in the direction of increasing the content of vitamins, minerals and food fibers, reducing the energy value and enriching the products with functional ingredients [4, 16]. The reason for choosing this subject was that the preparation of functional candies with the addition of rosehip powder is a new technology, opting to replace synthetic food additives with BIO products [5, 17].

The aim of the research was to evaluate the physico-chemical and sensory characteristics of the new functional product. In order to achieve the goal, the objectives were pursued: (1) the analysis of the global trends in the production of functional candies by studying, analyzing and systematizing the scientific literature and the patents of invention; (2) justification for choosing rosehip powder as a natural colorant; (3) determining the content of polyphenols, caratenoids and the acidity index of rosehip extract; (4) analysis of the results of scientific research.

Materials and methods

Materials

The collection of berries is a first step in preparing the raw materials needed to carry out the established research. The fruits of rosehip were harvested in quantities of 3–5 kg and then subjected to the convection drying process for a period of about 6 hours. The dried fruits were finely ground and sifted until an extra-fine powder was obtained. Experimental samples of dried rosehip fruits and powder used in the work are presented in Figures 1 and 2.

Figure 1. Dried rosehip fruits

Figure 2. Rosehip powder

Functional product preparation technology – BIO candies with added rosehip powder

The functional candy production technology has a number of features, but the basis is a single scheme that includes the following steps: (1) preparing the raw materials for production, (2) preparing the mixtures, (3) preparing the composition, (4) cooling the composition, (5) processing and forming of candies, (6) packaging them. In the process of developing functional candy production technology, it is necessary to develop techniques for processing raw materials and semi-finished products, in which minimal chemical changes of nutrients (isomalt, dietary fibers and proteins) are guaranteed, the optimal structural and mechanical properties of semi-finished and finished products.

Physico-chemical methods of analysis

Determination of the dry matter. The sample taken for determination is exposed to a source of heat up to a constant weight. Weight loss, calculated as a percentage, represents the moisture content, and the remaining residue – the dry matter [6]. The dry matter content (X,%) in the analyzed sample is calculated using the following formula:

$$X=\frac{(m_2-m)}{(m_1-m)}\cdot 100\%,$$

where: m – mass of the vial with the glass rod and sand, g;
m_1 – mass of the vial with the glass rod and sand + the product before drying, g;
m_2 – the mass of the vial with the glass rod and sand after drying, g.

Antioxidant activity determination using free radical DPPH. Determination of the antioxidant activity of the lipophilic extracts was performed using LLG uniSPEC -2 spectrophotometer and expressed as a% inhibition of DPPH using the following equation [7]:

$$AA\% = \frac{A_0 - A_t}{A_0} \cdot 100\%$$

where:

A0 – absorbance of the DPPH solution at t = 0 s;

At – absorbance of the DPPH solution after 30 min;

A lower value of At in the analyzed sample shows a higher antioxidant activity.

Determination of the total polyphenols content. Determination of total polyphenols content was performed according to Sturza (2016) on the same spectrophotometer, at ʎ = 765 nm, using a 10 mm quartz cuvette [6, 8]. The results of the total polyphenols content, expressed in mg GA / 100 g of vegetal material, were obtained using the gallic acid calibration curve (y = 1.4x + 0.0037, R2 = 0.999).

Determination of the total content of assimilating pigments (chlorophyll a, chlorophyll b, total carotenoids). For the determination of the content of assimilating pigments, was measured the absorbance at wavelengths of 663 nm for chlorophyll a, 647 nm for chlorophyll b and 470 nm for total carotenoids, to 10 ml of extract versus the deodorized refined oil (blank). The carotenoid content were determined by the following equations [9-12]:

$$C_a(mgL^{-1}) = (12{,}25 \times A_{663.2}) - (2{,}79 \times A_{646.8}) \quad (3)$$

$$C_b(mgL^{-1}) = (21{,}5 \times A_{646.8}) - (5{,}1 \times A_{663.2}) \quad (4)$$

$$C_{a+b}(mgL^{-1}) = \frac{(1000 \times A_{470} - 1.82 \times C_a - 85.02 \times C_b)}{198} \quad (5)$$

where:

$A_{663.2}$ – solution absorbance at λ = 663.2 nm;

$A_{646,8}$ – solution absorbance at λ = 646.8 nm;

A_{470} – solution absorbance at λ = 470 nm;

Determination of antioxidant capacity – HPSA. For the determination of HPSA, in the titration flasks, 1 ml of sample was mixed with 1 ml of hydrogen peroxide solution H_2O_2 (0.1 mM). Then 2 drops of ammonium molybdate, 10 ml of H2SO4 (2M) sulfuric acid and 7 ml of KI potassium iodide (1.8 M) were added. The obtained solution was titrated with sodium thiosulfate N2S2O3 (5.09 mM) until the yellow colour disappeared. The volume (V1) of sodium thiosulfate Na2S2O3 (5.09 mM) used for titration was recorded.

$$\%\, H_2O_2 = \frac{V_0 - V_1}{V_0} \cdot 100\%$$

where:

V_0 – volume of sodium thiosulphate $N_2S_2O_3$ (5,09 mM) spent for titration of the control sample in the presence of hydrogen peroxide (without sample);

V_1 – volume of sodium thiosulphate $N_2S_2O_3$ (5,09 mM) (5.09 mM) spent for titration of the sample in the presence of hydrogen peroxide.

Determination of acid value (AV). Determination of AV was performed by the volumetric method and the results obtained were calculated according to the following equation [13]:

$$AV = \frac{V_{KOH} \cdot N_{KOH} \cdot 5.611}{m}, \text{ [mg KOH/g]}$$

where:

V_{KOH} – volume of the potassium hydroxide, [ml];

N_{KOH} – concentration of the potassium hydroxide, [mol/dm^3];

m – mass of the sample, g.

Gastrointestinal in vitro digestion. The samples were weighed 10 g of product and dissolved in 100 ml of HCl solution with pH = 1.5–2.0, 15 mg pepsin was added. At the same time, similar samples of 10 g of product where dissolved in 100 ml $NaHCO_3$ solution with pH = 8.2, 15 mg trypsin was added. The samples were thermostated at 37±0.1 °C by continuous stirring at 95 rpm for 60 minutes. From the initial samples (0 minutes of thermostat) as well as after 60 minutes, 120 minutes and 180 minutes, respectively, aliquots were taken in order to spectrophotometrically determine the antioxidant activity using the free radical DPPH. Each aliquot was centrifuged for 10 min (6000 rpm), then the filtrate (1 ml each) was subjected to the analysis. The direct reaction was determined by the antioxidant activity of the aliquots: 3.9 ml of DPPH solution and 0.1 ml of the analyzed sample were introduced. As a reference sample, methanol was used. The reaction took place for 30 min in a dark place. During this time the absorbance was read at the spectrophotometer "LLG uniSPEC -2" [14].

Sensory evaluation. The functional food products were determined by a sensory panel of 10 members. They rated the samples for appearance, aroma, taste, and overall acceptability by using a five-point Hedonic scale (5 and 1 representing “like extremely” and “dislike extremely” respectively) *[10]*.

Statistical analysis. Variance analysis of the results was carried out by least square method with application of Microsoft Office Excel program. Differences were considered statistically significant if probability was greater than 95% (q < 5%). All assays were performed at room temperature, 20±1 ºC. Experimental results are represented according to standard rules.

Results and discussions

Physico-chemical and antioxidant properties of rosehip powder

The physical-chemical characteristics of a product have an essential role in the evaluation of its food quality and safety. In this regard, several indexes have been determined in order to analize qualitatively the investigated horticultural raw material.

According to the data from Table 1, the low value of the water weight fraction of rosehip powder, 5.20±0.01%, was established. This fact argues for the possibility of preserving the rosehip powder for a long time and using it for other products elaboration [3].

Table 1

Physico-chemical properties of rosehip powder

Nr	Parameter	Value,%
1	Weight fraction of water,%	5.20±0.01
2	Acid Value, mg KOH/l	0.12±0.01
3	Antioxidant activity,% HPSA	16.5±1.2
4	Polyphenols content, mg AG/100 g plant	1981.28±3.57

The composition of food products contains acidic substances that cause an acid reaction to them [6]. Acidic substances can be present in raw materials, as well as formed while technological processes or during storage [5]. Acidity is an important property for the appreciation of food quality, because it directly contributes to the taste formation and is used as the indicator of some products freshness [12]. Following the determination of the acidity index of analyzed rosehip extract, it was showed that the obtained value, 0.12±0.01 mg KOH/l, did not exceed the maximum permissible limits [6]. This fact encouraged us to use the rosehip powder in new functional products obtaining [4].

The dried and ground fruits were mixed with a deodorized refined oil in the ratio 1:15 and with 50% ethyl alcohol in the ratio 1:10 to obtain liposoluble and hydroalcoholic extracts. The obtained compositions were stirred for 3 hours at 37 °C.

The extracts were separated by centrifugation at 7000 rpm for 10 minutes, stored in dark-colored glass vials and kept in the refrigerator (t =±4 °C).

Hydrogen Peroxide Scavenging Activity (HPSA) reflects the level of system resistance against oxidative deradation, caused by the presence of free oxygen – the main oxidizing agent, regardless of how oxidation reactions are initiated [9]. In the case of analyzed rosehip extract, HPSA is 16.5±1.2%, which positively argues for the possibility of synthetic additives substitution with natural antioxidants obtained from horticultural sources such as rosehip fruits.

Polyphenols are biologically active compounds that exhibit antioxidant character by the inhibition of free radicals and the deceleration of oxidative and alteration processes in food products [7]. The determination of extracts polyphenol content was performed using the Folin-Ciocalteu reagent by spectrophotometric methods. The obtained data showed that the polyphenol content was 1981.28±3.57 mg GA/100 g plant.

Carotenoids take part of the compounds class that is characterized by coloring capacity, beneficial health and anti-obesity effects [10]. Carotenoids are also widely used in many industrial fields, such as the foods, pharmaceuticals and cosmetics [11].

It was established [1–3] that carotenoid content could vary between 1 and 20 mg/L depending on the region of cultivation, season and climatic conditions in the region. The content of α and β chlorophyll, β-carotene, lycopene and zeaxanthin in the liposoluble extract of analyzed rosehip was determined spectrophotometrically (Figure 3).

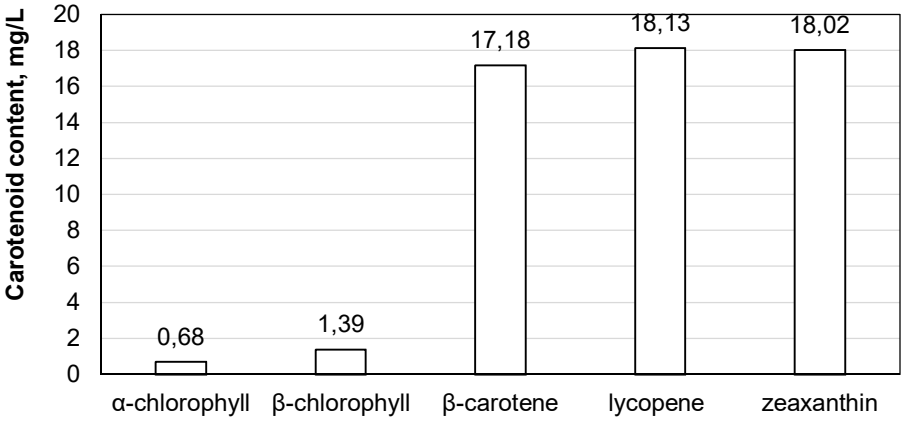

Figure 3. Carotenoid content in obtained rosehip extracts

According to Figure 3, the analyzed rosehip extract is characterized by a high carotenoid content. Generally, carotene are orange pigments – red to yellow. In this respect, the following results were obtained: 17.18±0.01 mg/L β-carotene; 18.13±0.03 mg/L lycopene; 18.02±0.02 mg/L zeaxanthin. It was also showed the presence of chlorophyll – the group of green pigments from plants and other photosynthetic organisms: 0.68±0.01 mg/L α-chlorophyll and 1.39±0.02 mg/L β-chlorophyll.

Antioxidants are substances that slow down or stop the harmful action of oxidants [7]. The main characteristic of antioxidant substances is the ability to capture free radicals [8]. Phenolic compounds, polyphenols, carotenoids, flavonoids are antioxidant compounds that inhibit free radicals (peroxides, hydroperoxides) and respectively inhibit the mechanism of oxidation itself [12]. Forest berries, especially rosehip, are considered very rich in antioxidant compounds.

The analysis of the antioxidant activity was performed using the free radical DPPH in order to estimate the antioxidant potential of studied rosehip extracts (Figure 4).

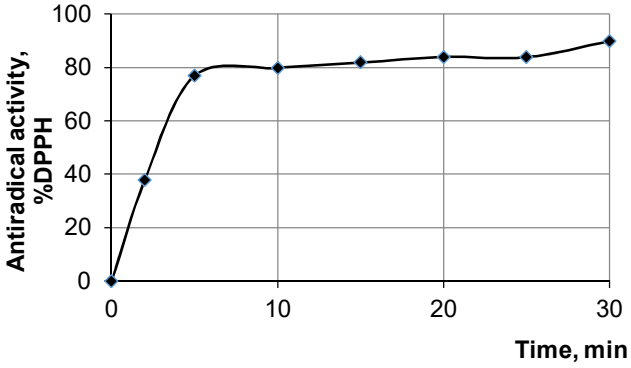

Figure 4. The antioxidant activity of rosehip lipidic extract

It has been established that rosehip powder is characterized by a high antioxidant capacity, because the value of DPPH free radical inhibition capacity after a 30-minute action period constitutes 90.84±0.86%. This fact is explained by the rich content of biologically active compounds with antioxidant character in the analyzed extract and, respectively, in the rosehip powder [2].

Bioavailability of biologically active compounds according to *in Vitro* simulation of gastrointestinal digestion

The bioavailability of biologically active compounds is the ratio of the amount of active substance to the rate at which it is transferred, absorbed into the body, reaches the site of action and manifests its biological effect [14]. Numerous researches [1, 2, 7, 8, 9] have been carried out regarding the content of biologically active substances with antioxidant character in fruits, fruit extracts, etc. The digestion process directly influences the composition of the extracts depending on the conditions under which the physiological digestion processes and the multitude of processes that take place in the gastrointestinal tract are performed. In order to study the evolution of the antioxidant activity of functional products with the addition of rosehip powder, the simulation of gastric and intestinal digestion over time was performed (Figures 5 and 6).

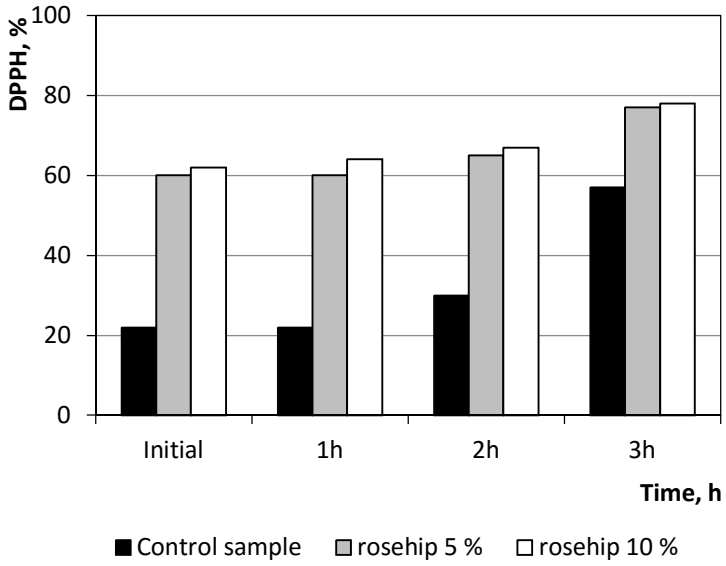

Figure 5. Bioavailability of biologically active compounds in acidic medium (gastric digestion)

In consonance with data obtained by the induced gastric digestion (acidic medium), the samples with rosehip addition show an essential increase of antioxidant activity in comparison with the control samples, for which values vary between 24.38 and 53.57%. These values range within 60.36–72.75% for the samples with 5% rosehip and within 65.80–77.85% for the samples with 10% rosehip, respectively.

The sequential increase of antioxidant activity over 3 hours is explained by the gradual release of biologically active compounds in the digestion process. The important factor refers to the influence of solution pH and enzymatic interactions in the investigated product. It has been shown that the increased polyphenol content enhance the antioxidant capacity of the obtained samples. The essential activity deviation of the samples with the addition of rosehip powder in comparison with the control samples can be also explained by the presence of other substances that increase the antioxidant capacity of the product as a result of in Vitro digestion processes. These biologically active compounds such as amino acids, peptides are released during digestion and undergo modifications that can subsequently affect the ability of free radicals inhibition. The another hypothesis consists in the loss of volatile substances during gastric digestion due to the increased antioxidant capacity of the product.

The obtained data show that gastric digestion doesn`t essentially change the qualitative and quantitative composition of biologically active compounds with antioxidant character in the analyzed product. This fact suggests that these compounds have high stability in the conditions of low pH. Both the acidic medium and digestive enzymes favor the release of biologically active compounds, that respectively influence positively on the antioxidant capacity of the products based on rosehip powder [14].

Simultaneously with the analysis of gastric digestion processes, the simulation of the intestinal digestion phase was carried out by the samples incubation in alkaline medium (pH = 8.2), determining the product antioxidant activity over a 3-hour period (Figure 6).

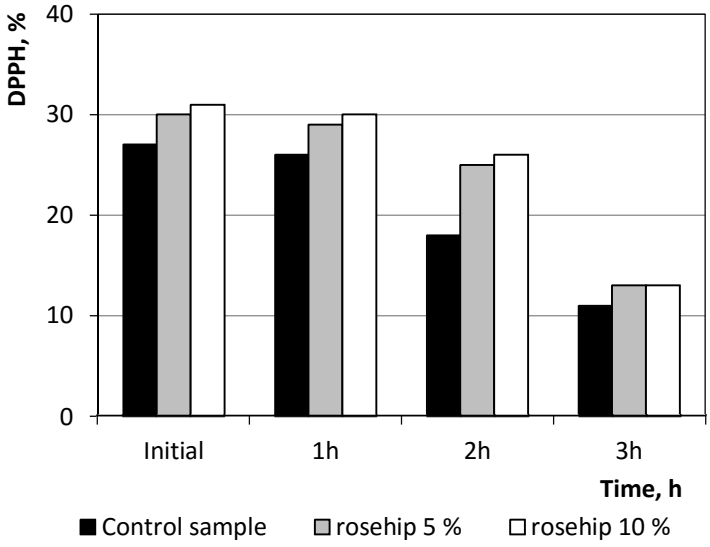

Figure 6. Bioavailability of biologically active compounds in alkaline medium (intestinal digestion)

The obtained data show that the antioxidant activity of samples based on rosehip powder, both 5% and 10% samples, is higher compared to the control sample and vary within 31.21–14.32% and 29.72–13.11%, respectively. Whereas the values of the control samples vary within 26.38–10.95%.

The gradual decrease of the antioxidant activity within 3 hours both for the samples with rosehip addition and for the control samples was established while the intestinal digestion simulation. This fact can be explained by the low stability of biologically active compounds under alkaline conditions (pH = 8.2) and the formation of metabolites that inhibit the antioxidant activity of biologically active compounds in the investigated products.

Weight fraction of water and acidity index of functional products with the rosehip powder

The weight fraction of water for the control samples as well as the samples with Rosehip (5 and 10%) are within the allowable limits (30.0%) for candies on the base of dried fruit. In the case of samples with the rosehip, the weight fraction of water shows a slight decrease, which ensures a higher degree of stability compared to the control sample.

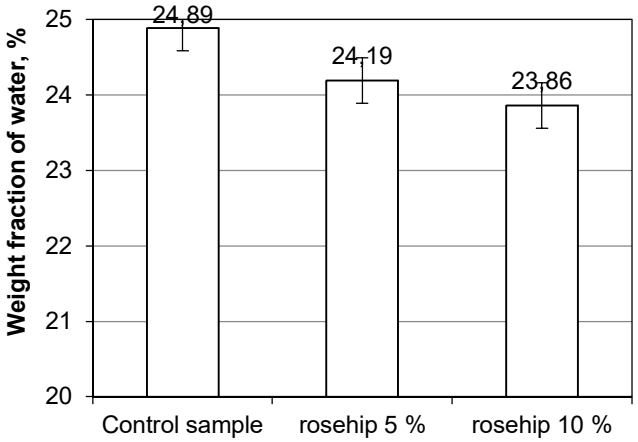

Figure 7. Weight fraction of water in functional candies with the rosehip powder,%

Acidic substances may come from raw materials, technological processes or may be formed during storage [13]. Acidity is an important property in the appreciation of the quality of the food products as it directly contributes to the formation of the taste and for some products it is an indicator of their freshness [4].

The acidity index of the control sample is 1.14±0.01, and in the case of samples with of 5 and 10% rosehip, it values 1.15±0.01 acidity grade and 1.17±0.01 acidity grade respectively.The obtained values are within the maximum permissible limits (A = 4.0 max. acidity grade), which encourages us to use rosehip powder in obtaining functional food products.

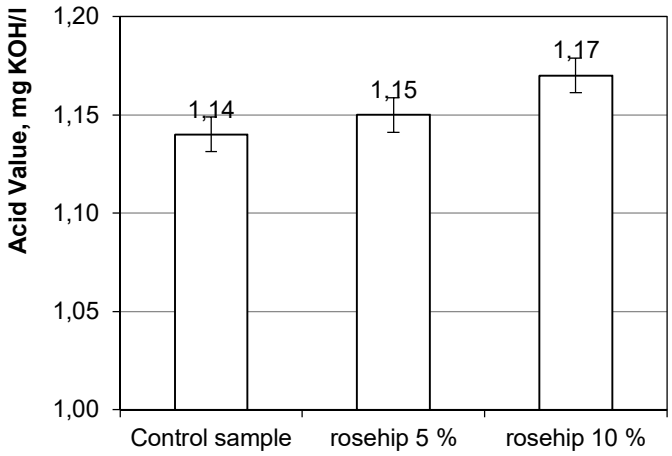

Figure 8. Acidity index in functional candies with rosehip powder, acidicy grade

Sensory analysis of candy with the rosehip powder

It was established that the sensory properties of the sample with 5% rosehip powder are characterized by a good consistency, pleasant taste and fine odor.

Figure 9. BIO candy with cashew and rosehip powder (5%)

Figure 10. BIO candy with cashew and rosehip powder (10%)

According to the tasters' appreciation, this does not differ from the control sample which does not contain rosehip powder. Although, sample with 10% rosehip powder has a pleasing shape and odor, but tasters noted a bitter taste that is due to the increased powder content. The higher amount of powder, the more bitter taste intensifies.

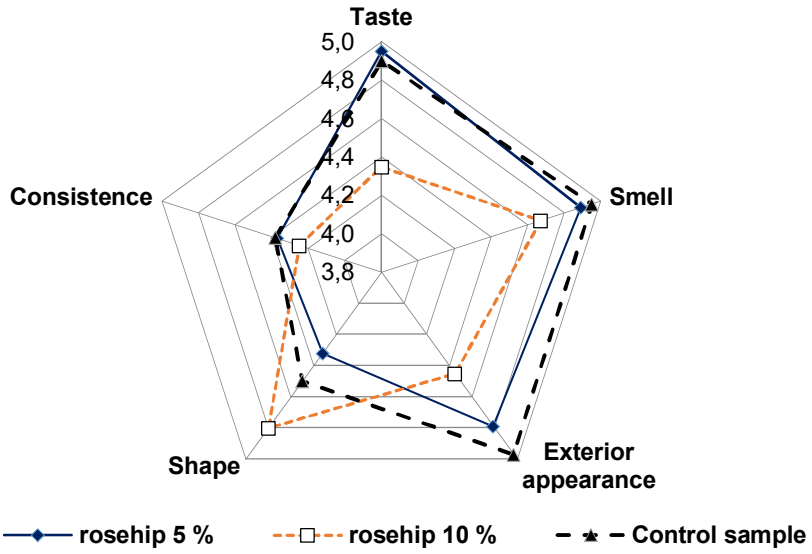

Figure 11. Sensory evaluation of functional candies with rosehip powder

As a result of the 5-point hedonic tests applying (Figure 11), it was established that the tested samples are positively appreciated and represent BIO products.

The use of rosehip powder presents a good possibility to increase the biological value of the product. Candies obtained on the base of rosehip powder represent a new product with functional properties, that do not induce the risk for consumers health.

Conclusions

The functional candies with rosehip powder have definite advantages in comparison to products obtained by the classical recipe. The rosehip high content of carotenoids (17.18±0.01 mg/L β-carotene; 18.13±0.03 mg/L lycopene; 18.02±0.02 mg/L zeaxanthin), enhanced antioxidant activity (up to 91%) and the bioavailability of biologically active compounds, according to *in Vitro* simulation of gastrointestinal digestion, demonstrates the benefits of its use as natural antioxidants and colorants in the different foods. This fact allows the partial or total substitution of some synthetic preservatives with harmful action on human body, developing new technologies for functional food products obtaining. It was established that physico-chemical parameters of functional confenctionery products with *rosa canina* powder (1,14–1,17 mg KOH/l, 23–25 weight fraction of water,%) correspond to normative documents. The sensory indices of the BIO candies are characterized by a good consistency, pleasant taste and fine odor and can be recommended for all categories of consumers.

Acknolegements
Authors gratefully thank the young researchers project **06/26.10.18A** "*Functional products obtained by using natural texture agents and carotenoids*" for support. This research was partially supported by World Federation of Scientists.

References

1. Kharazmi A (2008), Laboratory and preclinical studies on the anti-inflammatory and anti-oxidant properties of rosehip powder – Identification and characterization of the active component GOPO®, *Osteoarthritis and Cartilage*, 16(1), pp. S5–S7.
2. Stralsio L., Alklint Ch., Olson M.E., Sjoholm I. (2003), Total folate content and retention in Rosehips (Rosa ssp) after Drying, *J. Agric. Food Chem*., 51, pp. 4291–4291.
3. Popovici V., Covaliov E., Capcanari T., Popovici C., Radu O. (2019), Evolution of total carotenoid content in food products enriched with rosehip (*Rosa Canina*) powder, *Proceedings of the 8th International Specialized Scientific and Practical Conference "Resource and Energy Saving Technologies of Production and Packing of Food Products as the Main Fundamentals of Their Competitiveness", National University of Food Technologies, Kyiv, Ukraine, September 12, 2019*, p. 170.
4. Martirosyan D. (2011), Functional Foods and Chronic Diseases, Science and Practice. *Food Science*, p. 255.
5. Ciobanu C., Deseatnicov O., Sturza R., Curchi D. (2005), Procedeu de fabricare a produselor de panificație îmbogățite cu fier, *Brevet de invenție nr, MD-2895*, 31.10.2005, publicat BOPI Nr. 10/2005.
6. Sturza R. (2016), Principii moderne de analiză a alimentelor, *Monografie*, UTM, Chișinău.
7. Saykova I., Tylkowski B., Popovici C., Peev G. (2018), Extraction of phenolic and flavonoid compounds from solid wastes of grape seed oil production by cold pressing. *Journal of Chemical Technology and Metallurgy*, 53(2), pp. 177–190.
8. Popovici C. (2013), Soxhlet extraction and characterisation of natural compounds from walnut (*Juglans regia* L.) by-products, *Ukrainian Food Journal,* 2(2), pp. 328–336.
9. Šarolić M., Gugić M., Tuberoso C.I.G., Jerković I., Šuste M., Marijanović Z., Kuś P.M. (2014), Volatile Profile, Phytochemicals and Antioxidant Activity of Virgin Olive Oils from Croatian Autochthonous Varieties Mašnjača and Krvavica in Comparison with Italian Variety Leccino, *Molecules*, 19, pp. 881–895.
10. Tesfaye B., Abebaw A., Reddy M.U. Determination of Cholesterol and β-Carotene content in some selected Edible Oils, *International Journal of Innovative Science and Research Technology*, 2(7), pp. 14–18.
11. Biehler E., Mayer F., Hoffman L. (2009), Comparison of 3 Spectrophotometric Methods for carotenoid determination in frequentlz consumed fruits and vegetables, *Journal of Food Science*, pp. C1–C7.
12. Necula V. (2010), Analiza senzorială a alimentelor, *Note de curs*, pp. 2–4.
13. (1999), AOCS Official Method Cd 3d-63. AcidValue. *Sampling and Analysis of commercial fats and oils.*
14. Pavan V., Soriano Sancho R.A., Pastore G.M. (2014), The effect of in vitro digestion on the antioxidant activity of fruit extracts (Carica papaya, Artocarpus heterophillus and Annona marcgravii), *LWT – Food Science and Technology,* 59(2), Part 2, pp. 1247–1251.
15. Pakhomova I.V., Tkachenko A.S. (2015), Vplyv netradytsiinoi syrovyny na zberezhenist zhyrovmisnykh kondyterskykh vyrobiv, *Tovaroznavchyi visnyk*, 8. pp. 212–217.
16. Mariia Ianchyk, Oleksandra Niemirich (2016), Definition indicators of quality of the confectionery semi-finished product with powders from banana and carrot, *Ukrainian Journal of Food Science*, 4(1), pp. 76–84.
17. Ira Taneva, Petar Panayotov (2019), Analysis of vitamin C enriched yoghurt by direct extraction of rosehip fruit in cow's milk during storage, *Ukrainian Journal of Food Science*, 7(1), pp. 61–69.

Influence of technological parameters on the degree of enzymatic hydrolysis of high-protein products

Lesia Avdieiea, Eduard Zhukotskyi, Hanna Dekusha

Institute of engineering thermophysics of National Academy of Sciences of Ukraine, Kyiv, Ukraine

Keywords:

Protein
Hydrolysis
Proteases
Amino acids

Article history:

Received 21.10.2018
Received in revised form 12.09.2019
Accepted 28.11.2019

Corresponding author:

Lesia Avdieiea
E-mail:
tbds_ittf@ukr.net

DOI: 10.24263/2304-974X-2019-8-4-13

Abstract

Introduction. Research have been conducted to determine the influence of technological parameters on the degree of hydrolysis of soy and whey proteins, as well as their mixtures to obtain balanced protein compositions with a high degree of hydrolysis.

Materials and methods. Researched here are isolated soy protein, whey protein concentrate and mixtures at different ratio thereof that were hydrolyzed by proteases «Protamex», «Bioprotease N100L» and «Profix 6500». A degree of protein hydrolysis was evaluated by spectrophotometric method, the amino acid composition of hydrolysates was determined using ion exchange chromatography.

Results and discussion. To obtain a highly hydrolyzed isolated soy protein rational modes of its proteolysis were determined, namely: mass concentration of protein in an aqueous solution – 9%, mass concentration of protease – 5%, pH 6.5–7.0, hydrolysis temperature 55–60 °C and duration of the process – 60 min. Under these conditions, the degree of hydrolysis of isolated soy protein is 80–82% obtained with «Protamex», 50–51% – with «Bioprotease N100L» and 30–33% – with «Profix 6500».

Hydrolytic effect of the above mentioned proteases on the degree of hydrolysis of whey protein concentrate under the same conditions is slightly less and amounts to 45–46% for «Protamex», 30-33% for «Bioprotease N100L» and 19–20% for «Profix 6500» which can be explained by the smaller specificity of this substrate to the enzymes.

To achieve a balanced composition of essential amino acids relative to human milk, it is rational to combine a whey protein concentrate and isolated soy protein in a mass ratio of 1:1 respectively. In doing so, the degree of hydrolysis of this mixture is high and amounts to more than 80% under the action of «Protamex» at a concentration of 5% by weight of protein, a temperature of 55–60 °C and a duration of 60 minutes.

Conclusions. For the first time the rational technological parameters for the proteolysis of isolated soy protein, whey protein concentrate and their mixtures were determined to obtain a high degree of hydrolysis.

Introduction

A process of enzymatic protein hydrolysis is an interesting scientific and practical problem. It is of relevance because it allows to solve the problems of enrichment of food products with valuable biologically active components. The hydrolysis application increases the nutritional and biological value of proteins, improves their absorption and changes their functional properties as well [1, 2].

Furthermore, proteolysis is an effective way to reduce the antigenic properties of food proteins. Depending on the type of protease and the conditions of the process, peptides with different molecular weights and free amino acids are formed. Such properties make them possible to introduce to the composition of dietary products, medical [3, 4], sports nutrition [5, 6] as well as in the production of hypoallergenic formulae for enteral and baby nutrition [7, 8].

Due to the complexity and multifactor nature of the process and taking into account the high social need for products with hydrolyzed protein, the determination of rational conditions for the process of proteolysis remains relevant.

To obtain hydrolysates, various raw materials of animal (dairy, meat, fish) and vegetable (soy, lentils, beans, chickpeas) origin with a high protein content are used. Thus, the protein component of modern hypoallergenic formulae for infants is represented by extensively or partially hydrolysated milk proteins [9], such as whey, casein proteins or mixtures thereof [10]. Although whey proteins have a balanced composition of essential amino acids [11], β-lactoglobulin, which accounts for 58% of whey proteins (12% of total protein), has the highest allergenic potential [12, 13]. To reduce its antigenic properties, milk raw materials can traditionally be heat-treated (145 °C during 2 to 3 s [14]), however, the thermal denaturation can lead to both destruction and exposure of hidden areas of antigenic determinants and also to the aggregation of protein molecules [15, 16].

Researchers offer different solutions to the problem of reducing antigenicity due to hydrolysis of proteins under different conditions by enzymes of animal (trypsin, pepsin), microbial (obrained from Bacillus licheniformis (commercially known as Alcalase), Aspergillus oryzae (Flavourzyme), Bacillus amyloliquefaciens (Neutrase) and etc.) and plant origin (bromelain, papain, physyn) or their complexes (Protamex).

Among the advantages of whey protein proteolysis are the high nutritional and biological value of the obtained hydrolysates [11, 17, 18], their increased digestibility and solubility even with a small degree of hydrolysis (5–20%) [19] as well as antioxidant activity [20]. It should be noted that different authors received slightly different data depending on the method for determiming and used equipment.

The main problem of protein hydrolysates is, as known, their bitter taste [21-23] due to what is believed to be the formation of peptides with hydrophobic amino acids [24]. They are trying to reduce it applying additional ultrafiltration [25, 26], cleavage with exo- and endopeptidases [27, 28] or adding taste-masking components [29].

Among other disadvantages, a significant duration of the process and the high cost of enzyme preparations, especially of animal origin, for example, trypsin should be taken into consideration [1].

Based on the results of modeling of the hydrolysis process with the Peptide Cutter program it was determined that from the point of view of residual antigenicity, the hydrolysis of whey proteins with Protamex, Alcalase and thermolysin is optimal [30, 31].

It is possible to achieve different degree of hydrolysis of whey proteins by changing the technological conditions and using different proteases. For instance, the degree of hydrolysis of whey proteins after proteolysis with trypsin, rennin, papain and pepsin within 4 hours

reached 61.4, 84.2, 95 and 100% respectively. Subsequent ultrafiltration of peptides further reduces antigenicity [25] but as a result there is an imbalance in the amino acid composition of milk proteins. While the hydrolysis of α-lactalbumin with trypsin its complete degradation in 15–120 minutes is noted. A complete cleavage of β-lactoglobulin requires an increase in the process duration up to 450–1200 min and depends on the type of combination of conditions mentioned above [32].

In addition to milk proteins, soy proteins are often used to obtain therapeutic mixtures with hydrolysates. They are characterized by a high molecular weight (up to 380 kDa [14]) which can also result in their antigenicity. Enzymatic hydrolysis of soy proteins improves its functional properties, such as emulsifying ability, solubility and formation of biologically active peptides [1]. Soy protein hydrolysates [14, 33, 34] have the same features as milk protein hydrolysates.

The degree of hydrolysis of soy proteins is low in most cases and only combined action of several proteases makes it possible to achieve the value up to 40%. An increase in the degree of hydrolysis is also possible due to physical destruction of the protein structure applying high pressure, soft treatment with acids, ultrasound or extrusion [1].

At the same time, the fraction of soy peptides with a molecular weight <10 kDa is characterized by the highest antioxidant activity, namely, the ability to act as a metal-ion chelator, cleanse from free radicals, prevent lipid oxidation and so on[1].

An analysis of the literature research results suggests that the existing technological parameters of enzymatic hydrolysis in most cases are characterized by a significant process duration and low degree of protein hydrolysis.To increase the efficiency of the process additional research is needed.

The purpose of research is to determine the effect of technological parameters on the degree of hydrolysis of isolated soy protein and whey protein concentrate and their mixtures for obtaining balanced protein compositions of high degree of hydrolysis.

Materials and methods

Object of research: process ofenzymatic hydrolysis of isolated soy protein, whey protein concentrates and their mixtures.

Research subjects:

- Isolated soy protein Supro 1751 (further ISP) (protein content – 90%, fat – 0,5%, ash – 5,5%, «Solae Europe, S.A.», USA);
- Whey protein concentrate WPC 80 (further WPC) (protein content – up to 82.5%, fat – 5,2%, ash – 2,3%, «Agri-MarkInc.», USA);
- Mixture of isolated soy protein Supro 1751 and whey protein concentrate WPC 80 at ratio 1:1 and 1:2 respectively.

Materials

Neutral protease from *Bacillus amyloliquefaciens* [35]and *Bacillus licheniformis* [36-38, 39] («Protamex», activity 1,5 AU/g, optimum pH 5,5-7,5, optimum temperature 35–60 °C, "Novozymes", Denmark), neutral protease from *Bacillus subtilis* [40] («Bioprotease N100L», activity minimum 100,000 c.u. NPU/ml, optimum temperature 55–60 °C, optimum pH 7,0-8,0, Kerry Food Ingredients (Cork) Ltd, Ireland), neutral protease from papaya tree fruits («Profix 6500», activity 6500 units/mg, optimum pH 7.0–8.0, optimum temperature

65–70 ºC, Kerry Food Ingredients (Cork) Ltd, Ireland) were used for hydrolys. All enzyme preparations are permitted for use in food industry [41].

Preparation of hydrolyzed proteins

Weighted protein samples were hydrated in distilled water at the temperature of 20 ºC ($\omega_{protein}$ = 2,2–12,5%), thoroughly mixed, heated to the optimum temperature and proteases were added ($\omega_{protease}$= 0,3–10% of protein mass). Protein hydrolysis was carried out at the optimum temperature of maximum enzyme activity for a certain time (τ=20–90min). To stop the hydrolysis, the samples were heated to 85–90 °C and kept for 5–7 min at this temperature [42].

3-chloro-acetic acid (5% in final mass concentration) was added to the samples to separate obtained hydrolysates from protein, and then they were centrifuged at Low speed centrifuge 310 (Poland) for τ=15 min at 15000 rpm [43].

Determination of degree of protein hydrolysis (HD)

HD was determined by spectrophotometric technique on spectrophotometer CF-26 by changing light absorption of supernatant at a wavelength of 280 nm. Calibration graph is based on bovine serum albumin [44, 45]. HD was calculated by spectrophotometric method according to the ability of aromatic amino acids (tryptophan, tyrosine, phenylalanine) to absorb ultraviolet light with a maximum absorption at 280 nm [46].

Determination of amino acid composition in samples

Amino acid analysis was carried out by ion-exchange chromatography technique using an Amino Acid Analyzer T-339 (“Mikrotechna”, Czech Republic) [47].

Results and discussion

Dependence of hydrolysis degree of ISP and WPC from protein concentration in water

One of the main process parameters that affects HD is mass concentration ofproteinin water ($\omega_{protein}$). Determining a rational amount of protein will provide necessary HD with minimum possible amount of water and reduction of energy consumption for moisture removal when the product is being concentrated and dried.

The determination of HD of ISP and WPC depending on mass concentration of protein in water was carried out at$\omega_{protein}$= 2,2; 3,2; 6,3; 9,0 and 12,5%. The mass concentration of the protease ($\omega_{protease}$) for all samples remained unchanged ($\omega_{protease}$=5% by weight of protein), the duration of hydrolysis was τ = 60 min at the temperature t=55–60 °C. The results of change in HD of ISP and WPC depending on $\omega_{protein}$ by different proteases are shown in Figure 1.

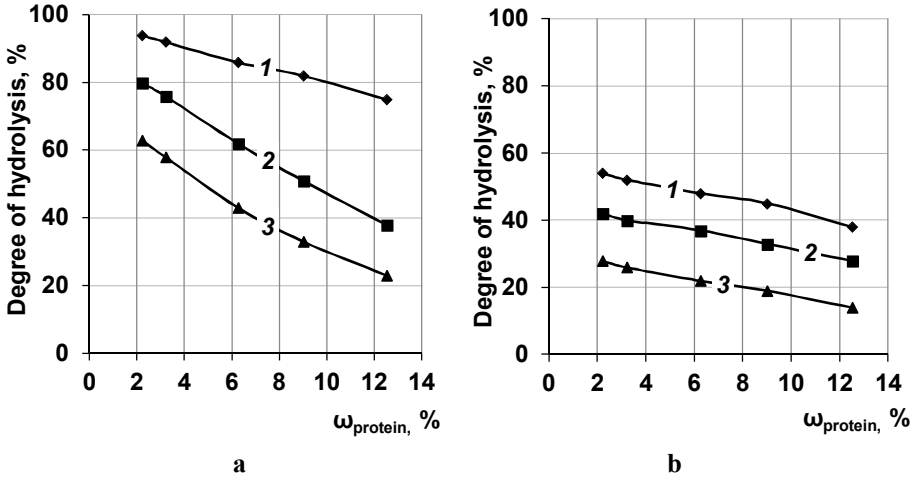

Figure 1. Dependence of hydrolysis degree of ISP (a) and WPC (b) samples from protein concentration in water ($\omega_{protein}$) hydrolyzed by:
1 – «Protamex», 2 – «Bioprotease N100L», 3 – «Profix 6500».

As seen in Figure 1, HD of all high-protein products was inversely proportional to the protein mass concentration ($\omega_{protein}$). Maximum HD of ISP was achieved at $\omega_{protein}$ = 2,2% under action of «Protamex» and amounts 90%. For data [35] Bacillus amyloliquefaciens, which is a part of «Protamex», showed significant improvement in nutritional quality and bioactivity by removing anti-nutritional factors as well as allergens. An aminopeptidase from Bacillus licheniformis, which is also is a part of «Protamex» showed high specificity for dipeptides with Leu, Val, Ala, Gly, and Phe at the N-terminus» as noticed in research [39]. In the hydrolysis of soy protein isolate Bacillus amyloliquefaciens preferred peptides with Leu, Glu, Gly, and Ala at the N-terminus by free amino acid analysis and preferred peptides with Leu, Ala, Ser, Trp and Tyr at the N-terminus by ultra performance liquid chromatograpy-MS/MS [39].

When using the «Bioprotease N100L» or «Profix 6500» the maximum HD of ISP was achieved at the same protein mass concentration and is about 80% and 63% respectively (Fig. 1a). But further reduction of $\omega_{protein}$ < 2,2% in water is impractical due to the fact that a large amount of water demands extra energy on moisture evaporation. And an increase in the mass concentration of ISP in an aqueous solution, for example, from $\omega_{protein}$ = 9% to $\omega_{protein}$ = 12,5%, leads to a decrease in its HD by 10-25%, depending on the type of protease.

Proteolysis of WPC by selected proteases at the same temperature-time parameters provided a significantly lower HD as compared with ISP (Figure 1b). It is hypothesized that B. licheniformis protease breaks down hydrophilic segments in the substrate and, therefore, preserves hydrophobic segments that aggregate once exposed to the solvent [37]. Thus, the highest degree of hydrolysis of WPC, obtained with $\omega_{protein}$ = 2,2% and using «Protamex», was 55-58% that also in some way confirmed in [38]. When «Bioprotease N100L» and «Profix 6500» were used HD of WPC was 2–2,5 times lower as comrared with ISP. Subsequent investigations were carried out at a mass concentration of all proteins of $\omega_{protein}$ = 9%.

Dependence of hydrolysis degree of ISP and WPC from protease concentration

Results of research of HD depending on mass concentration of selected proteases ($\omega_{protease}$) are shown in Fifure 2. Experimental research were carried out at $\omega_{protease}$ = 0,3; 0,5; 1; 2,5; 5 and 10% of mass of protein, $\omega_{protein}$= 9%, hydrolysis time period is τ = 60 min, temperature t =55-60 ºC.

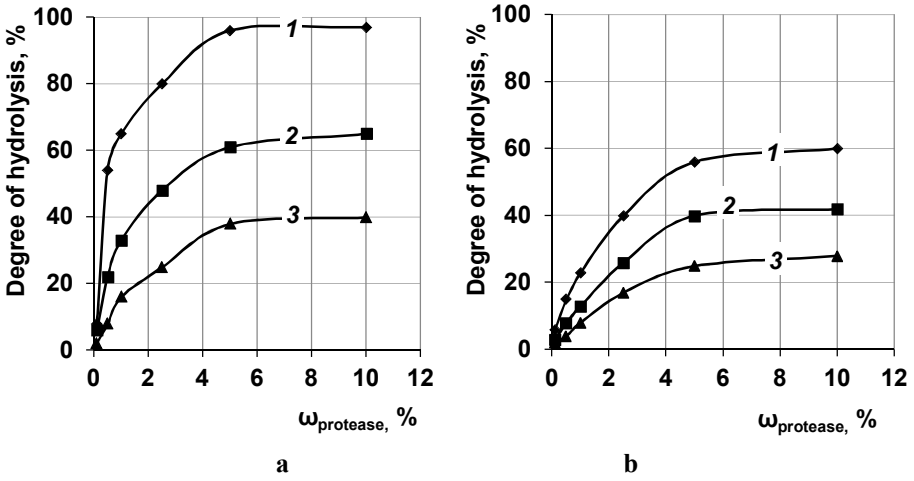

Figure 2. Dependence of hydrolysis degree of ISP (a) and WPC (b) from protease concentration $\omega_{protease}$: 1 – «Protamex», 2 – «Bioprotease N100L», 3 – «Profix 6500».

Given in Figure 2 curves demonstrate a growth of HD of proteins when increase in $\omega_{protease}$ in all hydrolyzated samples. The highest growth rate of HD was observed at $\omega_{protease}$= 0,3-5,0%, further increase in $\omega_{protease}$>6% have not provided significant change in HD. The highest HD by selected proteases was observed for ISP. Thus, proteolysis of ISP by «Protamex» allowed to obtain maximum HD (up to 90%) at $\omega_{protease}$= 5% (Figure 2a). «Bioprotease N100L» and «Profix 6500» cleavage ISP less than 60 and 40% respectively. The intensity of hydrolysis of WPC was significantly lower as compared to ISP when determined after 60 min (fig. 2b). Maximum values of HD were achieved when «Protamex», «Bioprotease N100L» and «Profix 6500» were used at $\omega_{protease}$ = 6–10% and accounted for 60, 40 and 25% respectively.

Dependence of hydrolysis degree of ISP and WPC from time

Another necessary parameter that influences on protein hydrolysis and describes process dynamic is aperiod of time. HD of proteins was determined every 20 min during 90 min. Curves of proteolysis of ISP and WPC obtained when $\omega_{protein}$ = 9%, $\omega_{protease}$ = 5% of mass of protein, temperature t = 55–60 °C are shown in Figure 3.

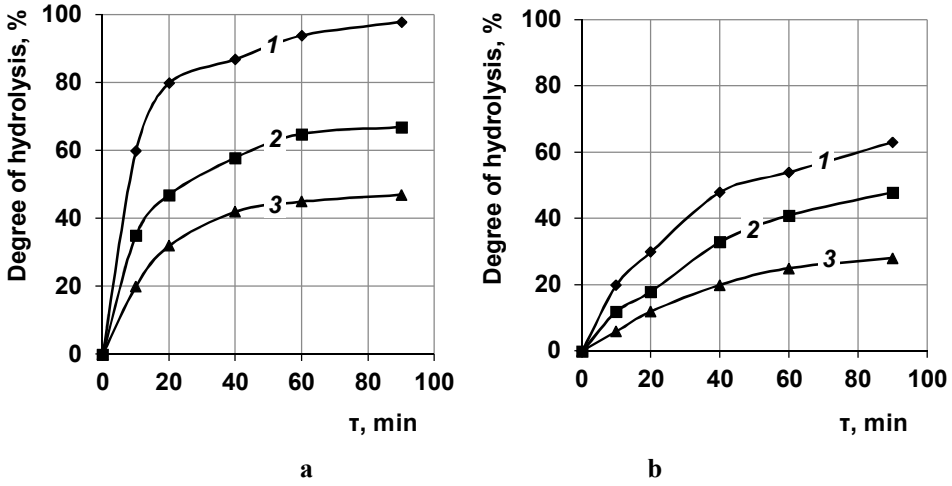

Figure 3. Dependence of HD of ISP (a) and WPC (b) from time: 1 – «Protamex», 2 – «Bioprotease N100L», 3 – «Profix 6500».

The highest process speedtook place during the first hourfor all samples. After that speed was slowed down and further hydrolysis gave only a slight increase in peptides (Figure 3). Reduction of the enzymatic reaction rate over timeis due to accumulation of reaction products and decrease in degree of saturation of the enzymes by substrate and partial inactivation of enzymes at given temperature and pH. Thus, the most considerable change in HD was observed in ISP samples and it significantly depended on type of protease: when using «Protamex» HD was 82%, «Bioprotease N100L» – 48% and «Profix 6500» – 35% after first 20 min. After 20 min the intensity of the hydrolysis process decreases and over the next 40 min the degree of hydrolysis of ISP and WPC grew by only 10–30%. Proteolysis of WPC was proceeding more slowly and in 60 min HD did not exceed 50–55% under effect of «Protamex», 40–45% – «Bioprotease N100L» and 25–27% – «Profix 6500».

Summarized results of studies of HD of high-protein products by chosen proteases at $\omega_{protein}$ = 9% and $\omega_{protease}$ = 5% in 60 minare given in Table 1.

Table 1

HD of ISP and WPC obtained by different proteases

Protein product	HD,%		
	«Protamex»	«Bioprotease N100L»	«Profix 6500»
ISP	90-95	60-65	40-45
WPC	50-55	43-45	20-23

Analysing results given in Table 1 it may be concluded that the highest HD of the high-protein products was achieved under activity of «Protamex», lower HD was observed when «Bioprotease N100L» was used and the lowest HD was noted for «Profix 6500». The rationale of using «Protamex» in the preparation of hydrolysates from whey proteins with a high degree of hydrolysis is confirmed by the results of [RU 2012158005, Method of

producing whey protein hydrolysate with high degree of hydrolysis and low residual antigenicity] and from SPI is shown in [RU 2299568C2 Method for the production of processed cheese, 48]. The effectiveness of the strain of Bacillus subtilis ("Bioprotease N100L") on the depth of hydrolysis of WPC was confirmed in studies [49, 50].

Composition of essential amino acids of WPC, ISP and their mixtures

Amino acid composition of ISP and WPC were balanced relatively to breast milk. The use of WPC adapts protein component of baby formulas to infant's organism needs, increase amount of tryptophan and cysteine and ensure high level of digestion.The use of ISP also improvesthe amino acid composition bringing it closer to breast milk, increases biological value and digestion of product, reduces osmolarity and therefore a strain on infant's kidneys.The presence of hydrolyzed soy proteins in infant formulas (for example, «Gerber Good Start Soy Stage», Nestle) have been demonstrated in other studies [33, 51].

Thereby, choice an appropriate ratio of WPC and ISP would bring closer essential amino acid composition to breast milk and baby's organism needs in optimal ratio, provide high level of amino acid assimilation and ensure physiological value of theend product.

Figure 4 demonstrates the composition of essential amino acids of ISP, WPC and their mixtures at different mass ratios as compared to breast milk.

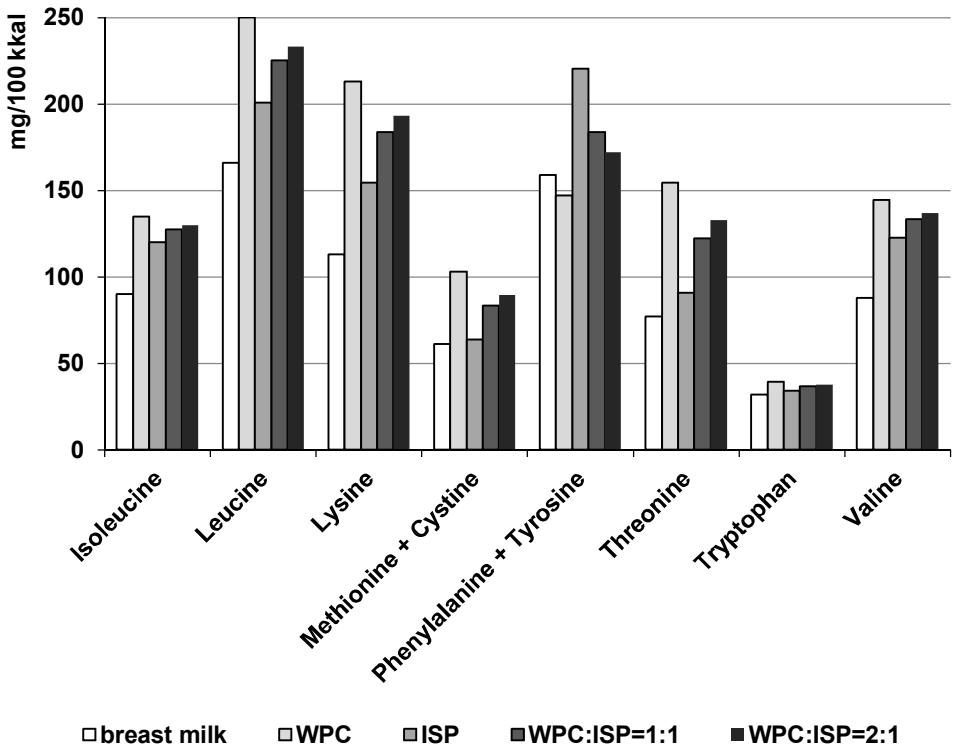

Figure 4. The composition of essential amino acids of WPC, ISP and their mixtures at mass ratio 1:1 and 2:1 respectively as compared to breast milk.

WPC and ISP at mass ratio of 1:1 and 2:1 respectively have a highly balanced formula of essential amino acids to breast milk. Content of essential is leucine, tryptophan, valine, phenylalanine, tyrosine and especially lysine and threonine are close to their content in breast milk.

Shown in Figure 5 is dependence of HD of WPC and ISP mixtures from mass concentration of «Protamex» with ratio of 1:1 and 2:1 respectively at the temperature t = 55–60 °C in 60 min.

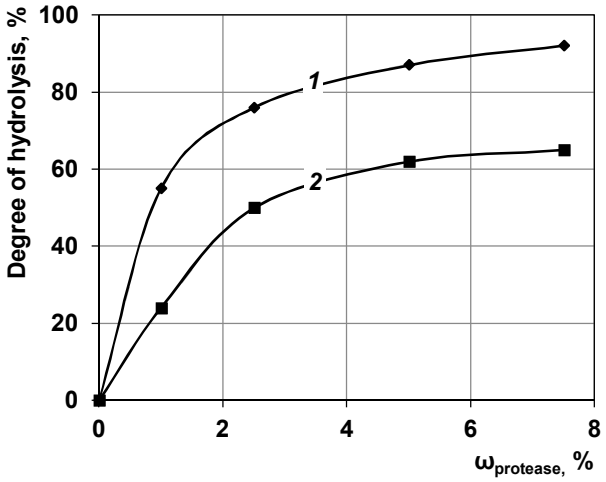

Figure 5. Dependence of HD of WPC and ISP mixtures from mass concentration of «Protamex» with mass ratio: 1 – 1:1, 2 – 2:1

The results (Figure 5) indicated high efficiency of «Protamex» application for proteolysis of WPC and ISP mixture with both ratios. The highest intensity of HD growth was observed in samples that contained $\omega_{protease}$ = 2,5%. Further increase in mass concentration of «Protamex» didn't provide a significant increase in HD. Maximum HD was observed in sample containing mixture of ISP and WPC with mass ratio of 1:1, respectively, when $\omega_{protease}$ = 7,5%, although a high value of HD was already achieved at $\omega_{protease}$ = 5% and was 70–75%.

Thus, conducted studies allowed to characterize proteolysis of dry high-protein products and their mixtures, obtain kinetic dependences depending on changing technological conditions and type of enzyme and choose rational technological parameters to achieve the goal.

Conclusion

Research of the influence of technological parameters on the degree of enzymatic hydrolysis of ISP and WPC by proteases «Protamex», «Bioprotease 100L» and «Profix 6500» were carried out.

Dependence of degree of enzymatic hydrolysis of ISP and WPCand their mixtures from mass concentration of proteins, proteases and incubation time are shown. Rational

technological parameters for each of the high-protein products and their mixtures were chosen: the mass concentration of protein is $\omega_{protein}$ = 9% under the action of «Protamex» ($\omega_{protease}$= 5%) for 60 min. The degree of protein hydrolysis for these conditions of enzymatic hydrolysis for ISP is up to 90%, for WPC is up to 55%, for a mixture of ISP and WPC in a ratio of 1:1, respectively, is 85%.

The rational ratio of ISP and WPC for maximum approximation to the composition of the essential amino acids of human milk is 1:1 respectively.

Obtained hydrolysates can be the basis of protein component in infant's hypoallergenic formulas.

References

1. Dong X. (2011), Enzymatic hydrolysis of soy proteins and the hydrolysates utilization, *International Journal of Food Science and Technology*, 12(46), pp. 2447–2459.
2. Wouters A., Rombouts I., Fierens E. et. al (2016), Relevance of the functional properties of enzymatic plant protein hydrolysates in food systems, Comprehensive Reviews in Food Science and Food Safety, 15, pp. 786–800.
3. Chalamaiah M., Yu W., Wu J. (2018), Immunomodulatory and anticancer protein hydrolysates (peptides) from food proteins: A review, *Food chemistry,* 245, pp. 205–222.
4. Zadak Z., Kent-Smith L. (2009), Basic in clinical nutrition: Commercially prepared formulas, *e-SPEN*, *the European e-Journal of Clinical Nutrition and Metabolism*, 4(5), pp. 212–215.
5. Schaafsma G. (2009), Safety of protein hydrolysates, fractions thereof and bioactive peptides in human nutrition, *European Journal of Clinical Nutrition*, 63, pp. 1161–1168.
6. Meghan A. (2018), Whey protein hydrolysate supplementation accelerates recovery from exercise-induced muscle damage in females, *Applied Physiology, Nutrition and Metabolism,* 43(4), pp. 324–330.
7. American Academy of Pediatrics. Committee on Nutrition Hypoallergenic infant formulas. (2000), *Pediatrics,*106(2), pp. 346–349.
8. Koletzko S., Niggemann B., Arato A. et. al (2012), Diagnostic approach and management of cow's milk protein allergy in infants and children: ESPGHAN Gl committee practical guidelines, *Journal of pediatric gastroenterology and nutrition*, 55(2), pp. 221–229.
9. Tutelian V.A., Kon I.Ia. (2004), *Rukovodstvo po detskomu pitaniiu*, Meditsinskoe informatsionnoe agentstvo, Moskva.
10. Rigo J., Schoen S., Verghote M. et. al (2019), Partially hydrolyzed whey-based formulae with reduced protein content support adequate infant growth and are well tolerated: results of a randomized controlled trial in healthy term infants, *Nutrients*, 11, pp. 1654–1669.
11. Pihlanto A. (2011), Whey proteins and peptides, *Nutrafoods*, 10(2-3), pp. 29–42.
12. Orcajo J., Lavilla M. (2015), Cow's milk allergen β-lactoglobulin immunoreactivity affected by pulsed light treatment, *Clinical and Translational Allergy*, 5(3), p. 50.
13. Rangel A.H., Sales D.C., Urbano S.A. et al. (2016), Lactose intolerance and cow's milk protein allergy, *Food science and Technology*, 36(2), Available at: http://www.scielo.br/scielo.php?script=sci_arttext&pid=S0101-20612016000200179.
14. Maubois J.-L., Lorient D. (2016), Dairy proteins and soy proteins in infant foods nitrogen-to-protein conversion factors, *Dairy Science and Technology*, 96(1), pp. 15–25.
15. Joyce A.M., Brodkorb A., Kelly A.L. et al. (2017), Separation of the effects of denaturation and aggregation on whey-casein protein interactions during the manufacture of a model infant formula, *Dairy Science and Technology*, 96, pp. 787–806.

16. Wijayanti H.B., Bansal N., Deeth H.C. (2014), Stability of whey proteins during thermal processing: a review, *Comprehensive reviews in Food Science and Food Safety,* pp. 13(6), 1235–1251.
17. Dullius A., Goettert M.I. (2018), Whey protein hydrolysates as a source of bioactive peptides for functional foods – Biotechnical facilitation of industrial scale-up, *Journal of Functional Foods,* 42, pp. 58–74.
18. Raikos V., Dassios T. (2014), Health-promoting properties of bioactive peptides derived from milk proteins in infant food: a review, *Dairy Science and Technology*, 94(2), pp. 91–101.
19. Sindayikengera S., Xia W. (2006), Nutritional evaluation of caseins and whey proteins and their hydrolysates from Protamex, *Journal of Zhejiang University-Science B*, 7(2), pp. 90–98.
20. Naik L., Mann B., Bajaj R. et al. (2013), Process optimization for the production of bio-functional whey protein hydrolysates: adopting response surface methodology, *International Journal of Peptide Research and Therapeutics*, 19(3), pp. 231–237.
21. Liu X., Jiang D., Peterson D.G. (2014), Identefication of bitter peptides in whey protein hydrolisate, *Journal of Agricultural and Food Chemistry*, 62(25), pp. 5719–5725.
22. Spellman D., O'Cuinn G., FitzGerald R.J. (2009), Bitterness in Bacillus proteins hydrolysates of whey proteins, *Food Chemistry*, 114(2), pp. 440–446.
23. Sujith P.A., Hymavathi T.V. (2011), Recent developments with debittering of protein hydrolysates, *Asian Journal of Food and Agro-Industry*, 4(06), pp. 365–381.
24. Saha B.C., Hayashi K. (2001), Debittering of protein hydrolyzates, *Biotechnology Advances*, 19(5), pp. 355–370.
25. Quintieri L., Monaci L., Baruzzi F., et al. (2017), Reduction of whey protein concentrate antigenicity by using a combined enzymatic digestion and ultrafiltration approach, *Journal of food science and technology*, 54(7), pp. 1910–1916.
26. Cho M.J., Unklesbay N., Hsieh F.H. et al. (2004), Clarke AD Hydrophobicity of bitter peptides from soy protein hydrolysates, *Journal of Agricultural and Food Chemistry*, 52(19), pp. 5895–5901.
27. Tchorbanov B., Marinova M., Grozeva L. (2011), Debittering of protein hydrolysates by Lactobacillus LBL-4 Aminopeptidase, *Enzyme Research*, 10, Available at: https://cyberleninka.org/article/n/910978/viewer.
28. FitzGerald RJ, O'Cuinn G. (2006), Enzymatic debittering of food protein hydrolysates // *Biotechnology advances*, 24(2), pp. 234–237.
29. Leksrisompong P., Gerard P., Lopetcharat K. et al. Bitter taste inhibiting agents for whey protein hydrolysate and whey protein hydrolysate beverages, *Journal of Food Science,* 77(8), pp. 282–287.
30. (2019), *PeptideCutter*, Available at: https://web.expasy.org/peptide_cutter/.
31. Borisova G.V., Novoselova M.V., Bondarchuk O.N., Malova Y.S (2012), Choice enzyme preparation to obtain whey hydrolyzate low allergenicity, *Fundamental research*, 11, pp. 1164–1167.
32. Mota M.V., Ferreira I., Olivera M. et al. (2006), Trypsin hydrolysis of whey protein concentrates: Characterization using multivariate data analysis, *Food chemistry*, 94(2), pp. 278–286.
33. (2017), Gilbaugh A., Kerner R.D. and John, *Pediatric formula comparison guide*, Available at: http://med.stanford.edu/content/dam/sm/peds/protected/core/green-team-gastro/nutrition/Stanford_Kerner_formula_guide_2017.pdf.
34. Olivera C.F., Folmer Correa A.P., Daroit D.J. et al. (2015), Soy protein hydrolysis with microbial protease to improve antioxidant and functional properties, *Journal of Food Science and Technology*, 52(5), pp. 2668–2678.

35. Chi C.-H., Cho S.-J. (2015), Improvement of bioactivity of soybean meal by solid-state fermentation with Bacillus amyloliquefaciens versus Lactobacillus spp. and Saccharomyces cerevisiae, *Food Science and Technology*, 68, pp. 619–625.
36. Rey M.V., Ramaiya P., Nelson B.A. et al. (2004), Complete genome sequence of the industrial bacterium Bacillus licheniformis and comparison with closely related Bacillus species, *Genome Biology*, 5(10), Available at: https://www.ncbi.nlm.nih.gov/pmc/articles/PMC545597/.
37. Creusot N., Gruppen H. (2007), Hydrolysis of whey protein isolate with Bacillus licheniformis protease: fractionation and identification of aggregating peptides, *Journal of Agricultural and Food Chemistry*, 55(22), pp. 9241–9550.
38. Silvestre M., Moris H.A. (2012), Hydrolysis of whey proteins by a Bacillus licheniformis protease, *Ci. Agr. Eng*, Ponta Grossa, 18(2), pp. 85–94.
39. Lei F., Zhao Q., Lin L. et. al (2017), Evaluation of the hydrolysis specificity of an aminopeptidase from Bacillus licheniformis SWJS33 using synthetic peptides and soybean protein isolate, *Journal of Agriculture and Food Chemistry*, 65(1), pp. 167–173.
40. Jeske S., Zannini E., Cronin M.F. (2018), Impact of protease and amylase treatment on proteins and the product quality of a quinoa-based milk substitute, *Food and Function*, 9(6), pp. 3500–3508.
41. Mine Y., Shahidi F. (2005), Nutraceutical proteins and peptides in Health and Disease, Taylor and Francis Group, Boca Raton, Available at: https://www.ulprospector.com/en/na/Food/Detail/4497/331898/ Protamex.
42. (2019) *Protamex*, Available at:http://symbiotech.ru/products/protein-hydrolysis/protameks/.
43. Scopes R.K. (1985), *Protein purification*, Moskva.
44. Simonian M.H., Smith J.A. (2004), Spectrophotometric and colorimetric determination of protein concentration, Current Protocols in Molecular Biology, 10(10.1A).
45. Gerhardt P., Murray R. G. E., Wood W. A. et al. (1994), *Methods for General and Molecular Bacteriology*. American Society for Microbiology, Washington, D.C.
46. GerhardtP. (1981), *Methods for General Bacteriology*, American Society for Microbiology edition, Washington D.C.
47. Lazarus W. (1973), Purification of plant extracts for ion-exchange chromatography of free amino acids, *Journal of Chromatography A*, 87 (1), pp. 169–178.
48. NguyenP.M. (2015), Bioactive peptides from soybean hydrolysis using Protamex, *Bulletin of Environment, Pharmacology and Life Sciences*, 4(7), pp. 10–19.
49. Alvarado Y., Muro C., Illescas J. et al. (2019), Encapsulation of Antihypertensive Peptides from Whey Proteins and Their Releasing in Gastrointestinal Conditions, *Biomolecules*, 9, p. 164.
50. Mayda E. EL, Paquet D., Ramet J.P., Linden G. (1986), Proteolitic activity of a Bacillus subtilis neutral protease preparation upon caseins and whey proteins of cow's milk, *Journal of Dairy Science*, 69, pp. 305–310.
51. Fiocchi A., Schunemann H.J., Brozek J. (2010), World allergy organization (WAO) Diagnosis and Rationale for Action against Cow's Milk Allergy (DRACMA) Guidelines, *WAO Journal*, 21, pp. 57–161.

Effect of basil seed gum, xanthan gum and carrageenan on rheological and sensory properties of suspended barberry pulp in syrup

Maryam Maleki[1], Seyyed Ali Mortazavi[1], Samira Yeganehzad[2], Ahmad Pedram Nia[1]

1 – Islamic Azad University, Sabzevar Branch, Sabzevar, Iran
2 – Research Institute of Food Science and Technology, Mashhad, Iran

Keywords:

Barberry
Carrageenan
Basil
Xanthan
Gum
Rheology

Article history:

Received 19.02.2019
Received in revised form 09.09.2019
Accepted 28.11.2019

Corresponding authors:

Samira Yeganehzad
Email: s.yeganehzad@rifst.ac.ir

DOI: 10.24263/2304-974X-2019-8-4-14

Abstract

Introduction. *Berberis vulgaris* is a native plant in Iran and the seedless type gained a reputation for the southern regions of Khorasan. The effect of adding mixture of basil seed gum-carrageenan and xanthan-carrageenan gum on rheological behavior and stability of suspended barberry pulp in syrup was investigated.

Materials and methods. Sugar 4.8% (w/v), glucose syrup 21%(w/v), barberry concentrate 17%(w/v), water 54%(w/v), and barberry pulps2%(w/v) were weighed. Different ratios of hydrocolloids (1.20%(w/v)), including basil seed gum-carrageenan and xanthan-carrageenan were prepared. The gum solution and other ingredients were heated to 60 ºC for 10 minutes. To prepare the final product, the pulps of barberry were directly added to the solution. Rheological and sensory properties were evaluated.

Results and discussion. The highest apparent viscosity belonged to sample with 100% basil seed gum, and the lowest value was for the sample containing 100% carrageenan. Samples containing xanthan-carrageenan had lower apparent viscosity compared to sample with basil seed gum-carrageenan. Increasing the amount of basil seed gum by formation of a three-dimensional network of continuous phase increases viscosity and make suitable conditions for suspending barberry pulp. It was found that the most suitable model for predicting the flow behavior of the samples was the Herschel-Bulkley model. Samples containing 70% basil seed gum and 30% carrageenan, due to the proper appearance and appropriate suspension of barberry particles, gained the highest scores in terms of sensory properties by the panelists and the lowest scores belonged to the sample containing 100% xanthan gum. The samples containing 100% basil seed gum and 100% xanthan gum showed the highest density and the lowest density, respectively.

Conclusions. According to the results obtained the sample containing 70% basil seed gum and 30% carrageenan showed the highest score in terms of sensory properties, stability and suspension assessment compared to other sample and could be introduced as a suitable formulation of barberry suspended pulp in the syrup.

Introduction

Barberry is a large group of evergreen barbed shrubs that are very important because of their many uses and applications, such as fruit consumption. Barberry with scientific name *Berberis vulgaris* is a native plant in Iran and the seedless type gained a reputation for the southern regions of Khorasan, especially Qaen and Birjand (Figure 1) [1].

In all parts of barberry plant, there are Berberine, Oxycontin and Berbamine alkaloids. The amount of alkaloids in the root of the barberry is more than other parts of the plant. Barberry fruit contains about 4% cinnamon, 65% malic acid and tartaric acid and some gum [1]. Barberry has phenolic compounds (725.558 mg of gallic acid in 100 ml of extract), anthocyanin (208.392 mg / l), antioxidant activity (84.26%) and vitamin C [2].

A global look at barberry is primarily a medicinal plant that has the potential for extraction of active ingredients, and the second look is an ornamental plant. Medicinal herbs containing Berberine have been used predominantly as antidiarrheal during a thousand-year period in China and India [1].

The consumption of barberry in freshly form because of sour taste is not common. Innovations in the production of barberry products and the production of various pulp products such as jam, marmalade, juice, soft drinks, pasta, sauce, jelly or hydrogel are growing nowadays.

Hydrocolloids are used in the formulation of fruit snacks to increase stability due to the ability to maintain water, improve the texture, and affect flavor release and other structural and sensory properties in the desired product [3].

Basil *(Ocimum bacilicum)* is a member of the family of mint, a species that is spread in Iran. According to the report of Iran to the International Conference on Genetic Resources FAO (1996), basil plant is introduced as a native plant in Iran (Figure 2) [4].

Figure 1. Fresh barberry fruit.

a ***b*** ***c***

Figure 2. *a* – basil plant; *b* – basil seed; *c* – basil seed gum powder.

Polysaccharides extracted from basilicum consist of two main parts of glucomannan (43%) with cross links (1 → 4) xylan (24.29%) and a small portion of glucan (2.31%). Also, the presence of arabinogalactan is highly secreted in addition to glucomannan and xylan [5].

Basil gum is a unique hydrocolloid that is classified as anionic gum with pH 8.1. This gum contains 63.79% carbohydrates and 32.1% protein. Glucose, galactose and mannose are 6.29, 16.1, 9.8% of the major sugars and potassium with 64.2% of the major ions present in this gum [6]. In addition to the pseudo-plastic behavior of basil gum, the existence of stress tolerance suggests the ability to suspend particles by this hydrocolloid, which makes it a good stabilizer in some nutritional formulations such as mayonnaise sauce and salad dressings.

Carrageenan, a linear polysaccharide family, is high molecular weight gum extracted from algae mostly from *Crispus chondrus* red algae and several other types [7].

Commercial solutions of carrageenan are available with the 5–800 mPa viscosities and measured at a temperature of 75 °C and a concentration of 1.5% (w/w). Solutions with viscosities less than 100 mPa have very close proximity to the Newtonian behavior [8].

Xanthan gum is a high molecular weight extracellular hetero polysaccharide extracted from *Xanthomonos campestris*. Xanthan is composed of (1–4) β -D glucose connections and has side chains (two mannose molecules and one glucuronic acid unit), which is available in the form of white powder soluble in cold and hot water. Xanthan gum is widely used in the food industry as a thickener, emulsifier, foaming agent and a temperature resistant stabilizer [9].

Liang et al. (2006) examined the effect of different hydrocolloids on pulp deposition, white sediment, turbidity and viscosity of carrot juice concentrate and concluded that the addition of 0.2% of guar gum and xanthan gum and 0.3% of CMC gum and a mixture of 0.015% and 0.1% of xanthan gum reduced the amount of pulp deposition and white sediment [10].

Ghannadi, movahhed, & ahmadi chenarbon (2018) investigated the effect of xanthan and pectin on the stability of suspension of orange juice pulp. According to the results, the amount of suspension of pulp particles in the treatment containing 0.2% of xanthan was acceptable and the treatment of 0.2% pectin was favorable in terms of most of the characteristics [11].

Considering the previous studies no published data is found on suspension of barberry pulp in the syrup. The aims of this study were: 1) to study the effect of basil seed gum as a native gum with mixture of carrageenan on suspension of barberry pulp; 2) to formulate a barberry suspension in syrup using commercial hydrocolloids.

Materials and methods

Materials

Barberry concentrate with brix 65 and acidity of 7.8–8.3 were prepared from khushe Sorkh Company (Iran). Glucose syrup was purchased from Glucose Nemuneh Toos Company (Iran). Carrageenan was purchased from Parand Khorasan Co. (Iran). Basil seed gum was supplied by Reyhan Gum Parsian Company (Iran) and xanthan was purchased from Fu Feng Company (China).

Preparation of barberry suspensions with barberry pulp

To produce barberry suspensions with barberry pulp, sugar 4.8% (w/v), glucose syrup 21% (w/v) , barberry concentrate 17%(w/v), water 54%(w/v), barberry pulps 2% (w/v), were weighed. Different ratios of hydrocolloids (1.20%(w/v)), including basil seed gum-carrageenan and xanthan-carrageenan were prepared (Based on pretests).

The gum solutions, water, barberry concentrate, sugar, glucose syrup and other ingredients were heated to 60 ºC for 10 minutes. To prepare the final product, the pulps of barberry were directly added to the solution. Ratios were as below:

Ratio of basil seeds gum: carrageenan was (70:30, 30:70, 50:50, 0:100, 100:0) and xanthan-carrageenan was (70:30, 30:70, 50:50, 0:100, 100:0)

Flow behavior and apparent viscosity test

Flow behavior test for 10 barberry syrup samples with different ratios of carrageenan – basil seed gum and carrageenan-xanthan (without pulp) in the shear rate range of 0.1- 85 1/S were determined using SC4-27 spindle rotary viscometer (RV DVIII Ultra Brookfield. Co, USA) and equipped with a water circulating system (Julabo, Japan).The sample temperature was kept constant at 35 °C during experiment.

The shear stress was plotted against shear rate in a range of 0.1 to 85 per second. The data obtained were fitted to four different models Newtonian, Power law, Herschel-Bulkley and Sisco) using MATLAB program and the best model (according to the highest R-square(R^2) and the lowest Root Mean Square Error(RMSE) was used to describe flow behavior of the syrup. The apparent viscosity was reported at shear rate of 43/s [12].

Stability test

To measure the product stability, the amount of 20 g of each sample (with pulp) was poured into plastic tubes and kept in constant condition at 4 °C. The rate of pulp separations of samples was determined by separating the upper transparent phase and weighing it and its expression based on percentage of total weight of the sample [13] .

Turbidity test

To measure turbidity, 10 cc of samples were centrifuged for 10 minutes at1500 rpm.Using centrifuge model 2-16 sigma making Germany. Absorption of the upper portion was measured at 660 nm [14].

Density test

A 50-millimeter pycnometer was cleaned with 96-degree ethyl alcohol and washed several times with distilled water. The pycnometer was placed in an oven for 3 hours at 105 ±5 °C. The pycnometer was weighted at 20 °C, and then was filled with freshly boiled and cooled distilled water at 20 °C. The pycnometer was evacuated and dried. It was filled with sample at 20 °C and weighed as below [15].

Calculation method:

$$P = \frac{M3 - M1}{M2 - M1}$$

M_1 = Weight of pycnometer at 20 °C in gram

M_2 = Weight of pycnometer with distilled water at 20 °C in gram

Brix test

Refractometer method was used. First, the device (atago, Japan) was adjusted to zero with distilled water. Then, a few drops of sample were placed at 20 °C on the sample location in a refractometer. Then, the percentage of soluble solids was read as Brix. [15]

Sensory evaluation

For sensory evaluation 5 point hedonic test was used. For this purpose, sensory evaluation forms were prepared for 50 panelists (20 to 50 in ages and 31 women and 19 men). For each treatment, a three-digit code was considered. Panelists were asked to give scores between 1(dislike extremely) to 5 (like extremely). Panelists were asked to drink water between samples [9].

Statistical analysis

All experiments were performed at least as triplicates. The results of treatments were expressed as mean±SD. Data were analyzed and compared using Duncan's multiple range test at significance level of 5% via SPSS.

Results and discussion

Effect of basil seed gum, xanthan and carrageenan gum on flow behaviour and apparent viscosity of barberry syrup samples containing barberry pulp

Flow behavior of barberry syrup was determined to predict stability and physical changes. According to the results the data was fitted appropriately to the Herschel-Bulkley model (Higher R^2 and the least RMSE) in comparison to other models.

$$\sigma = K\dot{\gamma}^n + \sigma_0$$

where σ is shear stress (Pa), K is the consistency coefficient(Pa.s^n), $\dot{\gamma}$ is shear rate(s^{-1}), n is the flow behavior index and σ_0 is the yield stress(Pa).

The flow behaviour parameters for Herschel-Bulkley model are presented in Table (1). The experimental data indicated that all samples had yield stress. The yield stress means the minimum shear stress to start the flow in a fluid so that at lower values of shear stress the fluid behaves like a solid and is unable to flow [16].

Table 1

Flow behavior Parameters of the Herschel-Bulkley model of barberry syrup containing different concentrations of basil seed gum –carrageenan and xanthan-–carrageenan

Sample code	Sample description	σ_0 (pa)	k(pa.s^n)	n (-)
1	Basil seed gum70%- carrageenan30%	5.18±0.33	1.42±0.05	0.73±0.02
2	Basil seed gum30%- carrageenan70%	1.38 ±0.10	2.76±0.13	0.57±0.02
3	Basil seed gum50%- carrageenan50%	1.77±0.10	4.61±0.20	0.56±0.02
4	Basil seed gum0%-carrageenan100%	6.62±0.46	0.67±0.09	0.90±0.03
5	Basil seed gum100%-carrageenan0%	7.51±0.68	12.4±1.07	0.36±0.05
6	Xanthan0%- carrageenan100%	2.36±0.16	2.18±0.13	0.44±0.03
7	Xanthan30%- carrageenan70%	2.42±0.20	2.05±0.07	0.45±0.02
8	Xanthan50%- carrageenan50%	3.26±0.14	2.00±0.15	0.45±0.03
9	Xanthan70%- carrageenan30%	5.06±0.12	1.49±0.07	0.58±0.02
10	Xanthan100%- carrageenan0%	4.50±0.12	2.71±0.16	0.49±0.02

The results showed that the sample containing the highest amount of basil seed gum (100%w/v basil seed gum), showed the highest yield stress and the lowest yield stress was related to the sample containing 30% w/v basil seed gum and 70% w/v carrageenan. Such behavior expresses the strong interaction of basil seed gum and other components of the formulation. Sample containing 70% xanthan and 30% carrageenan showed the highest yield value (5.06 Pa).

Results indicated that the highest concentration of basil seed gum had the highest effect on the consistency coefficient and flow behavior index. The consistency coefficient of the sample containing the highest concentration of basil seed gum was at the maximum level (12.4 Pa·s). In general, consistency coefficient changes in the samples containing basil seed gum was in parallel to the increase in the concentration of the gum except in the sample with 70%w/v of basil seed gum. At this concentration, the hydrocolloid may undergone phase separation and thus have a negative effect on viscosity and consistency. The increase in consistency coefficient in different treatments, especially the treatments containing basil seed gum, may be due to the intermolecular forces and the expansion of hydrogen bonds between water and soluble compounds (basil seed gum), thereby limiting the movement of the water molecule and increasing system consistency [17]. In samples containing xanthan gum the k values were almost the same in the narrow range of 2 to 2.71 Pa. As shown in the Table 1, the flow behavior index in all treatments were below 1, indicating a pseudo-plastic and shear thinning behavior of the syrups containing two gums as stabilizers.

In this study, apparent viscosity increased with increasing basil seed gum. The results of statistical analysis of data showed that the combination of basil seed gum-carrageenan gum had a significant effect on the apparent viscosity of the sample compared to the xanthan-carrageenan gum composition. One of the reasons is the higher apparent viscosity of carrageenan and basil gum individually compared to xanthan [18].

As shown in Figure 3 the highest apparent viscosity related to sample with 100% w/v basil seed gum, and the lowest value was for the sample containing 100% w/v carrageenan. In samples containing xanthan gum-carrageenan, the highest apparent viscosity belonged to sample with 100% xanthan.

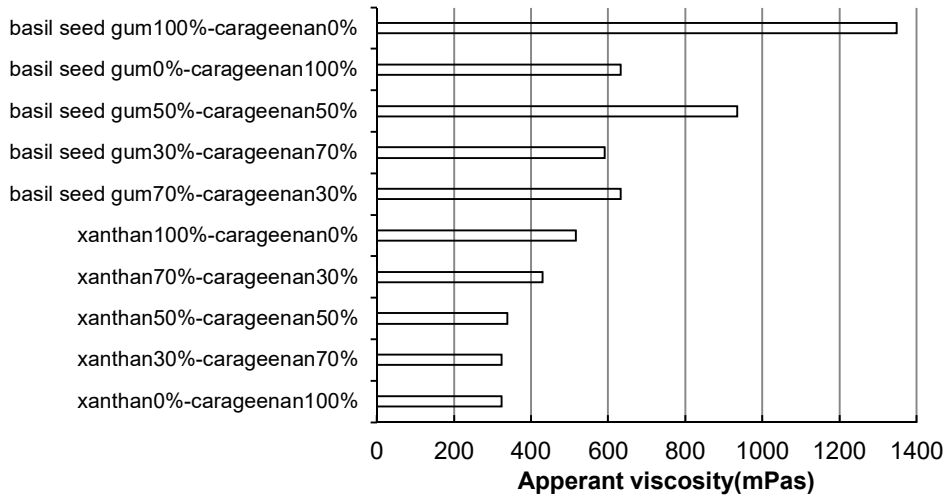

Figure 3. Apparent viscosity of barberry syrup treatments containing different concentrations of basil, carrageenan and xanthan gum as stabilizers

Effect of adding basil gum, xanthan and carrageenan gum on the stability of barberry syrup containing barberry pulp

The results showed that among all samples, in the sample 70% w/v basil seed gum and 30% w/v carrageenan, barberry was distributed uniformly throughout the solution from top to bottom, while in other samples, the pulp was not equally distributed and was floating more on top of the syrup. In other samples, barberry pulp couldn't suspend properly due to low viscosity or compact network. Hydrocolloids increase the stability of some food systems by increasing the apparent viscosity of the product or by acting on colloid interactions such as spatial suppression and electrostatic interactions [19]. Therefore, reduce the movement of particles and reduce the speed of the separation of phases from one another [20]. In fact, the reason for uniform distribution in treatments containing carrageenan-basil seed gum was the presence of a three-dimensional network, resulting barley pulp being trapped in this network. Increasing the amount of basil seed gum by formation of a three-dimensional network of continuous phase increases viscosity and make suitable conditions for suspending barberry pulp. Enough force is required to break down the three-dimensional structure of liquid gels. Therefore, the particles should disconnect the existing network and then move it. If a particle is trapped inside this network and the other forces are not enough to disperse the structure of the liquid gel, the particle will remain suspended. Liang et al. (2006) investigated the effect of adding guar, xanthan, gellan, and carboxymethyl cellulose hydrocolloids on the amount of particle precipitation in carrot juice. According to the results, the addition of these gums reduced the amount of sediment in the carrot juice and the concentration of sediment was lower in higher concentrations [10].

Effect of adding basil seed gel, xanthan and carrageenan on turbidity of barberry syrup containing barberry pulp

According to the results of the Table 2 samples containing basil seed gum-carrageenan compared to xanthan-carrageenan showed higher turbidity. It could be due to the brown color of basil gum compared to white color of xanthan. Also, the reason for the increase of the turbidity in different treatments was the accumulation of double helixes and the trapping of components in the network. Weak gels showed less turbidity in comparison to strong gels. Higher turbidity of the sample containing basil seed gum- carrageenan, may indicate the formation of a stronger gel by these gum compared to the xanthan-carrageenan composition.

Liang et al. (2006) stated that the addition of xanthan, guar, gellan, and carboxymethyl cellulose gums in carrot juice increased turbidity compared to control treatment [10]. In 2011, Kanha also investigated the impact of adding zinc, gellan, pectin and carboxymethyl cellulose gum on ginger drink. The results of this study showed that the addition of pectin and xanthan increased turbidity in treatments compared to control sample and treatments containing gellan and carboxymethyl cellulose [21].

Effect of adding basil gum, xanthan and carrageenan gum on the density of barberry syrup samples containing barberry pulp

The effect of adding basil seed gum, xanthan, and carrageenan gum on the density of barberry syrup samples containing barberry pulp is shown in Table 2.

According to the results, the density of samples containing xanthan-carrageenan is lower than samples containing basil seed gum-carrageenan. The highest density belonged to samples containing 100% w/v carrageenan and samples containing 100% w/v xanthan

showed the lowest density. Density depends on various factors such as concentration of solution, pressure and temperature. In the present study, the reason for increasing the density could be related to increased dry matter and the direct relation of mass with density. The results matched with the results of the research of Tabib Loghmani and Ehsan Doust (2013). They stated that flax and xanthan gum increased the density of ketchup and led to an increase in dry matter content due to the application of gum in the formulation [22].

Effect of adding basil gum, xanthan and carrageenan on Brix of barberry syrup containing barberry pulp

Percentage of soluble solids (Brix) of the samples did not differ significantly with different ratios of xanthan, carrageenan and basil seed gum. Results are shown in Table 2.

Table 2

Soluble solids in water measurement results, turbidity and density of samples

Sample code	Sample description	Density (g/ml)	Turbidity (NTU)	Brix (%)
1	Basilseedgum100%-carrageenan0%	1.1874±0.01	432.7±15	40.8±1
2	Basil seed gum70%- carrageenan30%	1.1965±0.05	471.3±20	41.8±0.5
3	Basil seed gum50%- carrageenan50%	1.1990±0.04	228.5±22	42.1±1
4	Basil seed gum30%-carrageenan70%	1.2069±0.07	344±14	41.8±0.7
5	Basil seed gum0%-carrageenan100%	1.2143±0.03	329±10	39.4±0.5
6	Xanthan0%- carrageenan100%	1.1925±0.02	88.15±6	41±0.6
7	Xanthan30%- carrageenan70%	1.1752±0.07	135.7±5	41.8±1
8	Xanthan50%- carrageenan50%	1.1699±0.03	135.5±5	41.2±0.8
9	Xanthan70%- carrageenan30%	1.1390±0.04	185.3±10	40.7±1
10	Xanthan100%- carrageenan0%	1.0703±0.02	199 ±8	41.6±1

Effect of adding basil seed gum, xanthan and carrageenan seeds on the sensory properties of barberry syrup containing barberry pulp

Appearance and taste of the samples were evaluated by the panelists (Table 3). According to previous researches, although hydrocolloids are capable of stabilizing two-phase food systems, they can also have negative effects on the final sensory properties [9].

Generally, samples containing 70% w/v basil seed gum and 30% w/v carrageenan, due to the proper appearance and appropriate suspension of barberry particles, were scored higher by the panelists, and the lowest scores belonged to the sample containing 100% w/v xanthan gum. The colorless and tasteless properties of xanthan gum was the reason for higher scores in odor and color compared to basil seed gum. In spite of the better color of the samples containing xanthan gum compared to basil seed gum, due to instability of barberry pulp and distribution throughout the sample, these sample were less favorable in terms of appearance and overall acceptance. It is worth mentioning that excessive addition of gum causes undesirable viscosity and therefore reduces the acceptability of the final product from the consumer's point of view, also the high percentage of hydrocolloids decrease the sample's fluidity, which is one of the desirable characteristics [9].

Table 3

Results of sensory evaluation of barberry syrup containing different ratios of xanthan, carrageenan and basil seed gum

Sample code	Sample description	Taste	Color	Odor	Mouth feel	Appearance	Overall acceptance
1	Basilseedgum100%-arrageenan0%	2±0.1	2±0.2	2±0.1	2±0.1	3±0.1	3±0.3
2	basil seed gum70%-carrageenan30%	3±0.11	3±0.3	3±0.1	4±0.1	4±0.05	4±0.14
3	basil seed gum50%-carrageenan50%	3±0.5	3±0.1	3±0.06	2±0.2	3±0.14	3±0.16
4	basil seed gum30%-carrageenan70%	3±0.3	3±0.1	3±0.2	3±0.1	3±0.18	3±0.12
5	basil seed gum0%-carrageenan100%	2±0.08	4±0.2	3±0.13	3±0.1	3±0.1	3±0.2
6	xanthan0%-carrageenan100%	2±0.07	3±0.3	2±0.3	3±0.3	3±0.1	2±0.1
7	xanthan30%-carrageenan70%	2±0.11	3±0.05	3±0.1	3±0.3	3±0.08	2±0.21
8	xanthan50%-carrageenan50%	3±0.09	4±0.3	3±0.07	3±0.1	2±0.1	2±0.12
9	xanthan70%-carrageenan30%	4±0.3	4±0.3	4±0.3	2±0.1	3±0.3	3±0.3
10	xanthan100%-carrageenan0%	4±0.3	3±0.3	4±0.3	3±0.3	2±0.1	2±0.2

Conclusion

According to the results, all samples of barberry syrup containing basil seed gum-carrageenan gum and xanthan-carrageenan gum were considered to be non-Newtonian fluids. Herschel-Bulkley was the most suitable model for predicting the flow behavior of the samples.

The results showed that the addition of 70% w/v basil seed gum and 30% w/v carrageenan in the formulation of barberry pulp suspension showed positive effect on pulp particle stability, turbidity, viscosity and was highly accepted by the panelists. The sample containing 100% w/v xanthan gum was scored the lowest in sensory properties. The sample containing 100% w/v basil seed gum showed the highest density and the lowest density was related to sample contaning100% w/v xanthan gum. Samples containing xanthan-carrageenan showed lower apparent viscosity and stability of barberry pulp was not proper in these samples. Samples containing carrageenan-basil seed gum showed more turbidity than those of xanthan-carrageenan. Total result of this research showed that production of suspended barberry pulp in barberry syrup is possible. This product could be consumed by people in different ages and could benefit from special mouthfeel and nutritional properties.

References

1. Balandari A., Cafi M. (2002), *Barberry. Production and processing technology*, Zaban & Adab, Mashhad.
2. Mortazavi S.A., Sharifi A., Maskooki A., Niakousari M., Elhamirad A.H. (2014), Optimisation of bioactive compounds extraction from barberry fruit (*Berberis vulgaris*) using response surface methodology, *Research and innovation in science and technology*, 3(1), pp. 11–24.
3. Goldfield G.S., Epstein L.H. (2002), Can fruits and vegetables and activities substitute for snack foods?, *Health Psychology*, 21(3), p. 299.
4. Hosseiniparvar H., Mortazavi A., motamedzadegan A., Razavi M.A., Matia-Merino l. (2009), Flow behavior of gum solutions extracted from Ocimum basilicum seeds mixed with Locust bean gum and Guar gum, *Food processing and storage*, 2(1), pp. 84–69.
5. Azuma J.I., Sakamoto M. (2003),Cellulosic hydrocolloid system present in seed of plants, *Trends in Glycoscience and Glycotechnology,* 15(81), pp. 1–14.
6. Hosseini-Parvar S., Matia-Merino L., Goh K., Razavi S.M.A., Mortazavi S.A. (2010), Steady shear flow behavior of gum extracted from Ocimum basilicum L. seed: Effect of concentration and temperature, *Journal of Food Engineering*, 101(3), pp. 236–243.
7. Milani J., Maleki G. (2012), *Food Industrial Processes–Methods and Equipment ed B*. In: *Hydrocolloids in food industry*, Benjamin Valdez, Intechopen, London.
8. Hashemiravan M., Yarmand M.S.(2008), *Application of hydrocolloids in the food industry and other industries*, Marze Danesh, Tehran.
9. Arabshirazi S., Movahhed S., Nematti H. (2012), Evaluation of addition of xanthan and hydroxyl propyl methyl cellulose gums on chemical and rheological properties of sponge cakes, *Scholars Research Library*, 3(2), pp. 589–594.
10. Liang C., Hu X., Ni Y., Wu J., Chen F., Liao X. (2006), Effect of hydrocolloids on pulp sediment, white sediment, turbidity and viscosity of reconstituted carrot juice, *Food hydrocolloids*, 20(8), pp. 1190–1197.
11. Ghannadi S., Movahhed S., Ahmadi Chenarbon H. (2018), Effect of xanthan gum and pectin on stability of suspension orange juice with pulp, *Journal of Food Science & Technology*, (2008–8787), 15(80), pp. 13–23.
12. Razavi M.A., Akbari R. (2009), *Biophysical properties of agricultural and food products*, Ferdowsi university, Mashhad.
13. Zohuriainpordel S., Aryanfar A. (2015), Effect of Pectin on fixweed Syrup Stabilization, *Special Issue of the Twenty-third National Congress of Iranian Food and Science*, (In Persian), Islamic Azad University Sabzevar Branch, Quchan.
14. Rivas A., Rodrigo D., Martinez A., Barbosa-Cánovas G., Rodrigo M. (2006), Effect of PEF and heat pasteurization on the physical–chemical characteristics of blended orange and carrot juice, *LWT-Food Science and Technology*, 39(10), pp. 1163-1170.
15. Anonymous. 2007, *Institute of Standard and Industrial Research of Iran (ISIRI), Fruit Juice. Test methods, No: 2685*, 1, pp. 13–37.
16. Steffe J.F. (1996), Rheological methods in food process engineering, Freeman press.
17. Soto-Caballero M., Valdez-Fragoso, A., Salinas-López A., Welti-Chanes J., Verardo V., Mújica-Paz H. (2016), Rheological parameters of xanthan gum/pectin solutions as a function of temperature and composition, *Revista Mexicana de Ingeniería Química*, 15(3), pp. 859–868.

18. Marcotte M., Hoshahili A. R. T., & Ramaswamy, H. (2001). Rheological properties of selected hydrocolloids as a function of concentration and temperature, *Food Research International*, 34(8), pp. 695–703.
19. Foroughinai S., Abbasi S., Hamidiesfahani Z. (2007), The Effect of Single and Combined Additives of Quiche, Saalb and Guar Gum on Dough Stabilization, *Journal of Nutrition Sciences and Food Technology of Iran*, 2, pp. 15–25.
20. Kiani H., Mousavi S.M.A., Emam-Djomeh Z. (2008), Rheological properties of Iranian yoghurt drink, Doogh, *International Journal of Dairy Science*, 3(2), pp. 71–78.
21. Kanha A. (2011), Use of hydrocolloids in textural stabilization of a yoghurt drink Ayran, *Food hydrocolloids*, 18, pp. 593–600.
22. Tabibloghmany F.S., Ehsandoost E. (2013), Investigation of Linseed (Linum usitatissimum L.) gum effects on rheological properties, and sensory quality of tomato ketchup during storage, *International Journal of Agriculture and Crop Sciences (IJACS)*, 6(2), pp. 70–76.

Effect of *Spirulina platensis* on the crumb firming of wheat bread during storage

Denka Zlateva[1], Rosen Chochkov[2]

1 – University of Economics, Varna, Bulgaria
2 – University of Food Technologies, Plovdiv, Bulgaria

Keywords:

Bread
Staling
Algae
Spirulina platensis
Crumb

Article history:

Received 21.12.2018
Received in revised form 24.06.2019
Accepted 28.11.2019

Corresponding author:

Rosen Chochkov
E-mail:
rosen4o4kov@abv.bg

DOI: 10.24263/2304-974X-2019-8-4-15

Abstract

Introduction. The effect of Spirulina platensis on the crumb firmness during storage (96 h) of wheat bread was studied by measuring the deformation properties (total, plastic and elastic deformation).

Materials and methods. Bread is obtained from wheat flour with the addition of Spirulina platensis (powder) in the amount of 2 or 4% by the weight of flour. The deformation properties of the bread crumb were studied 3, 24, 48, 72 and 96 hours after the baking. The deformation characteristics of the bread crumb are measured using automatic penetrometer, by immersion of a body with a certain mass for a certain time.

Results and discussion. The highest penetration, and therefore the greatest softness of the bread crumb is found in the bread with the addition of Spirulina platensis in the amount of 4% by weight of flour. In the both algae samples, the rate of firming of the crumb is slower and after 96 hours of storage the total deformation of the crumb decreases 2.75 times, while that of control sample decreases 3.6 times. Bread samples containing Spirulina platensis have a higher plasticity of the crumb during the whole period of storage (96 hours). Algae addition in the amounts of 2% and 4% by weight of the flour leads to an improvement in the plastic properties of the bread crumb and to their retention for a longer time than in the control sample. During storage in the control sample elasticity of the bread crumb gradually decreases and at the last measurement (96 hours after baking) it is 3.54 times lower compared to the first measurement – 3 h after baking. The elasticity of the bread crumb is affected by the addition of Spirulina platensis. Bread samples, which recipe includes 4% Spirulina platensis have a higher elasticity of the crumb throughout the storage period.

Conclusions. Crumb firmness decreased with the incorporation of Spirulina platensis powder. The addition of Spirulina platensis in the amount of 4% determines the greatest softness of the bread crumb.

Introduction

Bread staling is a process, that occurs during storage period. It is a complex phenomenon that affects the product characteristics by losing freshness in terms of flavour, texture, perceived moisture and other sensory characteristics.

Bread staling has been extensively studied for more than a century. The first research on staling was conducted by Boussingault [1], who pointed out that staling of bread is not due to loss of moisture and that stale bread could be freshened by moderate heating. Later, using X-ray diffraction, Katz [2] showed that crystallization of amylose and amylopectin was responsible for the firming of bread over time. However, despite intensive research efforts of many authors the complete molecular mechanisms for bread staling remain elusive [3].

Nowadays crumb-firming has been widely studied proposing different theories that involve numerous phenomena occurring simultaneously in the bread during storage (e.g. starch retrogradation, a modification of the gluten structure or moisture migration/ redistribution in the crumb) [4]. Different authors [5, 6] suggest that the retrogradation of starch is the main reason for the physico-chemical changes during storage. The retrogradation process occurs when amylose and amylopectin chains realign themselves, converting the gelatinized starch molecules to a more compacted and resistant crystalline form [7]. Other authors also point, that the migration of water molecules plays role to bread staling [8, 9]. It is well known, that after baking, migration of water occurs from bread crumb to crust due to the moisture gradient. The bread staling process starts along with the loss of moisture initiating the retrogradation of starch [10]. Water migrates from gluten to starch leading to plasticity loss of crumb and eventually to the reduction of molecular mobility. On the other hand, water is redistributed and incorporated in retrograded amylopectin crystals, leading to crumb hardening and bread staling during storage [7].

The mechanisms of action in molecular level of bread staling are still not fully understood. The change of starch in bread plays a crucial role and has been extensively studied [11]. Upon cooling, some starch chains began to reassociate into a different ordered structure [12, 13]. Studies confirm the central role of amylopectin retrogradation and water redistribution within the different polymers in determining bread staling [14].

Apart from starch and water molecules, gluten is also a factor to affect bread staling. The gluten network in fresh bread is flexible and elastic. It is noteworthy to pinpoint that the gluten network could reduce starch recrystallization, owing majorly to the interaction with starch granules via hydrogen bonds [15].

It can be assumed, that all the various components of bread composition will play a role in bread staling, as they undergo changes during the bread making process and during aging of the final product. Thus, the staling kinetics depend on a complex balance of input parameters (dough ingredients, yeast, enzymes), process parameters (mixing, proofing, baking, cooling) and storage parameters (humidity, temperature). To date, various food additives have been applied to bread and other bakery foods to retard staling.

Nowadays the consumption of marine products is increasingly gaining attention. Edible seaweeds or marine macro algae are one of the richest sources of valuable compounds, which are traditionally consumed by humans as food [16]. In the baking industry, hydrocolloids are of increasing importance as bread making improvers, where their use aims to improve dough handling properties, increase the quality of fresh bread, and extend the shelf life of stored bread [17]. Seaweed polysaccharides are a potential source of soluble dietary fibers. These compounds have higher water holding capacity than cellulosic (insoluble) fibers. Elleuch et al. point out that soluble dietary fibers demonstrate the ability to increase viscosity, form gels and/or act as emulsifiers [18].

Most of the authors focus their attention on the increase of nutritional and biological value of the algae-enriched bakery products, there are not enough studies on the textural properties and shelf-life of bread prepared with edible seaweeds. Lee et al. [19] evaluated the shelf-life and quality of breads made with 0.5, 1.0, and 2.0% of Myagropsis myagroides. It was concluded that the addition of 0.5% M. myagroides to breads has a good influence on improving the shelf-life and the overall quality of the products. Mamat et al. [17] find out that dried red seaweed species (*Kappaphycus alvarezii*) at amount 2-8% influenced dough and bread textural properties.

Bread prepared with the addition of *Ahnfeltia* had a greater shelf life than the traditional one; changes in the organoleptic and physicochemical parameters of the enriched bread during storage were less noticeable. At the same time, *Ahnfeltia* had more effective influence on the freshness retention of bread during storage than Costaria, probably due to the fact that in the composition of *Ahnfeltia tobuchiensis*, agaroids are predominate, they slow down the process of retrogradation of gelatinized starch and eventually prevent intensive staling of bread [20, 21].

However, the impact of algae on the keeping of bread freshness is not discussed extensively. It is worthwhile to find out how they affect the freshness of the bread during storage. The main manifestation of bread staling is crumb firming. Therefore, the purpose of the present study is to investigate the effect of *Spirulina platensis* on the crumb firmness during storage of wheat bread by measuring the deformation properties.

A number of objective methods can be used to characterize bread freshness:

- Methods based on determining the hydrophilicity of the bread crumb;
- Methods based on the determination of the content of water-soluble substances in the bread crumb;
- Methods based on the determination of the moisture in the bread crumb;
- Methods based on determining the physical properties of the bread crumb (such as firmness, plasticity, elasticity).

According to AACC (1999), bread firmness is defined as the force required to compress the crumb at a fixed distance or to evaluate freshness, defined as the distance that a fixed force will compress a crumb [22].

Materials and methods

Materials

For the preparation of the bread samples the following materials were used:

- Commercial wheat flour type 500 with the following properties: moisture content – 12.8%; gluten content – 27.07%; release of gluten – 6 mm; titratable acidity – 2 °H;
- Water – according to ISO 6107-1:2004
- Commercial yeast (Lesafmaya);
- Salt – according to Codex Standard for Food Grade Salt CX STAN 150-1985;
- *Spirulina platensis* powder (average chemical composition: protein 64g/100g; fat 8.2g/100 g of which saturated 3.42 g; carbohydrates 16.1g/100 g, of which sugars 0.52g, fiber 7g/100 g).

Methods

Dough and bread composition. The composition of the bread samples is presented in Table 1.

Table 1

Bread samples composition

Ingredients	Bread samples		
	Control sample	Sample with 2% Spirulina platensis	Sample with 4% Spirulina platensis
Wheat flour type 500, g	**250**	**245**	**240**
Water, cm^3	**140**	**145**	**155**
Yeast, g	3.37	3.37	3.37
Salt, g	3.25	3.25	3.25
Spirulina platensis, g	–	**5**	**10**

Bread preparation. Bread is obtained from type 500 wheat flour by a two-phase method. Initially, knead the yeast, flour and water dough in a 1:1 ratio in kneading machine (Labomix 1000, Hungary). Pre-mixed *Spirulina platensis* algae (powder) in the amount of 2% or 4% by the weight of flour are added to the mixing water. The dough thus prepared matures for 4 hours at 33 °C and then mix the dough to obtain a homogeneous mass by adding the remainder of the flour to the formulation and salt (1.3 kg/100 kg flour). The bread dough divides (440 g) and forms, matures for 55 minutes at 38 °C (Tecnopast CRN 45–12, Novacel ROVIMPEX Novaledo, Italy). After the final fermentation, the pieces of dough were put into an electric oven (Salva E-25, Spain) pre-heated to 200–220 °C. The baking time is 24 min, until the temperature in the center of the bread crumb reach 96-98 °C. After baking, the bread is allowed to cool down for 3 h at room temperature.

Determination of deformation properties of the bread crumb. The deformation properties of the bread crumb were studied – total, plastic and elastic deformation 3, 24, 48, 72 and 96 hours after the baking. The deformation characteristics of the bread crumb are measured using automatic penetrometer AP-4/2 (Germany), by immersion of a body with a certain mass for a certain time and are expressed in penetrometric units (PU) [23]. The measurement is made on a piece of bread crumb (from the center of the bread) 40 mm thick. Depending on the size of the test piece, the determination is made at three (or five) locations at least 30 mm apart from the crust. During the test, bread samples are stored under conditions that do not allow moisture exchange with the environment.

Statistical analysis. All experiments were conducted in triplicate and results were expressed as mean±standard deviation. Statistical analysis was carried out with SPSS version 21.0 (SPSS Inc., Chicago, IL, USA). A one-way-analysis of variance (ANOVA) and Duncan's multiple comparison tests were used to determine the significant differences at a level of 0.05.

Results and discussion

Effect of *Spirulina platensis* on the total deformation of bread crumb

Changes in the texture firmness of *Spirulina platensis*-enriched and control bread samples over 96 hours of storage are shown in Figure 1.

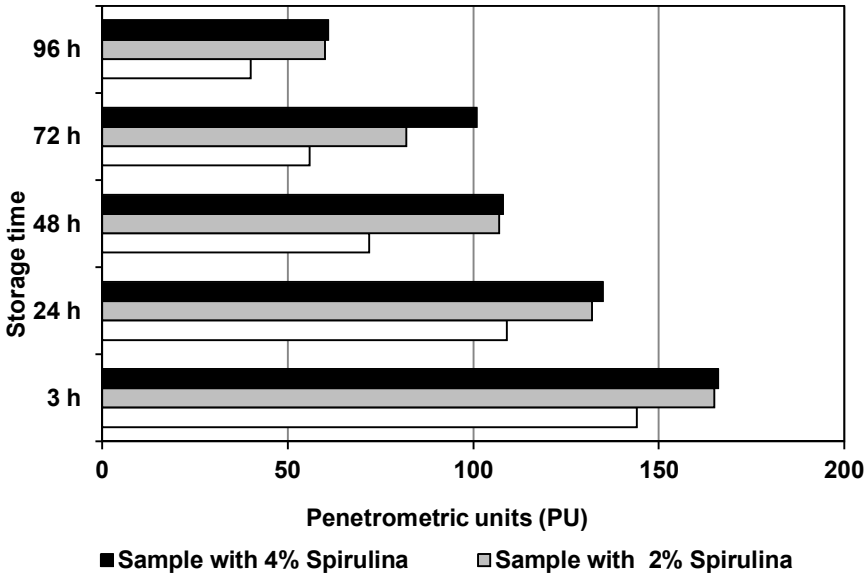

Figure 1. Total deformation of bread crumb (PU)

As can be seen from the figure, in all analyzed samples the total deformation of the crumb is reduced by extending the storage period. The lowest values, irrespective of the duration of storage of the bread (3, 24, 48, 72 or 96 h) are measured in the control sample. The highest penetration, and therefore the greatest softness of the bread crumb is measured in the bread, in which formulation *Spirulina platensis* is included (in the amount of 4% by weight of flour).

Throughout the period of storage, the crumb of the control sample had the least contractility and therefore – the highest firmness. 3 hours after baking, the total deformation is 144 penetrometric units (PU), which then decreases gradually, which indicates the hardening of the bread crumb. At the end of the storage (after 96 h) the total deformation of the crumb of the control sample is 40 penetrometer units (PU), i.e. it has decreased 3.6 times during the storage period. It is noteworthy that the reported values decrease with equal intensity. The bread crumb of the samples with *Spirulina platensis* is deformed to a greater extent in penetration and therefore features a softness that is retained throughout the period of storage. The amount of algae used (2% and 4%) does not significantly affect the total deformation. Three hours after bread baking, a total deformation of 165 PU is reported in both samples. Throughout the storage period the results for the both samples are quite similar, with only 72 hours after baking, the bread with 4% *Spirulina platensis* has a greater softness of the crumb. In the both algae samples, the rate of hardening of the crumb is slower and after 96 hours of storage the total deformation of the crumb decreases 2.75 times. After 48 hours, the algae containing samples have a firmness of the crumb recorded for the control sample after 24 hours of storage. *Spirulina platensis* contains hydrocolloids [24], and these types of polysaccharides are known to reduce the degree of moisture loss during storage of bakery products, thereby lowering the rate of crumb dehydration and hardening

Different studies have been carried out showing the potential use of seaweed hydrocolloids in the baking industry as an ingredient slowing down bread staling. According

to Rojas and coauthors [25] hydrocolloids can modify starch gelatinization and extend the overall quality of the product over time [26]. Guarda et al. [27] reported that breads containing hydrocolloids showed a lower loss of moisture content after baking due to higher water retention in the crumb. It is well known that moisture redistribution is one of the factors affecting bread staling and crumb firmness.

Effect of *Spirulina platensis* on the plastic deformation of bread crumb

The results obtained by determining the plastic deformation of the bread crumb are presented in Figure 2.

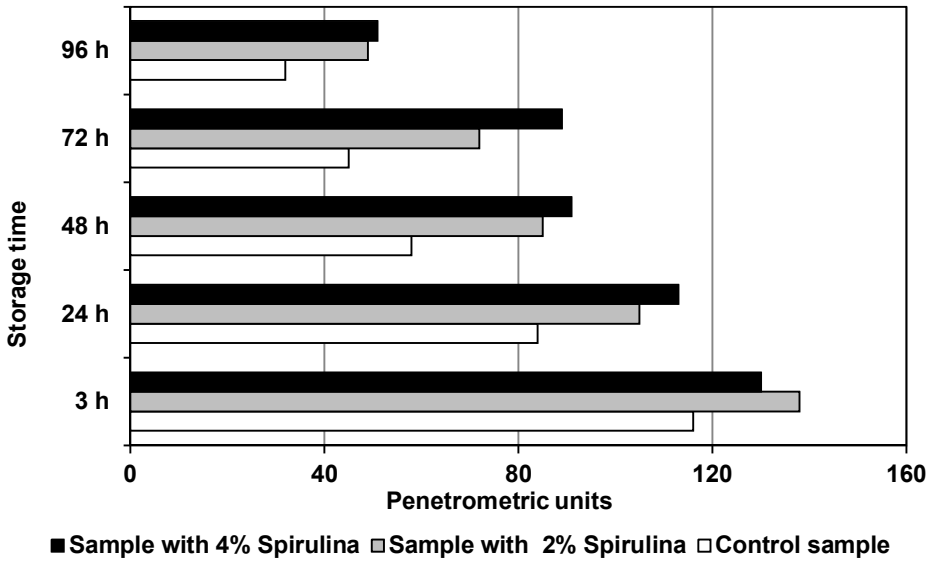

Figure 2. Plastic deformation of bread crumb

Algae containing samples have a higher plasticity of the crumb than the control sample. Regarding the bread with 2% *Spirulina platensis* at the beginning of storage, the reported value is 128 PU and is 1.2 times higher than that of the control sample. At the initial measurement (after 3 hours) the bread crumb of the sample with 4% *Spirulina platensis* falls behind in terms of its plastic properties in comparison to the bread crumb with 2% algae, but in the next measurements the sample containing 4% algae has better plastic properties and this regularity is maintained throughout the storage period. After 96 hours, the difference in plastic deformation of the enriched samples is only 2 PU. Whereas the control sample plastic deformation decreased 3.63 times within the period of storage, then the enriched samples the change was 2.81 times for the bread with 2% algae and 2.55 times for the bread with 4% *Spirulina platensis*.

In the samples prepared with the addition of algae, the bread crumb is distinguished by a higher plasticity and softness which is related to the higher porosity found during the experimental studies – figure 3.

a *b* *c*

Figure 3. Bread samples tested:
a – control sample; b – sample with 2% *Spirulina platensis*;
c – sample with 4% *Spirulina platensis*

72 hours after baking the bread with 4% *Spirulina platensis*, the plastic deformation value is 2 times higher than that of the control sample, and 1.24 times higher than that of the bread prepared with 2% algae. This proves that the addition of *Spirulina platensis* in the amounts of 2% and 4% by weight of the flour leads to an improvement in the plastic properties of the bread crumb and to their retention for a longer time than in the control sample.

These results are consistent with those of other researchers who also found that natural hydrocolloids in seaweeds improved dough characteristics and extended bread shelf life, also improve texture of the bread crumb [28]. Arufe and coauthors [29] investigate the effect of brown seaweed powder on physical and textural properties of wheat bread. They emphasize that a maximum of 4% (flour base) seaweed powder could be added, without impairing the crumb texture of enriched breads. Otherwise, using higher amounts, crumb firmness increases.

Effect of *Spirulina platensis* on the elastic deformation of bread crumb

The results obtained by determining the elastic deformation of the bread crumb are presented in Figure 4.

The experimentally established results show that as the bread storage time increases, the elasticity of the bread crumb decreases and this trend occurs in all samples subjected to testing.

During storage for 96 h in the control sample, the elasticity of the bread crumb gradually decreases and at the last measurement (96 hours after baking) it is 3.54 times lower compared to the beginning of storage – 3 h after baking the product. This is explained by the changes occurring in the starch fraction of the bread, and in particular with retrogradation of the amylopectin. Bread staling is inevitably associated with the deterioration of the structural properties of the bread crumb – reducing the softness and elasticity.

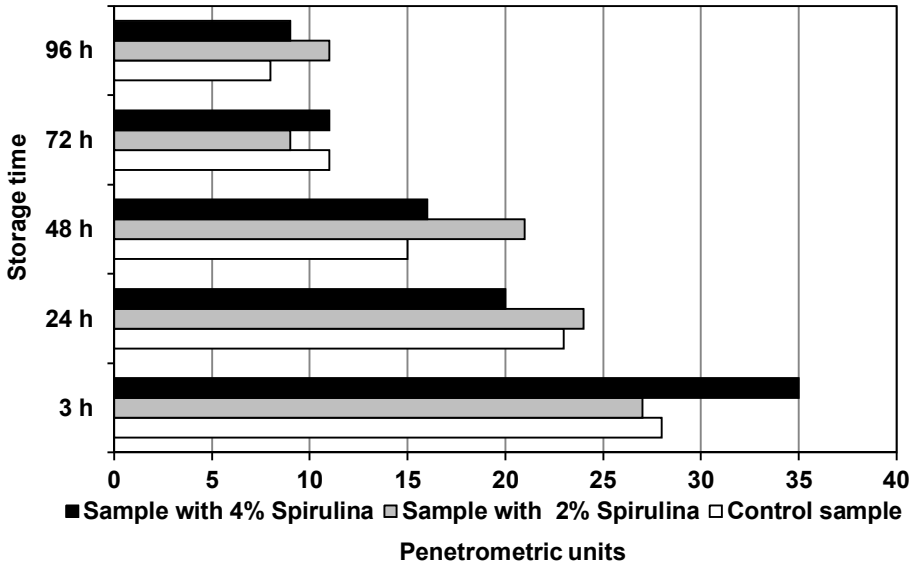

Figure 4. Elastic deformation of bread crumb

The elasticity of the bread crumb is affected by the addition of *Spirulina platensis*. For the sample with the addition of 4% algae at the beginning of storage, the value of the elastic deformation is 7 penetrometric units higher than that for the control sample. The values decrease by lengthening the storage period, as a more intensive decrease of elasticity is recorded at the beginning of storage (between the 3rd and 24th hour). The bread samples, which recipe includes 4% algae are characterized by a higher elasticity of the crumb throughout the storage period.

The results obtained by examining the deformation characteristics of the sample with 2% *Spirulina platensis* algae indicate that after 48 hours of storage, the elasticity of the bread crumb is identical to that recorded in the control sample after 24 hours of storage. It is noteworthy that in this sample the elasticity decreases 2.45 times for the whole period of storage (96 hours), while for the control sample – 3.5 times. Furthermore, in the middle of storage (between 24th and 72nd hours), the elasticity decreases at a slower rate than in the other samples.

This gives ground to point out that the samples of bread with the addition of *Spirulina platensis* retain their elasticity for a longer time and increase the time it takes for the bread crumb to harden. This finding is also supported by results published by other authors. Guarda et al. [27] reported that seaweeds because of the alginates showed an anti-staling effect on bread. The ability of alginates to decrease the staling rate of bread samples is attributed to inhibiting interactions between gluten and starch [30].

Conclusion

In this study the addition of 2 and 4% *Spirulina platensis* powder, as a novel approach of bread preparation, was investigated. Results obtained showed that crumb firmness of the

bread decreased with the incorporation of seaweed powder *Spirulina platensis*. The addition of *Spirulina platensis* in the amount of 4% determines the highest contractility and therefore the greatest softness of the bread crumb. After 48 hours, the samples containing algae have firmness of the crumb recorded in the control sample after 24 hours of storage. Bread crumb in samples with the addition of *Spirulina platensis* is characterized by a higher plasticity and softness. This gives ground to conclude that bread samples with the addition of *Spirulina platensis* store softness and elasticity for a longer time and the firming of the bread crumb occurs more slowly.

Acknowledgements. Authors would like to thank to the Ministry of Education and Science of Bulgaria about the subsidy by Regulation № 3 from 27.11.2015 – in accordance with the Ordinance on the Terms and Procedure for the Evaluation, Planning, Allocation and Expenses of the State Budget Funds for the Financing of the Inherent Research Activities of the State Higher Education Institutions. The acknowledgements are also to the academic management of University of Economics – Varna for the allocations in project NPI-16/2018 "Innovative approaches to increase the quality and biological value of foods".

References

1. Boussingault J. B. (1852), Expériences ayant pour but de déterminer la cause de la transformation du pain tendre en pain rassis, *Annales de chimie et de physique*, 36, pp. 490–494.
2. Katz J. R. (1928), The X-ray spectrography of starch and gelatinization and retrogradation of starch in the bread staling process, In R. P. Walton (Ed.), A comprehensive survey of starch chemistry NY, *Chemical Catalog Co*, pp. 68–76.
3. Gray J. A., Be Miller J. N. (2003), Bread staling: Molecular basis and control, *Comprehensive Reviews in Food Science and Food Safety*, 2, pp. 1–21.
4. Amigo J. M., Olmo A., Engelsen M. M., Lundkvist H., Engelsen S. B. (2019), Staling of white wheat bread crumb and effect of maltogenic α-amylases. Part 2: Monitoring the staling process by using near infrared spectroscopy and chemometrics, *Food Chemistry*, 297, pp. 1–9.
5. Goesaert H., Slade L., Levine H., & Delcour J. A. (2009b), Amylases and bread firming-an integrated view, *Journal of Cereal Science*, 50, pp. 345–352.
6. Hallberg L. M., Chinachoti P. (2002), A fresh perspective on staling: The significance of starch recrystallization on the firming of bread, *Journal of Food Science*, 67, pp.1092–1096.
7. Slade L., Levine H., Reid D. S. (1991), Beyond water activity: Recent advances based on an alternative approach to the assessment of food quality and safety, *Critical Reviews in Food Science and Nutrition*, 30, pp. 115–360.
8. Baik M. Y., Chinachoti P. (2000), Moisture redistribution and phase transitions during bread staling, *Cereal Chemistry*, 77, pp. 484–488.
9. He H., Hoseney R. C. (1990), Changes in bread firmness and moisture during long-term storage, *Cereal Chemistry*, 67, pp. 603–605.
10. Zeleznak K. J., Hoseney R. C. (1986), The role of water in the retrogradation of wheat starch gels and bread crumb, *Cereal Chemistry*, 63(5), pp. 407–411.
11. Tao H., Zhang B., Wu F. F., Jin Z. Y., Xu X. M. (2016), Effect of multiple freezing/thawing-modified wheat starch on dough properties and bread quality using a re-constitution system, *Journal of Cereal Science*, 69, pp. 132–137.

12. Wang S. J., Li C. L., Copeland L., Niu Q., Wang S. (2015), Starch Retrogradation: A Comprehensive Review, *Comprehensive Reviews in Food Science and Food Safety*, 14, pp. 568–585.
13. Fu Z., Chen J., Luo S. J., Liu C. M., Liu W. (2015), Effect of food additives on starch retrogradation, *A review. Starch/Stärke*, 67, pp. 69–78.
14. Fadda C., Sanguinetti A. M., Del Caro A., Collar C., Piga A. (2014), Bread staling: Updating the view, *Comprehensive Reviews in Food Science and Food Safety*, 13, pp. 473–492.
15. Ottenhof M.-A., Farhat I. A. (2004), The effect of gluten on the retrogradation of wheat starch, *Journal of Cereal Science*, 40, pp. 269–274.
16. Gupta S., Abu-Ghannam N. (2011), Recent developments in the application of sea-weeds or seaweed extracts as a means for enhancing the safety and quality attributes of foods, *Innovative Food Science & Emerging Technologies*, 12(4), pp. 600–609.
17. Mamat H., Matanjun P., Ibrahim S., Amin S., Hamid M., Rameli A. (2014), The effect of seaweed composite flour on the textural properties of dough and bread, *Journal of Applied Phycology*, 26(2), pp. 1057–1062.
18. Elleuch M., Bedigian D., Roiseux O., Besbes S., Blecker C., Attia H. (2011), Dietary fibre and fibre-rich by-products of food processing: Characterisation, technological functionality and commercial applications: A review, *Food Chemistry*, 124 (2), pp. 411–421.
19. Lee C., Choi J., Song E., Lee S., Kim K., Kim S., Jung J. (2010), Effect of Myagropsis myagroid esextracts on shelf-life and quality of bread, *Korean Journal of Food Science and Technology*, 42(1), pp. 50–55.
20. Smertina E. S., Fedyanina L. N., Kalenik T. K. (2011), Costaria Costata is a functional component in enriched bakery products, *Storage and processing of agricultural raw materials*, 3, pp. 71–74.
21. Fedyanina L. N., Smertina E. S., Kalenik T. K., Fischenko E. S., Medvedeva E. B. (2012), Functional foods with BAS on the basis of the hydrobiont of plant and animal origin as functional ingredients, *Goods expert of foodstuffs*, 4, pp. 17–20.
22. AACC (1999) Approved methods of the American Associations of Cereal Chemists, *American Association of Cereal Chemists*, St. Paul
23. Vangelov A., Karadhzov G. (1993), *Bread and pastry technology – a guide for labratory work*, Zemizdat, Sofia.
24. Raposo M. F. J., de Morais R. M. S. C., de Morais A. M. M. B. (2013), Bioactivity and applications of sulphated polysaccharides from marine microalgae, *Marine Drugs*, 11, pp. 233–252.
25. Rojas J. A., Rosell C. M., Benedito de Barber C. (1999), Pasting properties of different wheat flour-hydrocolloids systems, *Food Hydrocoll*, 13, pp. 27–33.
26. Rosell C. M., Rojas J. A., Benedito de Barber C. (2001), Influence of hydrocolloids on dough rheology and bread quality, *Food Hydrocoll*, 15, pp. 75–81.
27. Guarda A, Rosell C. M., Benedito de Barber C., Galotto M. J. (2004), Different hydrocolloids as bread improvers and antistaling agents, *Food Hydrocoll*, 18, pp. 241–247.
28. Rodge A. B., Sonkamble S. M., Salve R. V., Syed Imran Hasmi. (2012), Effect of hydrocolloid (guar gum) Incorcopration on the Quality Characteristics of Bread, *J. Food Process Technol*, 3:2.
29. Arufe S., Della Valle G., Chiron H., Chenlo F., Sineiro J., Moreira R. (2018), Effect of brown seaweed powder on physical and textural properties of wheat bread, *European Food Research and Technology*, 244, 1, pp. 1–10.
30. Davidou S., Le Meste M., Debever E., Bekaert D. (1996), A contribution to the study of staling of white bread: effect of water and hydrocolloid, *Food Hydrocoll*, 10, pp. 375–383.

Modeling and synthesis of systems of intensive mass exchange

Anatolii Sokolenko, Oleksandr Shevchenko, Kostyantyn Vasylkivskyi, Oleksii Boiko, Anastasiia Shevchenko

National University of Food Technologies, Kyiv, Ukraine

Keywords:

Exchange
Intensification
Synthesis
Medium
Inertion

Article history:

Received 12.03.2019
Received in revised form 16.07.2019
Accepted 28.11.2019

Corresponding author:

Oleksandr Shevchenko
E-mail: tmipt@ukr.net

DOI: 10.24263/2304-974X-2019-8-4-16

Abstract

Introduction. The development of the theory of synthesis of systems of intensive mass exchange processes at the expense of energy potentials of liquid or gas-liquid flows provides the realization of actual needs.

Materials and methods. The paper analyzes the physical basis of methods and ways of intensification of processes in liquid and gas-liquid systems and phenomenological generalizations based on known laws of nature with mathematical formalization of relationships between geometric, kinematic and hydrodynamic parameters.

Results and discussion. The study shows the possibility of synthesis of inertial fields due to the variable geometric parameters of pipelines, namely, the cross-sectional area, and due to the alternation of curvilinear and straight sections and trajectories of variable curvature.

The generalized representation of the factor of intensification of mass exchange processes relates to force actions in the form of the consequences of pressure redistribution as a result of the redistribution of kinetic and potential energy potential.

Possibilities of variations by values of force influences due to combinations of gravitational field and inertial fields of different orientation and frequency of effects have been shown, including with the possibility of reproduction of dynamic shocks in zones of change of signs of radii of curvature. Synthesis of inertial fields in such systems is achieved by such factors as variable flow velocity or change in flow direction. The combination of these two factors is more effective.

Energy support of the intensification of mass exchange refers to the initial conditions of flow creation, and the overall positive result is ensured by accurate localization of processes.

Conclusions. The factors of intensification of mass exchange processes are represented by the synthesis of inertial fields due to changes in the velocity and direction of the flow of the medium.

Introduction

Intensive mass exchange of liquid, gas-liquid or solid-medium media is an important component in a large number of chemical, food and microbiological technologies. Supplementation of mass exchange processes by chemical reactions, destruction or synthesis of substances, changes in chemical, thermodynamic and hydrodynamic parameters in the final result determine the speed of the target processes and the productivity of technological devices. These relationships are reflected in their geometry, total volume, process length etc.

So the cultivation of baker's yeast is carried out on sugar-containing media in machines with a capacity of 70–100 m^3. With the same or much larger volumes, the apparatus is used in anaerobic fermentation technologies in the brewery, winemaking, and alcohol industries. In each case, however, there are known limitation factors that make it necessary to use high-volume devices. For example, in aerobic fermentation technologies the processes are inhibited by the activity of yeast, including because of the limited concentration of dissolved oxygen. Anaerobic processes are limited by the osmotic pressure of solutes, etc., but in such cases, the output is sought due to the intensification factors that are realized in the local zones. In this regard, modeling of turbulent flows [1], flows in pipelines with special diaphragms [2], the study of features of transients [3–5], the potentials of mass forces [6, 7] are developed. Theory and numerical analysis allow to use the scientific potential of the Navier-Stokes equations, computational methods in fluid dynamics [8, 9], modern models of hydrodynamics of liquid and gas-liquid media [10–14]. Thus, the applied character of the search for technical solutions determines the relevance of the research and the creation of systems of intensive mass exchange at the expense of internal energy potentials.

Materials and methods

The paper analyzes the physical basis of methods and ways of intensification of processes in liquid and gas-liquid systems and phenomenological generalizations based on known laws of nature with mathematical formalization of relationships between geometric, kinematic and hydrodynamic parameters.

The object of the study is the technology of intensification of mass transfer processes in systems with limited local zones of interaction [6].

The subject of the research is the factors of intensification as a consequence of the redistribution between potential and kinetic energies in the form of variable kinematic parameters, orientation of flows in the gravitational field, variable pressures, variable geometry of cross sections of flows and curvature of pipeline routes [7].

Methods for investigating the intensification of liquid and gas-liquid systems are related to the use of relationships between kinematic and dynamic flow parameters based on generally accepted mathematical formalizations for straight and curved sections with the determination of dynamic shocks in the zones of change of signs of radii of curvature.

The procedure of the study was determined on the basis of the phenomenological generalization using the laws of nature in the courses of processes with force inertial effects in combination with the effects of the gravitational field.

The final part of the research was related to the analysis of the obtained mathematical models and the formulation of conclusions.

Results and discussion

The potential cause of force interaction between solid, gas or liquid fractions and their combinations is the presence of a potential field. So the gravitational field is almost without exception inherent in all technologies of mankind, creating a force of gravity proportional to the mass of the body or medium. The vector characteristic of this field is its overtension $\bar{g}$ in the form of the relation of force $\bar{F}$ to the mass of the object [1, 2].

A considerable number of technological processes on the basis of mass and energy exchange in food technologies are carried out in potential fields, due to which the pressure is varied. As for solids, such variations are possible due to the action of external forces and the redistribution of pressures between other bodies at constant indexes of the force potential field. In case of liquid, gas medium (flows) or their combinations, one of two conditions is required [3].

Condition one: Local fluxes are created in liquid, gas or gas-liquid medium in the potential field, in which, according to the Bernoulli and Navier-Stokes equations, the redistribution between potential and kinetic energies and pressures, respectively is carried out. The same redistribution of pressures accompanies the interaction of liquids and gases in the flow of solids, which is accompanied by the occurrence of flows with relative velocities. On this basis, a considerable number of technological methods have been created, which include the use of the aerodynamic profile of the aircraft wing, aircraft screws and helicopters, structures, blades of mixers, ejection devices, etc.

Condition two: the sealing of the local volume of liquid or gas is created and has the manifestation of an increase in the mass quantity of the medium due to external force factors through solids with appropriate energy costs, or the change of the localized sealed volume, or transmission (withdrawal) of heat to the static volume is carried out.

Regarding the first condition, it is noteworthy that the characteristics of the potential field is crucial in the pressure changes. Devices that create artificial force fields based on centrifugal forces are widespread. The principle of their action is based on the movement of curvilinear trajectories with the occurrence of normal accelerations.

The movement of material bodies or flows along curved trajectories means that they have material connection with the centers of curvature in the form of lacs or contact surfaces of curvilinear form.

The force interaction between the streams and the pipes in which they are formed has differences with respect to straight and curved sections. In accordance with the condition of continuity of the flow of the ideal substance in a cylindrical tube with a constant cross-section, the velocity is assumed constant at all points of the latter, and for the uncompressed fluid, the velocity is the same for all sections.

The movement of fluid flows along curvilinear trajectories is accompanied by the creation of fields of centrifugal forces with the action of the latter on each material particle. The combination of centrifugal force and the shell reaction leads to the emergence of a local pressure zone. Since the action and counteraction are mutually compensated, this means that an increased pressure field arises only in the area of the centrifugal force field. The external consequence of the existence of an increased pressure field is an increase in the pressure drop ΔP along the length of the curved pipe as the friction forces between the flow and the wall increase. So according to the recommendations [3] pressure loss in the coil pipe is:

$$\Delta P_{cp} = \Delta P_{st} \psi \,, \tag{1}$$

where ΔP_{st} is the loss of pressure on the straight pipe section, and a dimensionless correction factor $\psi > 1$ is determined by the formula:

$$\psi = 1 + 3.54\frac{d}{D}, \tag{2}$$

where d is the internal diameter of the pipe; D – diameter of the coil pipe.

Due to the given values of kinematic parameters, the tension of the field of inertia forces can significantly exceed the similar potential of the gravitational field. For example, for values of parameters V = 5 m/s, d = 0.1 m and D = 0.2 m we obtain:

$$a^n = \frac{2V^2}{D} = \frac{2 \cdot 25}{0.2} = 250\ m/s^2 \tag{3}$$

and the inertia force from the mass m in this curved section will be corresponding:

$$F_i = m\frac{2V^2}{D} = 250m,\ N\ . \tag{4}$$

In the last entry, the parameter F_i is defined as the resultant inertia force corresponding to the distributed pressure. It is important that the transition from the straight-line section to the curvilinear and vice versa is carried out under the condition of instantaneous change of acceleration a^n, which corresponds to the known phenomenon of soft impact in the dynamics and is estimated as a powerful factor of influence on the system in terms of interests of intensification of energy and mass exchange processes.

These changes in the physical parameters of the impact can have manifestations in limited time or in impulse modes and operate in the extended period of time [4, 5].

Given the proportional values of the tensions of the gravitational field and the field of forces of inertia, the orientation of the plane of curvature of the curvilinear trajectory of the flow can have value. Thus, in the horizontal orientation of the system in accordance with the principle of superposition, the total tension of potential fields is determined by their geometric sum:

$$\overline{a}_{sum} = \overline{g} + \overline{a}^n\ , \tag{5}$$

which remains constant throughout the site, if $\overline{a}^n$ is constant. In the vertical orientation of the specified plane, the values $\overline{a}_{sum}$ will be variable (Figure 1).

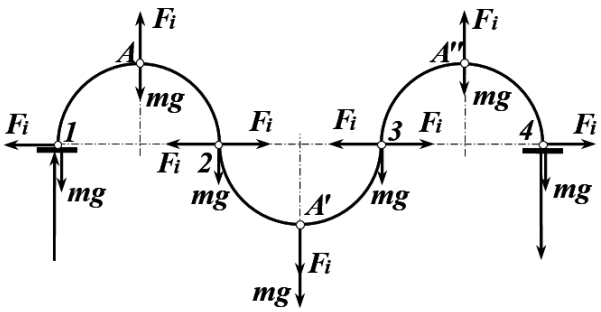

Figure 1. Scheme for determination of inertial force effects on a curvilinear section of a transport system with points of inflection of the trajectory

Along the whole trajectory, we obtain variable values of mass forces due to different combinations of directions $\overline{F_i}$ and $\overline{mg}$. In the case of a route with points of inflection of curvilinear sections with constant values of the radii of curvature, the forces of inertia remain constant, but their directions change by 180 °, which leads to the redistribution and action of friction forces between the flow and the pipeline and to changes in the hydrodynamic regime. Changing the direction of inertia forces relative to the flow plays the role of an intensification factor, which is especially important for combined media with the presence of liquid, gas and solid fractions.

Figure 2 shows the marking points of flow *A* and *B* and the directions of the resultant gravitational and inertial forces. As we can see, in the closed loop, the result of the gravitational force of unit mass *mg* on the sections of rectilinear displacement *2–3* and *4–1* relative to the flow has a multi-directional orientation, remaining vertical, and on the sections of curvilinear displacement, the unit mass rotates about 180 ° by vector *mg*. Such change in the relative position corresponds to a transient process which additional perturbations occur due to the occurrence of F_i inertia forces at points *3* and *1* (Figure 2).

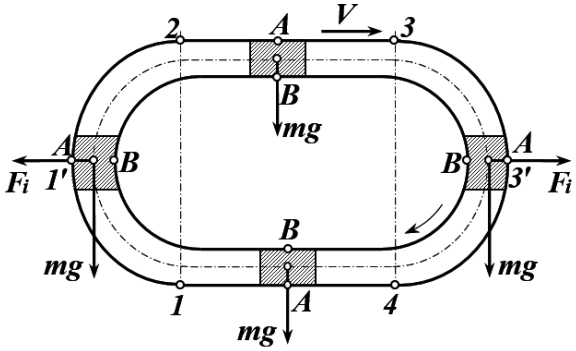

Figure 2. Scheme to determine the directions of force actions relative to the flow

The resultant *R* is determined by the expression:

$$\overline{R} = \overline{F_i} + \overline{mg}\,. \tag{6}$$

Since the orientation of the resultant of inertia forces F_i is related to the position of the radius vector $\overline{r}$, we determine its projections on the coordinate axis of the *OXY* system (Figure 3):

$$\begin{aligned} F_{i\,X} &= F_i \sin\phi = F_i \sin\omega t; \\ F_{i\,Y} &= F_i \cos\omega t \end{aligned} \tag{7}$$

where ω is angular velocity of single mass on a curved section; *t* – the time of movement of single mass in a curved section.

From the plan of forces (Figure 3) it can be seen that the resultant projection on the axis *OY* for the module is ($mg - F_i \cos\omega t$).

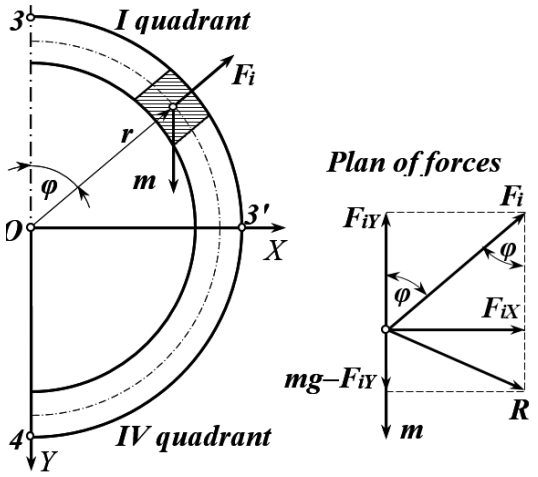

Figure 3. Scheme to determine the force

Then the value of the total resultant for the first quadrant will be

$$R^{I} = \sqrt{F_i^2 \sin^2 \omega t + \left(mg - F_i \cos \omega t\right)^2}\ , \tag{8}$$

and for the fourth quadrant –

$$R^{IV} = \sqrt{F_i^2 \sin^2 \omega t + \left(mg + F_i \cos \omega t\right)^2}\ .$$

The maximum value of the resultant in the first quadrant:

$$R^{I}_{\max} = \sqrt{F_i^2 + \left(mg\right)^2}\ , \tag{9}$$

and in the fourth quadrant – $R^{IV}_{\max} = mg + F_i$.(10)

At position *4* there is a R^{IV} jump to reduce the force to the value of *mg*, which corresponds to the mode of soft impact. Only *mg* is valid in section *4-1* of the mass force, and co-directed with the inertia force F_i in point *1* in shock mode. Calculating the angle φ = ωt from the vertical axis in the third quadrant, we determine:

$$R^{III} = \sqrt{F_i^2 \sin^2 \omega t + \left(mg + F_i \cos \omega t\right)^2}\ , \tag{11}$$

and for the second quadrant we obtain

$$R^{II} = \sqrt{F_i^2 \sin^2 \omega t + \left(mg - F_i \cos \omega t\right)^2} \tag{12}$$

Choosing a pipeline route in the shape of, for example, a sinusoid wave leads to variable radii of curvature [7].

It is known that the general sinusoidal dependence corresponds to the equation

$$y = A\sin(\omega_0 x + \varphi_0), \tag{13}$$

where amplitude $A > 0$ and circular frequency $\omega_0 > 0$.

This is a periodic function with period $T = 2\pi$ (Figure 4), the graph of which intersects the *OX* axis at points with coordinates $(n\pi; 0)$ (n is any integer). The points of inflection of the curve correspond to these coordinates. The tangents at these points form, with the positive direction of the axis *OX*, the angles $\pi / 4$ or $-\pi / 4$.

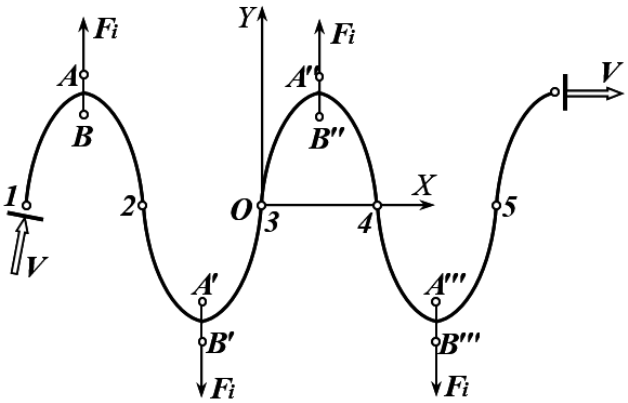

Figure 4. Scheme to determine the power parameters for the sinusoidal line

It is known that the curve y = y (x) is determined by the dependence:

$$K = \frac{y''(x)}{\left(1+\left(y'\right)^2\right)^{3/2}}, \tag{14}$$

and the radius of curvature is

$$r = \frac{1}{K} = \frac{\left(1+\left(y'\right)^2\right)^{3/2}}{y''(x)} \tag{15}$$

With the possibility of free transfer of the origin of the coordinate system OXY, we assume $\varphi 0 = 0$. Then

$$\begin{aligned} y &= A\sin\omega_0 x; \\ y' &= A\omega\cos\omega_0 x; \\ y'' &= -A\omega^2\sin\omega_0 x. \end{aligned} \tag{16}$$

Substituting values y' and y' we obtain

$$r = \frac{\left(1 + A^2\omega_0^2 \cos^2 \omega_0 x\right)^{3/2}}{-A\omega_0^2 \sin \omega_0 x}. \quad (17)$$

Let's determine the value of the radii of curvature at the inflection points and extrema. It should be noted that the complex in the numerator of the last dependence will be positive for all values of *x*, since the cosinus function is squared. This means that the sign of the radius of curvature depends only on the sign of sine, namely: in the first and second quadrants the radius is negative, and in the third and fourth – positive.

It should be noted that the notion of the positive and the negative value of the radius of curvature refers to convex and concave parts of a sine wave with respect to the chosen coordinate system, although from a physical point of view the radius of curvature cannot be negative. Figure 5 shows a general view of sinusoidal function and radii of curvature.

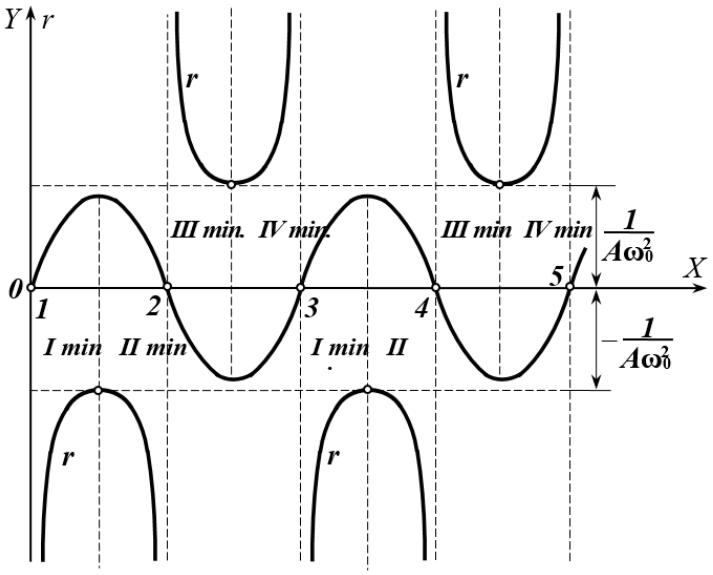

Figure 5. Scheme for determining the radii of curvature of a sinusoid

A change in the direction of the centrifugal force of inertia F_i corresponds to the discontinuity at the inflection points of the function $r = r(x)$.

From the point of view of increasing the power flow

F_i, it is advisable to have as little value of r as possible, since

$$F_i = m\frac{V^2}{r}. \quad (18)$$

The value $\omega_0 x = \pi/2$ and $\omega_0 x = 3\pi/2$ correspond to the extremes of dependence $r = r(x)$ and there is $r = -\frac{1}{A\omega_0^2}$ and $r = \frac{1}{A\omega_0^2}$ respectively. At inflection points, we obtain $|r| = \infty$ and $F_i = 0$.

Thus, in the case of a sinusoidal pipeline route, the inertia force acting on a mass unit m

$$F_i = m\frac{-V^2 A\omega_0^2 \sin\omega_0 x}{\left(1 + A^2\omega_0^2 \cos^2 \omega_0 x\right)^{3/2}} \tag{19}$$

is variable by magnitude and direction.

The methods of dynamic influences on liquid or gas-liquid are considered to be worthy of attention and are proposed for implementation, but in the extreme case the situation corresponding to a hydraulic shock should be considered.

Recognizing the changes in pressure as an important factor of intensification of massexchange processes in gas-liquid systems or systems with the addition of solid fraction, we conclude that the deformation is due to the presence of a dispersed gas fraction. This means activation in the interphase surface renewal, coalescence, re-dispersion, vapor phase formation and its collapse at the level of cavitation phenomena. It is important that all these phenomena and transformations occur in conjunction with the operations for transporting the medium. Achieving this result is possible through the use of mass exchange pipelines with variable dimensions and cross-sectional areas. One such option corresponds to the case of successive alternation of transitions from circular to elliptical sections. However, it is obvious that there is an option in which there are simultaneously variable cross-sectional area and trajectory of variable curvature [10].

Let's turn to the estimates of dynamic force manifestations in the latter case. The fundamental value in estimating the parameters of hydrodynamics is the interaction between the streams and the shells that form them. Such determination can be made on the basis of Euler's theorem about the change of the principal vector of quantities of motion of a system of material points. According to it, the sum of the major vectors of the bulk and surface forces, as well as the vectors of the second quantities of fluid flow through two sections of the pipe is zero if the vectors of the second quantities of motion are directed inside the selected cross-sections by volume [12, 13].

Let's turn to the example of the flow of fluid through a curved tube, the straight sections of which form an angle of 120° with velocity w, aiming to determine the additional dynamic pressure of the flow on the walls of the tube. The calculation scheme of this case is shown in Figure 6 in plan. The bulk force is the gravitational force of the fluid, which is perpendicular to the plane of the drawing. The reactions of the wall of the tube, applied to the particles of water in accordance with the law of equality of action and counteracting by the largest vector of the reaction shell are superior.

In the selected coordinate system, the X-axis is directed horizontally to the right and the Y-axis is vertically up. The vectors of the instantaneous quantities of the flow flowing through the sections 1 and 2 are depicted pointing them inside the volume (Figure 6b). Secondary mass of water is:

$$m_c = \rho f w, \tag{20}$$

where f is the cross-sectional area of the tube.

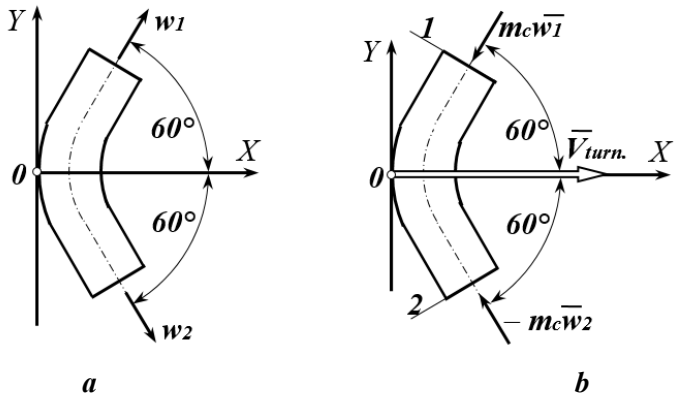

Figure 6. Calculation scheme for the case of determination of dynamic flow pressures

Using the Euler theorem, we write down the parameters of the system in the projection on the axis of the selected coordinate system:

$$V_{shell.x} + V_{turn.x} - m_c w_{1x} - m_c w_{2x} = 0; \quad (21)$$

$$V_{shell.y} + V_{turn.y} + m_c w_{1y} - m_c w_{2y} = 0. \quad (22)$$

In our case vector $\overline{V}_{shell}$ is perpendicular to the axes *X* and *Y*, and therefore the system of equations (21)-(22) will be written in the form:

$$V_{turn.x} - m_c w \cos 60° - m_c w \cos 60° = 0; \quad (23)$$

$$V_{turn.y} - m_c w \cos 30° + m_c w \cos 30° = 0, \quad (24)$$

where indexes at speeds are not written because $|w_1| = |w_2| = w$.

From this we get:

$$V_{turn.x} = 2m_c w \cos 60°; \qquad V_{turn.y} = 0. \quad (25)$$

Thus, the main vector of additional dynamic reactions of the walls of the tube is directed parallel to the axis *OX*. As $m_c = \rho f w$, then

$$V_{turn.x} = 2\rho f w^2 \cos 60°, \text{ N}. \quad (26)$$

The main vector N of forces of additional dynamic pressures on the walls of the tube is equal by modulus and in opposite by direction $V_{turn.}$, that is, horizontally to the left. This additional component acts only on the curved section and its largest value corresponds to the 180 ° rotation angle:

$$V_{turn.\max} = 2\rho f w^2, \text{ N}. \quad (27)$$

Such additional force interaction between flow and shell is perceived by the medium as an inertial component, the change of which is reflected in the Froude, Reynolds and Euler criteria. Thus, the flow of curvature-stretching sections should be attributed to the number of factors of intensification of mass exchange processes, and acceleration jump in magnitude w^2/r and additional dynamic loading in the form of a soft impact correspond to the transition zone from the curved section to the straight line. It is important that such impacts can be fully dosed and programmed.

Conclusion

The analysis of the peculiarities of mass exchange processes in liquid and gas-fluid systems and flows allows to note the following.

1. The generalized representation of the factor of intensification of mass exchange processes relates to force actions as a consequence of the redistribution between potential and kinetic energies in the form of alternating pressure.
2. Characteristics of a set of potential gravitational fields and artificially generated inertial fields are important in creating alternating pressure. The latter with different characteristics are synthesized at the expense of curvilinear trajectories of flows, which means the presence of their material connection with the centers of curvature in the form of surfaces of contact of curvilinear form.
3. Transitions from curvilinear to rectilinear sections of flow are accompanied by the phenomena of soft dynamic shocks.
4. The intensification factor of mass exchange processes is the geometry of pipeline with variable cross-sectional area. One of the possibilities of realizing such geometry concerns the alternation of circular and elliptical sections due to the corresponding residual deformations.
5. The displacement of flows by curvilinear sections is estimated as a factor of intensification of mass exchange processes, and variable radii of curvature of the route mean the realization of continuously acting influences of inertia forces with manifestations of dynamic shocks in the zones of change of signs of radii of curvature.

References

1. Belov I., Isaev S. (2001), *Modelirovanie turbulentnykh techenii: uchebnoe posobie,* Sankt-Peterburg.
2. Ganiev R. (2009), *Analiz techeniia v truboprovode so standartnoi diafragmoi sredstvami vychislitelnoi gidrodinamiki*, Kazan.
3. Piddubnyi V. (2008), *Naukovi osnovy i aparaturne oformlennia perekhidnykh protsesiv kharcho-vykh i mikrobiolohichnykh vyrobnytstv*, NUFT, Kyiv.
4. Roache P (1976), *Computational Fluid Dynamics*, Hermosa, Albuquerque
5. Sokolenko A., Piddubnyi V., Ukrainets A. (2007), Vykorystannia potentsialu masovykh syl dlia intensyfikatsii masoobminu v ridynnykh i hazoridynnykh potokakh, *Kharchova i pererobna promyslovist*, 3, pp. 15–17.
6. Shevchenko O.(2006), *Naukovi osnovy i aparaturne oformlennia protsesiv dovhostrokovoho zberihannia kharchovykh produktiv*, NUFT, Kyiv.
7. Sokolenko A., Khomenko M., Shevchenko O. (2007), Masoobmin u neliniinykh

truboprovodakh, *Kharchova i pererobna promyslovist,* 5, pp. 20–21.
8. Temam Roger (1979), *Navier-Stokes Equations. Theory and Numerical Analysis. 2nd Edition*, North Holland.
9. Fletcher K. (1991), *Vychislitelnye metody v dinamike zhidkostei. T. 1*, Mir, Moscow.
10. Frik P. (1998), *Turbulentnost: modeli i podkhody*, Perm.
11. Anderson John D., Jr. (1995), *Computational Fluid Dynamics: The Basics with Applications*, McGraw-Hill, New York.
12. Bajura R., Pellgrin M. (1977), Studies of pulsating incompressible flow through orifice meter, *U. S. Dep. Commer. Nat. Bur. Stand. Spec. Publ*, 84/2, pp.523–548.
13. Harvard Lomax, Thomas H. Pulliam, David W. Zingg (1999), *Fundamentals of Computional Fluid Dynamics*, University of Toronto Institute for Aerospace Studies, Toronto.
14. Hofmann G. (1996), Flotation Die Technik der Zukynf, *Der Deutsche Weinbau*, 1, pp. 20–21.

Justification of the neuro-fuzzy regulation in evaporator plant control system

Mykhailo Hrama, Viktor Sidletskyi, Igor Elperin

National University of Food Technologies, Kyiv, Ukraine

Keywords:

Sugar
Juice
Model
Evaporator
Neuro-fuzzy
Regulation

Article history:

Received 17.01.2019
Received in revised form 29.05.2019
Accepted 28.11.2019

Corresponding author:

Viktor Sidletskyi
E-mail: vmsidletskiy@gmail.com

DOI: 10.24263/2304-974X-2019-8-4-17

Abstract

Introduction. The purpose of the study is the determining the use of which type of regulation will achieve the best indicators of quality control for the regulation of the evaporator plant.

Materials and methods. The system of management of a five-body evaporator plant of a sugar refinery was researched. The method of synthesis of modal control was used for evaluating the results of the research.

Results and discussion. A comparison between FID and fuzzy regulator was made. Regulation of such responsible parameters as levels of concentrated juice in evaporator plant bodies, which directly affect the quality and value of manufactured products, was implemented. First, in the space of states in Matlab environment, a mathematical model was developed and the results obtained regarding the variation of the problem with respect to the initial conditions and perturbations were obtained. Due to them one can conclude that the time of the transition process is within the range from 0.8 to 1.2 seconds. However, the deviation levels in the evaporator plant bodies are too high. Secondly, a mathematical model with a PID-regulator was developed and transition processes for control schemes across all control channels were obtained. In this case, the time of transition processes is within the range of 60 seconds along the channel X1 to 145 seconds along the channel X2, but this led to a significant decrease in the deviation of levels in the bodies. Thirdly, a mathematical model with a fuzzy regulator is developed and transition processes for control schemes in all control channels were obtained. In this case, the time of transition processes is within the range from 50 seconds along the channel X1 to 110 seconds along the channel X2, which is the better result if compared to the PID regulator. Compared with the previous study, the levels in the bodies also significantly decreased. Therefore, the use of neuro-fuzzy regulation leads to an increase in qualitative parameters of the process compared with the system with PID-regulators.

Conclusions. The scientific substantiation of the feasibility of using neuro-fuzzy regulation during the implementation of optimal control systems is the novelty of the research results.

Introduction

An automated control system for an evaporator plant can be characterized as a system, which requires the intervention of a process operator in the process of its operation [1]. Process operator shall make adjustments in the tasks for regulators in charge of temperature conditions, material flows. Such adjustments can be explained as a change in the technological and qualitative indicators for the components at the input of evaporator plant, as well as the need to change them at the output from the site. In the process of making changes in the operation of the automation system the operator shall consider how the adjacent areas affect the work of the evaporator plant, as well as the influence of the evaporator plant on the work of adjacent sites, for example: defecosaturation devices, vacuum devices, desuperheating and pressure reducing system of CHPP; secondary steam of the last case shall be used for heating of pressed pulps and feed water for extraction plant [2].

Evaporation plants for the sugar industry shall be usually equipped with evaporator plants with natural circulation [3]. In the latter, in case of non-compliance with the optimal mode in the process of evaporation, there is a decrease in alkalinity due to decomposition and caramelization of sucrose, which leads to the decomposition of amides such as asparagine [4]. Condensate juices (ammonia water) and evaporator vapors contain carbon dioxide, carbon monoxide and ammonia. Sugar juice contains glucose ($C_6H_{12}O_6$); the aforementioned factors cause a change in its properties. Once the glucose temperature reaches the mark of 160 ° C and it remains unchanged for a long time, there is a splitting off of one of two molecules of water, which is glucose anhydride ($C_6H_{10}O_5$) [5]. Creation of crystallized sugar out of it is impossible. In case of further increase of temperature up to 220 ° C boilings without flavor or bitter assamar (a substance formed when heating products of animal and vegetable origin) that are not capable of fermentation is formed out of sugar juice. Therefore, the production of sugar out of such substances is impossible. Therefore, it is necessary to provide the best quality control parameters in order to prevent overexposure and overheating of sugar juice [6].

Analysis of recent studies and publications

Improvement of the evaporation process is an important task. In the study [7] the author considers the model of the evaporation process, which takes into account the balance of mass and energy in the three components of the evaporation process. There is a unique surface of the distributor of the juice heater in case if the total surface of the heater is fixed. In the study [8] the linearization process of a nonlinear model consisting of 14 nonlinear levels of the primary order, which is a dynamic model of the evaporator plant, was researched. A function for changing the concentration of the product on the deviation of the flow rate of the liquid was found for the first time in this study. In the study [9] a fuzzy evaporator plant model, which reduces the computational time using a Rankine cycle based evaporator plant, was suggested. The results indicated that fuzzy technology can significantly reduce the time of calculation by predicting the outlet of the supercritical evaporator in the waste heat treatment system. In the study [10] the author argues that with the help of intelligent control it is possible to provide a faster decrease in the temperature of the casing and to achieve a more stable control of overheating in the first evaporator plant. In the study [11] it has been proved that control over the evaporation can be implemented by recycling the liquid in the evaporation section or by feeding only the liquid into the evaporator plant. In this study [12] the fuzzy PID regulator was investigated as a discrete version of the usual PID regulator. Thus, it retains the same structure, but has an independent adjustable control factor. It is proved that it is possible to improve the classical PID regulator with certain adaptive control

ability. In this study [13] PID regulator of fuzzy logic is presented. This regulator is a fuzzy PID regulator with a computational efficient analytical scheme. The author proves that the regulator is stable with a restricted input / output. The need for upgrading the existing management systems is indicated in the study [14]. This study indicates some approaches that are used for a distributed level of control of technological processes. Explanation of these approaches is useful for better understanding of the processes that occur during the formation of a controlling influence, especially in cases when software programmers for industrial ACSs use a large number of settings for configuring the system. Such an approach is reasonable only for skilled professionals with significant work experience. However, knowledge of these processes by professionals can also provide more flexible work in structuring data. The study [15] indicates that one of the advanced methods of improving control systems is the addition of fuzzy and neuron-fuzzy logic. The method of dynamic regulation of power of steam boilers at the CHPP of low power according to the current needs of consumers is researched. Methods of dynamic power control of boiler systems were analyzed using fuzzy logic and adaptive neural networks. The use of fuzzy conclusions (the so-called fuzzy system) is one of the possible options for adjusting the boiler's power. The regulating action is formed by checking the coherence of the fuzzy rules on the actual parameters of the system. The rules are created according to the operator's experience, which reflects his / her actions when changing the technological parameters. In the study [16] the management of multiple evaporator plants with the full integration of fuzzy control and the use of wireless network sensors and actuators are described. The study [17] presents an overheating control of the evaporator plant using a fuzzy slider regulator. This research [18] presents a mathematical model for controlling overheating of the electronic evaporative expansion valve system with the explored management strategy. The study [19] indicates an analysis and simulation of the evaporator's electronic expansion valve with fuzzy adjustment, which was carried out. The model is identified by the least squares algorithm based on the minimized amount of square residues. The study [20] presents a fuzzy control for overheating of the evaporator plant. The research in the study [21] considers the use of a robust regulator in the process of evaporation. The author conducts a comparative analysis with the PID regulator and concludes that the suggested regulator provides better performance. In the study [22] a methodology for improving the use of steam was considered. In the study [23] the authors prove that the rate of evaporation decreases with time and performs a calculation, which indicates that liquid phase diffusion is a step that limits the speed for this system, in contrast to the evaporation of pure water. The study [24] presents a generalized stationary mathematical model for modeling a multichannel evaporator system. In the study [25] problems of troubleshooting industrial processes using dynamic neural networks by example of evaporator plant were considered. The considered neural network has a multilevel feed structure. In the study [26] the author researches the use of real-time optimization in the sugar plant evaporation section using methods that reduce the time for developing models. In the study [27] the authors consider the use of genetic algorithms in sugar production. The research [28] indicates the development of the structure of an automated control system using tensor methods in sugar production.

Aim and research objectives. The purpose of the study is to determine when the use of which type of regulation will achieve the best indicators of quality control for the regulation of the evaporator. The regulation of such responsible parameters as levels of concentrated juice in the evaporator's buildings, which directly affect the quality and cost of manufactured products, is carried out.

In this study it is suggested to research how the uses of neuro-fuzzy regulators in the evaporator plant control system that will improve the quality indicators of the regulatory

process in order to improve the efficiency of the functioning of the automation system. For this purpose, it is necessary to develop in Matlab environment a mathematical model of the process of evaporation, translating it into the space of states. Next, it is necessary to develop mathematical regulators with PID and neuro-fuzzy regulators and compare the simulation results with each other.

Materials and methods

Description of the automation scheme. The research deals with mathematical modeling and simulation of automatic control of five-hull evaporation station of a sugar mill. The apparatus consists of 5 evaporators, with the same characteristics arranged in series [29]. The process of sugar production consists of several stages. In this sense, evaporation is the unit of mass transfer operation where the sugar syrup is concentrated to 65-70% CP (dry matter). This is done in multi-body evaporators, where the amount of steam used in the first evaporation enclosure is used in the following [30].

Figure 1 indicates automation diagrams of temperature control loops, pressure and level control. The temperature control circuits use a resistance thermometer (TE) with a built-in converter into a uniform signal (TT) that connects to the analog signal of the microprocessor controller (a point on the input line of the analog IA to the PLC). From the PLC, this information is transmitted to the automated workplace (AW) of the operator, namely to the mnemonic circuit (intersection with line I – display), is stored in memory (intersection with line R – registration), with the further possibility to view the trends of its change in time, as well as to the alarm subsystem (intersection with line A – alarm, to display to the AW operator an alarm if the temperature goes beyond the set limits).

In the automatic control and level control circuits in the evaporation enclosures, a level meter (LE) with a built-in converter into a uniform electrical signal (LT), which is fed to the analog inputs of the controller (IA), is used to measure the level. This information enters the controller automatic controller unit (intersection with C – automatic control), as well as the automated workstation (AW) of the operator, in which the values of the levels are displayed on the computer screen (intersection with I) in the form of bar charts and stored in memory (R – logged with further trend viewer). In addition, an alarm (A) is generated if the value of the levels exceeds the set limits. The control signal produced by the controller is output from the corresponding analog outputs of the controller (AO) in the form of a uniform electrical signal. It is suggested to choose pneumatic actuators. The signal from the controller is fed to an electro-pneumatic converter (eg LY 9e), which converts an analog unified electrical signal. In turn, the actuator (eg 9f) changes the position of the control valves. The operator can control the position of the regulator in remote (manual) mode (intersection with C – remote control from the AW operator).In the control loops, resistance thermal converters TCM-1288 are used as sensors (1a). Pressure transducers PC-28 are used as sensors (6a) in the pressure control loop. Capacitance level indicators are used as sensors (10a) in the level control loop. The ITM-110 device, which is produced by "Microl" factory, was selected as secondary indicating device. Manual control units BRU-17 are used for switching the "Manual / Automatic" mode. Modicon M340 is used as a regulator. J4SPG1805 KRAFTt-AIR pneumatic seat valves with built-in throttling valves are used as an actuator.

Real operation variables were used: flow rate, temperature, pressure, concentration and level. From a management standpoint, the process is multidimensional, with multiple inputs and outputs, highlighting the concentration of juice at the outlet of the last housing [31]. In addition, the process has nonlinear characteristics, with a delay and large interactions between variables [32].

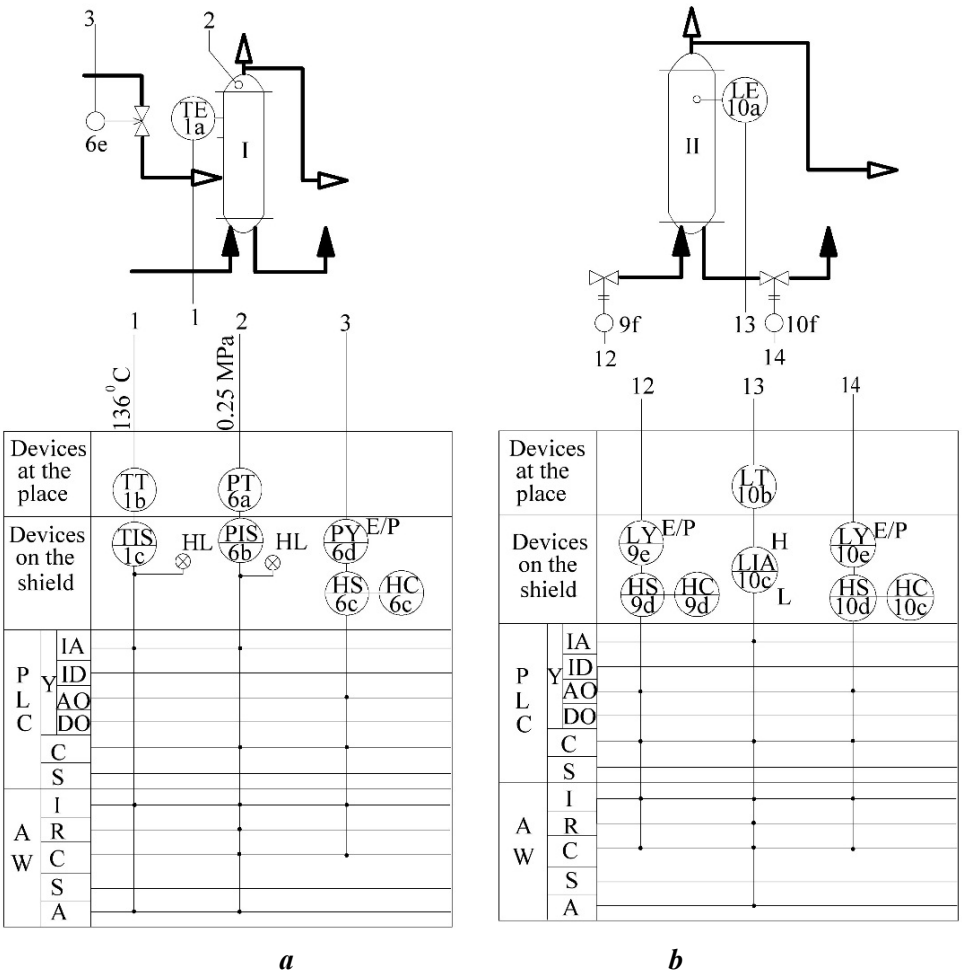

Figure 1. Automation of evaporator plant control loops:
a – temperature and pressure, b – level

This research uses PIDs and neuro-fuzzy regulators. Neuro-fuzzy regulators are based on fuzzy logic. In order to develop a neuro-fuzzy regulator, it is necessary to first define the input linguistic variables [33]. The next step is to define the linguistic variable that you want to get as a result. The final step is to define the rules for converting the resulting variable from the input [34].

A modal control synthesis method will be used to evaluate the results of the work. In order to achieve the necessary transitional character, modal control changes the eigenvalue module of the object matrix. In doing so, the task itself is to select such feedback that provides the necessary distribution of the roots of the characteristic equation in a closed system [35]. Therefore, in such systems, the required number of transients is achieved not through the use of corrective links, but through the introduction of appropriate feedback on the state of the object [36].

Description of the method of synthesis of modal control. In order to create a mathematical model, one shall take into account the following assumptions: due to the disturbance channels and the delay control in the juice pipeline, it should not be taken into account as insignificant for the dynamics of the evaporator plant; the parameters included in the equation are taken regardless of time and is average for the bodies; the evaporator plant shall be considered as an object with concentrated parameters as a link of complete mixing [37]. One shall transfer the control object to the space of the state variables. In order to do this, one shall first write down vectors (each component of the vector), i.e. x (t), u (t), w (t). Further, based on the mathematical model in the space of the state variables (1) and the system of differential equations (7)

$$\begin{aligned} \dot{x}(t) &= Ax(t) + Bu(t) + Fw(t), \\ y(t) &= Cx(t). \end{aligned} \tag{1}$$

Then we receive a stationary reverse (7) connection:

$$u(t) = -Kx(t) \tag{2}$$

where K – matrix, which has an order of m x n.

Equation of object (8) can be rewritten as follows:

$$\dot{x}(t) = Ax(t) - BKx(t) = [A - BK]x(t) \tag{3}$$

Then the MATLAB environment is used [38]. Matrices are created on the basis of expressions (7-11), using the synthesis of modal control. We introduce matrices: matrices A and D models have components that are equal to zero.

$$\text{Matrix C} = \text{diag}(1,1,1,1,1) \tag{4}$$

$$B = \begin{vmatrix} -0.2277 & 0 & 0 & 0 & 0 \\ 0.1466 & -0.1466 & 0 & 0 & 0 \\ 0 & 0.1978 & -0.1978 & 0 & 0 \\ 0 & 0 & 0.2011 & -0.2011 & 0 \\ 0 & 0 & 0 & 0.2534 & -0.2534 \end{vmatrix} \tag{5}$$

$$F = \begin{vmatrix} 0.2277 & -0.2277 & 0 & 0 & 0 & 0 \\ 0 & 0 & -0.1466 & 0 & 0 & 0 \\ 0 & 0 & 0 & -0.1978 & 0 & 0 \\ 0 & 0 & 0 & 0 & -0.2011 & 0 \\ 0 & 0 & 0 & 0 & 0 & -0.2534 \end{vmatrix} \tag{6}$$

The square roots of the imaginary axis of this object are on the verge of stability. This conclusion is due to the fact that the real part is equal to zero [37].

In order to construct the observation matrix Nk we shall use the following method: using the ctrb function, the input parameters of which are matrices A and B. We use the built-in rank function for determining the rank of the matrix Nk: Nk = ctrb (A, B), rank (Nk). The rank of the matrix is equal to 5. Since the rank of the matrix coincides with the dimensionality of the state spaces, the object is completely observable [39].

Results and discussion

Mathematical model of five-body evaporator plant

In the process of development of the automation system, the main inconvenience is that there are often no clear channels of control and perturbation in the mathematical models of the evaporator plant (Figure 2).

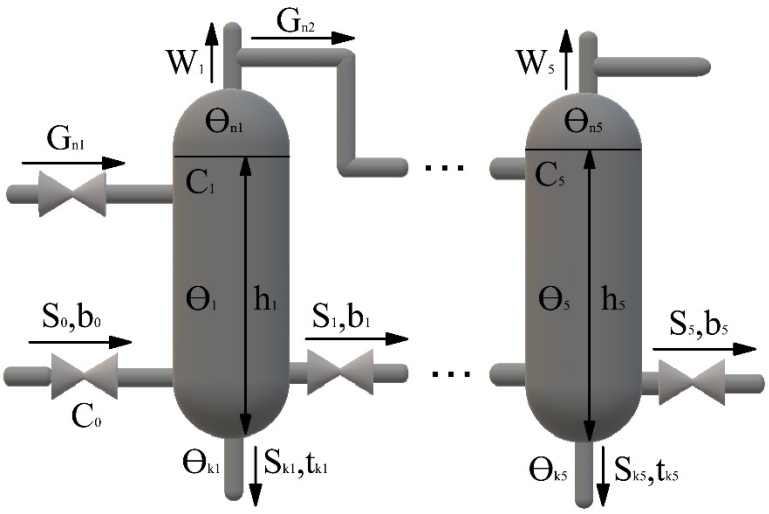

Figure 2. Mathematical model of evaporator plant:

Θ_i – the temperature of the boiling juice in the i-th body BC [°C];
i = 0–5 – corresponds to the number of body BC;
Θ_{ni} – steam temperature in the i-body of the evaporator plant [°C];
h_i– the level of juice, respectively, in the i-th body BC [m,% to the length of the tubes of the surface of the heating];
S_0,S_1,S_2,S_3,S_4,S_5– inflow of juice into the I body, an outflow of juice from the I body and an inflow into the II body, an outflow from the II body and an inflow into the III body, an outflow from the III body and an inflow into the IV body, an outflow from the IV body and an inflow into the V body, an outflow from V body accordingly [kg/f];
W_i – the flow of steam generated in the i-th body of the evaporator plant [kg/f];
G_{ni} – consumption of heating steam in the i-th case BC [kg/f];
b_i – concentration of dry matter in the i-body of the evaporator plant [%];
S_{ki}- – the flow of condensate in the i-th body of the evaporator plant [kg/f];
Θ_{ki} – condensate temperature in the i-th body BC [°C];
C_i – the content of sucrose in juice in the i-th body BC [%].

The indicated system was divided into subsystems. They are connected by essential links between variables, regulated by a similar scheme and described by mathematical models that are similar in structure.

Figure 3 shows a simplified parametric scheme for installing an evaporator plant with assigned subsystems [37].

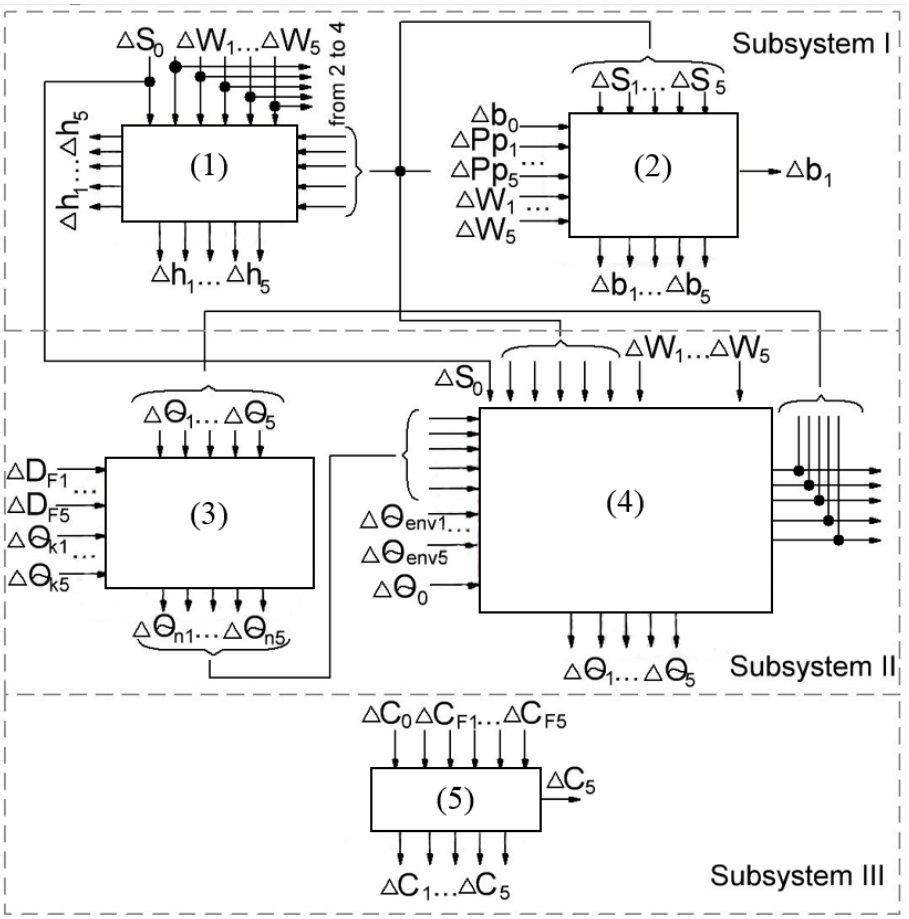

Figure 3. Parametric scheme of evaporator plant
equations describing the levels according to the bodies of the evaporator plant (7)

Below are indicated the differential equations for each of the subsystems of the nominal mode:

subsystem I:

$$\begin{cases} 4{,}391\dfrac{\partial(\Delta h_1)}{\partial t} = \Delta S_0 - \Delta S_1 - \Delta W_1, \\ 6{,}820\dfrac{\partial(\Delta h_2)}{\partial t} = \Delta S_1 - \Delta S_2 - \Delta W_2, \\ 5{,}056\dfrac{\partial(\Delta h_3)}{\partial t} = \Delta S_2 - \Delta S_3 - \Delta W_3, \\ 4{,}973\dfrac{\partial(\Delta h_4)}{\partial t} = \Delta S_3 - \Delta S_4 - \Delta W_4, \\ 3{,}974\dfrac{\partial(\Delta h_4)}{\partial t} = \Delta S_4 - \Delta S_5 - \Delta W_5. \end{cases} \quad (7)$$

$$\begin{cases} 187{,}34\dfrac{\partial(\Delta b_1)}{\partial t}+\Delta b_1=-0{,}2\Delta S_0+1{,}38\Delta b_0+0{,}72\Delta W_1-0{,}04\Delta Pp_1, \\ 589{,}17\dfrac{\partial(\Delta b_2)}{\partial t}+\Delta b_2=0{,}8\Delta S_1+1{,}67\Delta b_1+2\Delta W_2-0{,}066\Delta Pp_2, \\ 655{,}43\dfrac{\partial(\Delta b_3)}{\partial t}+\Delta b_3=-1{,}5\Delta S_2+1{,}5\Delta b_2+4{,}49\Delta W_3-0{,}1\Delta Pp_3, \\ 1131{,}42\dfrac{\partial(\Delta b_4)}{\partial t}+\Delta b_4=-1{,}67\Delta S_3+1{,}29\Delta b_3+7{,}46\Delta W_4-0{,}13\Delta Pp_4, \\ 853{,}1\dfrac{\partial(\Delta b_5)}{\partial t}+\Delta b_5=-1{,}01\Delta S_4+1{,}12\Delta b_4+9{,}37\Delta W_5-0{,}14\Delta Pp_5. \end{cases} \quad (8)$$

equations describing concentrations according to bodies of evaporator plants, where Ppi – loss of sugar during thermal decomposition in the i-th plant (8);

subsystem II:

$$\begin{cases} 13{,}89\dfrac{\partial(\Delta\Theta_1)}{\partial t}+\Delta\Theta_1=0{,}1868\Delta S_0+0{,}0482\Delta\Theta_0+0{,}9999\Delta\Theta_{n1}+ \\ \qquad +6{,}50\cdot10^{-6}\Delta\Theta_{env1}-0{,}1792\Delta S_1-0{,}9251\Delta W_1, \\ 21{,}78\dfrac{\partial(\Delta\Theta_2)}{\partial t}+\Delta\Theta_2=0{,}1620\Delta S_1+0{,}0315\Delta\Theta_1+0{,}9826\Delta\Theta_{n2}+ \\ \qquad +8{,}42\cdot10^{-6}\Delta\Theta_{env2}-0{,}1394\Delta S_2-0{,}8362\Delta W_2, \\ 22{,}50\dfrac{\partial(\Delta\Theta_3)}{\partial t}+\Delta\Theta_3=0{,}2136\Delta S_2+0{,}0266\Delta\Theta_2+0{,}9839\Delta\Theta_{n3}+ \\ \qquad +8{,}98\cdot10^{-6}\Delta\Theta_{env3}-0{,}1794\Delta S_3-1{,}28\Delta W_3, \\ 35{,}97\dfrac{\partial(\Delta\Theta_4)}{\partial t}+\Delta\Theta_4=0{,}2948\Delta S_3+0{,}0264\Delta\Theta_3+0{,}9815\Delta\Theta_{n4}+ \\ \qquad +1{,}45\cdot10^{-6}\Delta\Theta_{env4}-0{,}242\Delta S_4-2{,}1\Delta W_4, \\ 45{,}10\dfrac{\partial(\Delta\Theta_5)}{\partial t}+\Delta\Theta_5=0{,}4905\Delta S_4+0{,}0374\Delta\Theta_4+0{,}9704\Delta\Theta_{n5}+ \\ \qquad +2{,}58\cdot10^{-6}\Delta\Theta_{env5}-0{,}386\Delta S_5-4{,}26\Delta W_5. \end{cases} \quad (9)$$

equation (9) describes the temperature of the steam-juice mixture on the bodies of the evaporator plant, where Θ_{envi} – heat loss in the environment in the i-th device [°C].

$$\begin{cases} 7{,}07\dfrac{\partial(\Delta\Theta_{n1})}{\partial t}+\Delta\Theta_{n1}=0{,}7229\Delta G_{n1}+\Delta\Theta_1-0{,}0146\Delta\Theta_{k1}- \\ \qquad -0{,}9251\Delta D_{F1}, \\ 9{,}025\dfrac{\partial(\Delta\Theta_{n2})}{\partial t}+\Delta\Theta_{n2}=\Delta\Theta_2-0{,}076\Delta\Theta_{k2}-0{,}851\Delta D_{F2}, \\ 8{,}04\dfrac{\partial(\Delta\Theta_{n3})}{\partial t}+\Delta\Theta_{n3}=\Delta\Theta_3-0{,}0153\Delta\Theta_{k3}-1{,}3\Delta D_{F3}, \\ 13{,}19\dfrac{\partial(\Delta\Theta_4)}{\partial t}+\Delta\Theta_{n4}=\Delta\Theta_4-0{,}0138\Delta\Theta_{k4}-2{,}1445\Delta D_{F4}, \\ 14{,}28\dfrac{\partial(\Delta\Theta_5)}{\partial t}+\Delta\Theta_{n5}=\Delta\Theta_5-0{,}094\Delta\Theta_{k5}-4{,}4\Delta D_{F5}. \end{cases} \quad (10)$$

Equations (10) describe steam temperature according to bodies of evaporator plants, where D_{Fi} – the consumption of non-condensed gases in the i-th plant, subsystem III

$$\begin{cases} 398{,}59\dfrac{\partial(\Delta C_1)}{\partial t}+\Delta C_1 = 1{,}38\Delta C_0 - 0{,}04\Delta C_{F1}, \\ 753{,}49\dfrac{\partial(\Delta C_2)}{\partial t}+\Delta C_2 = 1{,}67\Delta C_1 - 0{,}04\Delta C_{F2}, \\ 1399{,}89\dfrac{\partial(\Delta C_3)}{\partial t}+\Delta C_3 = 1{,}5\Delta C_2 - 0{,}1\Delta C_{F3}, \\ 1948{,}73\dfrac{\partial(\Delta C_4)}{\partial t}+\Delta C_4 = 1{,}29\Delta C_3 - 0{,}13\Delta C_{F4}, \\ 1523{,}92\dfrac{\partial(\Delta C_5)}{\partial t}+\Delta C_5 = 1{,}12\Delta C_4 - 0{,}14\Delta C_{F5}, \end{cases} \quad (11)$$

equations (11) describe content of sucrose according to bodies of evaporator plant, where C_{Fi} – the amount of sucrose that decomposed in the i-th plant. For subsystem III, the creation of an optimal regulator is impossible, due to the fact that it contains only coordinates of disturbances and states. That is, the subsystem is uncontrolled. Practically, only the content of sucrose C_5 in the fifth body of the evaporator plant is controlled [37].

In order to calculate the amplification matrix of the regulator K using the algorithm of the modulator, one shall use the built-in library function place (p1 = 0,0003), the input parameters for which are the matrices A and B, and the result is the synthesized matrix K. The pzmap function shall be used for constructing the roots of a closed system, the input parameter for which is an object in the space of the variables of the state of ss-type, which is given using the ss format function: sys=ss(A_sys,F,C,D) (Figure 4.).

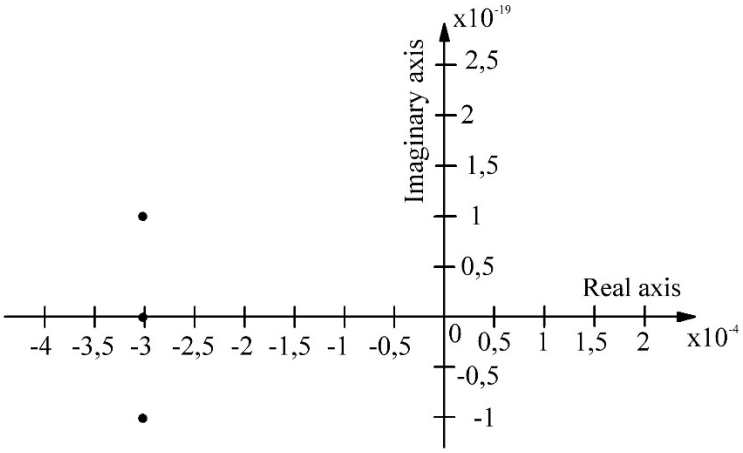

Figure 4. Pole-zero map for T=10000

Consequently, the closed system is stable, since the poles are located in the left half-plane of the complex plane.

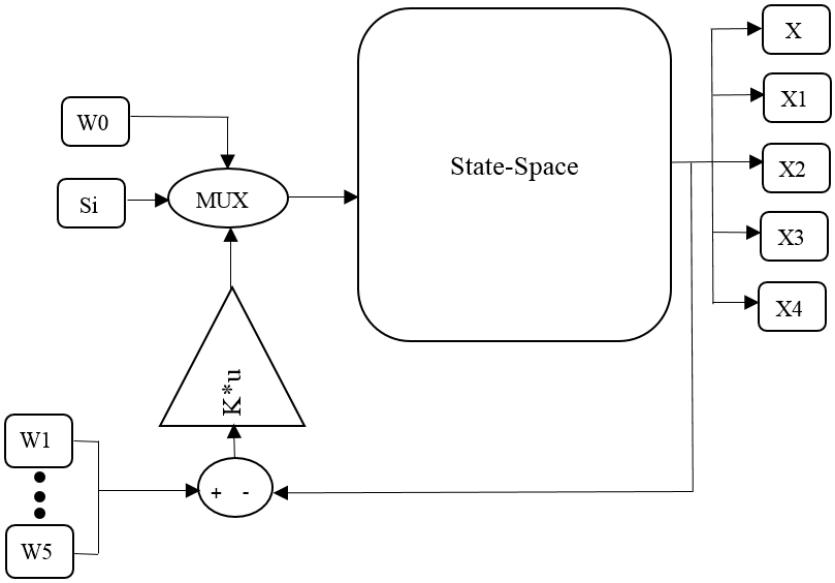

Figure 5. The schematic scheme of an object in the Simulink environment

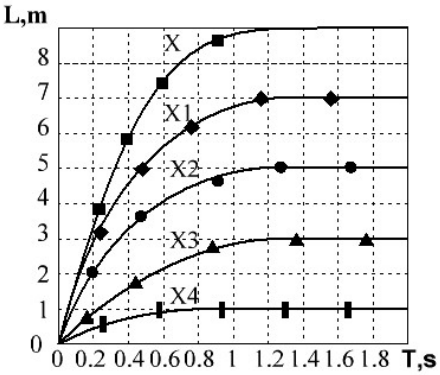

X – level tank I,
X1 – level tank II,
X2 – level tank III,
X3 – level tank IV,
X4 – level tank V.

Figure 6. Transition process via channels

Mathematic model with PID-regulator

Further on, in the Simulink environment, one shall use the State-Space block to enter an object in the space of the state variables in order to construct a schematic diagram of an object with a matrix regulator (Figure 5.). Due to the fact that the inputs and outputs of the State-Space block are vectors; it is additionally necessary to use the Mux and Demux blocks. The Step blocks are used for the task signals. The Initial conditions option in the State-Space object block is used for constructing the transient processes relative to initial deviations. The results for the task change are shown in Figure 6 [40].

The mathematical model with the PID regulator is shown in Figure 7.

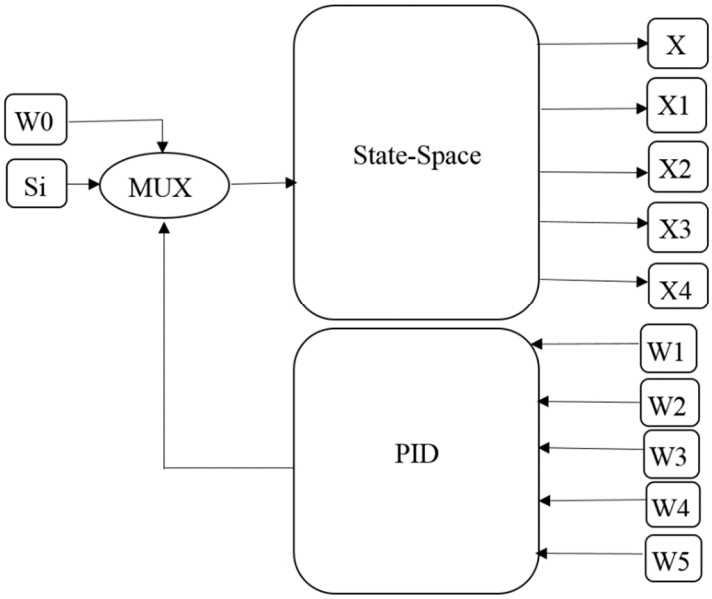

Figure 7. Mathematic model with PID-regulator

The settings for the regulator shall be calculated in the Matlab system:

By the channel X: proportional link: 1.36; integral: 0.08; differential: 0.95; by the channel X1: proportional: 4.85; integral: 0.64; differential: 1.47; by the channel X2: proportional: 0.65; integral: 0.02; differential: 0.12; by the channel X3: proportional: 2.38; integral: 0.21; differential: 0.9; by the channel X4: proportional: 2.99; integral: 0.42; differential: 0.7;

The transition process for each adjustment channel is shown in Figure 8.

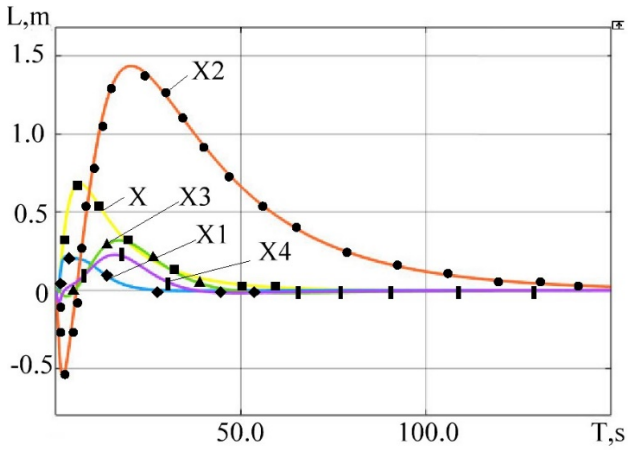

X – level tank I,
X1 – level tank II,
X2 – level tank III,
X3 – level tank IV,
X4 – level tank V

Figure 8. Transition process via channels

.

Mathematic model with fuzzy regulator

A mathematical model with a fuzzy regulator is shown in Figure 9.

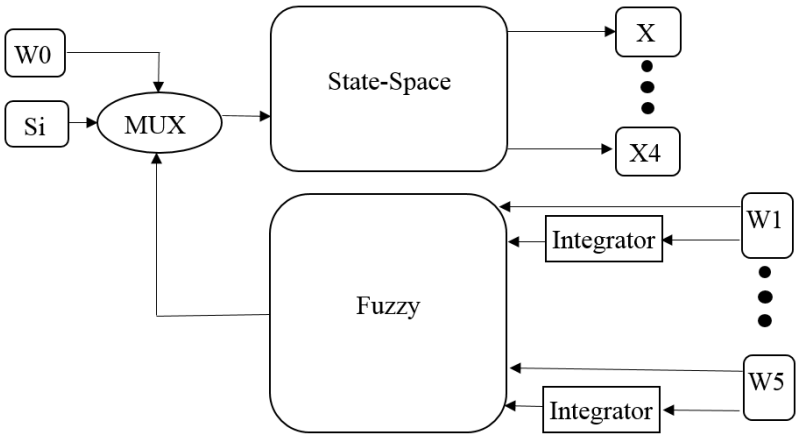

Figure 9. Mathematic model with fuzzy regulator

Setting of the fuzzy level regulator in body II is shown in Figures 10-11.

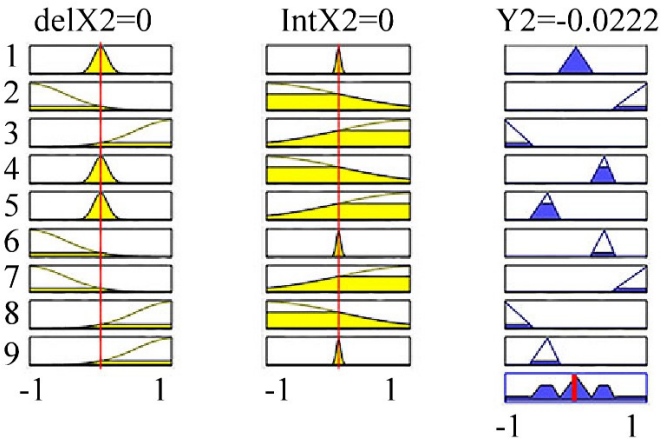

Figure 10. Graphical representation of the operation of the fuzzy conclusion algorithm: delX2 – proportional term; IntX2 – integral term; Y2 – result.

Similar settings are for other fuzzy regulators. Transition processes for each adjustment channel are shown in Figure 12.

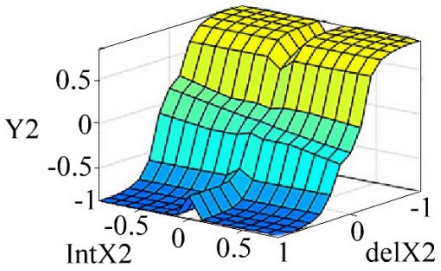

Figure 11. Reflecting surface of the response of the fuzzy algorithm: delX2 – proportional term; IntX2 – integral term; Y2 – result.

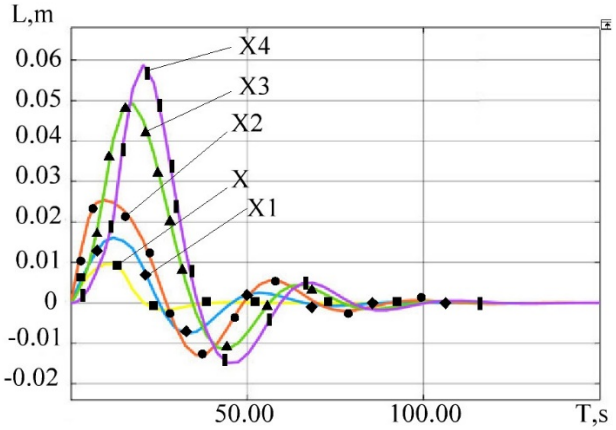

X – level tank I,
X1 – level tank II,
X2 – level tank III,
X3 – level tank IV,
X4 – level tank V.

Figure 12. Transition process via channels

Due to the aforementioned facts, it can be concluded that the use of a fuzzy regulator along the channel X gives a shorter time of the transient process (from 75 seconds with the use of the PID regulator to 55 seconds with the use of a fuzzy regulator) and a significant decrease in the amplitude of oscillations (from 0.68 m when using the PID regulator to 0.001 m using a fuzzy regulator). When comparing PID and fuzzy regulators along the X1 channel (Figure 13), one can see that using a fuzzy regulator one can receive a significant decrease in the amplitude of oscillations (from 0.6 m using the PID regulator to 0.016 m using a fuzzy regulator). When comparing PID and fuzzy regulators along the channel X2 it can be seen that the use of a fuzzy regulator allows for higher quality and shorter transition time (from 140s when using the PID regulator to 110 s using a fuzzy regulator), a significant decrease in the oscillation amplitude (from 1.3 m using the PID regulator to 0.025 m using a fuzzy regulator).

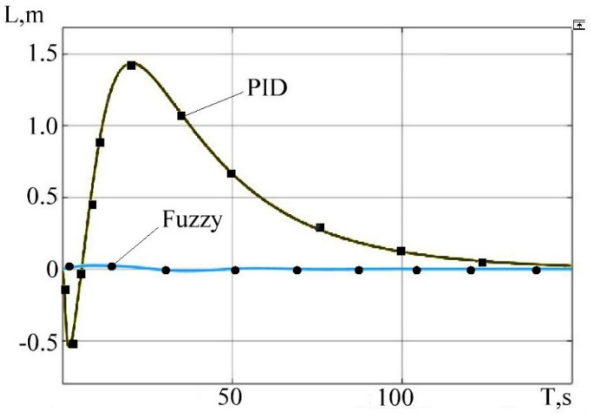

Figure 13. Transient processes of the operation of PID and fuzzy regulators (■ – for PID, ● – for Fuzzy)

Similarly, when comparing PID and fuzzy regulators along the X3 channel, it can be seen that the use of a fuzzy regulator allows for a shorter transition time (from 145 s when using the PID regulator to 110 s when using a fuzzy regulator) and a significant decrease in the amplitude of oscillations (from 0.25 m using the PID regulator to 0.05 m using a fuzzy regulator). When comparing PID and fuzzy regulators along the channel X4, it can be seen that when using a fuzzy regulator, one receives a significant decrease in the amplitude of oscillations (from 0.2 m when using the PID regulator to 0.06 m using a fuzzy regulator).

Conclusion

In order to increase the efficiency of the functioning of the automation system in this study, it was suggested to research how the use of neuro-fuzzy regulators in the control system of the evaporator plant will improve the quality parameters of the regulation process; since a number of problems will arise in case of failure to comply with the optimal mode during the process of evaporation. In this study, a comparison between PID and fuzzy regulator was made. The research was conducted in order to determine if a regulator type is used for achieving higher levels of quality of control of evaporator plant. The first step was the development of a mathematical model in the state space in Matlab environment (Figure 5). Figure 6 indicates transition processes when changing the task, it can be said that the transition time in the range from 0.8 to 1.2 seconds, which is a good result, but the values of the deviation of the levels in the cases for the evaporation process are too high (9 m according to channel X, 7 m according to channel X1, 5 m according to channel X2, 3 m according to channel X3 and 1 m according to channel X4). The next step was the development of a mathematical model with the PID regulator (Figure 7). Transition processes for control loops in all five control channels were obtained as a result of the simulation (Figure 8). In this case, the time of transitions is in the range of 60 seconds according to channel X1 to 145 seconds according to channel X2. Consequently, the time of regulation has increased in relation to the previous experiment, but this led to a significant decrease in the deviations of levels in the cases (0.68 m according to channel X, 0.6 m according to channel X1, 1.3 m according to channel X2, 0.25 m according to channel X3 and 0.2 m according to channel X4). Then a

mathematical model with a fuzzy regulator was developed (Figure 9). Transition processes for control circuits in all control channels were obtained during the simulation (Figure 12). In this case, the time of transition processes is in the range from 50 seconds along the channel X1 to 110 seconds along the channel X2, which is the best result compared to the PID regulator. Compared to the previous study, the levels in the cases also decreased significantly (0,001 m along the channel X, 0,016 m along the channel X1, 0,025 m along the channel X2, 0,05 m along the channel X3 and 0,06 m along the channel X4). Thus, comparing the control channels with the PID regulator and the fuzzy regulator (for example, Figure 13), one can see that the use of fuzzy regulation significantly increases the quality of transitions, namely: in all cases, the amplitude of oscillation decreases and in almost all cases the time of the transition process decreases. Taking into account the aforementioned facts, it is obvious that the use of neuro-fuzzy regulators is more appropriate, because it results in better quality control parameters compared to the system with PID regulators.

References

1. Skakovskij Yu., Babkov. A., Mandro O. (2018), Modernizaciya strukturi sistemi keruvannya viparnoyi stancziyi buryakoczukrovogo zavodu na bazi mikroproczesornikh tekhnichnikh zasobiv i program ukrayinskogo virobnicztva, *Automation of technological and business processes*, 10(2), DOI: 10.15673/atbp.v10i2.972, pp. 14-15.
2. Markitan S.V. (2001), Puti povysheniya tekhniko-ekonomicheskikh pokazatelej teplovykh skhem sakharnykh zavodov*, Czukor Ukrayini*, 5, pp.6–7.
3. Shtanheiev K. O. (2015), *Purpose installations and thermal schemes of sugar factories*, UNIDO, pp. 5-6.
4. Shtangeyev K.O., Khristenko V.I. (2002), Pro raczionalne vikoristannya pari v czukrovomu virobnicztvi, *Czukor Ukrayini*, 2, pp. 2-3.
5. Hrama M., Sidletskyi V., Elperin I. (2019), *Comparison between PID and fuzzy regulator for control evaporator plants, 2019 IEEE 39th International Conference on electronics and nanotechnology (ELNANO), Conference proceedings*, pp. 54–59.
6. Leviczkij Ya.G., Dmitruk A.P., Chernyakhovskij I.B. (2001), Opyt Chortkovskogo sakharnogo zavoda po snizheniyu raskhoda topliva, Czukor Ukrayini, 5, pp.19–20.
7. Chantasiriwan S. (2017), Distribution of juice heater surface for optimum performance of evaporation process in raw sugar manufacturing, *Journal of Food Engineering*, 195, pp. 21–30.
8. Verma O.P., Manik G., and Jain V. K. (2018), Simulation and control of a complex nonlinear dynamic behavior of multi–stage evaporator using PID and Fuzzy–PID controllers, *Journal of Computational Science*, 25, pp. 238–251.
9. Chowdhury J., Nguyen B., and Thornhill D. (2015), Modelling of Evaporator in Waste Heat Recovery System using Finite Volume Method and Fuzzy Technique, *Energies*, 8, 12, pp. 14078–14097.
10. Jolly P.G., Tso C. P., Chia P.K., and Wong Y. W. (2000), Intelligent Control to Reduce Superheat Hunting and Optimize Evaporator Performance in Container Refrigeration, *HVAC&R Research*, 6, 3, pp. 243–255.
11. Lahtinen S. (2001), Identification of fuzzy controller for use with a falling–film evaporator, *Food Control*, 12, 3, pp. 175–180.
12. Tang K. S., Kim Fung Man, Guanrong Chen, and Kwong S. (2001) An optimal fuzzy PID controller, *IEEE Transactions on Industrial Electronics*, 48, 4, pp. 757–765.

13. Carvajal J., (2000) Fuzzy PID controller: Design, performance evaluation, and stability analysis, *Information Sciences*, 123, 3–4, pp. 249–270.
14. Sidletskyi V.M., Elperin I.V., Polupan V.V. (2016), Analiz ne vymiriuvalnykh parametriv na rivni rozpodilenoho keruvannia dlia avtomatyzovanoi systemy, obiektiv i kompleksiv kharchovoi promyslovosti, *Naukovi pratsi Natsionalnoho universytetu kharchovykh tekhnolohi*i, 22(3), pp. 7–15.
15. Lapin M.V., Sidletskyi V.M. (2016), Vykorystannia system nechitkoi lohiky dlia dynamichnoho upravlinnia potuzhnistiu parovykh kotloahrehativ, *Naukovi pratsi Natsionalnoho universytetu kharchovykh tekhnolohii*, 22(4), pp. 24 – 31.
16. González–Potes A., Mata–López W., Ochoa–Brust A., and Escobar–del Pozo C. (2016), Smart Control of Multiple Evaporator Systems with Wireless Sensor and Actuator Networks, Energies, 9, 3, pp.142-143.
17. Zhang J., Zhang W., Hou G. (2011), Design of evaporator control system using fuzzy sliding mode controller, *The 2011 Internati onal Conference on Advanced Mechatronic Systems*, pp. 510–512.
18. Liu T., Wang Y., Yang X. (2013), Optimal fuzzy control of electronic expansion valve–evaporator system, *BioTechnology: An Indian Journal*, pp. 586 – 589.
19. Bao–hua Z. (2005), Simulation and analysis of evaporator superheat electronic expansion valve fuzzy control, *Energy Research and Utilization*, pp. 4 – 5.
20. Xiao-yang H. (2007), Fuzzy control for superheat of evaporator based on variable–universe method, *Journal of Guangxi University of Technology*, pp. 7 – 9.
21. Normey–Rico J. E., Merino A., Cristea S., and de Prada C. (2005), Robust dead–time compensation of an evaporation process in sugar production, *IFAC Proceedings Volumes*, 38(1), pp. 460–465.
22. Lavarack B.P., Hodgson J. J., Venning J. (2004), Improving the energy efficiency of sugar factories: Case study for Pioneer Mill, *International Sugar Journal*, 106(1266), pp. 337-342.
23. Roger K., Sparr E., Wennerström H. (2018), Evaporation, diffusion and self–assembly at drying interfaces, *Physical Chemistry Chemical Physics*, 20(15), pp. 10430–10438.
24. Srivastava D., Mohanty B., Bhargava R. (2013), Modeling and simulation of mee system used in the sugar industry, *Chemical Engineering Communications*, 200(8), pp. 1089–1101.
25. Patan K. and Parisini T. (2005) Identification of neural dynamic models for fault detection and isolation: the case of a real sugar evaporation process, *Journal of Process Control*, 15(1), pp. 67–79.
26. Merino A., Acebes L. F., Alves R., and de Prada C. (2018), Real Time Optimization for steam management in an evaporation section, *Control Engineering Practice*, 79, pp. 91–104.
27. Polupan V., Sidletskyi V. (2018), Genetic algorithm usage for optimization of saturator operation, *Ukrainian food journal*, 7(4), pp. 754–762.
28. Sidletskyi V., Korobiichuk I., Ladaniuk A., Elperin I., Rzeplińska–Rykała K. (2019), Development of the Structure of an Automated Control System Using Tensor Techniques for a Diffusion Station, AUTOMATION 2019, *Advances in Intelligent Systems and Computing*, pp. 175–185.
29. Khomichak L. (2007), *Peredovi tekhnologiyi virobnicztva czukru. Kharchova i pererobna promislovist: Shhomisyachnij naukovo–virobnichij zhurnal Derzhpromu*, Nacz. Universitetu kharchovikh tekhnologij ta TOV "Ukragropak", 4, pp. 20–23.
30. Borysyuk P.G. (2011), Some features of sugar market, *Tsukrovi buryaky*, 1, pp.4–5.

31. Krasnyak O.P. (2012), Trends of sugar market development in Ukraine: problems and prospects, *Zbirnyk naukovyh pratz Tavriyskogo derzhavnogo agrotehnologichnogo universytetu (ekonomichni nauky)*, 2(18), pp.261–269
32. Bondar V.S. (2010), Price trends on a world market of sugar and their influence on a domestic market of Ukraine, *Tsukrovi buryaky*, Available at: http://www.sugarbeet.org.ua/node/83 (Accessed 14 September 2013), pp. 9–10
33. Mudrak P.V. (2011), Price factors on a sugar market in a context of food security providing, *Naukovi pratsi Poltavskoyi derzhavnoyi akademiyi*, 2, pp.160–167.
34. Jantzen J. (2007), Foundations of Fuzzy Control, Wiley, pp. 152–153.
35. Besekerskij V.A., Popov E.P. (2003), Teoriya sistem avtomaticheskogo upravleniya, St. Petersburg, pp. 524–526.
36. Polupanov A.V., Romanov A.V., Frolov Yu.M. (2005), Synthesis of systems using modal control, Trudy Vserossijskoj studencheskoj nauchno-tekhnicheskoj konferenczii, *Prikladnye zadachi elektromekhaniki, energetiki, elektroniki*, pp. 134–137.
37. Lutskaya N.M., Vlasenko L.O. (2013), Development of multidimensional optimal controllers for sugarmill evaporation plant which operates in interval indetermination conditions, *Naukovi pratsi Natsionalnoho universytetu kharchovykh tekhnolohii*, 52, pp. 48–61.
38. Gardner E. S. (2006), Exponential smoothing: the state of the art – part II, *International Journal of Forecasting*, 22 (4), pp. 637–666.
39. Hyndman Rob J., Khandakar Yeasmin (2008), Automatic Time Series Forecasting, The forecast Package for R, *Journal of Statistical Software*, 27(3), pp. 1–22.
40. Hyndman Rob J., Koehler Anne B., Ord J. Keith, Snyder Ralph D. (2006), *Forecasting with Exponential Smoothing: the state space approach*, Springer-Verlag Berlin Heidelberg, pp. 17–18.

Influence of shungite treatment methods on its absorption properties and on water treatment quality for beverages production

Svitlana Oliynyk[1], Lyudmila Mel'nyk[1], Iryna Samchenko[1], Natalia Tkachuk[1], Olga Loginova[2], Ludmyla Kisterska[2]

1 – National University of Food Technology, Kyiv, Ukraine
2 – V. Bakul Institute of Superhard Materials, National Academy of Sciences of Ukraine, Kyiv, Ukraine

Keywords:

Water
Treatment
Shungit
Absorption
Nanosilver

Article history:

Received 11.04.2019
Received in revised form 18.09.2019
Accepted 28.11.2019

Corresponding author:

Natalia Tkachuk
E-mail: tkachuk2008@bigmir.net

DOI:
10.24263/2304-974X-2019-8-4-18

Abstract

Introduction. The prospect of treating shungite in various ways to increase its absorption properties and increase the efficiency of water treatment during beverage production is shown.

Materials and methods. Drinking water was prepared using shungite activated, activated and modified by nanosilver, activated, steam treated and modified by nanosilver. Photometric, spectrometric, chemical and potentiometric methods of analysis, theoretical generalization and comparison, a systematic approach were used in the work.

Results and discussion. The parameters of aggregation of nanoparticles in water-glycerol medium, adsorption and sorption-catalytic properties of shungite activated and nanomodified in various ways are investigated.

Additional treatment of activated shungite with steam and nanosilver allows to increase its adsorption activity for iodine and for adsorption of acetic acid, alkalinity of water infusion up to 1.2 times and to provide stabilization of the redox potential of the prepared water at the level of + 90–100 mV.

Steam treatment enhances part of the pores before diffusion and molecular sorption, and increases the adsorption activity of humic and fulvic acids by 40% by activated steam and silver nanoparticles by 40%.

Waste water costs during the preparation of activated steam and nanosilver shungite do not exceed 20 relative volumes of wash water per volume of material, allowing the transparency of the prepared water is at least 99%.

Pre-treatment shungite of steam before its activation with silver nanoparticles due to improving the wetting of the surface makes it possible to increase the duration of the filter cycle and the possibility of deepening the sorption of harmful water impurities: iron, manganese, nitrogen and organic compounds by 10–12%.

Conclusions The use of shungite activated steam treated and modified by nanosilver provides increased efficiency of cleaning of harmful impurities and stabilization of the redox potential of the prepared water.

Introduction

The production of beverages involves the use of high quality prepared water, which has additional requirements that are related to the peculiarities of the technology of preparation, shelf life and finished product destination [1]. The use of silver instead of the harmful chemicals (fluorine, chlorine and chlorine-containing compounds) makes water not only safe (it has been proved [2] that silver ions kill the vast majority of harmful microorganisms) but also beneficial as in absence of harmful microorganisms the color, smell and taste of water is much better [3].

Nowadays considerable scientific and applied interests are the possibility of using effective natural adsorbents in water purification processes [4]. One of the most promising materials is shungitis [5]. Shungite is a natural material–a rock that has the composition similar to anthracite and graphite [6]. The use of shungite in water treatment as a filter material is due to its high adsorption capacity [7], corrosion resistance [8], catalytic activity [9], low cost [10], ecological purity and safety [11]. The main properties of shungite are described in [12-15]. Mosin O. [6,8,16], Mel'nyk L. [7], Mukhin V. [17], Wang S. [18], and other researchers have shown the prospect of using shungite as a filter material in water treatment for the food industry [19,20], in different types of soft drinks production [21,22] and established the efficiency of purification from mineral impurities [7].

During the vodka preparation it was proposed to use a method of purifying water by sequential filtration through shungite and zeolite, followed by passing through a column of shungite. According to the authors, "the presence of shungite in the charge of the zeolite leads to a decrease in the alkalinity of water and the transition of pH to the neutral acid part", which increases the tasting evaluation of finished products [8].

Recently, more and more attention is being paid to water treatment methods that would help stabilize the water oxidation–reduction potential [24].

The method of metal cathode dispersing by the localized glow discharge in vacuum has developed an innovative one-stage combined "wet-dry" technology for the production of concentrated colloidal solutions of nano metals in liquid media of different physical and chemical nature, which allowed to create ready-to-use nanosilver suspension in food glycerol. The undeniable advantages of high-purity nanosilver, physically implanted into food glycerol and stabilized in it without additional chemical reagents, are exceptionally low toxicity to humans and animals along with high bactericidal properties, the method demonstrate high industrial productivity and a competitive price in comparison to European and world analogs [26].

The studies aimed at the simultaneous regulation the water oxidation–reduction potential and the harmful impurities removal are especially important [27]. Thus, research aimed at using natural shungite modified by nanosilver for water treatment technologies is necessary and relevant.

The provided studies were concentrated of water oxidation–reduction potential change true nature and the quantitative characteristics of the water preparation during its sorption purification using shungite treated in various ways: activation; treatment with nanosilver, without it and with steam pre-treatment. The main tasks of the research were: determination of the adsorption and sorption-catalytic properties of the shungite treated in various ways to stabilize the of water oxidation–reduction potential, the efficiency of its purification from high- and low-molecular organic compounds and toxic substances, compliance with the requirements of current regulatory standards for soft beverages.

Materials and methods

Materials under study

1. Drinking water of the Kyiv Artesian well and treated water,
2. Naturally activated specimens of shungite of the Zagozhin deposit (1.0 mm fraction).

Preparation of prototypes

Activation of natural shungite was carried out at a temperature of 150–180 °C during 2 hours. Further 100 g of the appropriate sample of shungite was loaded into a glass column, washed with distilled water to achieve the filtrate transparency at least 98% [15].

The modification of shungite by nanosilver was carried out by adsorption from solutions after sieving without pre-washing with distilled water and after pretreatment with the appropriate steam sample. The silver nanosuspension produced using ion-plasma technology at a pilot plant was used to modify the shungite. A detailed description of the methodology and installation for silver nanosuspension manufacturing is given in article [25].

To study the state and parameters of nanoparticle aggregation in aqueous-glycerol medium, the resulting suspension was irradiated with a helium-neon laser with X = 633 nm, scattered light which was recorded at an angle of 173° [28]. The absorption spectra were measured in a cuvette (1 cm) before and after ultrasound. Distribution of silver nanoparticles in solution before and after treatment and in triplicate repetition with different nanoparticle concentration was defined by laser photon correlation spectroscopy [28] on Zeta Sizer Nano S instrument (Malvern, UK) at 25 °C. The kinematic viscosity of the suspensions required to calculate the nanoparticle size distribution was measured on a Malvern SV-10 (Japan) vibration viscometer [28].

To evaluate the stability of the formed silver agglomerates in glycerol, the distribution of silver nanoparticles in solution before and after ultrasonic treatment and in three-fold repeatability with different nanoparticle concentrations was investigated [28]. Marking of the samples was as follows: 1.0–initial suspension of silver nanoparticles in glycerol, 1.1–diluted suspension in 2 times, 1.2–diluted suspension in 10 times.

Procedure of research conducting

Water filtration was carried out at temperatures from 18 to 22 °C in dynamic mode for three glass filters with a diameter of 50 mm. Each filter was filled up with a corresponding sample of shungite layer with a height of 500 mm each.

The process of sorption purification of water included the preparation of the material for operation, such as pre-washing before the filter cycle and the basic filter cycle.

Preparation of the material for work, the main filtering cycle through an appropriate sample of shungite was carried out by gravity from top to bottom of the filter at a speed of 10-12 m/h. Organoleptic and physic-chemical parameters of the prepared water were determined after every 500 cm^3 of the filtrate.

Description of methods

During the research, the adsorption characteristics of the shungite samples were determined by the methods used during the incoming control in the hard liquors distillery: total pore volume for water [29], adsorption activity for: iodine [29], alkalinity of water

infusion and adsorption of acetic acid [29], acid-base properties of water infusion and humic and fulvic acids [29].

Studies of water quality before and after its purification with a suitable sample of shungite were performed:

- Colorimetric method using the photoelectric colorimeter KFK-2 in determining the mass concentration of iron, manganese, nitrogen-containing substances [29],
- Spectrophotometric method (spectrophotometer Specord UV) in determining transparency [29, 30];
- Permanganometric method for determining permanganate oxidation [29],
- Potentiometric (pH-meter + ORP-meter pH-099 and pH-150 MI) when determining the redox potential [31, 32].

Determination of water purification efficiency by a suitable sample of shungite was carried out by spectrophotometric method in the ultraviolet region of the spectrum at a wavelength of 200–350 nm and a cuvette of length S = 50 mm [29].

Processing of research results

Experimental, mathematical and statistical methods were used in the work-planning and processing of experimental results. The research results were systematized and processed using mathematical and statistical methods on the basis of modern software [29–31].

Results and discussion

Aggregation parameters of nanoparticles in aqueous-glycerol medium

Absorption spectra of solutions of silver nanoparticles in glycerol before and after ultrasonic treatment during 10 min. is given in Figure 1. As shown on Figure 1, the data shows that the solution absorption spectra retain their shape during the dilution, ie dilution of the solution with water does not lead to structural changes in the sample.

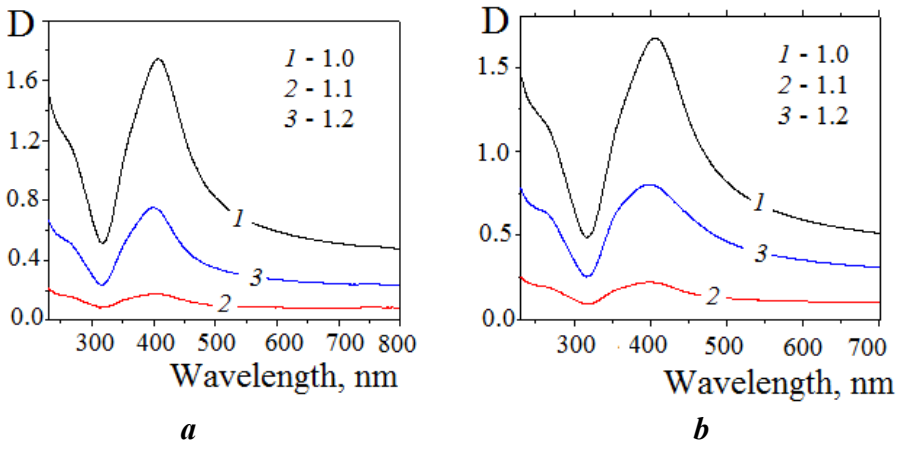

Figure 1. Absorption spectra of silver nanoparticles solutions in glycerol before (a) and after (b) ultrasonic treatment.

The distribution of silver nanoparticles before and after ultrasonic treatment is presented in Figure 2. As can be seen from Figure 2, the distribution of silver nanoparticles by size after ultrasonic treatment changes in the direction of a significant reduction in the size of agglomerates formed in solution (from almost 200 to 60 nm), that is, ultrasonic treatment of nanosilver solutions actively destroys agglomerates. This is the result we obtained earlier in article [26].

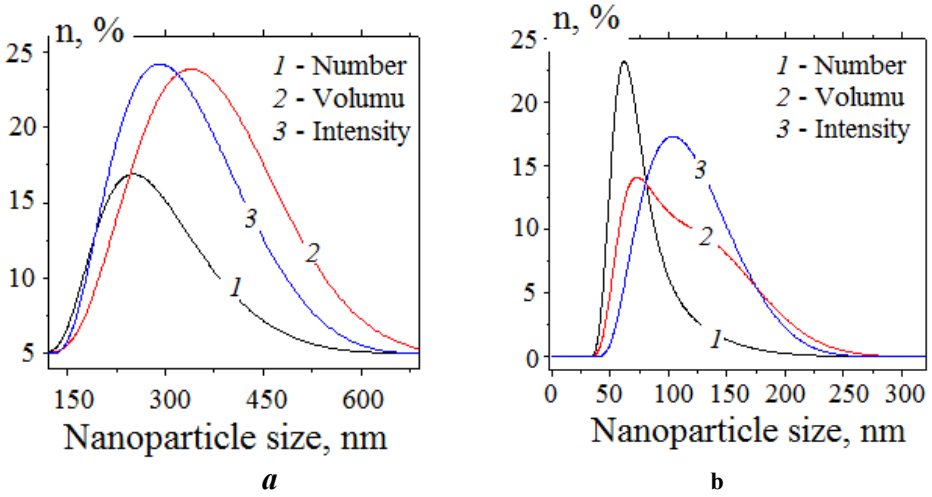

Figure 2. Distribution of silver nanoparticles in solution before (a) and after (b) ultrasonic treatment.

It is known that the aggregate stability of colloidal solutions (sols) is proportional to the charge of the colloidal particle, which is determined by the electrokinetic potential (ξ-potential). The ξ-potential arises on the slip plane of the double electric layer due to the separation of its diffuse part from the adsorbed bound fixed part, it determines the charge of the diffuse layer and is a measure of the intensity of electrokinetic phenomena in the interfacial region. The sign and value of the ξ-potential are widely used to characterize the electrical properties of a surface when considering adsorption, adhesion, aggregate stability of dispersed systems, structure formation in materials and in other processes where electrokinetic phenomena exist. The larger the ξ-potential of the system, the greater the value of the average electric charge of the colloidal particles. The presence of colloidal particles of the same charge leads to their mutual repulsion, preventing the possible sticking (agglomeration, aggregation) of the particles of the dispersed phase, informing the system of the aggregate stability.

The values of the size of silver nanoparticles and ξ-potential in the given suspensions are presented in Table 1. As can be seen from the data in Table 1, the aggregate stability of the original solution and diluted with water is stored at the level of 30–70 mV, ie after ultrasonic treatment, these solutions were stable at different dilutions. For theoretical limit of colloidal systems stability, the value of ξ – potential greater than 30 Mv is assumed [32,37].

Table 1

Value of the ξ-potential (mV) of silver nanoparticles in solutions

Sample	The value of the ξ-potential before ultrasonic treatment, mV	The value of the ξ-potential after ultrasonic treatment, mV
1.0	-65,2	-74,3
1.1	-11,5	-29,1
1.2	-51,5	-56,9

Sorption capacity of activated and modified nanosilver shungite

High-quality sorption-filtering material that can be used in water purification systems from high- and low-molecular-weight organic compounds and toxic substances for the soft drinks production should have high adsorption, sorption-catalytic properties, in addition to the optimal structure (Table 2).

The data shown in Table 2 proved that the modification of shungite by silver nanoparticles makes it possible to increase the total pore volume of water and the total volume of basic oxides by 1.2 times, thereby increasing its adsorption activity: iodine and acetic acid adsorption by 1.3 times, the alkalinity of the water infusion–2.0 times, which will contribute to a longer filter cycle and the possibility of in-depth sorption of harmful water impurities.

Table 1

Adsorption and sorption-catalytic properties of shungite treated in various ways

Indicator name	Indicator value for shungite sample		
	Activated	Activated and modified by nanosilver	Activated, Steam treated and modified by nanosilver
Total pore volume by water, cm^3/g	0,45	0,55	0,6
Total amount of oxides, mol/m^3:			
– acid	0,3	0,32	0,35
– basic	0,4	0,5	0,7
Adsorption activity by:			
– iodine,%	45	57	65
– alkalinity of water infusion, cm^3	2,5	5,0	5,8
– adsorption of acetic acid, cm^3	40	55	62

Pre-treatment with steam indicates the positivity of its application to the main stage of modification of shungite by nanosilver, resulting in an increase: total pore volume by 1.2 times, total volume of basic oxides by 1.4 times, indicators of adsorption activity for iodine, alkalinity of aqueous infusion and adsorption of acetic acid by 1.1–1.2 times. This is proved by the studies shown by us in article [7], that is, the adsorption activity of the steam-treated shungite increases by improving the wetting of the surface with aqueous solutions.

The presence of humic acids and fulvic acids significantly impairs the organoleptic characteristics of prepared water [1], so it was necessary to determine the adsorption activity for these substances. Figure 3 presents the adsorption activity of the samples by humic acids and fulvic acids. It is confirmed that, compared to activated shungite, the adsorption activity of nanosilver-treated shungite is higher by 25%, the adsorption activity of steam-treated and nanosilver-treated is higher by 40%.

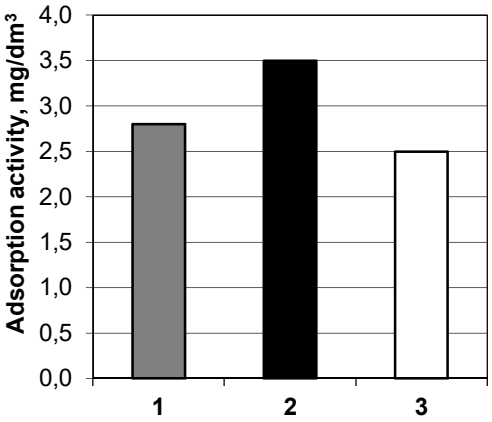

Figure 3. Shungite samples adsorption activity on humic and fulvic acids:
1 – shungite sample activated and modified by nanosilver;
2 – shungite sample activated, steam treated and modified by nanosilver;
3 – shungite sample activated.

This is due to the fact that the adsorption of humic and fulvic acids on shungite is carried out on the surface of the pores of the material, the effective diameter of which exceeds the size of their molecules contained in the solution. Thus, most of the pores treated with steam and treated with nanosilver are available in size for the diffusion of humic acid molecules, the absorption of humic and fulvic acids, as well as their salts, which is provided due to molecular sorption, as that was confirmed by the data obtained from carbonaceous materials [39].

The effectiveness of shungite samples washing at the stage of preparation for work was evaluated by the transparency indicator, which should not be less than 99%, according to the requirements of the current regulatory documents [1]. The analysis of the obtained data shows (Figure 4) that the consumption of flushing water at the stage of shungite preparation, to achieve standardized water transparency of 99% for shungite treated with steam and nanosilver is rising to 20 relative volumes of flushing water per volume of material. For activated shungite and nanosilver-treated shungite, there is an increase in the cost of flushing water, which will negatively affect the resource costs of production and will increase the cost

of water treatment, which was confirmed by other researchers [1,4]. It is possible to conclude from the given data that to reduce the consumption of flushing water at the preparatory stage, before further processing of shungite with silver, shungite must be activated and treated with steam.

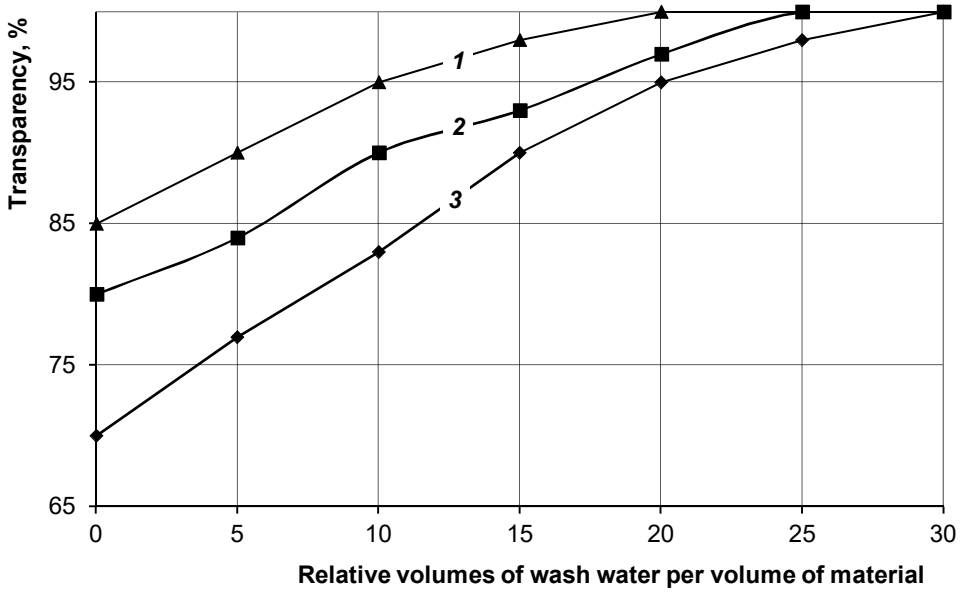

Figure 4. The consumption of flushing water at the stage of shungite preparation:
1 – shungite sample activated, steam treated and modified by nanosilver;
2 – shungite sample activated;
3 – shungite sample activated and modified by nanosilver.

During the production of beverages, a particular attention is paid to the value of permanganate oxidation, which characterizes the content of organic compounds in the prepared water, as well as the efficiency of water purification from iron, manganese and nitrogen-containing compounds (Figure 5) [1]. The effect of water purification from impurities of iron, manganese, nitrogen and organic compounds is higher by 10-12% when using a sample of shungite, which was activated, treated with steam and nanosilver, which is explained and confirmed by its better adsorption properties.

The properties of water are determined by its micro- and macro-component composition, as well as by its structure [1]. Prepared water, unlike natural water, has no pleasant refreshing effect, fullness of taste, characterized by disordered structure [23].

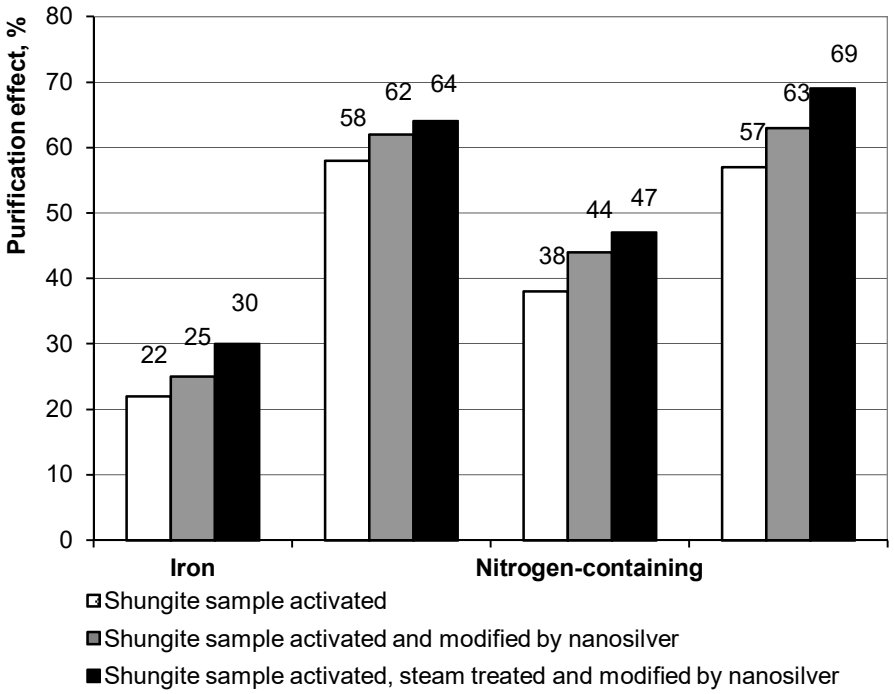

Figure 5. Efficiency of water purification using shungite treated in various ways

In modern conditions of production and consumption of different types of beverages (alcoholic and nonalcoholic), not only their chemical composition but also the physical indicators of beverages, which directly influence the processes of ensuring human life, are of particular importance [33]. One such indicator is the water oxidation–reduction potential [34]. This indicator of water characterizes the degree of activity of electrons in redox reactions indicates the biological activity and antioxidant property of water [35].

Regulatory documents that set requirements for the quality of drinking water and prepared value of the water oxidation–reduction potential is not regulated. In natural water, without its additional technological treatment, the value of the water oxidation–reduction potential varies widely from − 400 mV to +700 mV [33,34]. However, during water treatment the water oxidation–reduction potential increases to +200 – +400 mV [33, 34]. In order to achieve a positive technological effect with the maximum preservation of natural properties and physicochemical characteristics of water, the influence of shungite treated in various ways the water oxidation–reduction potential was investigated (Figure 6).

The results obtained indicate a gradual decrease the water oxidation–reduction potential of the prepared water from +250 mV and the achievement value of +70 mV on the seventeenth volume of the prepared water to the volume of the shungite treated with nanosilver; for steam and nanosilver treated shungite the water oxidation–reduction potential reaches + 40 mV. In the further prepared water volume there is an increase of the index of the water oxidation–reduction potential and its stabilization at the values of + 150–170 mV during the treatment of shungite with nanosilver, +90–100 mV–during the treatment of shungite with steam and nanosilver.

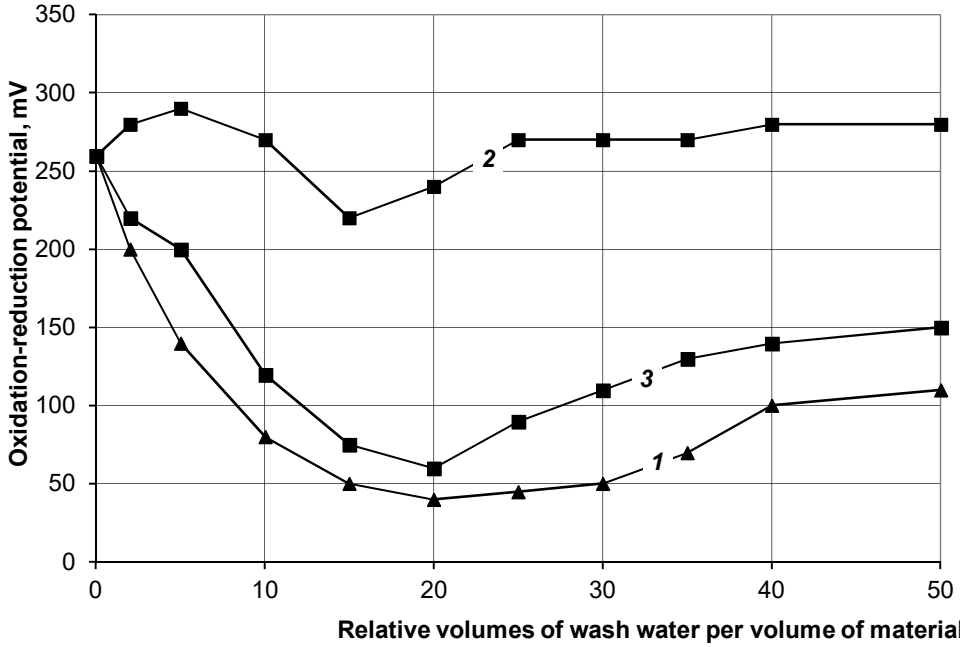

Figure 6. Water oxidation–reduction potential of the prepared water using activated shungite, activated and treated by nanosilver shungite, activated, steam and nanosilver treated shungite.

Thus, the use of shungite treated with steam and nanosilver is effective for stabilizing the water oxidation–reduction potential, which is confirmed by the acquisition of water antioxidant properties [35]. The additional decrease of the water oxidation–reduction potential of water prepared by shungite treated with steam and nanosilver from + 70 to + 40 mV can be explained by the presence of a negative charge of nanoparticles on the surface, as evidenced by the value of the ξ potential [25].

Conclusions

The urgency of shungite treated in different ways use for water purification in the production of different types of beverages is substantiated. The most effective method to increase the adsorption activity of the material, to reduce the consumption of flushing water during shungite preparation to the filter cycle, to stabilize the redox potential of the treated water is the preliminary preparation of the shungite, which includes activation, steam and nanosilver treatment.

The use of nanomodified and steam-treated shungite is effective for stabilizing the redox potential of the material, indicating the acquisition of water antioxidant properties.

References

1. Kuzmin O., Topolnyk V., Loviagyn A., Kuzmyn V. (2011), *Vodka: technology, quality, innovation,* Donetsk., DonNUET.
2. Landsdown Alan BG (2006), Silver in healthcare: Antimicrobial effects and safety in use. *Curr Probl Dermatol.* 33, pp. 17–34.
3. Kibardin G. (2010), *Shungit i ego celebnie svoistva*, Moscow, Amrita-Rus.
4. Ryabchikov B. (2013), *Sovremennaya vodopodgotovka [Modern Water Preparation]*, Moscow.
5. Mosyn O., Yhnatov Y. (2015), Research of Influence of Shungite on Mountain Water from Bulgaria. Mathematical Models of Water Influenced from Shungite and Zeolite, *Journal of Medicine, Physiology and Biophysics,* 12, pp. 1–19.
6. Mosyn O., Yhnatov Y. (2013), Sostav y strukturne svoistva pryrdnoho fulerenosoderzhashcheho mynerala shunhyta, *Byotekhnosfera,* 1(25), pp. 29–33.
7. Mel'nik L., Tkachuk N., Turchun O., Diyuk V., Ishchenko O., Byeda O., Kisterska L., Loginova O., Lysovenko S., Gontar O., Garashchenko V. (2017), Adsorption properties of shungite in purification of water–alcohol solutions, *Journal of Superhard Material,* 39(6), pp. 416–421, DOI: 10.3103/S1063457617060053
8. Mosin O., Ignatov I. (2013), The structure and compositions of natural carbonaceous fullerene containing mineral shungite, *International Journal of Advanced Scientific and Technical Research*, 3(11), pp. 9–21.
9. Kulikova V. (2006), *Treatment shungite*, Moscow.
10. Mosyn O. (2011), Novyi pryrodnyi myneralnyi sorbent – shunhyt, *Santehnika*, 3, pp. 34–36.
11. Musyna U. (2014), Koksuevskye shunhytystye porody v protsessakh obespechenyia ekolohycheskoho ravnovesyia, *Yzvestyia Sankt-Peterburhskoho hosudarstvennoho tekhnolohycheskoho ynstituta*, 23(49), pp. 79–82.
12. Pushmyna Y., Khorunzhyna S., Permiakova L. (2009), Yspolzovanye tseolytov Sybyry v proyzvodstve napytkov, *Pyvo y napytky*, 3, pp. 18–19.
13. Kornev V., Rybakov Yu., Chyrykov S. (2015), Sravnytelnaia otsenka strukturы chastyts y adsorbtsyonnыkh svoistv shunhyta y bentonyta, *Vestnyk nauky y obrazovanyia*, 9(11), pp. 20–23.
14. Shpileuski M. E., Shpileuski E. M., Stelmach V. F. (2001), Fullerenes and fullerene-like structures, *Journal of engineering physics and thermophysics,* 76(6), pp. 25–28.
15. Kuzmyn O. (2014), *Usovershenstvovanye protsessov proyzvodstva alkoholnoi produktsyy*, DonNUET, Donetsk.
16. Mosyn O. (2013), Perspektivy ispolzovaniya prirodnogo fullerensoderzhchego minerala shungita v vodopodgotovke, *Voda i vodoochisni tehnologii*, 3(13), pp. 41–49.
17. Muhin V., Klushin V. (2012), *Production and using of carbon adsorbents*, RXTU, Moscow.
18. Wang S., Peng Y. (2010), Natural zeolites as effective adsorbents in water and wastewater treatment, *Chemical Engineering Journal*, 156(1), pp. 11–24.
19. Borisov B., Egorova E., Zaynullin R. (2014), *Vodopodgotovka v proizvodstve pishchevykh produktov i napitkov*, Professiya Publ, Sankt Petersburg.
20. Shrestha R., Joshi D. R., Gopali J. (2009), Oligodynamic fraction of silver, copper and brass on enteric bacteria isolated from water of Kathmandu Valley, *Nepal Journal of Science and Technology,* 10, pp. 189–193.
21. Moghazy El. (2011), Netraditsionnyye sposoby vodopodgotovki v proizvodstve syvorotochnykh napitkov, *Tekhnika i tekhnologiya pishchevykh proizvodstv*, 4, pp. 72–77.
22. Stounbjerg L., Vestergaard C., Andreasen B., Ipsen R. (2018), Beverage clouding agents: Review of principles and current manufacturing, *Food Reviews International*, 34(7), pp. 613–638.

23. Kovalchuk V.P. (2005), Umovy zabezpechennya bysokoi yakosti likero-gorilchanyx napoiv na stadii vodopidgotovky. (2011), *Xarchova i pererobna promyslovist*, 11, pp. 24–27.
24. Kilcast D., Subramaniam P. (2011), *Food and beverage stability and shelf lift*, Woodhead Publishing Limited.
25. Novikov M. V., Kisterska L. D., Sadokhin V. V., Sadokhin V. P., Perevertailo V. M. (2012), Environmentally friendly technology: plasma sputtering of conductive materials and dispersion of nanoparticles in various liquids as one-step production cycle, *Powder metallurgy and metal ceramics,* 51(1-2), pp. 26–34. DOI: 10.1007/s11106-012-9392-7
26. Kisterska L., Loginova O., Sadokhyn V., Sadokhyn V. (2015), Innovatsiina tekhnolohiia vyrobnytstva biosumisnykh nanodezinfektantiv novoho pokolinnia, *Visnyk NAN Ukrainy*, 1, pp. 39–48.
27. UkrainetsA., Bolshak Yu., Marynin A. (2018), Okysno-vidnovnyy balans pytnoy vody – pokaznyk yy yakosti ta fiziologichnoy povnoczinnosti, *Harhova promyslovist*, 24, pp. 6–14.
28. Particle Characterization: Light Scattering Methods (2002), Kluwer Academic Publishers New York, Boston, Dordrecht, London, Moscow, pp. 1–398: DOI DOI: 10.1007/0-306-47124-8
29. Polyhalyna H, (2006), *Analytycheskyi kontrol proyzvodstva vodok y lykerovodochnykh yzdelyi,* DeLy prynt, Moscow
30. Koroliuk T., Usatiuk S., Kostinova T., Filipchenko I. (2017), *Metodyka kontroliu kharchovykh produktiv*, Kyiv, NUFT.
31. Abramova Y., Abramova Y., Medryshch M., Pavlenko S. (2013), Ynnovatsyy v sfere kontrolia kachestva alkoholnыkh napytkov, *Spyrtnye napytky*, 5, p. 52.
32. Schulz H., Fischer W. (2000), Comparison of Different Methods for Redox Potential Determination in Natural Waters, *Redox fundamentals, Prosseses and Applications*, pp. 42–54.
33. Bolshak Yu. (2015), *Byolohycheskaia aktyvnost y zakonomernosty formyrovanyia bezreahentno modyfytsyrovannoi vody,*. Knyha-plius, Kyiv.
34. Xiaorong Z, Haibo Li, Yinghua Li, Fei G, Zhongxin Ya. (2018), *Int J Environ Res Public Health*, Available at: http://10.3390/ijerph15122790
35. Copeland A, Darren A Lytle (2014), Measuring the oxidation–reduction potential of important oxidants in drinking water, Available at: DOI: 10.5942/jawwa.2014.106.0002.
36. Rahman S.M.E., Khan I. (2016), *Comprehensive Reviews in Food Science and Food Safety*, Available at: DOI: 10.1111/1541-4337.12200.
37. Sigg L. (2000), Redox Potential Measurement in Natural Waters: Significance, Concepts and Problems, Redox Fundamentals*, Processes and Applications*, pp. 1–12.
38. Cavchrina L. A., Koganovskiy A. M., Klimenko N. A., Topkin U. V. (2002), Adsorbciya fulvokyslot aktivnymy uglamy raznoy poristoy structury, *Ximiya i texnologiya vody*, 24(3), pp. 226–237.
39. Cheremisinoff N.P. (2002), *Handbook of water and wastewater treatment technologies*, Butterworth Heinemann–Pollution Engineering, Woburn.
40. Liudmyla Melnyk, Zynoviy Melnyk, Volodymyr Kryvorotko (2013), Methods of recovering schungite's adsorptive properties after processing red beet juice, *Ukrainian Journal of Food Science*, 1(2), pp. 223–227.
41. Liudmyla Melnyk, Olena Turchun, Natalia Tkachuk, Anatolii Kutz, Zynovii Melnyk (2014), Water-alcohol adsorbing cleaning out of higher alcohols by shungite, *Ukrainian Journal of Food Science*, 2(2), pp. 312–317.

Анотації

Харчові технології

Вплив ультратонкого помелу вторинної сировини від переробки сої на її функціональні властивості

Фанг Ванг[1, 2], Валерій Сукманов[1], Цзе Цзен[2]
1 – Сумський національний аграрний університет, Суми, Україна
2 – Хенанський інститут науки і технологій, Сіньсян, Китай

Вступ. Основними інгредієнтами вторинної сировини від переробки сої є харчові волокна та білок, що мають високу харчову цінність та корисні для здоров'я людини властивості. Ультратонкий помел дає змогу збільшити вміст харчових волокон, покращити смак та якість продукту, виробленого з додаванням борошна з цієї сировини.

Матеріали і методи. Подрібнювач надтонкого помелу KCW-701S; лазерний вимірювач розміру частинок BT-9300H; сканувальний електронний мікроскоп. Відходи переробки сої подрібнювали при частоті помелу 50, 40, 30 та 20 Гц; контрольні зразки обробляли за традиційною технологією помелу.

Результати і обговорення. Розчинність у воді та набухання оброблених зразків зросли порівняно з контрольними зразками. Із зменшенням частоти подрібнення розчинність у воді та набухання суттєво змінюються: при частоті 30 Гц розчинність у воді становила 20,84%, а набухання – 11,03 мл/г. Із зменшенням частоти помелу вологоутримувальна здатність має тенденцію до зменшення: при частоті 20 Гц вологоутримувальна здатність досягала найнижчого значення 6,53 г/г, якщо порівняти з контрольними зразками (10,92 г/г). Жироутримувальна здатність суттєво не змінилася.

Колір досліджуваних зразків після надтонкого помелу зазнав суттєвих змін. Значення яскравості (L^*) підвищилося, колір змінився від пшенично-жовтого до кремово-білого. Значення a^* і b^* поступово зменшувалися. Сканування електронним мікроскопом структура досліджуваних зразків свідчить, що із зменшенням частоти помелу вони стають більш дрібними і гладкими, їх розмір поступово зменшується. При частоті помелу 30 Гц середній діаметр становив 47,95 мкм, але при частоті вище 30 Гц цей розмір збільшувався.

Висновки. Ультратонкий помел сировини від переробки сої суттєво впливає на фізичні та хімічні властивості хлібобулочних виробів. Розчинність і набухання у воді значно покращилося порівняно з контрольними зразками. Частота 30 Гц є раціональною і може бути використана при ультратонкому помелі відходів переробки сої та подальшому їх використанні у виробництві хлібобулочних виробів.

Ключові слова: *ультратонкий помел, соя, відходи, функціональність.*

Стабілізація харчових дисперсних систем

Андрій Горальчук, Ольга Гринченко, Ольга Рябець, Олег Котляр
Харківський державний університет харчування та торгівлі, Харків, Україна

Вступ. Огляд проведено з метою систематизації інформації про чинники, що впливають на створення і стабілізацію пін та емульсій.

Матеріали і методи. Аналітичні дослідження праць з одержання та стабілізації емульсій пін і поліфазних дисперсних систем на основі публікацій за останні 20 років. Предметами дослідження є піни, емульсії, піноемульсійні системи та системи, що одночасно являють собою піну, емульсію та суспензію.

Результати і обговорення. Піни та емульсії, хоч і мають схожість, однак їх утворення відрізняється швидкістю диспергування, що обумовлено швидкістю адсорбції поверхнево-активних речовин. Процес емульгування відбувається швидше, ніж піноутворення, тому одержання піноемульсій можливе лише послідовно. Коалесценція як чинник, що призводить до руйнування, характерний як для пін, так і для емульсій, визначається властивостями поверхнево-активних речовин. Інші чинники обумовлені властивостями дисперсійного середовища. Систематизовано чинники, які забезпечують стійкість дисперсних систем. Ефективним чинником стабілізації пін та емульсій є структурно-механічний. Реалізація цього чинника здійснюється за рахунок використання лише білків або твердих частинок з частковим змочуванням, або сумісного використання білків з низькомолекулярними поверхнево-активними речовинами чи сумісного використання білків з полісахаридами. Реалізація структурно-механічного чинника стабілізації в поліфазних системах, зокрема в піно емульсіях, передбачає підбір поверхнево-активних речовин для регулювання реологічних властивостей міжфазних адсорбційних шарів, послідовності створення дисперсних фаз, що забезпечує їх просторове розташування в харчовому продукті.

Висновки. Встановлено, що при забезпеченні стійкості харчових дисперсних систем визначальну роль відіграють реологічні властивості міжфазних адсорбційних шарів, сформованих за участю білків, поверхнево-активних речовин, полісахаридів, а також підвищення в'язкості дисперсійного середовища.

Ключові слова: *емульсія, піна, стабілізація, реологія, плівка.*

Вплив сортів і стадій зрілості на в'язко-пружні характеристики і механічну міцність полуниці

Сергіу Падурет
Університет «Штефан-чел-Маре», Сучава, Румунія

Вступ. Мета цього дослідження – визначити вплив сортів і стадій зрілості на в'язко-пружні характеристики полуниці та оцінити їхню механічну міцність.

Матеріали і методи. Зразки свіжої полуниці (сорти *Vibrant*, *Elsanta* і *Magic*) були піддані випробуванню на плинність, а для визначення в'язко-пружних характеристик використана механічна модель Бюргера, що враховує чотири елементи моделі Кельвіна-Фойхта. Зразки полуниці були розділені на три групи за стадіями зрілості: недозріла (S1), зріла (S2) і перезріла (S3).

Результати і обговорення. Зразки полуниці проаналізовані за вмістом вологи, кількістю розчинних речовин, активною (pH) і загальною кислотностями. Вміст вологи знаходився в діапазоні від 87,38% до 89,67%, причому в зразках, які

знаходяться на стадії перезрівання (S3), прослідковуються більш високі значення вологості порівняно з недозрілими зразками (S1), $p<0,05$. Найбільша кількість розчинних речовин була зафіксована для сортів *Elsanta* на стадії перезрівання, *Magic* (11,91) і *Vibrant* (11,57).

Миттєво-пружна деформація полуниці перебувала в діапазоні 1,057–3,135 мм, а під час уповільнення, яке корелюється з періодом зберігання, варіюється від 10,92 до 140,83 с. Матриця кореляції Пірсона між фізико-хімічними (вміст вологи, концентрація Брікса, активна і загальна кислотності) та в'язко-пружними характеристиками (уповільнена і миттєво-пружна деформація, час уповільнення, в'язка деформація, деформація плинності і поверхня відгуку кривих плинності) показує позитивний значний взаємозв'язок між уповільненою пружною деформацією ($\varepsilon 2$) і деформацією плинності ($p<0,01$).

Висновки. Сорт полуниці *Vibrant* володів найвищою стійкістю до механічних впливів, а також високою механічною стійкістю до стиснення завдяки найнижчим значенням миттєвої й уповільненої пружної деформації.

Ключові слова: *полуниця, модель Бюргера, плинність, деформація.*

Перехід поліфенольних сполук у білково-рослинні концентрати при осадженні *Plantago major L.* протеїнів молока

Олена Грек[1], Лариса Чубенко[1], Аміт Кумар[2],
Володимир Хареба[3], Алла Тимчук[1], Олена Онопрійчук[1]
1 – Національний університет харчових технологій, Київ, Україна
2 – Інтегральний університет, Лакнау, Індія
3 – Відділ аграрної економіки і продовольства НААН України

Вступ. Актуальним напрямом є реалізація принципів науково-обґрунтованого використання молочної і рослинної сировини з функціонально-технологічними властивостями.

Матеріали і методи. Сировиною для отримання білкових концентратів було молоко нормалізоване. Як коагулянт при осадженні білків використано сік прямого віджиму з наземної частини Plantago major L. Ідентифікацію та кількісне визначення поліфенолів і флаваноїдів в зразках соку подорожника та отриманій сироватці здійснювали методом високоефективної рідинної хроматографії за допомогою системи Prominence LC-20 Shimadzu (Японія). Порівняння проводили із зовнішніми стандартними зразками.

Результати і обговорення. Представлено дослідження якісного складу та кількісного вмісту поліфенолів і флавоноїдів у білково-рослинних концентратах, отриманих при осаджені білків молока соком прямого віджиму наземної частини Plantago major L. Процес відбувався за підвищених температур. Згідно з аналізом спектрів поглинання дослідних зразків соку з подорожника встановлено, що максимум знаходиться при довжинах хвиль 225–350 нм. Такий результат корелюється з тим, що з 22 виділених флавоноїдів 9 речовин містять 6-оксифлавони, для яких характерне наявність максимуму в межах 2550285 нм.

Різниця між показниками вмісту поліфенолів у соці Plantago major L. та сироватці показує ступінь переходу поліфенольних сполук у білково-рослинні концентрати. Загальний вміст флавоноїдів у всіх досліджуваних зразках дорівнював вмісту речовин, які мають схожість зі стандартами флавоноїдів (фенольні кислоти, катехіни,

флавоноли, флавонони та флавони), за винятком катехіноподібних речовин. Флавоноли представлені глікозидами мірицитину. Нарингін і гесперидин входять до складу флавононів. Флавони в кількісному значенні мають найменшу вагу і представлені лютеоліном та його глікозидами. Вміст фенольних кислот коливався на рівні 12,36 мг/л для соку подорожника і 0,07 мг/л для забарвленої сироватки.

Висновок. Визначено ступінь переходу поліфенольних сполук у білково-рослинний концентрат на рівні 77% від загальної кількості, з них 74% – флавоноїди.

Ключові слова: *молоко, Plantago major L., коагуляція, білок, поліфенольні сполуки.*

Порівняльне дослідження хімічного складу і антибактеріальної ктивності насіння гуньби (*Trigonella Foemum graecum L.*) та кмину (*Cumin cyminum L.*)

Хасна Бухенні[1], Кула Доукани[1], Назім Чекероглу[2],
Севгі Гезічі[2], Сухіла Табак[1]
1 – Університет Ібн-Халдуна, Тіарет, Алжир
2 – Університет Кіліс 7 Аралік, Кіліс, Туреччина

Вступ. Завданням цього дослідження є визначення фізико-хімічних характеристик гуньби (*Trigonella Foenum graecum L.*) та кмину (*Cumin cyminum L.*) та оцінка їхніх антибактеріальних властивостей щодо *Staphylococcus aureus ATCC25923*, *Escherichia coli ATCC 25922* та *Bacillus subtilis ATCC 6633* .

Матеріали і методи. Проаналізовано різні сорти гуньби та кмину на масу в 1000 насінинах та швидкість проростання. Визначено фізико-хімічні властивості – активну (pH) і титровану кислотності, вологість, золу, розчинні тверді речовини, електропровідність, в'язкість, вміст білків, жирів, сирої клітковини, пектину, загальних та редукуючих цукрів і мінералів. Антибактеріальну активність екстрактів оцінювали методом дискової дифузії стосовно випробувальних бактеріальних штамів.

Результати і обговорення. Отримані результати показали, що алжирський сорт гуньби та сирійський сорт насіння кмину давали найбільшу вагу зі значенням 16,8 г та 13,9 г відповідно та краще проростання на рівні 70%. Активна та титрована кислотності насіння гуньби та кмину коливалися від 5,6 до 6,5 та від 2,8 до 3% відповідно. Вміст вологи та золи коливався від 3 до 2,8% та 3 до 7% відповідно. Загальна кількість розчинних твердих речовин, електропровідність, в'язкість коливались від 2,8 до 5,5 Brix, від 18,1 до 42,8 mvs і від 2,4 до 2,8 МПа·с відповідно. Гуньба і кмин містять велику кількість білків – від 23,1 до 26,8%, вміст жирів – від 8,8 до 21%. Кількість сирої клітковини та пектину коливалась від 5,1 до 7,9% та від 1,9 до 2,8% відповідно. Вміст загальних і редукуючих цукрів коливався від 5,2 до 6,7 % та від 0,5 до 1 % відповідно. Гуньба та кмин містять у максимальній кількості калій як основний мінерал, сульфур, фосфор, кальцій, магній, залізо, цинк і бор, мідь, свинець, нікель, хром, молібден, кобальт і кадмій. Результати антибактеріальної активності екстрактів рослин з метанолом стосовно трьох бактеріальних штамів *S. aureus*, *E. coli* та *B. Subtilis* показали чутливість цих штамів до рослин-екстрактів з ДЗГ (діаметр зони гальмування) 21 мм, 12 мм, 18 мм для кмину та 10 мм, 8 мм, 9 мм для гуньби відповідно.

Висновок. Загальна оцінка проведених досліджень показує, що обидві спеції (гуньба і кмин) мають хороший хімічний склад, і підтверджує їхню чутливість до випробуваних штамів бактерій.

Ключові слова: *кмин, гуньба, насіння, антибактеріальний.*

Дослідження впливу поглиначів кисню на стабільність варених сосисок

Анатолій Українець, Василь Пасічний, Андрій Маринін, Юлія Желуденко
Національний університет харчових технологій, Київ, Україна

Вступ. Визначали вплив пакування з використанням поглиначів кисню українського та китайського виробництва на мікробіологічну та окисну стабільність варених сосисок протягом зберігання.

Матеріали і методи. Досліджували варені сосиски запаковані з різними поглиначами кисню. Мікробіологічні показники, зокрема кількість мезофільних аеробних і факультативно-анаеробних мікроорганізмів (МАФАнМ), плісеневі гриби та дріжджі визначали методом Пастера. Кислотне та пероксидне число визначали методом титрування.

Результати і обговорення. Час повного видалення кисню в упакованому зразку скорочується зі зменшенням об'єму, з якого видаляється кисень. З динаміки відновлення мінімального вмісту кисню в запакованих зразках видно, що здатність до відновлення МАР спрацьовує тільки при одноразовому відкритті пакетів. МАФАнМ для незапакованих зразків становив $4,5\times10^2$ КУО/г. На 8-у добу зберігання МАФАнМ для зразків з поглиначами кисню китайського виробництва та контролю, що зберігалися за температури від 0 до 6 °С, значно не відрізнялися ($5,0\times10^3$ КУО/г та $6,5\times10^3$ КУО/г відповідно) і були значно нижчими, ніж для зразка з поглиначами кисню українського виробництва ($1,9\times10^4$ КУО/г). На 13-у добу зберігання значення МАФАнМ для зразка 3 було нижчим, ніж для зразка 2 ($1,2\times10^4$ КУО/г та $6,9\times10^4$ КУО/г відповідно). У той же час цей показник для контролю був набагато вищим. Зразок 2 і зразок 3 показали стабільні значення плісеневих грибів протягом усього дослідження (<10 КУО/г) і були нижчими за контрольні показники ($3,0\times10^1$ КУО/г на 13-у добу). Усі зразки показали значне зростання кількості дріжджів під час зберігання, не спостерігалась значна різниця порівняно з контролем ($7,0\times10^1$ – $4,8\times10^2$ КУО/г та $5,0\times10^2$ КУО/г відповідно). Початкове значення кислотного числа на 1 день зберігання становило 1,41 мг КОН/г. На 13-й день зберігання ковбаси, упаковані з поглиначами кисню, що зберігалися за температури від 0 до 6 °С, показали найменше зростання порівняно з контролем (3,57–3,76 мг КОН/г та 3,98 мг КОН/г відповідно). Пероксидне число для зразків 2 і 3 не відрізнялося після 13 діб зберігання, але було значно нижчим порівняно з контролем (3,14½ ½Оммоль/кг, 3,36 ½Оммоль/кг і 4,05 ½Оммоль/кг).

Висновки. Пакування з використанням поглиначів кисню сповільнює мікробіологічне псування та окисні процеси для варених сосисок порівняно з контролем. Це дає змогу рекомендувати використання поглиначів кисню для пакування варених сосисок.

Ключові слова: *сосиски, стабільність, поглиначі кисню, зберігання.*

Фізико-хімічна характеристика рицинової олії

Тарік Панхвар[1], Сарфараз Ахмед Махесар[1], Афтаб Ахмед Кандро[2],
Сид Туфіал Хуссейн Шеразі[1], Абдул Хамед Корі[1],
Захід Хуссей Лагхарі[1], Джаміль-ур-Рехман Мемон[2]
1 – Національний центр передового досвіду в аналітичній хімії, Університет Сінду, Пакистан
2 – Інститут хімії ім. доктора М. А. Казі, Університет Сінду, Пакистан

Вступ. Ця стаття надає повний профіль фізико-хімічних властивостей і жирнокислотного складу місцевих сортів рицини з Сінду, Пакистан.

Матеріали і методи. Олія була видобута методом вилучення Сокслета з подальшим фізико-хімічним дослідженням необхідних параметрів (значення йоду, значення пероксиду, значення омилення, в'язкість і вологість). Для якісного аналізу касторової олії були використані методи GCMS та FTIR.

Результати і обговорення. Вміст олії спостерігався в межах 44–48%. Вміст вологи та золи в насінні рицини становив 4,22–5,16% та 5,66–6,49% відповідно. Композиційний аналіз GCMS показав, що рицинова кислота (88,5–93,1%) є помітною жирною кислотою у всіх місцевих сортах. Вміст інших жирних кислот: пальмітинові (0,4–0,8%), стеаринова (0,8–1,0%), лінолева (2,8–3,3%) та екосеноєва (0,2–1,5%). Встановлено, що значення вільних жирних кислот для всіх сортів рицинової олії становить від 0,16 до 0,53%. Інші параметри якості, такі як IV, PV та SV різних сортів касторової олії, визначалися в межах 79,16–90,03 гI_2/100г, 1,62–1,89 ммоль/кг і 188,12–204,76 мгКОГ/г відповідно. Спектри FTIR сортів рицинової олії були майже схожими. При ретельному дослідженні значень інтенсивності кожної функціональної групи, наявної в олії, було виявлено деякі зміни сортів насіння рицини**.**

Висновок. Досліджено важливі параметри місцевих сортів рицини з достатнім вмістом олії (> 40%). Інтенсивність смуги FTIR деяких функціональних груп корелює з важливими параметрами рицинової олії**.**

Ключові слова: *олія, рицина, насіння, FTIR.*

Виділення протеїнових фракцій β-LG, α-LA та BSA із сироватки молока

Володимир Юкало[1], Катерина Дацишин[1], Ольга Крупа[1], Наталія Павлістова[2]
1 – Тернопільський національний технічний університет імені Івана Пулюя, Тернопіль, Україна
2 – Могильовський державний університет харчування, Могильов, Республіка Білорусь

Вступ. Метою дослідження є отримання протеїнових фракцій β-LG, α-LA і BSA із сироватки молока препаративним диск-електрофорезом.

Матеріали і методи. Сироватку отримували із свіжого коров'ячого молока після ізоелектричного осадження протеїнів казеїнового комплексу. Концентрацію протеїнів сироватки молока визначали на спектрофотометрі за поглинанням при λ=280 нм. Гель-фільтрацію проводили на колонках для рідинної хроматографії. Для гель-фільтрації використовували сефадекси G-25 і G-100. Фракційний склад і гомогенність протеїнів сироватки аналізували диск-електрофорезом у пластинках поліакриламідного гелю.

Результати і обговорення. З урахуванням ефективності і наявності денатуруючих факторів для препаративного виділення гомогенних фракцій протеїнів-попередників біоактивних пептидів із сироватки молока була відібрана система диск-електрофорезу в нативних умовах для кислих і нейтральних протеїнів. У результаті гель-фільтрації для препаративного фракціонування отримано взірець протеїнів сироватки, очищений від низькомолекулярних сполук.

Оптимальна кількість взірця протеїнів сироватки для забезпечення ефективного розділення в модифікованій електрофоретичній камері апарата Стадієра не повинна перевищувати 10 $см^3$. Занадто великий за своїм об'ємом зразок не дає змоги ефективно розділити протеїни сироватки. Тривалість процесу екстракції окремих протеїнових фракцій після препаративного диск-електрофорезу становила близько 55…60 хв.

З допомогою аналітичного диск-електрофорезу встановлено ступінь гомогенності отриманих протеїнових фракцій, зокрема для фракції β-LG, BSA – 95…97%, для α-LA – 89–91%. Розраховано сумарний вихід гомогенних фракцій протеїнів сироватки молока β-LG, α-LA і BSA, який становив 49–61% (від протеїнів сироватки молока, взятих для розділення).

Висновки. Запропонований варіант диск-електрофорезу дає змогу виділити із сироватки молока електрофоретично гомогенні фракції β-LG, α-LA і BSA в нативних умовах. Електрофорез і екстракція протеїнів тривають близько 4 годин. Середній вихід гомогенних фракцій від протеїнів сироватки становить 55±6%.

Ключові слова: *протеїн, сироватка, молоко, диск-електрофорез.*

Вплив насіння винограду на реологію тіста із пшеничного борошна: оптимальна кількість та розмір частинок

Мадаліна Юга, Сільвія Міронеаса
Університет Штефан чел Маре, Сучава, Румунія

Вступ. Для розроблення хліба, збагаченого виноградним насінням, важливо передбачити зміни, які можуть відбутися в процесі його виготовлення.

Матеріали і методи. Досліджувався вплив кількості борошна з виноградних кісточок (GSF) (від 3 до 9%) і розміру частинок (великої L>500 μm, середньої 200 μm>M<500 μm та малої фракції S<200 μm) на фізико-хімічні характеристики борошна з кісточок винограду і пшениці та реологічні властивості тіста.

Результати і обговорення. Вміст білка і золи із додаванням GSF збільшується, а вологість та число падіння зменшилуються залежно від розміру частинок та рівня додавання. Зменшення числа падіння зі зменшенням розміру частинок GSF та збільшення рівня додавання вказує на збільшення активності альфа-амілази у складі борошна. Зберігання (G '), втрат (G' '), складного модуля (G *) і дотичної втрати (tan δ) тіста збільшувались із збільшенням розміру частинок та рівня додавання. Отримано зменшення максимальної висоти тіста (Hm), максимальної висоти газоутворення (H'm) і загального обсягу виробництва вуглекислого газу (Vt) із збільшенням рівня GSF у рафінованому пшеничному борошні. Коефіцієнт утримання газу (Rc) збільшується зі зменшенням розміру частинок GSF. Параметри бродіння тіста та динамічні реологічні властивості були адекватно передбачені досягнутими моделями регресії. Результат процесу оптимізації показав, що невеликі розміри часток GSF із сорту білого винограду в кількості 3,01% бажано замінити очищеним хлібом із пшеничного борошна з метою забезпечення належних реологічних характеристик. В цих

оптимальних умовах характеристики бродіння тіста та динамічні реологічні властивості були такими: Hm – 55,98 мм, Vt – 1274,11 мл, Rc – 81,22%, G' – 28,54·10^3 Па, G" – 9,79· 10^3 Па, G* – 0,17 ·10^3 Па, tan δ – 345.50·10^{-3}.

Висновки. Це дослідження підтверджує цінність насіння винограду від місцевих виробників вина та можливість використання цього побічного продукту з метою розробки нових збагачених хлібобулочних виробів**.**

Ключові слова: *пшеничне борошно, виноград, насіння, тісто, реологія.*

Фізико-хімічні та органолептичні властивості функціональних кондитерських виробів з борошном шипшини

Віоліна Попович[1], Оксана Раду[1], В'ячеслав Губеня[2],
Євгенія Ковалев[1], Татьяна Капканарь[1], Крістина Попович[1]
1 – Технічний університет Молдови, Кишинеу, Молдова
2 – Національний університет харчових технологій, Київ, Україна

Вступ. Метою дослідження було визначення фізико-хімічних та органолептичних властивостей кондитерських виробів, виготовлених з додаванням борошна шипшини.

Матеріали та методи. У дослідженнях використано вид Шипшина звичайна (*Rosa canina),* зібрану в Республіці Молдова (центральний регіон). Показники якості розроблених функціональні кондитерських виробів оцінювали за допомогою фізико-хімічних та органолептичних методів досліджень.

Результати та обговорення. Борошно з шипшини можна використовувати як джерело антиоксидантів і натуральних барвників у технологіях біо-цукерок функціонального призначення. Індекс кислотності у цих продуктах, порівняно з контрольним зразком, становить 0,12±0,01%, що в межах допустимих значень, а високий вміст каротиноїдів зумовлює червоно-помаранчевий колір продуктів, що доводить можливість використання борошна з шипшини у технологіях функціональних кондитерських виробів. Функціональні цукерки характеризуються позитивними органолептичними та фізико-хімічними властивостями, значення індексу кислотності становить 1,15±0,01 мг КОН/$дм^3$, вологість 24,19±0,01%. Збільшення дозування борошна шипшини надає виробам помаранчевого кольору, а також призводить до зростання кислотності продукту. Це вважають недоліком екстракту шипшини, проте дає поштовх новому напряму досліджень. Цукерки з невеликим вмістом борошна шипшини мають прийнятні органолептичні показники якості, що дає додаткові підстави використовувати харчові добавки рослинного походження з натуральними барвниками у технологіях функціональних харчових продуктів. Суттєвим аспектом досліджень є те, що були одержані харчова добавка і натуральний барвник, вилучений з плодів шипшини. Замінюючи синтетичну, натуральна добавка надає готовим цукеркам приємного смаку та запаху цвіту шипшини.

Висновок. Підтверджується функціональність та високі показники якості кондитерських виробів, в яких синтетичні харчові добавки замінено натуральними барвниками, які вилучено з рослинних продуктів.

Ключові слова: *цукерка, кондитерський, шипшина, борошно, функціональність.*

Вплив режимних параметрів на ступінь ферментативного гідролізу високобілкових продуктів

Леся Авдєєва, Едуард Жукотський, Ганна Декуша
Інститут технічної теплофізики Національної академії наук України, Київ, Україна

Вступ. Проведено дослідження з метою визначення впливу технологічних параметрів на ступінь гідролізу білків сої та молочної сироватки, а також їхніх сумішей для отримання збалансованих білкових композицій з високим ступенем гідролізу.

Матеріали і методи. Досліджувалися концентрат білковий з молочної сироватки, ізольований соєвий білок та їхні суміші у різних масових співвідношеннях, які гідролізували ферментними препаратами «Протамекс», «Біопротеаза N100L» та «Профікс 6500». Ступінь гідролізу білків визначався спектрофотометричним методом, амінокислотний склад гідролізатів – методом іонообмінної хроматографії.

Результати і обговорення. Для отримання високогідролізованого ізольованого соєвого білка встановлено раціональні режими його протеолізу, а саме: масова частка білка у водному розчині – 9%, масова частка ферментного препарату 5 %, pH 6,5–7,0, температура гідролізу 55–60 ºС, тривалість процесу – 60 хв. За цих умов ступінь гідролізу ізольованого соєвого білка становить 80–82% при дії «Протамексу», 50–51% – «Біопротеазою N100L» та 30–33% – «Профіксом 6500».

Гідролітична дія зазначених вище ферментних препаратів на ступінь гідролізу концентрату білкового із молочної сироватки за тих же умов дещо менша і складає 45–46% для «Протамексу», 30–33% – для «Біопротеази N100L» та 19–20% – для «Профіксу 6500», що можна пояснити меншою специфічністю цього субстрату до ферментних препаратів.

Для отримання збалансованого складу незамінних амінокислот щодо жіночого молока раціональним є поєднання концентрату білкового з молочної сироватки та ізольованого соєвого білка у масовому співвідношенні 1:1 відповідно. При цьому ступінь гідролізу такої суміші білків є високим і становить більше 80% при дії «Протамексом» концентрацією 5% до маси білка, температурі 55–60 ºС та тривалості 60 хв.

Висновки. Вперше визначено раціональні технологічні параметри проведення протеолізу ізольованого соєвого білка, концентрату білкового із молочної сироватки і їхніх сумішей для отримання високого ступеня гідролізу.

Ключові слова: *білок, гідроліз, протеаза, амінокислоти.*

Вплив *Spirulina platensis* на черствіння м’якушки пшеничного хліба під час зберігання

Денка Златева[1], Росен Чочков[2]
1 – Економічний університет, м. Варна, Болгарія
2 – Університет харчових технологій, м. Пловдив, Болгарія

Вступ. Вивчено вплив *Spirulina platensis* на черствіння м’якушки під час зберігання (96 год) пшеничного хліба шляхом вимірювання деформаційних характеристик.

Матеріали і методи. Хліб отримували з пшеничного борошна з додаванням *Spirulina platensis* (порошок) у кількості 2 або 4% від маси борошна. Деформаційні

характеристики хлібної м'якушки вивчалися через 3, 24, 48, 72 та 96 год після випікання. Деформаційні характеристики хлібної м'якушки вимірювали за допомогою автоматичного пенетрометра шляхом занурення тіла з певною масою на певний час.

Результати і обговорення. Найбільше проникнення, а отже, найбільша м'якість хлібної м'якушки виявилася у зразках з додаванням *Spirulina platensis* у кількості 4% від маси борошна. В обох зразках хліба з водоростями швидкість черствіння м'якушки повільніша, а після 96 год зберігання загальна деформація м'якушки зменшилася в 2,75 раза, тоді як у контрольному зразку зменшилась в 3,6 раза. Зразки хліба, що містять *Spirulina platensis*, мають більшу пластичність м'якушки протягом усього періоду зберігання (96 год). Додавання водоростей у кількості 2 та 4% від маси борошна призводить до поліпшення пластичних властивостей хлібної м'якушки та довшого їх утримування, ніж у контрольному зразку. Під час зберігання в контрольному зразку пластичність хлібної м'якушки поступово знижується і при останньому вимірюванні (через 96 год після випікання) вона в 3,54 раза нижча порівняно з першим вимірюванням – через 3 год після випікання. Додавання *Spirulina platensis* позитивно впливає на пластичність хлібної м'якушки. Зразки хліба, рецептура яких включає 4 % *Spirulina platensis*, мають більшу пластичність м'якушки протягом усього періоду зберігання.

Висновки. Черствіння м'якушки уповільнилося при внесенні порошку *Spirulina platensis*. Додавання *Spirulina platensis* у кількості 4% забезпечує найвищу пластичність хлібної м'якушки.

Ключові слова: *хліб, черствіння, водорості, Spirulina platensis, м'якушка.*

Процеси і обладнання

Моделювання і синтез систем інтенсивного масообміну

Анатолій Соколенко, Олександр Шевченко, Костянтин Васильківський, Олег Степанець, Олексій Бойко, Анастасія Шевченко
Національний університет харчових технологій, Київ, Україна

Вступ. Розвиток теорії синтезу систем інтенсивних масообмінних процесів за рахунок енергетичних потенціалів рідинних або газорідинних потоків забезпечує реалізацію актуальних потреб.

Матеріали і методи. У статті використано аналіз фізичного підґрунтя методів і засобів інтенсифікації процесів у рідинних та газорідинних системах і феноменологічні узагальнення на основі відомих законів природи з математичною формалізацією взаємозв'язків між геометричними, кінематичними та гідродинамічними параметрами.

Результати і обговорення. В дослідженні показано можливість синтезу інерціальних полів за рахунок змінних геометричних параметрів трубопроводів, зокрема площі поперечного перерізу, а також за рахунок чергування криволінійних та прямолінійних ділянок і траєкторій змінної кривини.

Узагальнене представлення фактора інтенсифікації масообмінних процесів стосується силових дій у формі наслідків перерозподілу тиску в результаті перерозподілу потенціалу кінетичної і потенціальної енергій.

Показано можливості варіацій значеннями силових впливів за рахунок

комбінацій гравітаційного поля та інерціальних полів різної орієнтації і частоти впливів, зокрема з можливістю відтворення динамічних ударів в зонах зміни знаків радіусів кривини. Синтез інерціальних полів у таких системах досягається за рахунок таких факторів, як змінна швидкість потоку або зміна напрямку потоку. Більш ефективною прогнозується комбінація з цих двох факторів.

Енергетичне забезпечення інтенсифікації масообміну стосується початкових умов створення потоків, а загальний позитивний результат забезпечується точною локалізацією процесів.

Висновки. Фактори інтенсифікації масообмінних процесів представлені синтезом інерціальних полів за рахунок зміни швидкості і напрямку потоку середовища.

Ключові слова: *масообмін, інтенсифікація, синтез, середовище, інерція.*

Обґрунтування нейро-нечіткого регулювання в системі керування випарною станцією

Михайло Грама, Віктор Сідлецький, Ігор Ельперін
Національний університет харчових технологій, Київ, Україна

Вступ. Проведено дослідження використання нейро-нечітких регуляторів у системі керування випарною станцією. Метою дослідження є визначення типу регулювання, що забезпечить досягнення найвищих показників контролю якості для регулювання випарника.

Матеріали і методи. Досліджувалася система керування п'ятикорпусною випарною станцією цукрового заводу. Для оцінки результатів роботи використовувався метод синтезу модального керування.

Результати і обговорення. Проведено порівняння між ПІД і нечітким контролером. Здійснюється регулювання таких відповідальних параметрів, як рівні концентрованого соку в корпусах випарника, які безпосередньо впливають на якість і вартість виробленої продукції. По-перше, в просторі станів у середовищі Matlab була розроблена математична модель та отримані результати щодо варіації задачі відносно початкових умов і збурень, які підтвердили, що час перехідного процесу в межах від складає 0,8 до 1,2 с, але значення відхилення рівнів у корпусах для процесу випарювання є занадто високими. По-друге, розроблена математична модель з ПІД-регулятором і отримані перехідні процеси для схем управління по всіх каналах керування. З'ясовано, що час перехідних процесів знаходиться в межах від 60 с по каналу X1 до 145 с по каналу X2, але це призвело до суттєвого зменшення відхилення рівнів у корпусах. По-третє, розроблена математична модель з нечітким контролером і отримані перехідні процеси для схем управління у всіх каналах керування. При цьому час перехідних процесів знаходиться в межах від 50 с по каналу X1 до 110 с по каналу X2, що є кращим результатом порівняно з ПІД-регулятором. Порівняно з попереднім дослідом також суттєво зменшилися рівні у корпусах. Отже, застосування нейро-нечіткого регулювання призводить до збільшення якісних параметрів процесу порівняно з системою з ПІД-регуляторами.

Висновки. Новизною результатів досліджень є наукове обґрунтування доцільності використання нейро-нечіткого регулювання під час реалізації систем оптимального керування.

Ключові слова: *цукор, сироп, модель, випарник, нейро-нечіткий, регулювання.*

Вплив способів оброблення шунгіту на його абсорбційні властивості та якість очищення води для напоїв

Світлана Олійник[1], Людмила Мельник[1], Ірина Самченко[1],
Наталія Ткачук[1], Ольга Логінова[2], Людмила Кістерська[2]
1 – Національний університет харчових технологій, м. Київ, Україна
2 – Інститут надтвердих матеріалів ім. В. М. Бакуля Національної академії наук України, м. Київ, Україна

Вступ. Показано перспективність оброблення шунгіту різними способами для підвищення його абсорбційних властивостей і збільшення ефективності очищення води під час виробництва напоїв.

Матеріали і методи. Досліджували воду питну та підготовлену шунгітом активованим; активованим і обробленим наносріблом; активованим, обробленим парою та наносріблом. Використовували фотометричні, спектрометричні, хімічні та потенціометричні методи аналізу, теоретичне узагальнення і порівняння, системний підхід.

Результати і обговорення. Досліджено параметри агрегації наночастинок у водно-гліцериновому середовищі, адсорбційні та сорбційно-каталітичні властивості шунгіту активованого та наномодифікованого різними способами.

Додаткове оброблення активованого шунгіту парою та наносріблом дає змогу збільшити його адсорбційну активність за йодом і за адсорбцією оцтової кислоти, лужністю водного настою до 1,2 раза та забезпечити стабілізацію окисно-відновного потенціалу підготовленої води на рівні +90–100 мВ.

Обробка парою сприяє збільшенню частини пор до дифузії та молекулярної сорбції, а також підвищує на 40% адсорбційну активність за гуміновими та фульвокислотами для активованого шунгіту за рахунок додаткової його обробки парою та наночастками срібла.

Витрати промивної води на етапі підготування активованого шунгіту обробленого парою та наносріблом не перевищують 20 відносних об'ємів промивної води на об'єм матеріалу, при цьому прозорість підготовленої води становить не менше 99%.

Попередня обробка активованого шунгіту парою перед його обробкою наночастинками срібла за рахунок покращення змочування поверхні дає змогу збільшити тривалість фільтрувального циклу та можливість поглиблення сорбування шкідливих мікродомішок води: заліза, марганцю, азотовмісних та органічних сполук на 10–12%.

Висновки. Використання шунгіту активованого, обробленого парою, забезпечує ефективність очищення від шкідливих мікродомішок і стабілізацію окисно-відновного потенціалу води підготовленої.

Ключові слова: *вода, шунгіт, наночастинки, модифікація.*

Instructions for authors

Dear colleagues!

The Editorial Board of scientific periodical
"**Ukrainian Food Journal**"
invites you for publication of your research results.

Requirements to all texts:
Language – English.
Recommended size of the article – 15–20 pages.
Font – Times New Roman, font size – 14, line intervals – 1, margins on both sides – 2 cm.

The structure of the article:

1. The title of the article
2. Authors (full name and surname)
3. Institution, where the work has been performed.
4. Abstract (2/3 of a page). The structure of the abstract should correspond to the structure of the article (Introduction, Materials and methods, Results and discussion, Conclusion).
5. Keywords.
6. The main body of the article should contain the following parts:
   - Introduction
   - Materials and methods
   - Results and discussion
   - Conclusion
   - References

   If you need you can add another parts and/or divide them into subparts.
7. The information about the author (Name, surname, scientific degree, place of work, email and contact phone number).

All figures should be made in graphic editor, the font size 14.

The background of the graphs and charts should be only in white color. The color of the figure elements (lines, grid, text) – in black color.

Figures and EXCEL format files with graphs additionally should be submitted in separate files.

Photos are not recommended to be used as graphical materials.

Website of Ukrainian Food Journal: http://ufj.ho.ua

Email for all submissions and other inquiries: ufj_nuft@meta.ua

Шановні колеги!

Редакційна колегія наукового періодичного видання «**Ukrainian Food Journal**» запрошує Вас до публікації результатів наукових досліджень.

Вимоги до оформлення статей

Мова статей – англійська.

Мінімальний обсяг статті – **10 сторінок** формату А4 (без врахування анотацій і списку літератури)**.**

Для всіх елементів статті шрифт – **Times New Roman**, кегль – **14**, інтервал – 1.

Всі поля сторінки – по 2 см.

Структура статті:

1**.** УДК**.**
2. **Назва статті.**
3. Автори статті (ім'я та прізвище повністю, приклад: Денис Озерянко).
4. *Установа, в якій виконана робота.*
5. Анотація. **Обов'язкова** структура анотації:
   - Вступ (2–3 рядки).
   - Матеріали та методи (до 5 рядків)
   - Результати та обговорення (пів сторінки).
   - Висновки (2–3 рядки).
6. Ключові слова (3–5 слів, але не словосполучень).

Пункти 2–6 виконати англійською і українською мовами.

7. Основний текст статті. Має включати такі обов'язкові розділи:
   - Вступ
   - Матеріали та методи
   - Результати та обговорення
   - Висновки
   - Література.

За необхідності можна додавати інші розділи та розбивати їх на підрозділи.

8. Авторська довідка (Прізвище, ім'я та по батькові, вчений ступінь та звання, місце роботи, електронна адреса або телефон).
9. Контактні дані автора, до якого за необхідності буде звертатись редакція журналу.

Рисунки виконуються якісно. Скановані рисунки не приймаються. Розмір тексту на рисунках повинен бути **співрозмірним** (!) тексту статті. **Фотографії можна використовувати лише за їх значної наукової цінності.**

Фон графіків, діаграм – лише білий. Колір елементів рисунку (лінії, сітка, текст) – чорний (не сірий).

Рисунки та графіки EXCEL з графіками додатково подаються в окремих файлах.

Скорочені назви фізичних величин в тексті та на графіках позначаються латинськими літерами відповідно до системи СІ.

В списку літератури повинні переважати англомовні статті та монографії, які опубліковані після 2010 року.

Правила оформлення списку літератури

В Ukrainian Food Journalвзято за основу загальноприйняте в світі спрощене оформлення списку літератури згідно стандарту Garvard. Всі елементи посилання розділяються **лише комами**.

1. Посилання на статтю:

Автори А.А. (рік видання), Назва статті, Назва журналу (курсивом), Том (номер), сторінки.

Ініціали пишуться після прізвища.

Всі елементи посилання розділяються комами.

1. Приклад:
   Popovici C., Gitin L., Alexe P. (2013), Characterization of walnut (Juglans regia L.) green husk extract obtained by supercritical carbon dioxide fluid extraction, *Journal of Food and Packaging Science, Technique and Technologies,* 2(2), pp. 104–108.

2. Посилання на книгу:

Автори (рік), Назва книги (курсивом), Видавництво, Місто.

Ініціали пишуться після прізвища.

Всі елементи посилання розділяються комами.

Приклад:

2. Wen-Ching Yang (2003), *Handbook of fluidization and fluid-particle systems*, Marcel Dekker, New York.

Посилання на електронний ресурс:

Виконується аналогічно посиланню на книгу або статтю. Після оформлення даних про публікацію пишуться слова ***Available at:*** та вказується електронна адреса.

Приклади:

1. (2013), *Svitovi naukovometrychni bazy*, available at: http://www1.nas.gov.ua/publications/q_a /Pages/scopus.aspx
2. Cheung T. (2011), *World's 50 most delicious drinks [Text]*, Available at: http://travel.cnn.com/explorations/drink/worlds–50-most-delicious-drinks–883542

Список літератури оформлюється лише латиницею. Елементи списку українською та російською мовою потрібно транслітерувати. Для транслітерації з українською мови використовується паспортний стандарт, а з російської – стандарт МВД (в цих стандартах використовуються символи лише англійського алфавіту, без хвостиків, апострофів та ін).

Зручні сайти для транслітерації:

З української мови – http://translit.kh.ua/#lat/passport

З російської мови – http://ru.translit.net/?account=mvd

Додаткова інформація та приклад оформлення статті – на сайті

http://ufj.ho.ua

Стаття надсилається за електронною адресою: ufj_nuft@meta.ua

УДК 663/664

Ukrainian Food Journal публікує оригінальні наукові статті, короткі повідомлення, оглядові статті, новини та огляди літератури.

Тематика публікацій в Ukrainian Food Journal:

Харчова інженерія
Харчова хімія
Мікробіологія
Фізичні властивості харчових продуктів
Якість та безпека харчових продуктів
Процеси та обладнання
Нанотехнології
Економіка та управління
Автоматизація процесів
Упаковка для харчових продуктів

Періодичність виходу журналу 4 номери на рік.

Результати досліджень, представлені в журналі, повинні бути новими, мати чіткий зв'язок з харчовою наукою і представляти інтерес для міжнародного наукового співтовариства.

Ukrainian Food Journal індексується наукометричними базами:
Index Copernicus (2012)
EBSCO (2013)
Google Scholar (2013)
UlrichsWeb (2013)
Global Impact Factor (2014)
Online Library of University of Southern Denmark (2014)
CABI full text (2014)
Directory of Research Journals Indexing (DRJI) (2014)
Universal Impact Factor (2014)
Directory of Open Access scholarly Resources (ROAD) (2014)
European Reference Index for the Humanities and the Social Sciences (ERIH PLUS) (2014)
Directory of Open Access Journals (DOAJ) (2015)
InfoBase Index (2015)
Chemical Abstracts Service Source Index (CASSI) (2016)
Emerging Sourses Citaton Index (2018)

Рецензія рукопису статті. Матеріали, представлені для публікування в «Ukrainian Food Journal», проходять «Подвійне сліпе рецензування» двома вченими, призначеними редакційною колегією: один є членом редколегії і один незалежний учений.

Авторське право. Автори статей гарантують, що робота не є порушенням будь-яких авторських прав, та відшкодовують видавцю порушення даної гарантії. Опубліковані матеріали є правовою власністю видавця «**Ukrainian Food Journal**», якщо не узгоджено інше.

Політика академічної етики. Редакція «Ukrainian Food Journal» користується правилами академічної етики, викладених в роботі Miguel Roig (2003, 2006) "Avoiding plagiarism, self-plagiarism, and other questionable writing practices. A guide to ethical writing". Редакція пропонує авторам статей і рецензентам прямо слідувати цьому керівництву, щоб уникнути помилок у науковій літературі.

Інструкції для авторів та інша корисна інформація розміщені на сайті
http://ufj.ho.ua

Редакційна колегія

Contents of Volume 8 (Year 2019)

Зміст тому 8 (2019 рік)

Olga Mazurenko, Liliia Kharchenko, Dmytro Kolomiets, Oleksandr Mazurenko Method of thermometric determination of thermophysical characteristics of thermolabs materials	133-154	*Ольга Мазуренко, Лілія Харченко, Дмитро Коломієць, Олександр Мазуренко* Спосіб термометричного визначення теплофізичних характеристик термолабільних матеріалів
Liudmila Strelchenko, Igor Dubkovetskyi, Ivan Malezhyk Influence of differential heat treatment on foodstuffs with apples obtained by the convection-thermoradiation method of drying	155-168	*Людмила Стрельченко, Ігор Дубковецький, Іван Малежик* Вплив диференційно-термічної обробки на харчові продукти з яблук, отриманих конвективно-терморадіаційним сушінням
Issue 2		**N2**
Oleksandr Shevchenko, Anatolii Sokolenko, Oleg Stepanets, Sergii But Determination of the parameters of the recovery systems of heat potentials of streams of the gas-steam media	317-328	*Олександр Шевченко, Анатолій Соколенко, Олег Степанець, Сергій Бут* Визначення параметрів систем рекуперації теплових потенціалів потоків газопарових сумішей
Valentyn Petrenko, Yaroslav Zasyadko, Mykola Pryadko Modeling of heat transfer deterioration regimes when concentrating solutions in industrial film evaporators	329-342	*Валентин Петренко, Ярослав Засядько, Микола Прядко* Моделювання режимів погіршення тепловіддачі під час концентрування розчинів у промислових плівкових випарних апаратах
Iryna Dubovkina, Borys Davydenko, Veronica Rikhter Modelling of the hydrodynamic conditions throughout liquid system treatment by alternating impulses of pressure	343-354	*Ірина Дубовкіна, Борис Давиденко, Вероніка Ріхтер* Моделювання гідродинамічних умов при обробленні рідких систем знакозмінними імпульсами тиску
Vitalii Rachok, Volodymyr Telychkun, Yevgenii Shtefan, Yuliya Telychkun, Stanka Damyanova Modeling of the process of kneading the yeast dough by cam operating elements	355-367	*Віталій Рачок, Володимир Теличкун, Євгеній Штефан, Юлія Теличкун, Станка Дамянова* Моделювання процесу замішування дріжджового тіста кулачковими робочими елементами
Issue 3		**N3**
Liudmyla Kryvoplias-Volodina, Oleksandr Gavva, Taras Hnativ, Kateryna Rivna Investigation of ejection process in mechatronic functional modules of packaging machines	620-633	*Людмила Кривопляс-Володіна, Олександр Гавва, Тарас Гнатів, Катерина Рівна* Дослідження процесу ежекції в мехатронних функціональних модулях пакувальних машин
Valerii Myronchuk, Oleksandr Obodovych, Vitalii Sydorenko Influence of discrete-pulse energy input on the distribution of plant biomass	634-644	*Валерій Мирончук, Олександр Ободович, Віталій Сидоренко* Вплив дискретно-імпульсного введення енергії на дисперсність біомаси рослинної сировини
Issue 3		**N3**
Anatolii Sokolenko, Oleksandr Shevchenko, Kostyantyn Vasylkivskyi, Oleksii Boiko, Anastasiia Shevchenko Modeling and synthesis of systems of intensive mass exchange	861-872	*Анатолій Соколенко, Олександр Шевченко, Костянтин Васильківський, Олег Степанець, Олексій Бойко, Анастасія Шевченко* Моделювання і синтез систем інтенсивного масообміну

Наукове видання

Ukrainian Food Journal

Volume 8, Issue 4
2019

Том 8, № 4
2019

Підп. до друку 28.11.2019 р. Формат 70x100/16.
Обл.-вид. арк. 16.46. Ум. друк. арк. 16.11.
Гарнітура Times New Roman. Друк офсетний.
Наклад 100 прим. Вид. № 14н/19.

НУХТ. 01601 Київ–33, вул. Володимирська, 68

Свідоцтво про державну реєстрацію
друкованого засобу масової інформації
КВ 18964–7754Р
видане 26 березня 2012 року.